

**The Design, Synthesis and Biological testing of  
Novel Antimicrobials for Food Safety and  
Human Health**



A thesis submitted to The University of Reading in fulfilment  
for the degree of Doctor of Philosophy

School of Pharmacy

Charlotte Frances Marriott

September 2018

## Abstract

It has been predicted that by 2050, 10 million deaths will occur as a result of resistant microbials. This is a growing concern which is creating an urgent need for the development of new antimicrobials as well as additional selective media for the identification of these bacteria. When designing new antimicrobial compounds, their selectivity to different bacterial strains, and their solubilities, must be optimised, for example through prodrug strategies. Since some bacterial strains are documented to have different levels of glycosidase enzymes, glycoside based prodrugs have proven of interest in antibacterial strategies. The overarching aim of this work was therefore to design, synthesise and analyse a range of glycoside prodrugs both as antibacterial agents and agents for the selective recovery of bacteria. Through this work, structure-activity relationships for the parent compounds and the prodrugs against a range of gram-negative and gram-positive bacteria could also be determined based on minimum inhibitory concentration values which were determined using a bioscreen or agar method.

Therefore,  $\beta$ -glucosides and  $\beta$ -galactosides of 2-benzylphenol and bis(2-hydroxyphenyl)methane were synthesised using an aq. Michael addition method. All the  $\beta$ -glycosides had MIC values of  $>128 \mu\text{g/mL}$ . 2-Benzylphenol was found to have MIC values of  $64 \mu\text{g/mL}$  for *Streptococcus agalactiae*, *Streptococcus pneumoniae* and *Streptococcus pyogenes* which is similar to the MIC value for cefaclor and cefaxil, which are used in the clinic. Using a different synthetic route based on phase transfer catalysis,  $\beta$ -glucosides and  $\beta$ -galactosides of 7-hydroxyflavone, chrysin and 7,8-dihydroxyflavone were synthesised. All the  $\beta$ -glycosides had MIC values of  $>128 \mu\text{g/mL}$  whilst 7,8-dihydroxyflavone and 7-hydroxyflavone had values of 25 and  $6.25 \mu\text{g/mL}$  for *Staphylococcus epidermidis* and 50 and  $12.5 \mu\text{g/mL}$  for *Staphylococcus aureus*, respectively. These compounds were also tested using an MTT assay, against the breast cancer MCF-7 and MDA-MB231 cell lines to obtain toxicity

data to evaluate their anticancer properties. The preliminary cell assays concluded that all compounds had an  $IC_{50} > 2$  mM.

1,2,3-Triazole derivatives of azidothymidine were also prepared using 'click' chemistry, with copper catalysed reactions affording the 4' isomers, and ruthenium catalysed reactions affording the 5' isomers. 3'-Deoxy-3'-(5-hydroxymethyl-1,2,3-triazol-1-yl)- $\beta$ -D-thymidine had comparable MIC values to azidothymidine, against *Escherichia coli* and *Klebsiella pneumoniae*, specifically 8 and 0.5  $\mu$ g/mL, respectively. To probe the antiviral activity of these compounds, the compounds were fitted using Pymol into the active site of the HIV reverse transcriptase enzyme, which is central for antiviral activity. All compounds were found to fit into the active site; however, further studies are needed to definitively determine their antiviral activity.

The work presented in this report display further advances the knowledge of structure-activity relationships within the three different classes of compounds. This can be used to further design better antimicrobials for potential use as selective media or clinical uses.

## **Acknowledgements**

There are many people for whom I would have been at a loss to try and finish this PhD project without them. Firstly, I would like to thank my university and industrial supervisors, Prof. Helen Osborn, Dr. Richard Bovill, and Dr. John Brazier. They allowed me to undertake this project and provided constant guidance and help which was greatly appreciated. I would also like to thank BBSRC and Thermofisher for funding my research project.

This project would have been significantly harder without the help of the technical staff at the University of Reading, namely Dr. Radek Kowalczyk (NMR), Gez Griffin and Philip Mason (Stores), and Martin Reeves and Nicholas Michael (MS). I would also like to thank Mark Hutchins and the people who work in the chemistry and clinical R&D sections in Oxoid, Thermofisher, their knowledge and support while I was performing my microbiological studies was invaluable. To all the members of Lab 228, both past and present, thank you for being amazing colleagues and putting up with my crazy ideas: Rebecca Thomson, Cidalia Pereira, Esmie Wescott, Irene Boz, Ibrahim Shah, Adam Gadd, Jack Cheeseman, Laura Bryant, Rosanna Fanelli, and Daniel Townsend. I would also like to extend my deepest thanks to Az Natfji for his help and guidance with the tissue culture studies. I would also like to thank Dr. James Hall for helping me understand and set up my fitting models software, and Ruth Cawdron and Ryan Coones for their proof-reading skills.

This work could not have been completed without the support of my family and friends. Thank you for all the good times and Frisbee that was played. My family also had a major role in helping me through this Ph.D. To my Dad, Mum, Joshua, Victoria and James: I cannot thank you enough.

And lastly I would like to thank my rock- Diarmuid Coffey. You helped me and were willing to go the extra mile to make sure I was doing well. Thank you.

## **Declaration**

The work described in the following thesis was carried out jointly between the School of Pharmacy at the University of Reading and Thermofisher (Oxoid, Basingstoke) between October 2014 and August 2018.

I declare that this thesis has been composed solely by myself and that it has not been submitted, in whole or in part, in any previous application for a degree. Except where states otherwise by reference or acknowledgment, the work presented is entirely my own.

Charlotte Frances Marriott

## Table of Contents

Chapter 1-Introduction.....	1
1.1 Antibiotics.....	2
1.1.1 The Discovery of Antibiotics.....	3
1.1.2 Classes of Antibiotics .....	4
1.1.3 Mechanism of action of antibiotics.....	6
1.1.3.1 Cell Wall Synthesis.....	7
1.1.3.2 Fatty acid synthesis.....	9
1.1.3.3 Protein/ RNA synthesis.....	11
1.1.3.4 Folate metabolism.....	13
1.1.3.5 DNA synthesis .....	14
1.1.4 Antibiotic resistance .....	15
1.1.4.1 Mechanism of resistance.....	18
1.1.5 Uses of antibiotics.....	20
1.1.5.1 Clinical use .....	20
1.1.5.2 Biocides in clinical practice .....	21
1.1.5.3 The use of antimicrobials in the detection of microorganisms in media .....	22
1.1.5.4 Selective recovery of bacteria from media .....	25
1.2 Methods for drug design .....	27
1.2.1 Prodrugs .....	29
1.3 Carbohydrates in drug design .....	32
1.3.1 Natural Carbohydrates and their presence in drugs .....	32
1.3.2 Glycosylations in chemistry.....	34
1.3.3 Carbohydrate uptake system.....	36
1.3.4 Carbohydrate prodrugs .....	37
1.4 Overall aims and objectives .....	40

1.4.1 Overall aims of the project.....	40
1.4.2 Overall objectives of the project.....	40
Chapter 2 – The synthesis and microbiological evaluation of carbohydrate prodrugs containing a bisphenol moiety .....	41
2.1 Aims and objectives of the bisphenol containing compounds.....	42
2.1.1 Aims for the bisphenol moiety containing prodrugs .....	42
2.1.2 Objectives of the bisphenol moiety containing prodrugs .....	43
2.2 Introduction.....	43
2.2.1 Polychlorinated compounds.....	44
2.2.2 Justification for drug design .....	47
2.3 Results and discussion .....	50
2.3.1 Synthesis .....	50
2.3.1.1 Synthetic route to synthesising the target molecules <b>33</b> and <b>34</b> .....	50
2.3.1.2 Optimisation of the glycosylation reaction .....	52
2.3.1.3 Mechanism by which the reaction occurs.....	54
2.3.1.4 Optimisation of the purification for the target compounds.....	58
2.3.1.5 Yields and purity of the target compounds.....	59
2.3.2 Microbiology data for the bisphenol series.....	60
2.3.2.1 Bioscreen method .....	60
2.3.2.2 Justification for organisms used .....	62
2.3.2.3 Microbiological results .....	65
2.3.2.4 Microbiological results for $\beta$ 2 benzylphenol glycosides and $\beta$ bis(2 hydroxyphenyl)methane glycosides .....	65
2.3.3 Structure-activity relationships between the bisphenol moiety glycosides .....	71
2.4 Conclusion .....	72
Chapter 3 – The synthesis and microbiological evaluation of triazole containing compounds based on azidothymidine .....	75
3.1 Introduction.....	76

3.1.1 Aims for the triazole based compounds.....	76
3.1.2 Objectives of the triazole based compounds.....	77
3.1.3 The history and further development of AZT.....	78
3.1.4 Nucleoside based prodrugs .....	82
3.1.4.1 1,2,3-Triazoles .....	84
3.1.5 Justification for drug design .....	90
3.3 Results and discussion .....	92
3.3.1 Synthesis .....	92
3.3.1.1 Synthetic route .....	92
3.3.1.2 Optimisation of the formation of the 1, 4 isomer .....	97
3.3.1.3 Chemical analysis of the triazole containing compounds <b>44-51</b> .....	99
3.3.1.4 Yields and purity of the target compounds <b>44-51</b> .....	101
3.2.1 Microbiology data for the triazole containing compounds.....	102
3.2.1.1 Microbiological results .....	102
3.2.1.2 Microbiological results for AZT <b>52</b> using the bioscreen method.....	103
3.2.1.3 Microbiological results for the 1,4-1,2,3-triazole derived compounds <b>44-47</b> using the bioscreen method.....	105
3.2.1.4 Microbiological results for the 1,5-1,2,3-triazole derived compounds <b>48-51</b> using the bioscreen method.....	109
3.3 SAR for the target compounds in the triazole containing compounds .....	115
3.4 Antiviral properties of AZT and its modifications .....	116
3.4.1 HIV reverse transcriptase.....	118
3.5 Conclusion .....	121
Chapter 4 – The synthesis and microbiological evaluation of carbohydrate prodrugs containing a flavonoid moiety to probe SAR's .....	123
4.1 Introduction.....	124
4.1.1 Aims for the glycosidic flavonoid compounds <b>92-97</b> .....	124
4.1.2 Introduction to Flavonoids.....	125

4.1.3 Flavonoid as antimicrobial agents .....	126
4.2 Chrysin.....	129
4.2.1 Mechanism of action.....	130
4.2.2 Derivatives of chrysin.....	130
4.3 Justification for design.....	133
4.4 Results and discussion .....	135
4.4.1 Synthesis .....	135
4.4.1.2 Synthetic route .....	135
4.4.1.3 Yields and purity.....	140
4.4.1.4 Optimisation of the synthetic route.....	141
4.4.1.5 Chemical analysis .....	145
4.4.2 Microbiology data for the flavonoid containing compounds.....	147
4.4.2.1 Microbiological results .....	147
4.4.2.2 Microbiology data for the parent flavonoid compounds <b>103, 110</b> and <b>111</b> . in agar .....	147
4.4.2.3 Microbiology data for the parent flavonoid compounds ( <b>103, 110</b> and <b>111</b> ) and their respective glycosides <b>92-97</b> .....	151
4.4.3 SAR of the target compounds <b>103, 110</b> and <b>111</b> and their respective glycosides <b>92 97</b> .....	157
4.5 Conclusion .....	158
Chapter 5 – Conclusions and Future work.....	161
5.1 Overall summary of this project .....	162
5.2 The carbohydrate prodrugs containing a bisphenol moiety .....	162
5.2.1 Future work for the carbohydrate prodrugs containing a bisphenol moiety.....	165
5.3 The triazole containing compounds based on azidothymidine .....	166
5.3.1 Future work for the triazole containing compounds based on azidothymidine .	169
5.4 The carbohydrate prodrugs containing flavonoids .....	170
5.4.1 Future work for the carbohydrate prodrugs containing flavonoids .....	174

5.4.1.2 Anticancer and in vitro toxicity for the glycosidic flavonoids <b>92-97</b> ...	175
5.4.1.3 Glycosidic compounds used in cancer therapy .....	176
5.4.1.4 In vitro toxicity experiment .....	177
5.5 Future work.....	179
5.5.1 Kinetic studies.....	179
5.5.2 Analysis with resistant bacteria .....	180
5.5.3 Possible future glycoside strategies .....	181
5.5.3.1 Pleuromutilin compounds .....	181
5.5.3.2 Carvacrol compounds .....	184
5.5.3.3 Azido moiety containing antimicrobials.....	185
5.5.4 Further biological analysis.....	185
Chapter 6 – Experimental .....	187
6.1 Equipment and Materials .....	188
6.1.1 NMR Spectroscopy .....	188
6.1.2 Mass Spectrometry .....	188
6.1.3 HPLC .....	188
6.1.4 Infrared Spectroscopy .....	188
6.1.5 Polarimetry.....	189
6.1.6 Thin layer Chromatography.....	189
6.1.7 Column Chromatography .....	189
6.1.8 Melting points .....	189
6.1.9 Chemicals.....	189
6.1.10 Microorganism strain list.....	189
6.1.11 Preparation of bacteria .....	191
6.1.12 Preparation of broths.....	191
6.1.13 Preparation of plate media .....	191
6.1.14 Determination of MIC of desired compounds using the bioscreen method ....	191

6.1.15 Determination of MIC of desired compounds using the agar method.....	191
6.1.16 Cell culture.....	192
6.1.17 Cell sub culturing.....	192
6.1.18 Preparation of MTT .....	193
6.1.19 MTT assay .....	193
6.2 The glycosidic compounds with a bis-phenol moiety <b>33-34</b> .....	194
6.2.1 General procedure for the synthesis of <b>33-34</b> .....	194
6.1.2.1 Synthesis of 2-benzyl phenol- $\beta$ -D-glucopyranoside ( <b>33a</b> ).....	195
6.1.2.2 Synthesis of Bis(2-hydroxyphenyl)methane- $\beta$ -D-glucopyranoside ( <b>33b</b> ) .....	196
6.1.2.3 Synthesis of 2-benzyl phenol- $\beta$ -D-galactopyranoside ( <b>34a</b> ) .....	197
6.1.2.4 Synthesis of Bis(2-hydroxyphenyl)methane- $\beta$ -D-galactopyranoside .....	
( <b>34b</b> ).....	198
6.3 The compounds based on azidothymidine containing a triazole moiety <b>44-51</b> .....	200
6.3.1 General Procedure for synthesis of 1,4 triazoles via click reactions .....	200
6.3.1.1 Synthesis of 3' Deoxy 3' (4 hydroxymethyl 1,2,3 triazol 1 yl) $\beta$ D thymidine ( <b>44</b> ).....	201
6.3.1.2 Synthesis of 3' Deoxy 3' (4 benzyl 1,2,3 triazol 1 yl) $\beta$ D thymidine ( <b>45</b> ) .....	202
6.3.1.3 Synthesis of 3' Deoxy 3' (4 4'' fluoro benzyl 1,2,3 triazol 1 yl) $\beta$ D thymidine ( <b>46</b> ).....	203
6.3.1.4 Synthesis of 3' Deoxy 3' (4 3'' fluoro benzyl 1,2,3 triazol 1 yl) $\beta$ D thymidine ( <b>47</b> ).....	204
6.3.2 General Procedure for synthesis of 1,5 triazoles via click reactions .....	206
6.3.2.1 Synthesis of 3' Deoxy 3' (5 Hydroxymethyl 1,2,3 triazol 1 yl) $\beta$ D thymidine ( <b>48</b> ).....	207
6.3.2.2 Synthesis of 3' Deoxy 3' (5 benzyl 1,2,3 triazol 1 yl) $\beta$ D thymidine ( <b>49</b> ).....	208

6.3.2.3 Synthesis of 3' Deoxy 3' (5 4'' fluoro benzyl 1,2,3 triazol 1 yl) $\beta$ D thymidine ( <b>50</b> ).....	209
6.3.2.4 Synthesis of 3' Deoxy 3' (5 3'' fluoro benzyl 1,2,3 triazol 1 yl) $\beta$ D thymidine ( <b>51</b> ).....	210
6.4 The glycosidic flavonoid containing compounds 92-97 and 112-117.....	211
6.4.1 General Procedure for synthesis of O-acetylated flavonoid glycosides <b>112-117</b> ....	211
6.4.1.1 Synthesis of 7 hydroxyflavone $\beta$ D 2,3,4,6 tetra-O-acetate glucopyranoside ( <b>112</b> ) .....	212
6.4.1.2 Synthesis of 7 hydroxyflavone $\beta$ D 2,3,4,6 tetra-O-acetate galactopyranoside ( <b>113</b> ).....	213
6.4.1.3 Synthesis of chrysin $\beta$ D 2,3,4,6 tetra-O-acetate glucopyranoside ( <b>114</b> ) .....	214
6.4.1.4 Synthesis of chrysin $\beta$ D 2,3,4,6 tetra-O-acetate galactopyranoside ( <b>115</b> ). .....	215
6.4.1.5 Synthesis of 7,8-dihydroxyflavone $\beta$ D 2,3,4,6 tetra-O-acetate glucopyranoside ( <b>116</b> ) .....	216
6.4.1.6 Synthesis of 7,8-dihydroxyflavone $\beta$ D 2,3,4,6 tetra-O-acetate galactopyranoside ( <b>117</b> ).....	218
6.4.2 General procedure for deprotection of the flavonoid glycosides <b>92-97</b> .....	220
6.4.2.1 Synthesis of 7 hydroxyflavone- $\beta$ -D-glucopyranoside ( <b>92</b> ) .....	221
6.4.2.2 Synthesis of 7 hydroxyflavone- $\beta$ -D-galactopyranoside ( <b>93</b> ).....	222
6.4.2.3 Synthesis of chrysin- $\beta$ -D-glucopyranoside ( <b>94</b> ) .....	223
6.4.2.4 Synthesis of chrysin- $\beta$ -D-glucopyranoside ( <b>95</b> ) .....	224
6.4.2.5 Synthesis of 7,8-dihydroxyflavone- $\beta$ -D-glucopyranoside ( <b>96</b> ) .....	225
6.4.2.6 Synthesis of 7,8-dihydroxyflavone- $\beta$ -D-galactopyranoside ( <b>97</b> ) .....	226
Chapter 7 – References .....	228
Appendix.....	i

## List of Abbreviations

**μmol** - micromole

**ac** - acetyl

**ACP** - acyl carrier protein

**add** - apparent doublet of doublet

**AIDS** - acquired immune deficiency syndrome

**aq.** – aqueous

**as** - apparent singlet

**ATCC** – american type culture collection

**ATP** - adenosine triphosphate

**AZT** - azidothymide

**BCP** – bromochlorophen

**BLW** – block-localised wavefunction

**BP** – β-2-benzylphenol

**br** - broad

**CLSI** – clinical and laboratory standards institute

**CuAAC** – copper catalysed azide-alkyne cycloaddition

**d** - doublet

**DCM** - dichloromethane

**dd** - doublet of doublets

**DMF** - dimethylformamide

**DMSO** – dimethyl sulfoxide

**DNA** - deoxyribonucleic acid

**DP** - dichlorophene

**dt** - doublet of triplets

**dThd** - deoxythymidine

**dTMP** – thymidylate

**ELSD** – evaporative light scattering detector

**eq.** - equivalence

**ESI** - electrospray ionisation

**EUCAST** – European committee on antimicrobial susceptibility testing

**FAS** - fatty acid synthase

**FDA** - US food and drug administration

**FTIR** - fourier transform infrared spectroscopy

**Gal** – galactose

**GlcNAc** -  $\beta$ -1, 4-linked *N*-acetylglucosamine

**Glu** – glucose

**GLUT** - glucose transporters

**h** - hour

**hex** – hexachlorophene

**HIV** - human immunodeficiency virus

**HPLC** – high-performance liquid chromatography

**HPM** –  $\beta$ -bis(2-hydroxyphenyl)methane

**HPr** – histidine-protein

**hTK1** – human thymidine kinase 1

**HTS** – high throughput screening

**Hz** - hertz

**ID<sub>50</sub>** – infectious dose

**INH** - isonicotinylnhydrazine

**LBDD** - ligand-based drug design

**M** - molar

**m** - multiplet

**MBC** – minimum bacterial concentration

**MeCN** - acetonitrile

**MHA** – Mueller-Hinton agar

**MHB** – Mueller-Hinton broth

**MIC** - minimum inhibitory concentration

**min** - minute

**MRD** – maximum recovery diluent

**MRSA** - methicillin-resistant *Staphylococcus aureus*

**MSSA** - methicillin-susceptible *Staphylococcus aureus*

**MTCC** - microbial type culture collection and gene bank

**MurNAc** - *N*-acetylmuramic acid  
**NAD** - nicotinamide adenine dinucleotide  
**NB** - nutrient broth 2  
**NBO** – natural bond orbital  
**NCTC** - national collection of type cultures  
**NDP** – nucleoside-diphosphate  
**NGP** - neighbouring group participation  
**NMR** - nuclear magnetic resonance  
**NP** – normal phase  
**OCC** - oxoid culture collection  
**OD** – optical density  
**ONPG** - *ortho*-nitrophenyl- $\beta$ -galactoside  
**PABA** - *para*-amino benzoic acid  
**PBP** – penicillin-bound proteins  
**PEP** - phosphoenolpyruvate  
**P-HPr** - phospho-histidine-protein  
**ppm** - parts per million  
**PTC** – phase transfer catalysis  
**PTS** - phosphotransferase system  
**q** - quartet  
**QAC** - quaternary ammonium chloride  
**QSAR** - quantitative structure–activity relationship  
**R<sub>f</sub>** - retention factor  
**RNA** - ribonucleic acid  
**RP** – reverse phase  
**RT** - room temperature  
**RuAAC** – ruthenium catalysed azide-alkyne cycloaddition  
**s** - singlet  
**saKAS III** - *Staphylococcus aureus*  $\beta$ -Ketoacyl acyl carrier protein synthase III  
**SAR** – structure-activity relationship  
**SBDD** - structure-based drug design  
**t** - triplet

**TB** - tuberculosis

**TBAHS** - tetrabutylammonium hydrogensulfate

**TK1** – thymidine kinase 1

**TLC** – thin layer chromatography

**tRNA** - transfer ribonucleic acid

**TSA** – tryptic soya agar

**TTS-12** - tigogenin 3-*O*- $\beta$ -D-xylopyranosyl- (1 $\rightarrow$ 2)-[ $\beta$ -D-xylopyranosyl (1 $\rightarrow$ 3)]- $\beta$ -D-glucopyranosyl-(1 $\rightarrow$ 4)-[ $\alpha$ -L-rhamnopyranosyl-(1 $\rightarrow$ 2)]- $\beta$ -D-galactopyranoside

**TTS-15** - tigogenin 3-*O*- $\beta$ -D-glucopyranosyl-(1 $\rightarrow$ 2)-[ $\beta$ -D-xylopyranosyl- (1 $\rightarrow$ 3)]- $\beta$ -D-glucopyranosyl-(1 $\rightarrow$ 4)- $\beta$ -D-galactopyranoside

**UDP-GluNAc** - uridine diphosphate-*N*-acetylglucosamine

**UDP-MurNAc** - uridine diphosphate -*N*-acetylmuramic acid

**UGTs** - UDP-glucuronosyltransferases

**UpTK** – *Ureaplasma parvum* thymidine kinase

**UV** - ultra-violet

**VB** – valance bond

**WHO** - world health organisation

**X-GAL** - 5-bromo-4-chloro-3-indolyl- $\beta$ -D-galactopyranoside

# **Chapter 1-Introduction**

## 1.1 Antibiotics

Antibiotics are compounds that have ‘*the ability to form a complex with a molecule essential for the growth of a bacterial cell, thus inhibiting its function*’.<sup>1</sup> These compounds can either block cell growth or induce apoptosis. Antibiotics may either be for a specific pathogen, or broad spectrum, meaning they kill a variety of pathogens.<sup>2</sup> A substance can be classified as an antibiotic if it has the required biological effect and if any one of the following conditions are met:

- (a) It is a product of a metabolism pathway.
- (b) It is a synthetic product formed as a structural analogue of a naturally occurring antibiotic
- (c) It antagonises the growth or survival of one or more species of microorganisms
- (d) It is effective in producing a biological effect at low concentrations.<sup>3</sup>

The use of antibiotics could have prevented many epidemics. An example of this is the plague, also known as Black Death. This disease was caused by a gram-positive bacterium called *Yersinia pestis* and caused both strains of the plague: bubonic and pneumonic. There were two major outbreaks which were estimated to have killed nearly 40-60% of the European population at the time, dependant on location.<sup>4</sup> With the introduction of the use of antibiotics, the number of bacterial-based infections considered as fatal has drastically reduced. It has also stopped the spread of these infections, which in turn has reduced the number of bacterial epidemics. Diphtheria is a good example of how the introduction of a certain antibiotic, penicillin and later followed by erythromycin, has reduced the mortality rate. This disease is caused by a gram-positive bacterium, *Corynebacterium diphtheriae*, and was the third leading cause of deaths in England and Wales in the 1930’s. With the introduction of an antibiotic vaccine, diphtheria

antitoxin followed by intravenous penicillins or erythromycin, the death toll has reduced and now, since 1994, there have been only three cases of diphtheria in England.<sup>5</sup>

### **1.1.1 The Discovery of Antibiotics**

It was Louis Pasteur who observed: *'if we could intervene in the antagonism observed between some bacteria, it would offer perhaps the greatest hopes for therapeutics'*.<sup>6</sup> This statement then initiated an area of medicine which is collectively named antibiotics. Paul Erlich, a pioneer in antimicrobial chemotherapy, also imagined a 'magic bullet'. This term represents a small molecule used to target the disease-causing pathogen, with the outcome of treating the said pathogen more effectively and in a more targeted fashion.<sup>7</sup> In 1909, he discovered the compound arsphenamine and investigated its use in the treatment of syphilis. This is considered the first modern antibiotic, though Erlich himself did not call it an antibiotic; he used the term chemotherapy. In 1928, Sir Alexander Fleming discovered the antibiotic penicillin and published his findings of mould juice, but could not isolate the active ingredient.<sup>8</sup> His discovery led the way for scientists to research this new field. It was not until 1945 that Sir Fleming received recognition for his discovery in the form of a Nobel Prize in medicine. He shared this prize with both Howard Florey and Ernest Chain. Florey and Chain isolated penicillin and started trials into the efficacy of penicillin as an antimicrobial. However, they had very little penicillin so their attention turned to large scale production. This antibiotic proved indispensable in World War II.

The term 'antibiotic' was coined by Selman Waksman. Considered the 'father of antibiotics', Waksman's approach was a stark contrast to that of Alexander Fleming. Sir Fleming's approach relied mostly on fortunate choices, whereas Waksman's approach was to apply a systematic screen that removes the luck element.<sup>5</sup> Waksman's research was based on screening soil-derived

*Actinomycetes*. This systematic screening process allowed for the discovery of streptomycin, the first effective compound to be used against tuberculosis.

### 1.1.2 Classes of Antibiotics

Since Waksman's platform was discovered and utilised, many families of antibiotics have been found, however, recently there has been a decrease in antibiotic discoveries. Over the past twenty years there have been only two new classes of synthetic antibiotics identified: fluoroquinolones and oxazolidinones. The oldest of the classes are the  $\beta$ -lactams, this family includes all penicillins, which all contain a  $\beta$ -lactam ring. These target the cell wall, attaching to the penicillin binding proteins found on the bacterial cell walls. Table 1 shows this family along with other examples of different antibiotics classes.

**Table 1:** A table showing examples of different classes of antibiotics. Table adapted from ref. 9 and 5.

Class of antibiotic	Examples in that class	Year of discovery	Mechanism of action
$\beta$ -lactam	Penicillins Penicillin G, penicillin V, methicillin, oxacillin, cloxacillin, dicloxacillin, nafcillin, ampicillin.	1928	Interference with cell wall synthesis <sup>10,11</sup>
Sulphonamide	Sulphanilamide, <i>para</i> -aminobenzoic acid, sulfadiazine, sulfisoxazole, sulfamethoxazole, sulfathalidine	1932	Inhibition of folic acid synthesis. <sup>12</sup>
Aminoglycoside	Streptomycin, neomycin, kanamycin, paromomycin, gentamicin, tobramycin, amikacin, netilmicin, spectinomycin, sisomicin, dibekacin, isepamicin	1943	Inhibits protein synthesis, its target is 30S ribosomal subunit <sup>13,14</sup>
Tetracycline	Tetracycline, chlortetracycline, demeclocycline, minocycline, oxytetracycline, methacycline, doxycycline, tigecycline, rifamycins Rifampicin.	1944	Inhibits protein synthesis, its target is aminoacyl-tRNA to the ribosomal acceptor site. <sup>15</sup>
Cephalosporin	<b>First generation:</b> Cephalothin, cephapirin, cephadrine, <b>Second generation:</b> Cefamandole, cefuroxime, cephalexin	1944 <sup>16</sup>	Interference with cell wall synthesis <sup>17</sup>

	<b>Third generation:</b> Cefotaxime. <b>Fourth generation:</b> Cefpirome <b>Fifth generation:</b> Ceftaroline		
Macrolide	Erythromycin, azithromycin, clarithromycin.	1948	Inhibits protein synthesis by binding to the 50S ribosomal subunit <sup>18,19</sup>
Monobactam	Aztreonam	1951 <sup>20</sup>	Interference with cell wall synthesis <sup>11</sup>
Glycopeptide	Vancomycin, teicoplanin, telavancin	1953	Inhibits the late stage cell wall synthesis <sup>21</sup>
Oxazolidinone	Linezolid	1955	Inhibits protein synthesis <sup>22</sup>
Quinolone	Nalidixic acid, oxolinic acid, norfloxacin, pefloxacin, enoxacin, ofloxacin/levofloxacin, ciprofloxacin, temafloxacin, lomefloxacin, fleroxacin, grepafloxacin, sparfloxacin, trovafloxacin.	1961	Converts DNA gyrase and topoisomerase IV into toxic enzymes <sup>23</sup>
Streptogramin	Quinupristin, dalfopristin, pristinamycin	1963	Inhibits protein synthesis by binding to the 50S ribosomal subunit <sup>18,24</sup>
Lincosamide	Lincomycin, clindamycin	1964 <sup>25</sup>	Inhibits protein synthesis by binding to the 50S ribosomal subunit <sup>18</sup>
Carbapenem	Imipenem, meropenem, doripenem	1976 <sup>26</sup>	Interference with cell wall synthesis <sup>27,28</sup>
$\beta$ -Lactamase inhibitor	Clavulanate, sulbactam, tazobactam	1976 <sup>26</sup>	Inhibits $\beta$ -lactamase
Lipopeptide	Daptomycin	1986	Anionic: Bind to the bacterial membrane, and cause rapid depolarisation of the membrane potential. <sup>29,30</sup>
Ketolide	Telithromycin	2000 <sup>19</sup>	Inhibits protein synthesis by binding to the 50S ribosomal subunit <sup>31,32</sup>
Others	Metronidazole, polymyxin B, colistin, trimethoprim		

### 1.1.3 Mechanism of action of antibiotics

There are differences between prokaryotic and eukaryotic cell structures, and this can allow antibiotics to selectively target one type of cell over the other. An example of a prokaryotic cell is a bacterium. Bacterial cells can be sub-divided into two separate classifications: gram-negative and gram-positive cells. Gram-negative bacteria have a thin peptidoglycan layer with an outer membrane. This extra outer layer is not present in gram-positive bacteria and this is the reason that once stained with crystal violet, only gram-positive bacteria are stained purple. This extra barrier also explains why gram-negative bacteria present an extra challenge when treating clinically.

Different antibiotics use different pathways to effectively affect bacteria. These pathways refer to the mechanism of action for the antibiotic, and this is shown in Figure 1.<sup>33</sup> Antibiotics can also be described as bacteriostatic or bactericidal agents. Bacteriostatic refers to the inhibition of growth of the bacterial cells, whereas bactericidal denotes the agents killing the bacteria. Clinically, however, this is not relevant without other information, such as pharmacokinetics.<sup>34</sup>

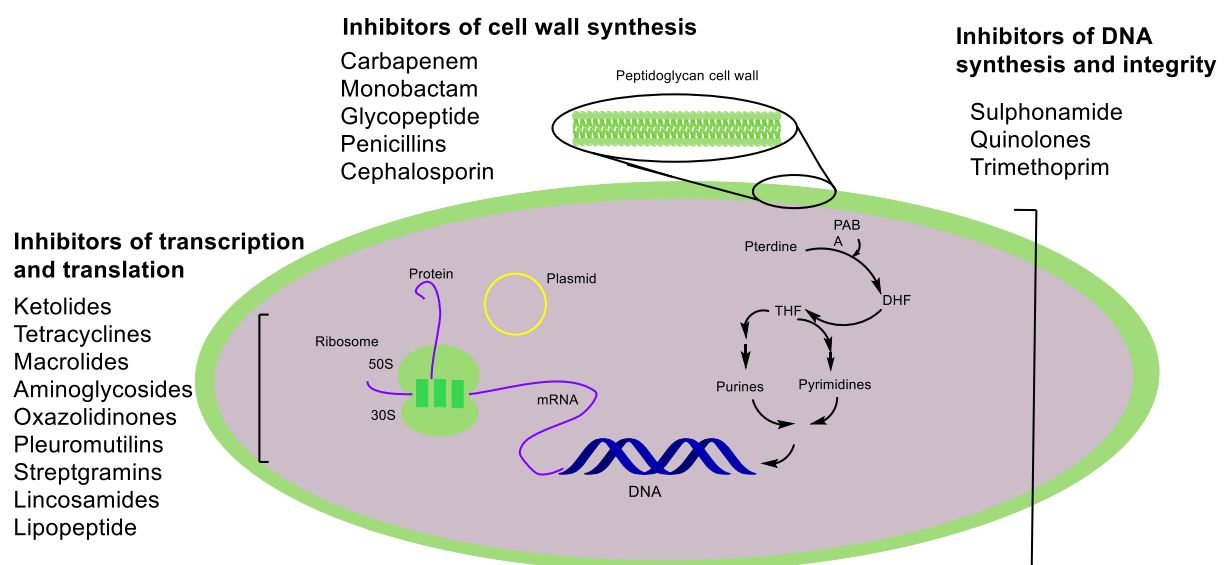


**Figure 1:** The sites of action for antimicrobial drugs. Adapted from a figure in ref. 33.

In designing antibiotics it has to be considered whether the antibiotic will affect the cells and kill the bacteria. There are five targets that are used when developing antibacterial compounds: cell wall synthesis, fatty acid synthesis, folate synthesis, deoxyribonucleic acid (DNA) synthesis and protein/ ribonucleic acid (RNA) synthesis. Each involves unique biological pathways which are exploited and targeted by the antibacterial molecule.

### 1.1.3.1 Cell Wall Synthesis

Cell wall synthesis is the most commonly exploited target for antibacterial agents. There is an inherent intrinsic target selectivity, as there is no counterpart found in human biology.<sup>35</sup> The cell wall is structured from peptidoglycan; this is a crossed linked polymer containing long glycan chains that are bridged to form elastic and flexible structures. The polysaccharide chains are  $\beta$ -1, 4-linked *N*-acetylglucosamine (GlcNAc) and *N*-acetylmuramic acid (MurNAc) subunits. The differences between the gram-positive and gram-negative cell walls are shown in Figure 2.<sup>36</sup> The initial stages of cell wall synthesis occur in the cytoplasm. The sugar nucleotide, UDP-*N*-acetylglucosamine (UDP-GluNAc) is used to synthesise UDP-*N*-acetylmuramic acid (UDP-MurNAc). This synthesis involves the enolpyruvyl functionality that is found in phosphoenolpyruvate (PEP) being attached to UDP-GluNAc by an enzyme called UDP-GlcNAc enolpyruvyl transferase, immediately followed by a reduction of the enol group to a lactyl group. Then, a peptide linker is added to increase flexibility and D-Ala-D-Ala is added via coupling reactions using adenosine triphosphate (ATP) as a source of energy. This, thus, creates the UDP-MurNAc-pentapeptide molecule. This molecule is then transported across the cytoplasmic membrane by a lipid carrier. The second stage sees the UDP-moiety of UDP-MurNAc being replaced with undecaprenyl phosphate. GlcNAc is then coupled to

MurNAc-pentapeptide, which is catalysed by a protein which has been encoded by the *murG* gene. The new compound, GlcNAc-MurNAc-pentapeptide, undergoes transglycosylation and cross-linking to assemble the peptidoglycan layer once it has been translocated to the extra-cellular side of the cytoplasmic membrane.<sup>37–39</sup>

Examples of antibiotics that interrupt and inhibit the cell wall synthesis include  $\beta$ -lactam and glycopeptide antibiotics. As previously mentioned, penicillins are part of the  $\beta$ -lactam family

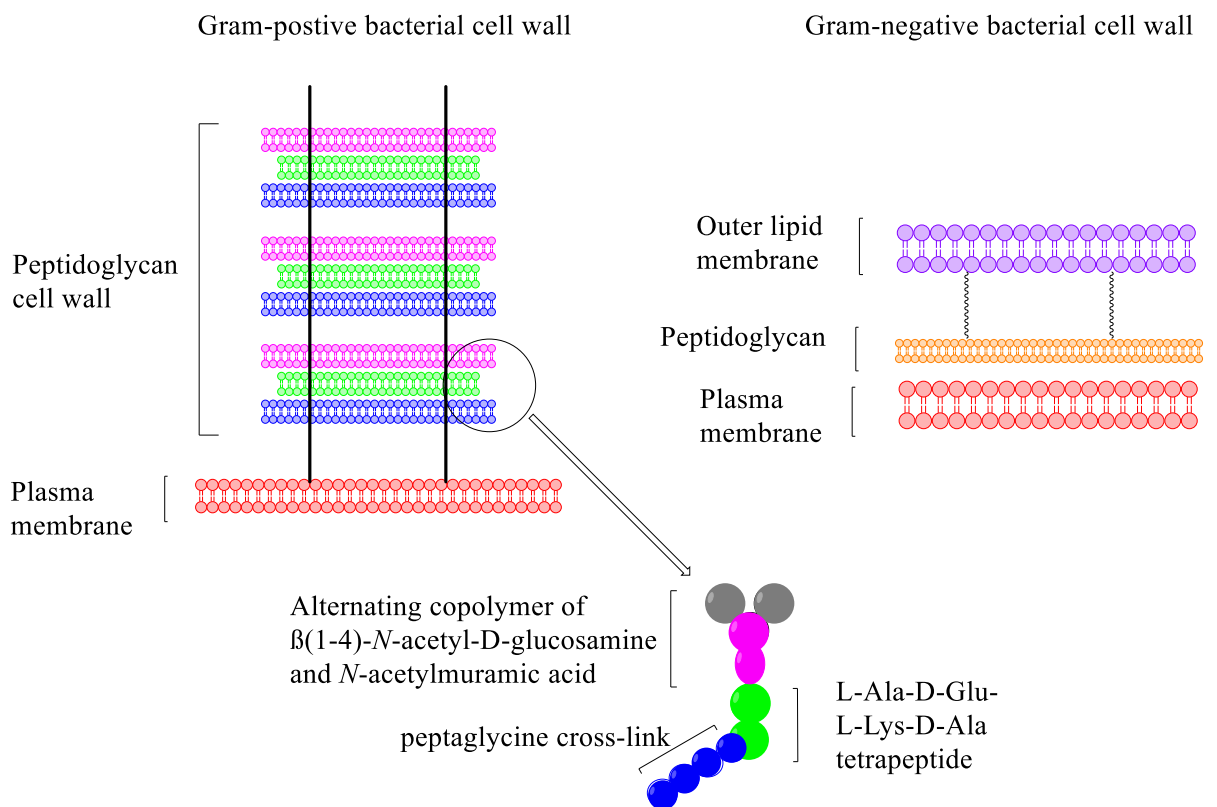


**Figure 2:** The structure of the cell walls for both gram-positive and gram-negative bacteria. Adapted from ref. 36.

and work by inhibiting the synthesis of the peptidoglycan layer in the cell wall. Facilitating the final step in the synthesis of peptidoglycan are penicillin-binding proteins (PBP). The 4-membered  $\beta$ -lactam ring is involved in binding to the enzyme DD-transpeptidase.<sup>40</sup> This therefore means that the enzymes cannot catalyse the formation of the cross-links, and an imbalance between cell wall production and degradation develops, causing the cell to rapidly die. The bacteria have, however, built resistance to this over time by synthesising an enzyme,

$\beta$ -lactamase, in gram-negative bacteria and penicillinases in gram-positive bacteria,<sup>41</sup> to attack the 4-membered ring before it binds to DD-transpeptidase. Minimum inhibitory concentration (MIC) data for penicillin in *Streptococcus pneumoniae* infection is  $\leq 0.06$   $\mu\text{g/mL}$  in susceptible strains and  $\geq 2$   $\mu\text{g/mL}$  in resistant strains (before 2008 for any syndrome).<sup>42</sup> Other examples of  $\beta$ -lactam antibiotics that work in a similar fashion are monobactams and cephalosporins. The second class of antibiotics, glycopeptides, also interfere with peptidoglycan synthesis; vancomycin and teicoplanin are examples of these types of antibiotics. They bind to the amino acids within the cell wall, preventing the addition of new units to the peptidoglycan. A specific configuration is needed to fit into a space left in the peptidoglycan wall. It is this specificity which allows glycoproteins to be selectively toxic to bacterial cell walls.<sup>21</sup>

### **1.1.3.2 Fatty acid synthesis**

The second most commonly exploited target for antibacterial agents is fatty acid biosynthesis. It is an attractive biosynthetic pathway for antibiotics to target as the fatty acid pathway in mammalian cells is different to that of bacterial cells, however, for the bacteria *Streptomyces* and *Actinomyces* it is not possible. This is because these bacteria are not able to produce fatty acid synthesis inhibitors due to the fatty acid synthetic pathway being so similar to polyketide biosynthesis. There are two molecular forms of fatty acid synthetic pathways: type I and type II. Type II refers to the enzymes used by bacteria, whereas type I refers to the enzymes used in mammalian cells.<sup>43</sup> This pathway can allow development of broad spectrum antibiotics to target the many enzymes.<sup>44</sup> There are three stages involved: initiation, elongation and termination.

The initiation step involves creating molecules that can be used in the elongation stage. The first reaction involved in this step is the transfer of an acetyl group to the pantothenate group of

the acyl carrier protein (ACP). The subsequent reaction is an additional transfer, from the pantothenate of the ACP to the cysteine sulfhydryl group on fatty acid synthase (FAS). This allows the pantothenate group to accept a malonyl group to permit the elongation to begin.

The elongation stage allows the fatty acid to grow in length and can be seen in Figure 3.<sup>45</sup> This cycle is started by the condensation of malonyl-ACP **2** with acyl-ACP **1** carried out by the enzyme  $\beta$ -ketoacyl-ACP synthase. A reduction is the next reaction to produce the aldol product **3**. A dehydration then occurs to create the alkene **4** and this is reduced to create an acyl-ACP two carbons longer than the original.

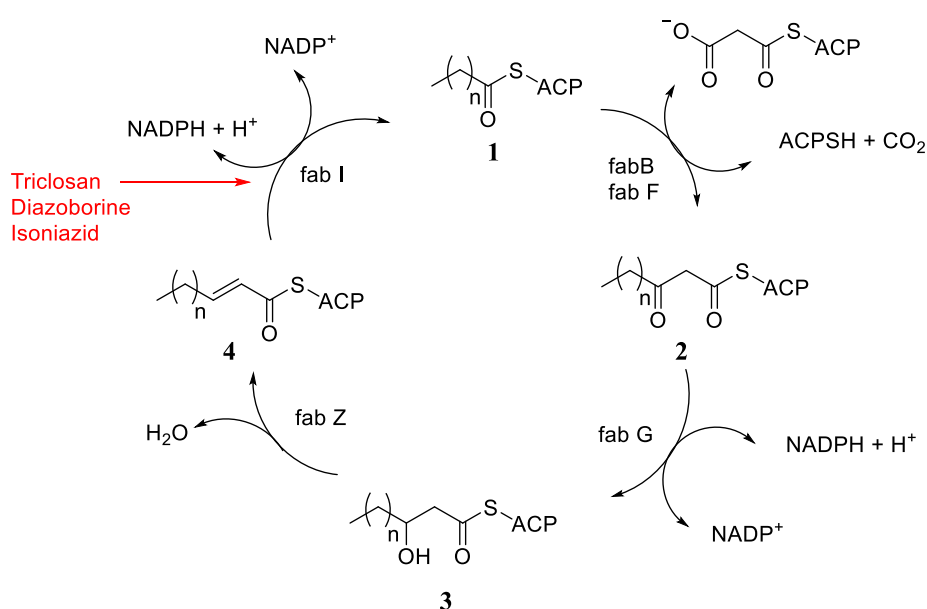


**Figure 3:** The elongation stage of fatty acid synthesis. The antibiotics are shown in red, displaying where they are effective. Modified from ref. 45.

Once the fatty acid has reached the correct length the termination sequence may begin. This stage terminates the signals to stop the growth of the fatty acid. *FabI/K* and enoyl ACP reductase are used to catalyse the end of the elongation.<sup>45</sup> There are many examples of drugs that target the fatty acid synthesis, these include triclosan and diazaborine. Triclosan targets the *FabI* step,

which involves enoyl-acyl carrier protein reductase. It forms a stable complex with nicotinamide adenine dinucleotide<sup>+</sup> (NAD<sup>+</sup>) and the protein, thus stopping the fatty acid synthesis pathway. Resistance to triclosan arises when the bacteria change the FabI gene through mutation of said gene.<sup>46</sup> Diazaoborine works in a similar fashion by targeting the enoyl-acyl carrier protein reductase.<sup>47</sup>

### 1.1.3.3 Protein/ RNA synthesis

Another mechanism used as a target for antibiotics is the exploitation of protein/ RNA synthetic pathways that occur at the ribosomes of bacteria. This synthetic target is split into four different stages: initiation, elongation, termination and recycling of the ribosome. Both bacterial and mammalian cells have ribosomes; however bacteria contain 30S, 50S and 70S ribosomes, whereas mammalian cells contain 80S ribosomes. This means that the ribosomes are of different molecular weights and shapes.

Aminoglycosides, tetracyclines, macrolides and streptogramins are all examples of protein synthesis inhibitors and are shown in Figure 4. The data shown below is the MIC values against *S. pneumoniae*.<sup>48,49</sup> Macrolides **9** and streptogramins **10** use the 50S ribosome to inhibit protein synthesis, whereas aminoglycosides and tetracyclines target 30S. The examples mentioned above that are 50S inhibitors work by stopping entry to the peptidyltransfer ribonucleic acid (tRNA)'s to the ribosome, which in turn blocks the elongation reaction by steric hindrance and eventually causes the dissociation of tRNA.<sup>50</sup> The mechanism of action of tetracycline **8** involves blocking the aminoacetyl tRNAs,<sup>51</sup> whereas aminoglycosides (such as streptomycin **7**) bind to the 16S RNA component of the ribosome.<sup>13</sup>

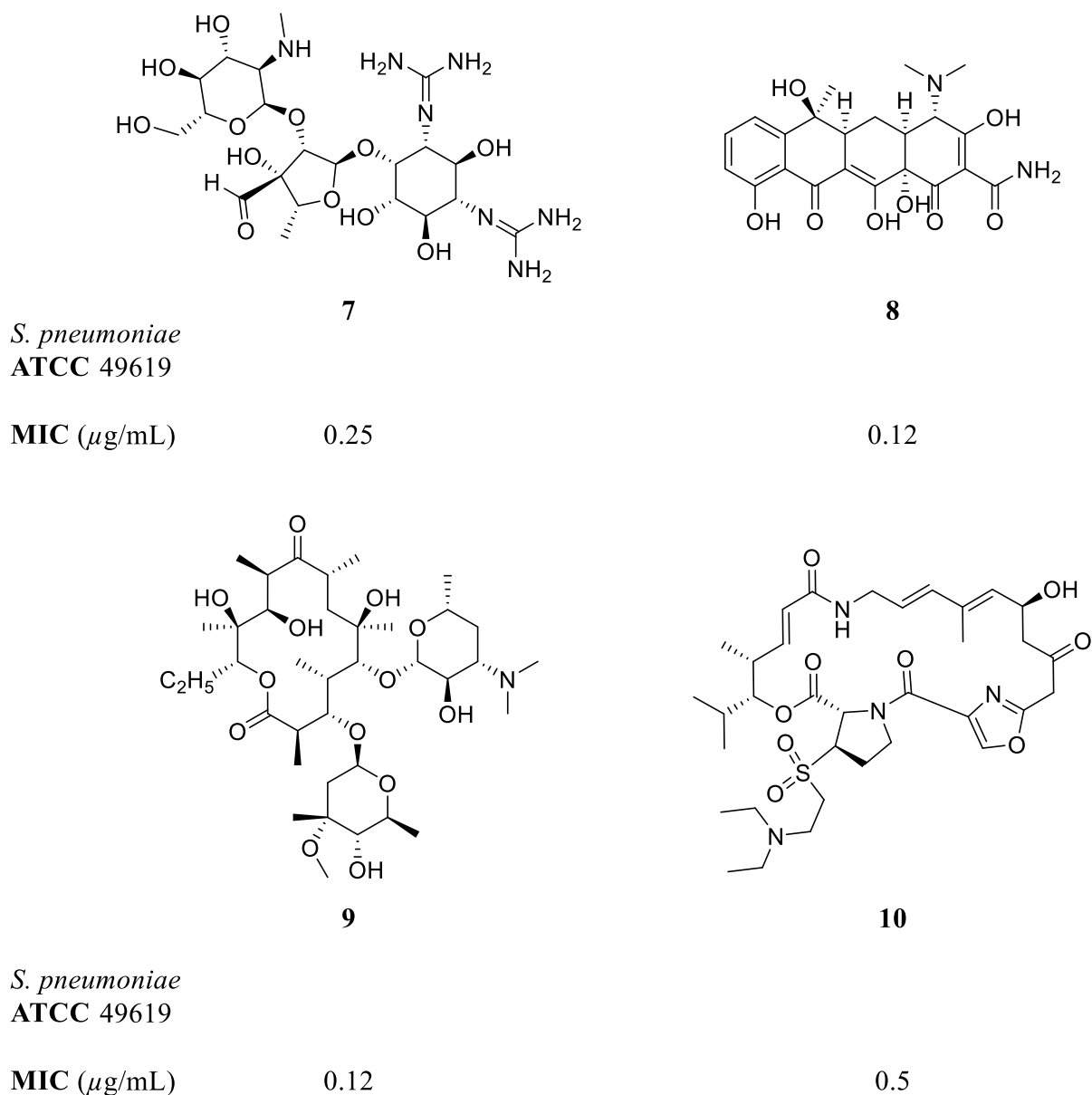


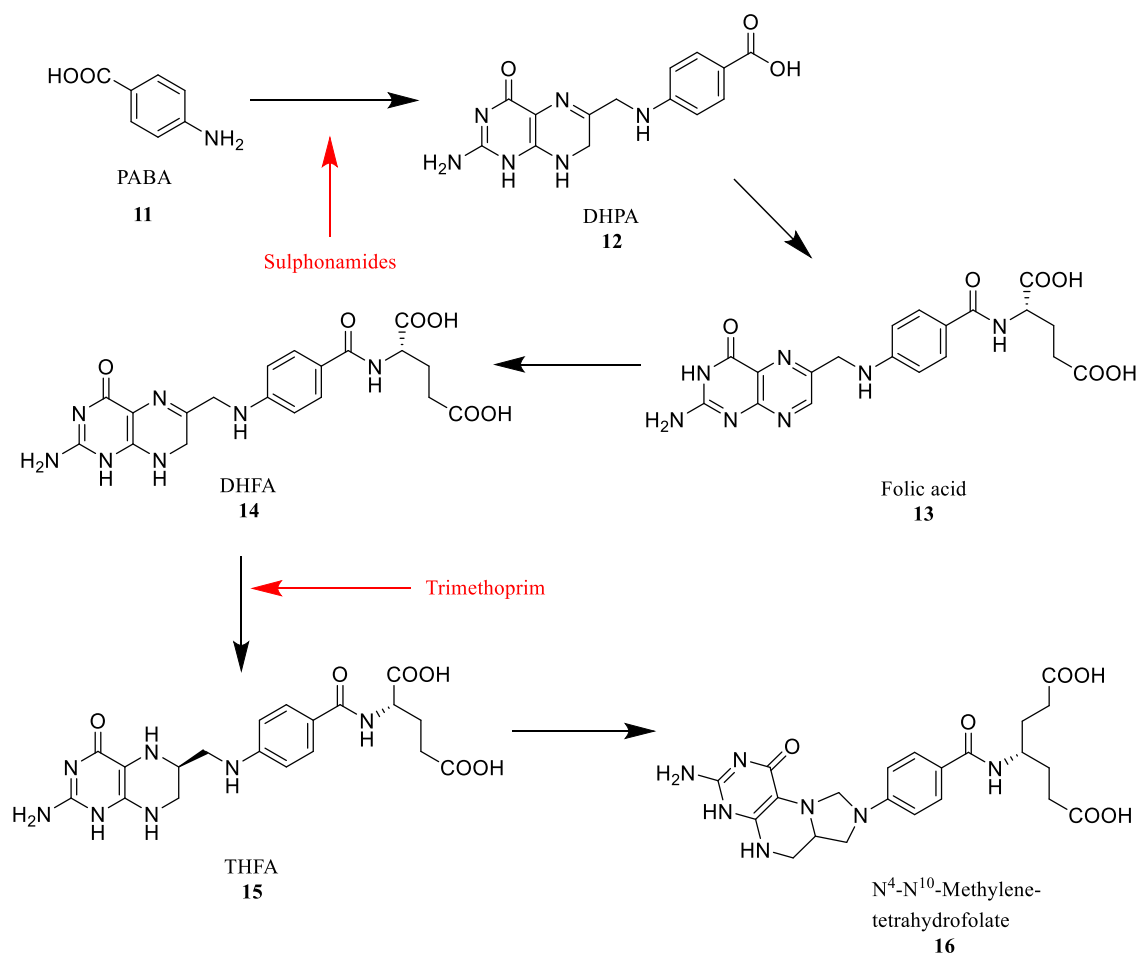
**Figure 4:** Examples of antimicrobials that affect the protein/ RNA synthesis. Streptomycin **7** is an example of an aminoglycoside. Tetracycline **8**<sup>48</sup>, erythromycin **9**<sup>48</sup> is a macrolide and dafopristin **10** is an example of a streptogramin<sup>49</sup>. The MIC data displayed shows their activities against *S. pneumoniae*.

#### 1.1.3.4 Folate metabolism

This is another pathway for antibiotics to target. This synthetic pathway is important since it allows DNA to be synthesised as it creates precursors for the base thymidine,

$N^4$ - $N^{10}$ -methylene-tetrahydrofolate **16** being the precursor. Bacteria can also be selectively eradicated by targeting their metabolic pathways. All cells require folic acid and it can diffuse easily into human cells. In bacteria, however, folic acid cannot enter, thus, the bacteria has to synthesise their own.

There are two examples of antibiotics that target folate synthesis: sulphonamides and trimethoprim. Where they stop the synthesis is shown below in Scheme 1.<sup>52</sup> Sulphonamides mimic the structure of *p*-amino benzoic acid (PABA) **11**.



**Scheme 1:** The pathway used for folate synthesis is displayed. Where the antibiotics are effective is summarised. Modified from ref. 52.

### **1.1.3.5 DNA synthesis**

There are four stages to DNA synthesis: initiation, elongation, termination and recycling. The initiation process is targeted by initiator proteins. The initiator proteins gather other proteins at the origin site and form a pre-replication complex, which unzips the double strand. Elongation starts at the replication fork using an enzyme called DNA polymerase. Nucleotides begin to align alongside the old strand, and are added together using DNA polymerase to start forming the new strand. To terminate the new DNA strand, a terminator protein interacts with the DNA to form a protein-DNA complex with the replication fork by antagonising the replicative helicase.<sup>53</sup>

Quinolones are a key group of antibacterials which target DNA synthesis in bacteria. Topoisomerase IV and gyrase are both enzymes which are used in the cleavage of DNA. Both of these are type II bacterial Topoisomerases, therefore both cut both strands of DNA helix simultaneously to manage DNA tangles and supercoils.<sup>54</sup> These are the two targets of quinolones. This class of antibiotics are also termed as topoisomerase poisons as they increase the concentrations of these enzymes. They non-covalently bind at the enzyme-DNA interface in the active site, intercalating into the DNA.<sup>23</sup>

### 1.1.4 Antibiotic resistance

There is a serious threat to the health of humans with the increase in drug-resistant bacteria. Antibiotic resistance occurs when the bacterium alters so that the drug is rendered ineffective in promoting apoptosis and inhibiting cell growth. Some restrictions on antibiotics have been put in place to try to control the rate of bacteria resistance. These restrictions have, however, caused a lack of interest to invest from pharmaceutical companies, thus slowing down the development of antibiotics.<sup>55</sup> There has been a steady decrease in the number of approved antibiotics, as seen in Figure 5, and since 1987 there has been no new class of antibiotics. In the graph, the data from 2008 shows that there is a resurgence in antibiotic research.<sup>56</sup> There have been several years (2002, 2003, 2006 and 2011) where no new antibiotic compounds were approved.<sup>57</sup> There was a dip in antibiotic research but with the recent pressures from governments there are new antibiotics coming through the system. Drug resistance is becoming a bigger problem as treatment options are becoming limited and resistant bacteria are problematic to treat. This leads to a rise in mortality rates for these diseases.<sup>58</sup>

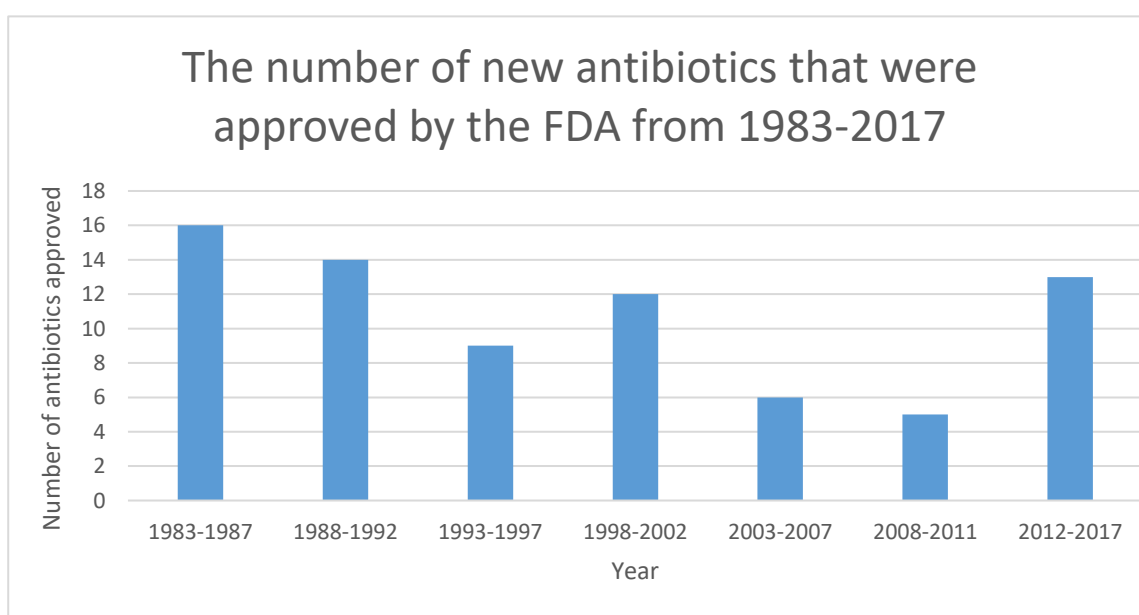


**Figure 5:** Systemic antibacterial new molecular entities approved by the US Food and Drug Administration from ref. 56.

There are certain organisms which have been looked into closely because resistance to these has proved particularly challenging. These include *Enterococcus faecium*, *Staphylococcus aureus*, *Klebsiella pneumoniae*, *Acinetobacter baumannii*, *Pseudomonas aeruginosa*, and *Enterobacter*, collectively known as ESKAPE organisms. The media in recent times has concentrated on the methicillin-resistant staphylococcus aureus (MRSA), which is also referred to as the superbug, and *Clostridium difficile*. Both have a high mortality rate once infection occurs, with the superbug being associated with hospitals. In 2016/2017, there was a study performed by Public Health England which stated that 97.2% cases of MRSA could be linked to mortality, this is 97.4% in *Clostridium difficile*.<sup>59</sup> Although associated with hospitals, MRSA can also be contracted in a community setting. In 2017, the world health organisation (WHO) published a list of bacteria that are in urgent need of new antimicrobials, they are shown in Table 2.<sup>60</sup> There are many reasons why resistance occurs but the main reason suggested is the incorrect use of antibiotics. Not finishing a course of antibiotics allows the bacteria that were not killed by the original antibiotics to mutate and change their genes to build a resistance to said antibiotics. This means that those bacteria would become harder to eradicate as the original antibiotics would not be able to kill the bacterial cells.

**Table 2:** A table showing the priority list provided by the WHO for which bacteria have become resistant and are in need of new antibiotics. Adapted from ref. <sup>60</sup>.

<b>The WHO list of bacteria who urgently need new antimicrobials</b>	
Priority 1: Critical	<i>Acinetobacter baumannii</i> , carbapenem-resistant
	<i>Pseudomonas aeruginosa</i> , carbapenem-resistant
	<i>Enterobacteriaceae</i> , carbapenem-resistant, ESBL-producing
Priority 2: High	<i>Enterococcus faecium</i> , vancomycin-resistant
	<i>Staphylococcus aureus</i> , methicillin-resistant, vancomycin-intermediate and resistant
	<i>Helicobacter pylori</i> , clarithromycin-resistant
	<i>Campylobacter</i> spp., fluoroquinolone-resistant
	<i>Salmonellae</i> , fluoroquinolone-resistant
	<i>Neisseria gonorrhoeae</i> , cephalosporin-resistant, fluoroquinolone-resistant
Priority 3: Medium	<i>Streptococcus pneumoniae</i> , penicillin-non-susceptible
	<i>Haemophilus influenzae</i> , ampicillin-resistant
	<i>Shigella</i> spp., fluoroquinolone-resistant

The rate at which antibiotic resistance occurs varies depending on the compound. The timeline in Figure 6 shows different drugs and when resistance started to develop.<sup>61</sup> An example of this is resistance to tetracycline when compared to vancomycin and Ceftaroline. Tetracycline is a protein inhibitor and it took nine years to notice resistance occurring. Vancomycin is a cell wall synthesis inhibitor and it took sixteen years for resistance to develop in *Enterococci* and a further twelve years for resistance to develop in *Staphylococci*. Ceftaroline took less than a year to acquire resistance.

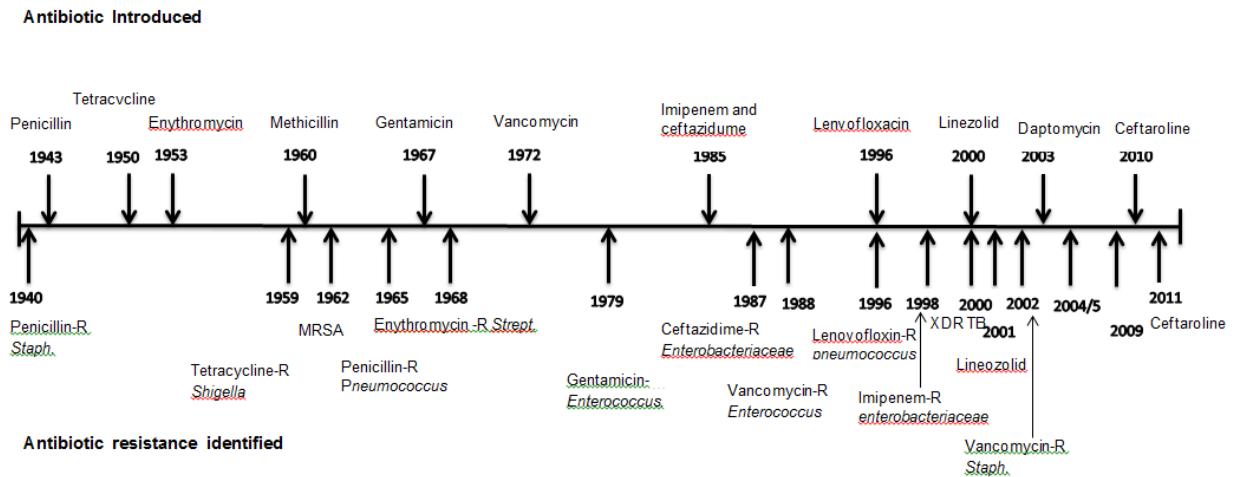


**Figure 6:** A timeline of when antibiotics were introduced and when resistance was identified. Adapted from ref. 61.

### 1.1.4.1 Mechanism of resistance

There are many mechanisms by which resistance can occur. The three fundamental mechanisms by which bacteria become resistant to antibiotics are enzymatic degradation of the drugs, alteration of bacterial proteins that are the targets for the antimicrobial agents, and changes in membrane permeability to antibiotics. Resistance to penicillin is one example of how enzymes are used to alter the drug to render it ineffective. Between the years of 1946-69 resistance to benzylpenicillin had risen from 14% to 80%.<sup>62</sup> The enzyme  $\beta$ -lactamase is produced in resistant bacteria; this enzyme opens the  $\beta$ -lactam ring. This, thus, does not allow the drug to bind to the PBP and, therefore, it cannot interfere with cell wall synthesis. Rifampin is another antibiotic used in the treatment of tuberculosis (TB). It is produced by a gram-positive bacteria *Amycolatopsis rifamycinica*. Its mechanism of action is to target RNA polymerase; however, bacteria have started to mutate the *rpoB* gene, encoding the beta subunit of RNA polymerase. This causes a decreased affinity for rifampin and, hence, resistance. This is a key example of how bacteria can alter their structural proteins to overcome the drug. There are more examples of how bacteria have started to build resistance to certain antibiotic families in Table 3.

**Table 3:**Relating antibiotic class to its target and mechanism of action.<sup>63</sup>

<b>Antibiotic class</b>	<b>Examples</b>	<b>Target</b>	<b>Mode(s) of resistance</b>
$\beta$ -Lactam	Penicillins, cephalosporins, penems, monobactams	Peptidoglycan biosynthesis	Hydrolysis, efflux, altered target
Aminoglycosides	Gentamicin, streptomycin, spectinomycin	Translation	Phosphorylation, acetylation, nucleotidylation, efflux, altered target
Glycopeptides	Vancomycin, teicoplanin	Peptidoglycan biosynthesis	Reprogramming Peptidoglycan biosynthesis
Tetracyclines	Minocycline, tigecycline	Translation	Monooxygenation, efflux, altered target
Macrolides	Erythromycin, azithromycin	Translation	Hydrolysis, glycosylation, phosphorylation, efflux, altered target
Lincosamides	Clindamycin	Translation	Nucleotidylation, efflux, altered target
Streptogramins	Synercid	Translation	C-O lyase ( type B Streptogramins), acetylation ( type A streptogramins), efflux, altered target
Oxazolidinones	Linezolid	Translation	Efflux, altered target
Phenicol	Chloroamphenicol	Translation	Acetylation, efflux, altered target
Quinolones	Ciprofloxacin	DNA replication	Acetylation, efflux, altered target
Pyrimidines	Trimethoprim	C <sub>1</sub> metabolism	Efflux, altered target
Sulfonamides	Sulfamethoxazole	C <sub>1</sub> metabolism	Efflux, altered target
Rifamycins	Rifampin	Transcription	ADP-ribosylation, efflux, altered target
Lipopeptides	Daptomycin	Cell membrane	Altered target
Cationic peptides	Colistin	Cell membrane	Efflux, altered target

### **1.1.5 Uses of antibiotics**

As previously mentioned, antibiotics have been utilised for many years, through different methods such as injections (intravenous) and tablets. Many of these methods are discussed in the following section. These groups of compounds can be used clinically, aiding human and animal health through use of antibiotics. They can also be used to reduce the harmful bacteria outside of the body; biocides render harmful organisms as inoffensive. Antimicrobials can also be used to create a selective media. This could produce a media that selectively inhibits certain bacteria growth or encourage the growth another certain species of bacteria. This could allow doctors to ascertain which bacterial infection is harming a person's health and prescribe clinical antibiotics as required.

#### **1.1.5.1 Clinical use**

Antibiotics have many uses; the most common is for clinical use. As previously described, antibiotics are compounds that have *'the ability to form a complex with a molecule essential for the growth of a bacterial cell, thus inhibiting its function'*.<sup>1</sup> They fit into several classifications, depending on how the antibiotics work. They can be considered broad or narrow spectrum. Broad spectrum refers to a compound that can kill a variety of bacteria, for example penicillins which have a broad spectrum range as they can be used to kill both gram-positive and gram-negative bacteria. Narrow spectrum refers to compounds which kill a specific bacteria or strain. Broad spectrum antibiotics are used when a) the infection cannot be treated by a certain drug or b) when they are unsure of what the infection is. The problem with these antibiotics, however, is that they give rise to antibiotic resistance, so physicians are trying to use alternatives.<sup>64</sup>

### **1.1.5.2 Biocides in clinical practice**

A biocide is defined as a chemical that is intended to destroy or render harmless any harmful organisms by chemical or biological means, similar to an antibiotic. These compounds are often found described as disinfectants, antiseptics or preservatives. Unlike antibiotics, biocides are not selective as to which bacteria they target. This creates a toxicity problem as they can be harmful to humans, dependant on which concentration is used.

There are many key stages by which a biocide interacts with the bacteria. Firstly, the biocide is taken up by the cell from a solution. This is followed by accumulation of a certain biocide. This then, eventually, leads to interaction with the target.<sup>65</sup>

**Table 4:** A table showing examples of biocides, their targets and mechanism of action. Adapted from tables from ref. 66,67.

<b>Biocide</b>	<b>Target region</b>	<b>Mechanism of interaction</b>	<b>Introduction/first used</b>
Aliphatic alcohols	Membrane integrity	Solvation of phospholipids	Early AD
Sodium hypochlorite	Amino groups in proteins	Halogenation	1827
Phenols (including triclosan, bisphenols and cresol)	Membrane integrity / cytoplasmic membrane	Penetration /partition into phospholipid bilayer/ displacement of phospholipid molecules	1867-1970's
Formaldehyde	Biomolecules	General alkylation reactions	1894
QAC's (quaternary ammonium chloride's)	Cytoplasmic membrane/ membrane-bound enzyme environment and function	Electrostatic interaction with phospholipids	1933
Chlorine dioxide	Thiol-containing cytoplasmic and membrane-bound enzymes	Oxidation of thiol groups	1946
Glutaraldehyde	Biomolecules	General alkylation reactions	1960's

#### **1.1.5.2 The use of antimicrobials in the detection of microorganisms in media growth**

Growth medium is used in microbiology to support the growth of microorganisms. These semi-solid, solid, or liquid scaffolds are full of nutrients in which allow microorganisms to grow. Different media are used depending on many factors, including which bacterial strain is growing. There are two groups of media: complex (or undefined) and defined. Complex medium contain plenty of nutrients, including water soluble extracts from plants or animal tissue and a sugar to serve as a main energy store and carbon source. The exact composition is

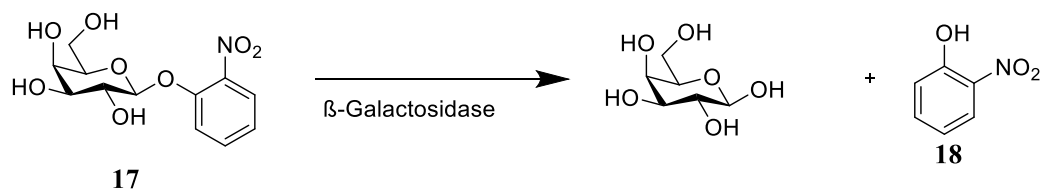
unknown; hence the media being described as undefined. Tryptic soy broth is an example of this media with composition casein peptone (pancreatic), dipotassium hydrogen phosphate, glucose, sodium chloride and soya peptone.<sup>68</sup> The casein peptone and soya peptone are the water soluble extracts and the glucose is the sugar source. Defined media are carefully composed with exact ingredients so the exact composition is known, hence its name. There are also sub-divisions within these two categories. Media can also be described as either selective or differential. Table 5 shows the difference between these four categories.

**Table 5:** A table showing the four different categories of culture media. Adapted from ref. 69.

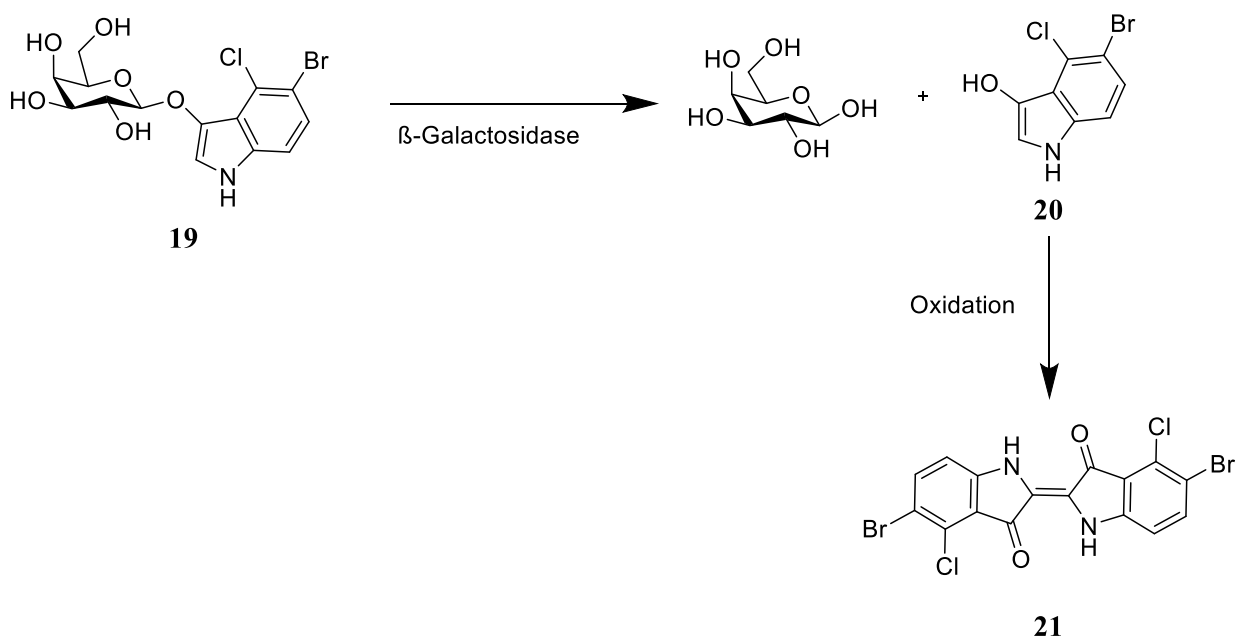
<b>Media</b>	<b>Purpose</b>
Complex/ undefined	Grow most heterotrophic organisms
Defined	Grow more specific heterotrophic organisms
Selective	Suppress unwanted microbes, or encourage desired microbes
Differential	Distinguished colonies of specific microbes from others

Chromogenic media are described as a differential media. The addition of a chromogenic substrate to the media can be used to distinguish different bacteria, and thus their identification. Chromogenic compounds contain substrates that can be cleaved by various biological pathways, usually via enzyme pathways, to release a substrate that produces a colour. An example of this is *ortho*-nitrophenyl- $\beta$ -galactoside (ONPG) **17**.  $\beta$ -Galactosidase cleaves this compound and releases galactose and *ortho*-nitrophenol **18**, as shown in Scheme 2. The latter compound is yellow in colour. It is used for the detection of the *Enterbacteriae* family.<sup>70</sup> This compound, however, has an affinity to diffuse in agar. To overcome this problem, 5-bromo-4-chloro-3-indolyl- $\beta$ -D-galactopyranoside (X-GAL) **19** can be used. In the presence of  $\beta$ -galactosidase, X-GAL **19** produces 4-Chloro-3-Bromo-indol-3-ol **20**. This then dimerises

in the presence of oxygen to form 4-Chloro-3-Bromo-indigo **21**, which is an insoluble blue precipitate. This reaction is shown in Scheme 3.



**Scheme 2:** The cleavage of the glycosidic bond, by  $\beta$ -galactosidase, to produce *ortho*-nitrophenol **18** and galactose.



**Scheme 3:** The cleavage of the glycosidic bond in X-GAL **19** to produce 4-chloro-3-bromoindol-3-ol **20**. This compound then dimerises to produce the insoluble indigo **21**.

Different bacteria contain varied glycoside profiles. As seen previously, **17** works due to cleavage to produce **18**. However, not all bacteria contain the enzyme glucosidase, which allows for the specific detection of certain bacteria. In Table 6, three different bacteria are shown to have different glycosidase profiles.<sup>71</sup>

**Table 6:** The different glycosidase profiles for three different bacteria: *Es. coli*, *B. cereus* and *P. aeruginosa*. Adapted from ref. 70. Key: glu=glucose, gal = galactose, man = mannose, Xyl = xylose, L-Fuc = L-fructose.

$\beta$ -substrate	Glu	Gal	Man	Xyl	L-Fuc	GluA	GluNAc	GalNAc	ManNAc
<i>Es. coli</i>									
ESI	+	+	-	-	-	-	+	-	+
UV	+	+	-	-	-	N/A	+	-	N/A
<i>B. cereus</i>									
ESI	+	+	+	-	-	+	+	-	+
UV	+	+	-	-	-	N/A	+	-	N/A
<i>P. aeruginosa</i>									
ESI	-	-	-	-	-	-	-	-	-
UV	-	-	-	-	-	N/A	-	-	N/A

#### 1.1.5.4 Selective recovery of bacteria from media

As previously mentioned, selective media can be used to selectively grow certain bacteria, while suppressing others. This is very useful when identifying a certain bacteria for diagnostic reasons and for selective recovery. When growing bacteria on culture plates, using an undefined media, the growth of certain bacteria could be hindered by the other microorganisms present. These competitive flora could mask the bacteria that needs to be observed.<sup>72</sup> The addition of selectivity to the media allows the desired bacteria to grow without the competition. There are

many examples of when a selective media has been used to selectively recover bacteria. These are shown in Table 7.

**Table 7:** A table showing examples of why selective media is used for certain bacteria

<b>Desired bacteria</b>	<b>Reason for selective media</b>	<b>Ref.</b>
<i>Pseudomonas aeruginosa</i>	<ul style="list-style-type: none"> <li>• Lung infection in cystic fibrous patients</li> </ul>	73, 74, 75
<i>Listeria monocytogene</i>	<ul style="list-style-type: none"> <li>• Detection in smoked fish for prevention of listeriosis.</li> </ul>	76, 77
<i>Staphylococcus aureus</i>	<ul style="list-style-type: none"> <li>• Detection in cystic fibrous patients</li> <li>• Food safety</li> </ul>	74, 78, 79
<i>Streptococcus anginosus</i>	<ul style="list-style-type: none"> <li>• Detection in cystic fibrous patients</li> </ul>	74, 80
<i>Achromobacter xylosoxidans,</i>	<ul style="list-style-type: none"> <li>• Detection in cystic fibrous patients</li> <li>• Detection in human ear discharge</li> </ul>	74, 81, 82
<i>Rothia mucilaginosa</i>	<ul style="list-style-type: none"> <li>• Detection in cystic fibrous patients</li> <li>• Oral health</li> </ul>	74, 83
<i>Gemella haemolysans.</i>	<ul style="list-style-type: none"> <li>• Detection in cystic fibrous patients</li> </ul>	74

From the list above, there are bacteria that are on the WHO watch list, Table 2, and these are likely to develop resistance.

To help provide this selectivity, antibiotics can be added to the media. The antibiotic can inhibit the growth of competition flora. An example of this is the FOXCA broth which was designed for the detection of MRSA. Several antibiotics were added, including cefoxitin, aztreonam and colistin. The cefoxitin was used to inhibit the growth of methicillin-susceptible *Staphylococcus aureus* (MSSA) due to the compound being able to induce methicillin resistances. Colistin is

active against *Pseudomonas* species, and aztreonam inhibits the growth of *Enterobacteraceae* species.<sup>84</sup> Other examples are shown in Table 8.

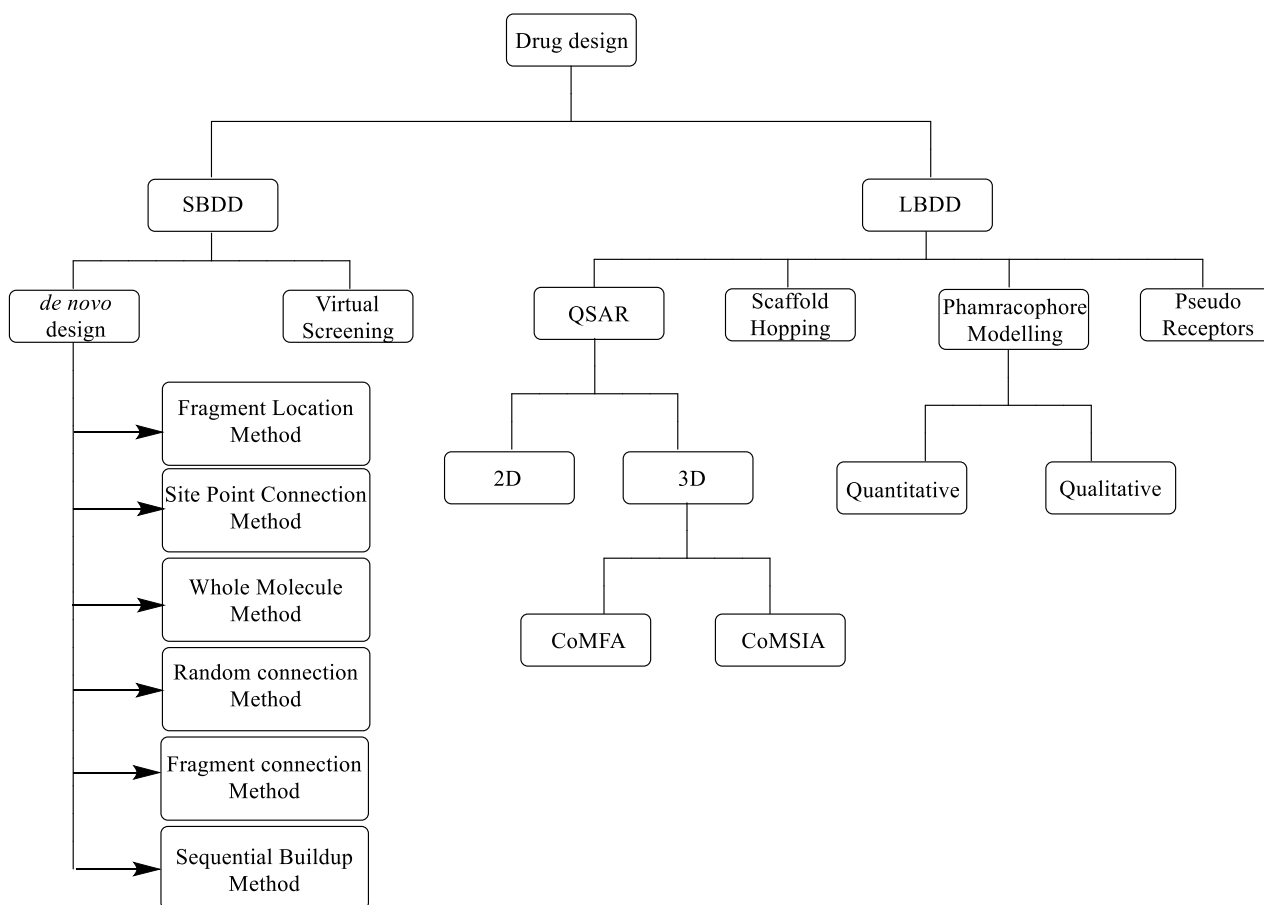
**Table 8:** A table showing examples of media used to selectively recover or grow certain bacteria. The names in red denote an antibiotic. \* Not technically an antibiotic but was added to provide selectivity.

Media used	Targeted bacteria	Ref.
VCAT (10% cooked horse blood, polyvitaminic supplement, <b>colistin</b> , <b>trimethoprim</b> , <b>vancomycin</b> and <b>amphotericin B</b> )	<i>Capnocytophaga</i> species	85
HPSPA formulation ( <b>vancomycin</b> , <b>amphotericin B</b> , <b>cefsulodin</b> , <b>polymyxin B</b> , <b>trimethoprim</b> , and <b>sulfamethoxazole</b> )	<i>Helicobacter pylori</i>	86
10% tryptic soy agar (TSA), sucrose, glycerol, Casamino Acids , NaHCO <sub>3</sub> , MgSO <sub>4</sub> -7H <sub>2</sub> O, K <sub>2</sub> HPO <sub>4</sub> , sodium lauroyl sarcosine (SLS), <b>trimethoprim</b> . For gram-negative crystal violet to eliminate gram-positive bacteria	<i>Pseudomonads</i> (fluorescent)	87
Humic Acid-Vitamin(HV) agar supplemented with <b>cycloheximide</b> *	<i>Actinomycetes</i>	88
FOXCA broth (Iso-Sensitest broth, NaCl, <b>cefoxitin</b> , <b>colistin</b> , and <b>aztreonam</b> )	MRSA	84
MS-SOB medium (Mitis Salivarius agar, <b>aztreonam</b> , <b>fosfomycin</b> , <b>bacitracin</b> and NaCl)	<i>Streptococcus sobrinus</i>	89

## 1.2 Methods for drug design

There are many routes by which a drug can be rationally designed. Two popular approaches that are explored when designing a drug are: Ligand-based drug design (LBDD) and structure-based drug design (SBDD). The different methods are shown in Scheme 4.<sup>90</sup>

**Scheme 4:** The different methods for drug design.



Structure based drug designs use the knowledge of the 3D structure of the biological target. This 3D information can be obtained through various analytical methods, including X-ray crystallography. If the structure is not available then computational methods can be employed to predict the intended target for the compound. Using this information, a prediction can be made as to whether a candidate drug will have a high affinity to the target.<sup>90</sup> SBDD is further

split into two separate groups: *de novo* design and virtual screening. Virtual screening refers to a computational technique that searches libraries of small molecules. The likelihood of a drug to bind to the target site comes from these libraries.<sup>91</sup> *De novo* design involves ligand molecules and building up compounds with the constraints of the binding pocket. This stepwise manner has an advantage of creating novel compounds not contained in any database.<sup>92</sup>

LBDD differs from SBDD as it uses the knowledge of other molecules that bind to the target. From these compounds a pharmacophore model may be derived. This model can outline the minimum structural requirements for the compound to bind to the target. This method can be further split into four categories: quantitative structure-activity relationship (QSAR), Scaffold hopping, Pharmacophore modelling and Pseudo receptors.

### 1.2.1 Prodrugs

Prodrugs have been described as '*a pharmacologically inactive compound that is converted to an active drug by metabolic biotransformation*'. The term was first coined by Adrien Albert in 1958. Ideally, prodrugs are converted to an active form of the drug once at the desired site, avoiding conversion too early or too late and it would be excreted before being converted to the target compound. This strategy has been used to increase the selectivity of the drug to the required site. The first prodrug to be used was methenamine, also known as hexamine, created by Schering in 1899. This compound decomposes at high acidity into formaldehyde and ammonia. It was used against urinary tract infections with the formaldehyde being bactericidal. Prodrugs are very useful to consider when designing a drug as they have many desirable properties, such as better lipophilicity or better solubility. An active drug can be converted to a prodrug by adding different functional groups to adapt its characteristics. There are many advantages to using this approach: drugs that were previously too toxic to administer can be

adapted so the prodrug is less toxic and once converted to the drug it will again be toxic or 'active'. If solubility is an issue, adding water soluble functionalities can improve the solubility and these groups can be metabolically cleaved after drug administration. Adding lipid soluble groups can improve absorption into certain cells depending where the active site is. How a prodrug works is shown in Figure 7.<sup>93</sup>

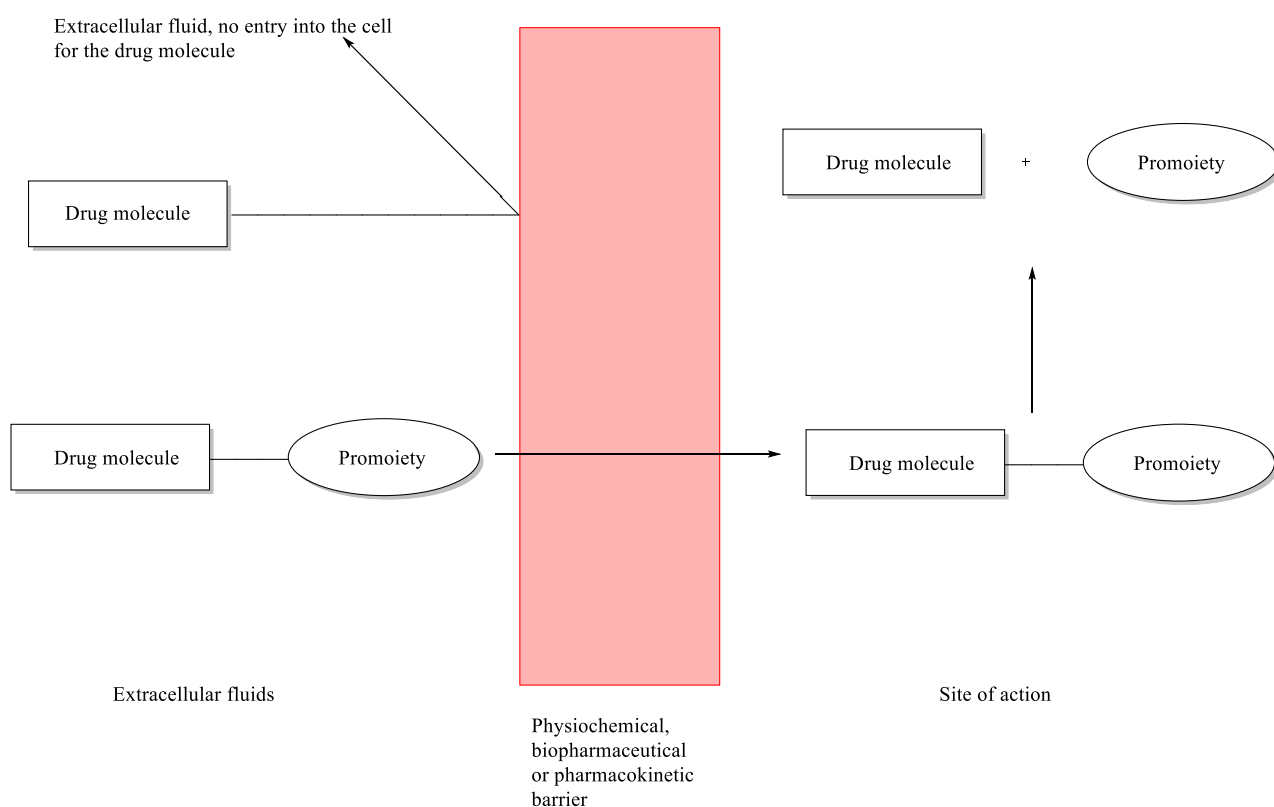


**Figure 7:** A simplified diagram of the prodrug concept. Modified from ref. <sup>93</sup>.

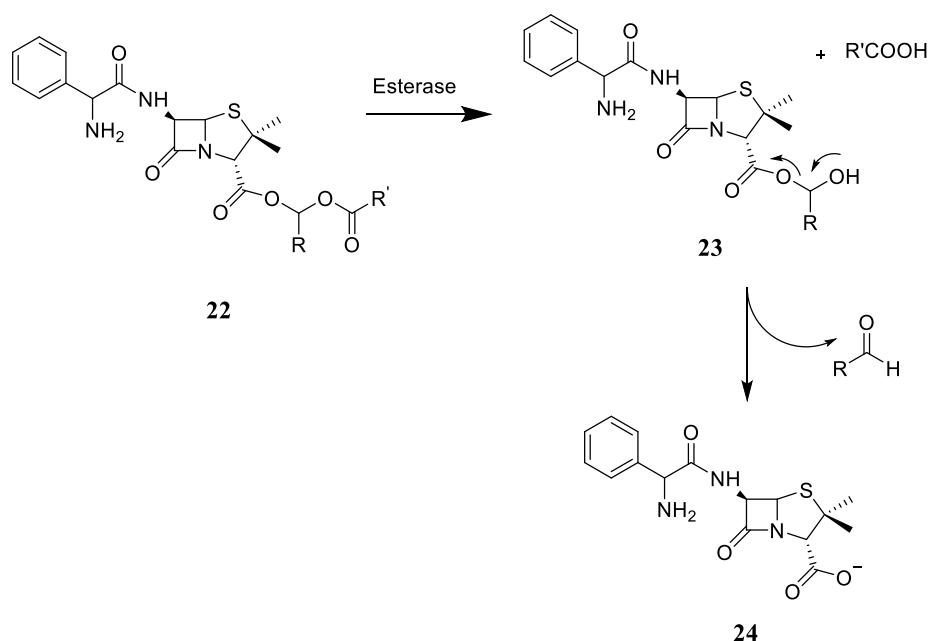
The intended target site for the drug will influence which prodrug is used. There are two different categories: carrier and bioprecursor. The carrier-prodrug principle consists of the active drug being attached to the carrier group which will thus change its physiochemical properties.<sup>93</sup> Bioprecursors are a result of a molecular modification of the active drug itself. This modification to a compound can enable the resulting compound to become the active principle, the ability to be transformed metabolically or chemically. There are several reaction mechanisms used on these drugs depending on which functional group is present. Oxidative

and reductive reactions are generally used *in vivo* but there are some functional groups which use reactions that do not alter their oxidative state.<sup>94,95</sup> A well-thought-out prodrug satisfies the following criteria:

1. The linkage between the drug substance and the transport moiety is usually a covalent bond
2. It is inactive or less active than the active compound in its natural form.
3. The linkage that connects the active drug and the carrier must be broken *in vivo*.
4. The carrier once it has been released must be nontoxic *in vivo*.
5. The generation of the active formula must take place with rapid kinetics to ensure effective drug levels at the target site and to minimise either direct prodrug metabolism or gradual drug inactivation.<sup>93</sup>

Carrier-linked prodrugs are further broken down into three categories: bipartite, tripartite and mutual. Bipartate prodrugs consist of one carrier attached to the active drug. Tripartate prodrugs are different from the bipartate drugs as they contain a linker connecting the drug and transport molecule. Ampicillin **24** belongs to the penicillin family, and is able to penetrate both gram-negative and gram-positive bacteria. It acts as an irreversible inhibitor of transpeptidase, so is an inhibitor of cell wall synthesis. Once administered, esterase attacks the prodrug **22** to create an intermediate **23** and a carboxylic acid. This then breaks down further to produce the active drug as exemplified in Scheme 5. Mutual prodrugs are two, usually synergistic, drugs attached

to each other. An example of this is pivampicillin which is used to treat  $\beta$ -lactamase producing bacteria.



**Scheme 5:** An example of a tripartite prodrug.

### 1.3 Carbohydrates in drug design

#### 1.3.1 Natural Carbohydrates and their presence in drugs

Carbohydrates, also known as saccharides or sugars, are the most abundant biomolecule and come in many forms including monosaccharides, polysaccharides and oligosaccharides. They are involved with many processes in nature, with inflammation, cell growth and development, cell surface recognition, and bacterial infections as a few examples. There are many diseases and disorders that can occur when there is a problem with the metabolism of certain sugars. An example of this is galactosemia. This term refers to all disorders involving galactose metabolism. Some of the problems arising from these disorders include: hepatocellular damage,

*Es. coli* sepsis and liver failure.<sup>96</sup> It has also been reported that glycosylations, particularly *N*-linked glycosylation, on a surface of the immunodeficiency virus limits the neutralising of the antibody response to simian immunodeficiency virus. This occurs due to sugar shielding the virus from immune recognition.<sup>97</sup>

Carbohydrates have been used for medicinal purposes for many conditions such as honey for antibacterial properties.<sup>98</sup> They are essential in glycoconjugates; these different drugs produce varying biological activities. They are found in many forms as drug conjugates. Figure 8 shows the most commonly used form of the sugar when attaching it to a drug. The data was compiled from the United States Pharmacopoeia/the National Formulary, European Pharmacopoeia, Japanese Pharmacopoeia sixth edition, and Chinese Pharmacopoeia 2010 (data was correct as of 2015).<sup>99</sup> The most common forms are polysaccharides and their derivatives which includes compounds containing cellulose and amylose.

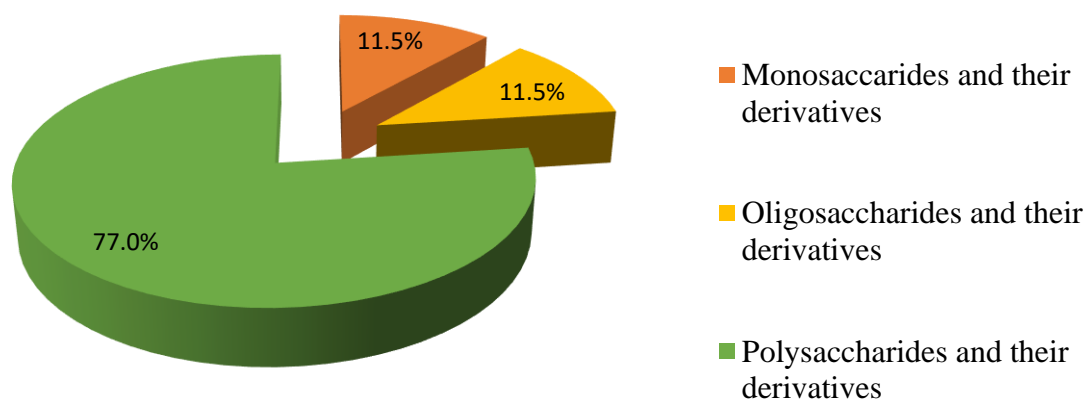
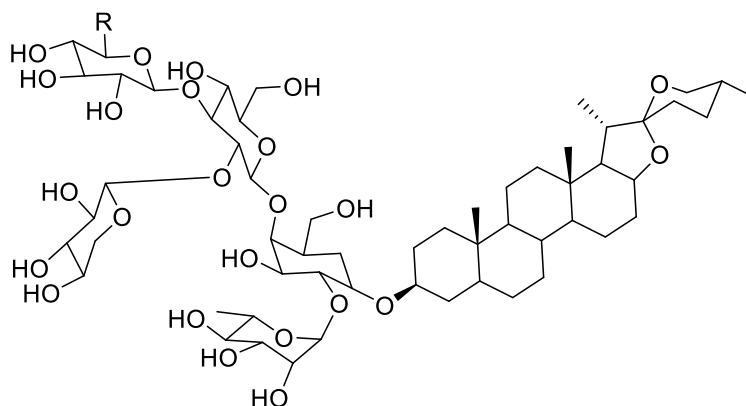


**Figure 8:** Data analysis of the composition of carbohydrate drugs records from the aforementioned pharmacopoeias. Adapted from ref. <sup>99</sup>.

A class of glycoconjugates are saponins. These are secondary metabolites which are found naturally in some plants and marine life. They are steroidal glycosides and can be used for a wide range of sicknesses. Some of these possess antimicrobial properties. Tigogenin 3-*O*- $\beta$ -D-xylopyranosyl- (1 $\rightarrow$ 2)-[ $\beta$ -D-xylopyranosyl (1 $\rightarrow$ 3)]- $\beta$ -D-glucopyranosyl-(1 $\rightarrow$ 4)-[ $\alpha$ -L-rhamnopyranosyl-(1 $\rightarrow$ 2)]- $\beta$ -D-galactopyranoside (TTS-12) **25** and tigogenin 3-*O*- $\beta$ -D-glucopyranosyl-(1 $\rightarrow$ 2)-[ $\beta$ -D-xylopyranosyl- (1 $\rightarrow$ 3)]- $\beta$ -D-glucopyranosyl-(1 $\rightarrow$ 4)- $\beta$ -D-galactopyranoside (TTS-15) **26** both have excellent activities against *Candida albicans* with MIC<sub>80</sub> 10 and 2.3 mg mL<sup>-1</sup>, respectively, and *Cryptococcus neoformans* with MIC<sub>80</sub> 1.7 and 6.7 mg mL<sup>-1</sup>, respectively.<sup>100</sup>



**25 R= H**

**26 R= CH<sub>2</sub>OH**

**Figure 9:** The structures of TTS-12 (**25**) and TTS-15 (**26**).

### 1.3.2 Glycosylations in chemistry

Glycosylations involve the reaction between a glycosyl donor, usually protected, and a glycosyl acceptor. The donor usually has a leaving group at the anomeric centre which allows the acceptor to attack the C-1 position.<sup>101</sup> The bond formed is called a glycosidic bond, there are many forms of this bond, with the most common being *O*-glycosidic bonds. This type of

glycosidic bond references the oxygen used to link the glycoside to the aglycone. This is the most common glycosidic bond as the most abundant disaccharides, sucrose, lactose and maltose, all contain this bond.<sup>102</sup> There are also *N*- (common in *N*-glycans)<sup>103</sup>, *S*- and *C*-glycosidic bonds.

Glycosylations are common reactions in nature; they result in glycosides, polysaccharides or glycoconjugates. There are, however, still difficulties when trying to perform these in a laboratory environment. They tend to be sensitive to water, especially if a halogenated leaving group is used; hydrolysis of the sugar tends to happen rather than the desired glycosylation. In nature, there are many pathways by which glycosylations occur; all involve the use of one or more enzymes to produce the desired product. There are five main groups of enzymes that are used during glycosylations in nature, examples of these are shown in Figure 10; glycosyltransferase (A), reverse glycosidase (B), glycan donor transferase (C) transglycosylation (D), and lipid-linked donor transferase.<sup>104</sup> Both examples of donor and acceptor pathways are shown.

These types of reactions are important in biological systems. Glycans themselves function as an energy source, structural components, and recognition compounds for carbohydrate binding proteins.<sup>105,106</sup> Defects in glycosylations can lead to problems with gene expressions and protein interactions.<sup>104</sup>

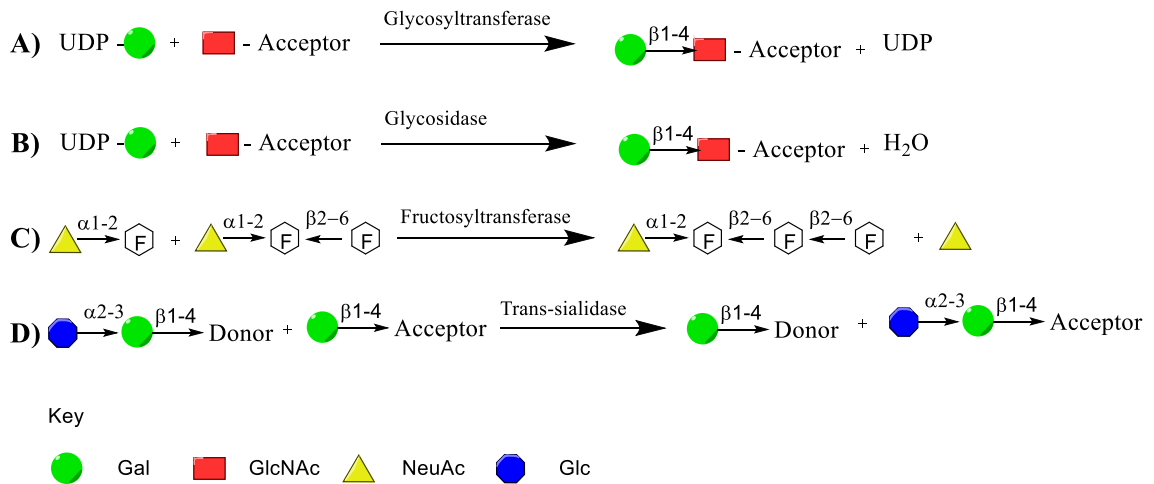
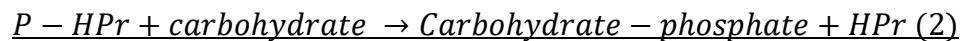
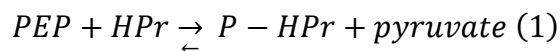


**Figure 10:** Four of the key enzymatic glycosylations in nature. Glycosyltransferase (A), reverse glycosidase (B), glycan donor transferase (C) transglycosylation (D).

Adapted from 104.

### 1.3.3 Carbohydrate uptake system

The PEP: phosphotransferase system (PTS) is the overall process utilised by bacterial cells to uptake carbohydrates. It was first discovered in *Es. coli* by Kundig *et al.* in 1964.<sup>107</sup> Equation 1 shows the general process used<sup>107,108</sup>:



**Equation 1:** The general process used in PTS.

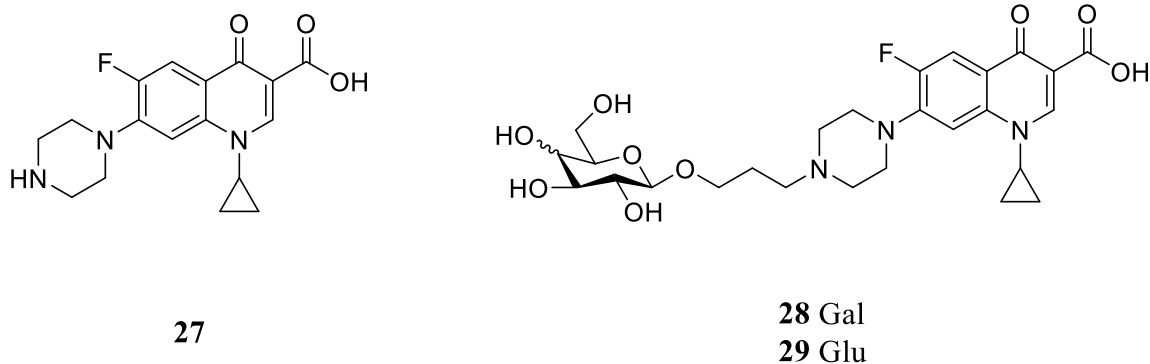
The system consists of two enzymes (EI and EII), Phospho-histidine-protein (P-HPr) and PEP. The PEP is used as an energy source as well as a donor for the phosphoryl group for the carbohydrates phosphorylation. There are several steps involved in the system, beginning with enzyme I (EI). This autophosphorylates the histidine-protein (HPr) to create P-HPr. The

phosphoryl group (P) is provided by PEP. The P group is then transferred onto the carbohydrate using enzyme II (EII). Unlike EI, EII are specific for one type of carbohydrate.<sup>109</sup> There are three domains which are found in this enzyme: IIA, IIB and IIC. IIA first becomes phosphorylated and passes on the phosphate to IIB. The IIC domains allow the intracellular carbohydrate phosphorylation.<sup>110,111</sup>

The phosphorylated carbohydrate is then used in glycolysis, via the Embden-Meyerhof-Parnas pathway, which occurs in the cell.<sup>112</sup> The glycolysis pathway allows for the release of energy from the carbohydrates. This is not the only metabolic pathway used, although it is the most common. Entner-Doudoroff pathway is another route used to convert carbohydrates into pyruvate. *Pseudomonas*<sup>113</sup> and *Azotobacter*<sup>114</sup> both use this pathway in preference to glycolysis. The uptake system is used to allow carbohydrates into the cell, which also includes drugs with carbohydrates attached.

#### **1.3.4 Carbohydrate prodrugs**

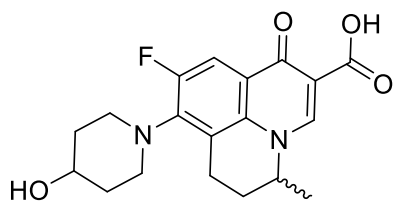
Glycosides have been used to create prodrugs for a variety of different biological activities. Carbohydrates are chosen as they can increase bioavailability, solubility, activity, and selectivity. For example, ciprofloxacin is an example of a fluoroquinolone, but since its introduction resistance to this compound has risen. Glycosides of the compound were synthesised and tested against various bacteria, these results are shown in Figure 11. The glycosides showed similar, but lower, activities to the parent compound, ciprofloxacin. These results suggested that the compounds can still reach their target enzymes and still inhibit them.<sup>115</sup>



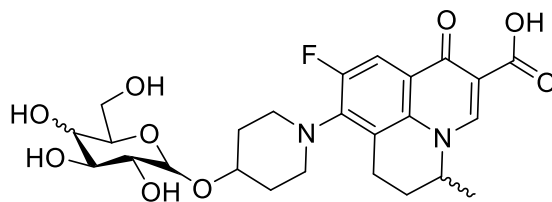
	<b>27</b>	<b>28</b>	<b>29</b>
<b>Zone of inhibition (cm)</b>			
<i>S. aureus</i> NCTC 6571	2.9	1.2	0.8
<i>S. aureus</i> NCTC 10399	2.9	1.3	1.2
MRSA (HG-1)	R	R	R
<i>S. epidermidis</i> NCTC 11047	3.1	1.2	1.1
<i>S. epidermidis</i> NCTC 2749	3.3	1.3	1.2
<i>E. coli</i> NCTC 10418	3.2	2.3	2.2
<i>E. coli</i> BIG 0046 (Cipro R)	R	R	R
<i>E. coli</i> BIG 0051 (Cipro R)	R	R	R
<i>P. aeruginosa</i> (Environmental) BIG 0039	3.1	1.2	0.9
<i>P. aeruginosa</i> (Clinical) BIG 0037	2.6	R	R
<i>P. aeruginosa</i> NCTC 10662	3.1	0.9	0.9
<i>P. aeruginosa</i> BIG 0063	3.2	R	R
<i>Serratia marcescens</i> BIG 0011	3.1	1.9	1.8

**Figure 11:** The structure of ciprofloxacin **27** with its glucose **28** and galactose **29** conjugates. The data shown is the diameter of the zone of inhibition in a disc diffuse assay. Data adapted from ref. 113.

Another example is glycosylation of nadifloxacin. These glycosides were synthesised and tested against various bacteria. As seen with previous glycosidic prodrugs, their activities were less than that of the parent compound. In most gram-positive bacteria, the glycosides completely lost their biological activity.<sup>116</sup> The structures and MIC data are shown in Figure **12**.



**30**



**31 Glu**

**32 Gal**

	<b>30</b>	<b>31</b>	<b>32</b>
<b>MIC (μg/mL)</b>			
<i>Citrobacter freundii</i>	2.0	>64	64
<i>Enterbacter cloacae</i>	1.0	32	2
<i>Cronobacter sakazakii</i>	1.0	>64	64
<i>Escherichia coli</i>	1.0	>64	32
<i>Hafnia alvei</i>	0.1	8	0.5
<i>Klebsiella pneumoniae</i>	0.1	8	0.5
<i>proteus mirabilis</i>	1.0	>64	64
<i>Salmonella typhimurium</i>	2.0	>64	>64
<i>Serratia marcescens</i>	4.0	>64	>64
<i>Enterococcus faecalis</i>	1.0	>64	>64
<i>Enterococcus faecium</i>	4.0	>64	>64
<i>Staphylococcus aureus</i>	0.1	32	16
<i>Staphylococcus epidermidis</i>	0.1	>64	>64
<i>Streptococcus agalactiae</i>	1.0	>64	>64
<i>Streptococcus pneumoniae</i>	1.0	>64	>64
<i>Streptococcus pyogenes</i>	1.0	>64	>64
<i>Streptococcus viridans</i>	1.0	>64	>64

**Figure 12:** The structure of nadifloxacin **30** with its glucose **31** and galactose **32** conjugates. The data shown is the MIC determined by the bioscreen method. Work adapted from ref. 114.

## **1.4 Overall aims and objectives**

### **1.4.1 Overall aims of the project**

The overall aim of this project was to create novel carbohydrate prodrugs, with a focus on antimicrobial activity. These compounds were designed to couple a sugar to an antimicrobial compound, to produce a glycoside which inhibits the growth of certain bacteria to be potentially used in selective media. This was done through the design and synthesis of the prodrugs followed by biological testing, including enzyme hydrolysis and MIC data. This allowed structure-activity relationships (SARs) to be derived. Within this project there were three different series containing three different antimicrobial compounds (bisphenol, flavonoids, 1,2,3-triazoles with the core that contains azidothymidine (AZT)).

### **1.4.2 Overall objectives of the project**

The aims for the project have been completed by firstly using different synthetic pathways to create the various prodrugs, including glycosylations and click chemistry methods. These prodrug compounds were then tested using a variety of biological methods. The MIC<sub>100</sub> data was collected using a bioscreen method, using different media, as well as using an agar method. The bacteria were chosen based on the pathogenicity, gram-positive and gram-negative bacteria were used. Where applicable, cell assays were used to study and evaluate the cancer properties of the flavonoid containing compounds. AZT was originally released onto the market as an anti-viral but was also found to have antimicrobial properties. A fitting model was used to explore the antiviral properties of the compounds that contain the 1,2,3-triazole core. AZT was originally released onto the market as an anti-viral but was also found to have antimicrobial

properties. This used Pymol to fit the compounds in the enzyme active site in HIV reverse transcriptase.

**Chapter 2 – The synthesis and  
microbiological evaluation of carbohydrate  
prodrugs containing a bisphenol moiety**

## 2.1 Introduction

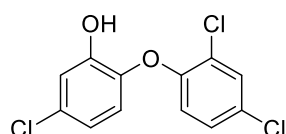
This series of compounds, the target molecules **33-34** which are shown in Figure 16, used a prodrug approach for drug design. The active drug would be released once the sugar moiety has cleaved in the target bacterial cell by glycosidase enzymes. Bacteria contain a range of these enzymes and different bacterial strains contain different glycosidase enzymes, as summarised Table 6. In this way, it has been hypothesised that it is possible to selectively deliver antimicrobial agents to specific bacterial strains by careful matching of glycoside prodrugs to the enzyme profiles present in the bacteria. In addition, the PTS, which is the transport protein system that is involved in bacterial carbohydrate uptake, will allow active uptake of the prodrugs within bacterial cells.<sup>108</sup>

### 2.1.1 Polychlorinated compounds

There are many poly-aromatic compounds which display excellent antimicrobial properties. Triclosan **38**, 2,4,4'-trichloro-2'-hydroxydiphenyl ether, is a broad spectrum antimicrobial agent which is considered part of the bisphenol class, its structure shown in Figure 13. It has been shown to have good activity against *S. aureus* (ATCC 29213) and *Es. coli* (ATCC 25922), with moderate activity against MRSA.<sup>117</sup> This compound **38** has good antimicrobial activity when compared to other antimicrobials which are also used as topical agents in dermatology, the data is presented in a table in Figure 13.<sup>118</sup> It was discovered in the 1970's, and has been used in a variety of different products, including deodorants, soaps and cosmetics<sup>119-121</sup>, and dermatological and topical preparations for protection of skin.<sup>118</sup> It has been used in these products as it contains antimicrobial properties while still being gentle on skin.<sup>119</sup> Using the right concentrations, triclosan **38** can also be used as a biocide.<sup>67</sup> In recent years, however, there

have been concerns over the safety of this compound, in animal studies it is thought to affect thyroid functions.<sup>122</sup> The major concern, however, is the resistance that bacteria have acquired to **38**. Triclosan **38** at a low concentration is a fatty acid synthesis inhibitor, whereas as a biocide has multiple cytoplasmic and membrane targets.<sup>123</sup> There are many mechanisms by which resistance to triclosan **38** has been acquired. These are also shown in Figure 13.

Bacterium	Mechanism of resistance	Antibiotic cross-resistance	Ref.
<i>Es. coli</i>	<i>fabI</i> mutations; efflux	Yes	124–126
<i>P. aeruginosa</i>	Multiple efflux systems	Yes	127,128
<i>S. aureus</i>	<i>fabI</i> mutations	No	129
<i>M. smegmatis</i>	<i>inhA</i> mutations	Yes	130
<i>M. tuberculosis</i>	<i>inhA</i> upregulating mutations	Yes	130,131



**38**

MIC data (ug/mL)	<i>S. aureus</i>	MRSA	<i>E. coli</i>
	0.125	64	0.5

**When compared to other antimicrobials:**

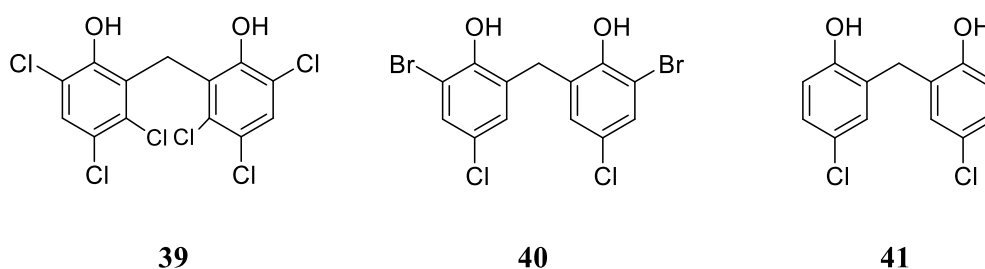
MIC (µg/mL)	Hexachlorophene		Gentamicin		
	<b>38</b>	Chlorquinaldol	Econazole		
<i>Staphylococcus aureus</i> (ATCC 13709)	0.01	0.3	3	1	3
<i>Streptococcus faecalis</i> (ATCC 10541)	10	3	>100	10	30
<i>Salmonella typhimurium</i> (NCTC 5710)	0.3	100	>100	1	>100
<i>Escherichia coli</i> (NCTC 86)	0.3	30	30	1	>100
<i>Pseudomonas aeruginosa</i> (NCTC 1999)	>100	30	>100	1	>100

**Figure 13:** The structure of triclosan **38**. The MIC data is also shown; data collected using a micro-dilution assay.<sup>115</sup> A table showing triclosan's **38** mechanism of resistance and antibiotic cross-resistance in different bacteria.

Hexachlorophene (hex) **39**, also known as 2,2'-methylenebis(3,4,6-trichlorophenol), is also another example of a bisphenol, structure shown in Figure 14. It was first patented as a broad-spectrum antimicrobial in 1941 by Gump.<sup>132</sup> The mechanism of action for this compound

(**39**) involves inhibition of the membrane bound part of the electron transport chain, at higher concentrations it can cause protoplast lysis and inhibit respiration.<sup>133–135</sup> It was used in soaps and cosmetics was taken off the market due to toxicity concerns, much like triclosan **38**.<sup>136,137</sup> Hex, **39**, was linked to brain lesions in infants before been taken off the market in 1975.<sup>138</sup> The drug was found to have a cumulative effect and was absorbed through the skin.<sup>139,140</sup>

Bromochlorophen (BCP) **40** and dichlorophene (DP) **41** are the anti-bacterial agents that have been used previously in cosmetics and deodorants, structures shown in Figure 14.<sup>141</sup> Notably, they all possess phenolic groups that allow for easy attachment to carbohydrates, through glycosylations, to form a range of glycoside prodrugs. Use of Hex **39** and BCP **40** has declined due to their toxicity; however, using the prodrug design can reduce the compounds toxicity and allow for compounds to be used more widely.



MIC ( $\mu\text{g/mL}$ )	39	40	41
<i>Citrobacter freundii</i>	16	>128	32
<i>Enterbacter cloacae</i>	4	>128	4
<i>Cronobacter sakazakii</i>	4	>128	16
<i>Escherichia coli</i>	8	>128	64
<i>Pseudomonas aeruginosa</i>	8	>128	128
<i>Klebsiella pneumoniae</i>	2	>128	64
<i>Proteus mirabilis</i>	8	8	8
<i>Salmonella typhimurium</i>	16	>128	32
<i>Serratia marcescens</i>	8	>128	64
<i>Enterococcus faecalis</i>	<0.5	4	8
<i>Enterococcus faecium</i>	<0.5	2	8
<i>Staphylococcus aureus</i>	<0.5	1	4
<i>Staphylococcus epidermidis</i>	<0.5	<0.5	4
<i>Streptococcus agalactiae</i>	<0.5	<0.5	1
<i>Streptococcus pneumoniae</i>	<0.5	<0.5	<0.5
<i>Streptococcus pyogenes</i>	<0.5	<0.5	<0.5
<i>Streptococcus viridans</i>	<0.5	1	4

**Figure 14** : The structures of bromochlorophen (BCP) **40**, dichlorophen (DP) **41** and hexachlorophene (hex) **39**. Data was collected using a bioscreen method.<sup>116</sup>

### 2.1.2 Justification for drug design

This series of compounds **35-37** has been designed based on previous work.<sup>142</sup> Dr. Brierley's work explored how attaching various bisphenolic compounds to a carbohydrate affected the activity of the phenolic compound. The glycosides of these compounds were synthesised and tested for the antibacterial efficacy and selectivity alongside the free anti-bacterial agents, the target compounds **35-37** are shown in Figure 15.

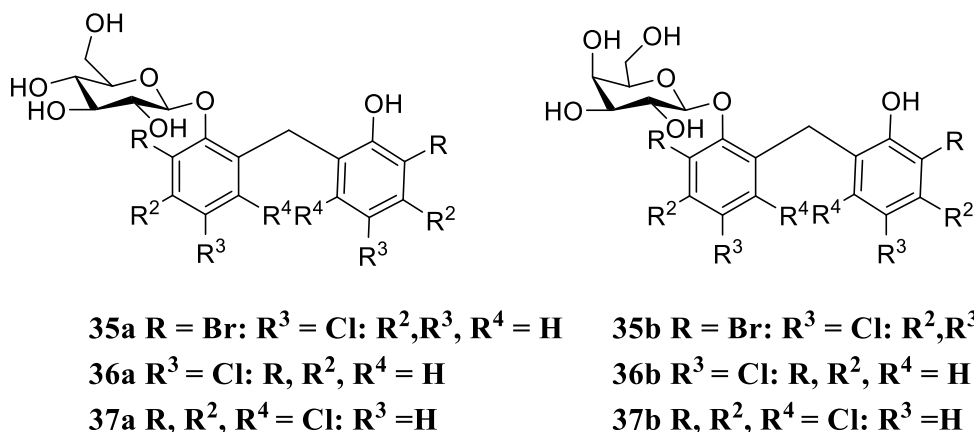


**Figure 15** : The structures of the previously synthesised glycosides from Dr. Brieley's work.<sup>116</sup>

Once compounds **35-37** were synthesised, their MIC values were determined and these are summarised in Table 9. The red lettered microbes are gram-positive bacteria, and the yellow highlighted values represent those with a MIC value of  $\leq 32$   $\mu\text{g/ml}$ . In the table, the glycoside derivatives are compared with the underivatized compounds. For hex, **39**, the MIC values for both gram-positive and gram-negative bacteria were under 32  $\mu\text{g/ml}$ . Due to the outer membrane of lipopolysaccharides and proteins found in gram-negatives, the MIC values were generally higher in the gram-negative bacteria when compared to the gram-positive bacteria. The glucosides are generally more active than the galactosides, and the carbohydrate prodrugs are less active than the free anti-bacterial agents. This is due to the extra step of the enzyme cleaving the carbohydrate to release the compound, so under the same time conditions would have expected a lower MIC value.

With all the above compounds there are halogens attached to the bisphenol moiety. The more halogens attached to the compound the lower its MIC. When designing the bisphenol compounds for preparation in this work, careful consideration was paid to which bisphenol moieties to use. In previous work, it was hypothesised that a free hydroxyl on the bisphenol moiety of the prodrug was responsible for the antibacterial activity. The hydroxyls in the *ortho*

position on the rings are vital for activity, once the hydroxyl groups are moved to the *para* position on the ring the MIC activity in *Es. coli* decreased from >40  $\mu\text{g/mL}$  with 2(2-hydroxybenzyl)-phenol to >100  $\mu\text{g/mL}$  with 4(4-hydroxyphenyl)-phenol. The hydroxyl forms hydrogen bond interactions with Y156 and with the 2'-hydroxyl group of  $\text{NAD}^+$  ribose ring. This allows for a stable enzyme-cofactor complex to form in FabI.<sup>118</sup> This was also taken into consideration when designing the target compounds for this work. Thus, glycosides were designed that incorporated a free phenolic group alongside the non-phenol counterpart. By preparing derivatives that do not have halogens, it was hypothesised that it would also be possible to compare the activities of the halogenated and the non-halogenated compounds to see the extent of the influence of the halogen on anti-bacterial properties. In this way, SARs can be determined.

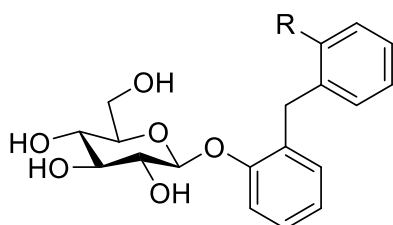
**Table 9:** A table showing the results of screening several bis-phenol compounds attached to various sugars against a range of bacterial strains, as performed by L. Brierley.<sup>142</sup> It is highlighted in yellow where the value  $\leq 32$   $\mu\text{g/ml}$ . The microbials labelled in red are gram-positive bacteria. The broth is CM5.

Organisms	MIC ( $\mu\text{g/ml}$ ) of various bis-phenyl moieties attached to various sugars.								
	39			40			41		
	Hex 39	35a	35b	BCP 40	36a	36b	DP 41	37a	37b
<i>B. cereus</i>	<0.5	16	16	1	16	16	2	128	32
<i>E. faecalis</i>	<0.5	32	16	4	32	32	8	>128	128
<i>E. faecium</i>	<0.5	64	16	4	32	32	8	>128	64
<i>S. aureus</i>	<0.5	32	16	1	32	32	4	>128	64
<i>S. epidermis</i>	<0.5	16	16	<0.5	16	32	4	>128	64
<i>St. agalactiae</i>	<0.5	16	8	<0.5	8	16	1	128	32
<i>St. pneumoniae</i>	<0.5	1	2	<0.5	8	8	<0.5	32	8
<i>St. pyogenes</i>	<0.5	64	2	<0.5	1	8	<0.5	128	8
<i>St. viridans</i>	<0.5	16	8	2	16	32	4	>128	>128
<i>C. freundii</i>	16	>128	128	>128	>128	>128	32	>128	>128
<i>Cr. sakazakii</i>	4	>128	128	>128	>128	>128	16	>128	>128
<i>En. cloacae</i>	4	>128	128	>128	>128	>128	4	>128	128
<i>Es. coli</i>	8	>128	128	>128	>128	>128	64	>128	>128
<i>K. pneumoniae</i>	8	>128	64	>128	>128	>128	64	>128	>128
<i>P. mirabilis</i>	2	>128	128	8	128	>128	8	>128	>128
<i>Ps. aeruginosa</i>	8	>128	128	>128	>128	>128	128	>128	>128
<i>Sa. typhimurium</i>	16	>128	128	>128	>128	>128	32	>128	>128
<i>Se. marcescens</i>	8	>128	64	>128	>128	>128	64	>128	>128

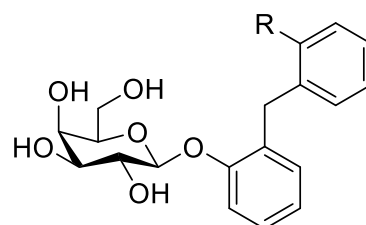
## 2.2 Aims and objectives of the bisphenol containing compounds

### 2.2.1 Aims for the bisphenol moiety containing prodrugs

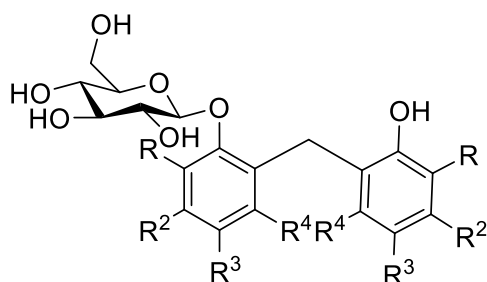
Previously, glycosides containing a bisphenol moiety have been synthesised and studied for their biological activity.<sup>143</sup> These compounds, **35-37**, are shown in Figure 16, they were used for the basis of the design of **33** and **34**. This series of compounds that have been synthesised are carbohydrate compounds attached to a bisphenol moiety, in keeping with a prodrug approach.



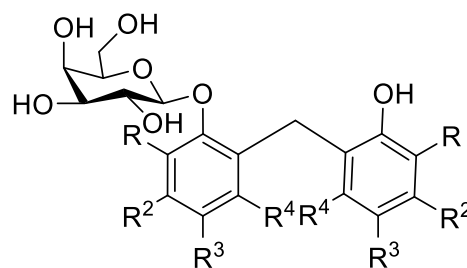
**33a** R=H  
**33b** R = OH



**34a** R=H  
**34b** R = OH



**35a** R = Br: R<sup>3</sup> = Cl: R<sup>2</sup>, R<sup>3</sup>, R<sup>4</sup> = H  
**36a** R<sup>3</sup> = Cl: R, R<sup>2</sup>, R<sup>4</sup> = H  
**37a** R, R<sup>2</sup>, R<sup>4</sup> = Cl: R<sup>3</sup> = H



**35b** R = Br: R<sup>3</sup> = Cl: R<sup>2</sup>, R<sup>3</sup>, R<sup>4</sup> = H  
**36b** R<sup>3</sup> = Cl: R, R<sup>2</sup>, R<sup>4</sup> = H  
**37b** R, R<sup>2</sup>, R<sup>4</sup> = Cl: R<sup>3</sup> = H

**Figure 16:** The previously synthesised compounds, **35-37**,<sup>116</sup> and the target structures, **33-34**, for the bisphenol containing carbohydrate compounds.

These compounds were designed to probe the structure-activity relationships (SAR) with other bisphenolic compounds that have previously been investigated.<sup>142</sup> Specifically, **33** and **34** were designed to probe whether the free hydroxyl, in the *meta* position the aromatic ring without a glycoside, had any bearing on the antimicrobial activity of the compounds. Also, compounds **35-37** were used to investigate the influence of halogens present on the bisphenolic rings on the antimicrobial activity.

### **2.2.2 Objectives of the bisphenol moiety containing prodrugs**

The aims for this chapter were achieved by utilising an aq. glycosylation method, a Michael style of reaction. A base was used to deprotonate the bisphenol and this allowed the deprotonated moiety to attack the anomeric centre of the halogenated sugar. These compounds were then deprotected to give the target compounds **33** and **34**. The MIC data was collected using a media method; using various media, namely Mueller-Hinton broth (MHB), CM5, and Nutrient broth 2 (NB).

## 2.3 Results and discussion

### 2.3.1 Synthesis

#### 2.3.1.1 Synthetic route to synthesising the target molecules 33 and 34

The target compounds **33-34** and the retrosynthetic route for these compounds are shown in Figure 17. As can be seen in the retrosynthetic analysis, the glycosidic bond between the carbohydrate and the bisphenol moiety was cleaved and this left the carbohydrate with a leaving group on the anomeric centre and hydroxylated bisphenol moiety. The difference between glucosides and galactosides is the stereochemistry of the hydroxyl position on the C-4 position on the carbohydrate ring.

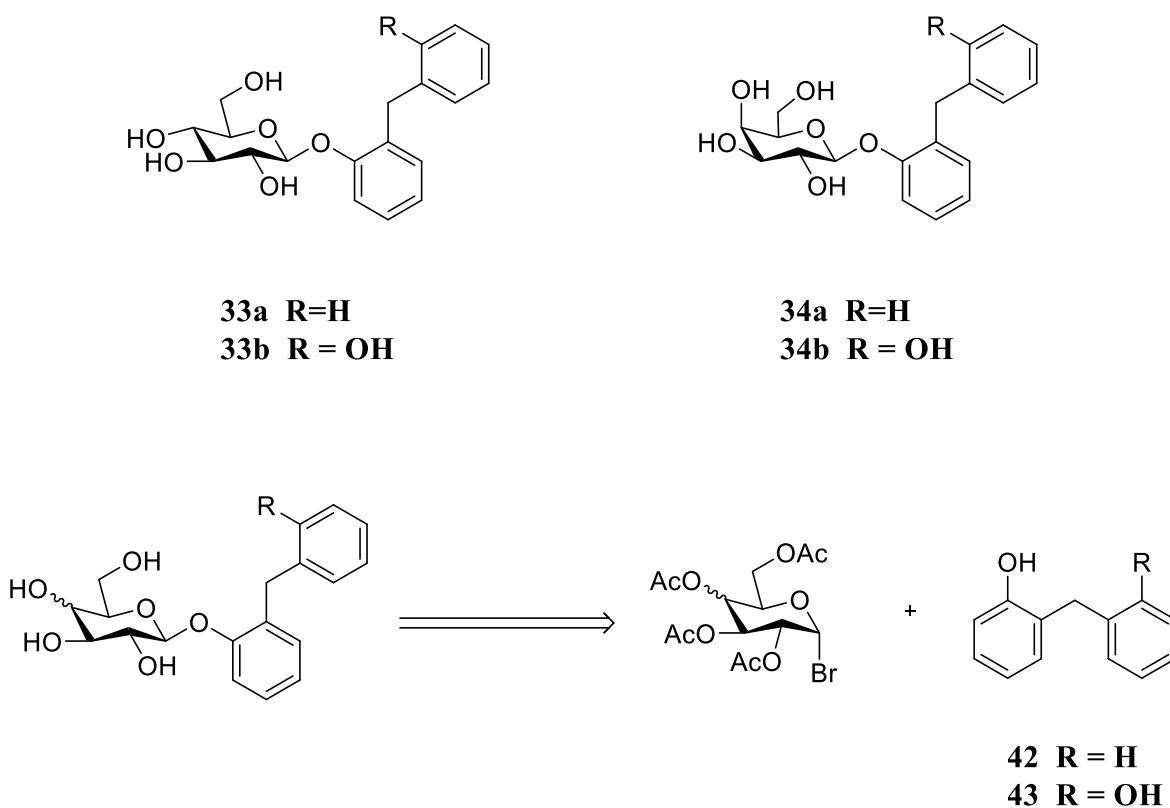
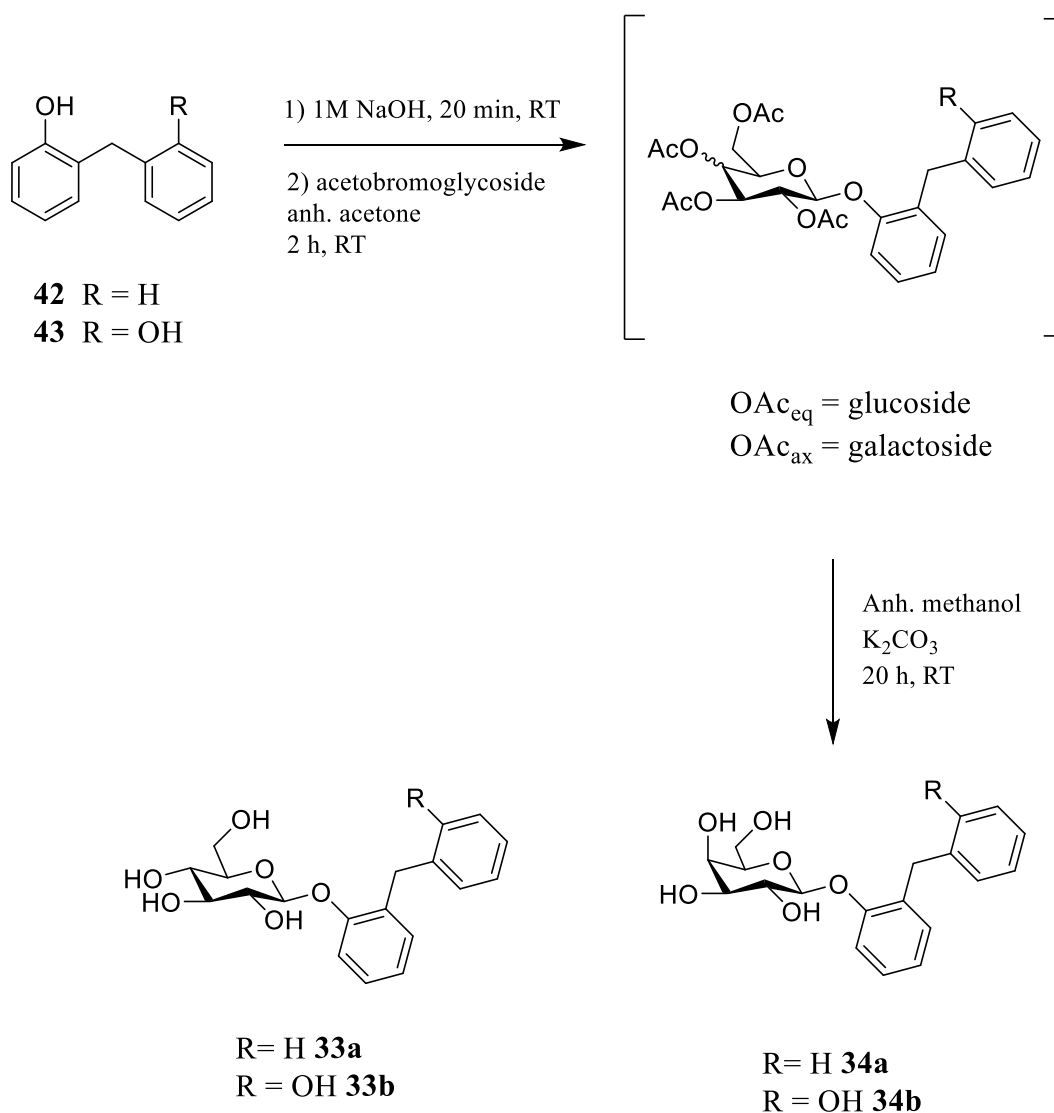


**Figure 17:** The target compounds **33-34**. The retrosynthetic route is also shown beneath the target compounds.

For the synthetic route, shown in Scheme 6, a glycosylation method involving NaOH was used. This reaction involved the aglycone (bisphenol) and the halogenated sugar. A brominated sugar, brominated at the anomeric centre, was used to provide a good leaving group in the sugar for the deprotonated aglycone to attack. A glycosyl halide was chosen as they are versatile and provide a halide, a good leaving group, in the anomeric position. The bromide was chosen in the anomeric centre as it is more reactive than its chloride and fluoride counterparts, it is also the most common halide used.<sup>144</sup> The fluoride and chloride are more stable, which therefore makes them inferior glycosyl donors. The glycosyl iodide compounds are more reactive than the corresponding bromide, however, are more useful for creating the  $\alpha$ -anomer.<sup>145</sup>



**Scheme 6:** The reaction scheme for the synthesis of **33** and **34**. The compound in the square bracket represents an intermediate that was partially purified.

The NaOH was added to the bisphenol firstly and allowed to stir for 20 min, to allow the deprotonation of one of the hydroxyls on the bisphenol compound before the sugar was added. The halogenated carbohydrate was then added to form the acetylated intermediate. The glycosylation only occurred at one of the free hydroxyls. This could be due to the ratios used in the reaction NaOH: bisphenol: sugar (1:1:1), so only one sugar molecule reacted with one bisphenol compound. Another theory could be that the oxygen present in the ring in the carbohydrate could hydrogen bond to the free hydroxyl, thus only single glycosylations are possible. This hydrogen bond is shown in Figure 18.

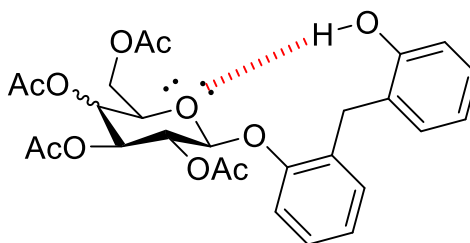
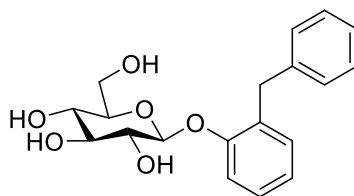


**Figure 18:** The possible hydrogen bond present in the acetylated intermediates in for the synthesis of **33b** and **34b**.

### 2.3.1.2 Optimisation of the glycosylation reaction

As previously mentioned, there are different routes in which to perform glycosylations. In this work, different glycosylation methods were used to try and optimise the yield. Phase transfer catalysis (PTC) was a reaction method which was used. PTC involves the use of a catalyst to enable the migration of a reactant from one phase to another, this then allows the reaction to occur. The catalyst used was tetrabutylammonium hydrogensulfate (TBAHS), with the  $K_2CO_3$  deprotonating the aglycone. The tetrabutylammonium ion forms a complex with the deprotonated bisphenol compound. This, in turn, allows a transition state between the halogenated sugar and the bisphenol to form, the bromide then acts as a leaving group and gives

the glycosylated bisphenol. The results for these reactions are shown in Figure 19. The compound **33a**, was the target compound for these reactions.



**33a**

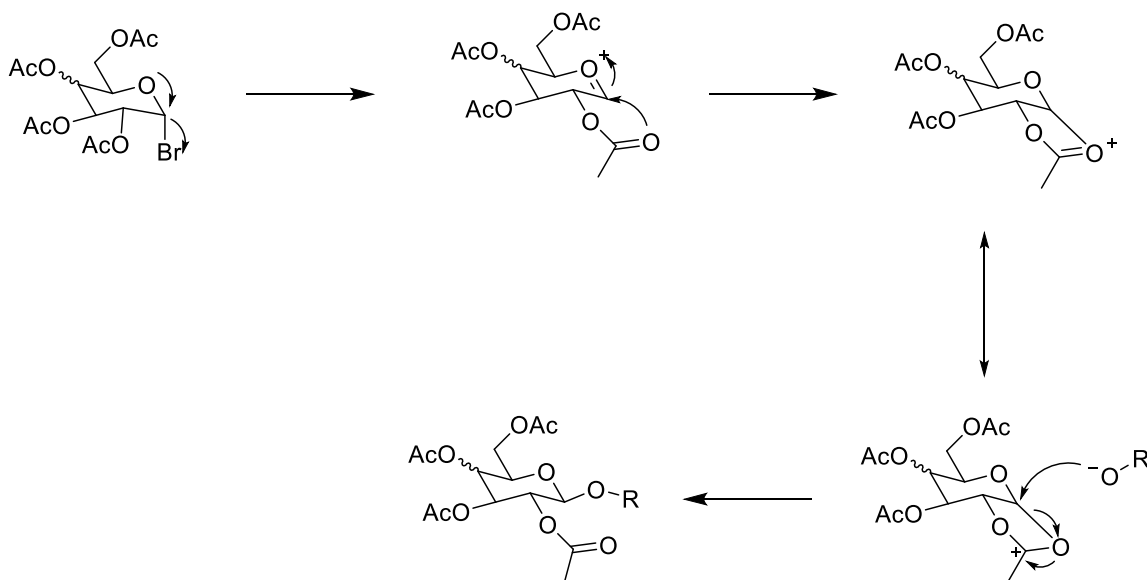
Glycosylation	Reactants used	Glycosyl donor used	Yield	Ref.
Aq. Michael addition	NaOH		9%	116
PTC	TBAHS, K <sub>2</sub> CO <sub>3</sub>		NR	146

**Figure 19:** A table showing the different glycosylation methods used. NR = no reaction.

As can be seen in Figure 19, only one of the methods was successful. The PTC reaction did not afford the product; this could be due to the base not being able to deprotonate the bisphenol moiety. From these results, the synthetic route chosen was aq. Michael addition.

### 2.3.1.3 Mechanism by which the reaction occurs

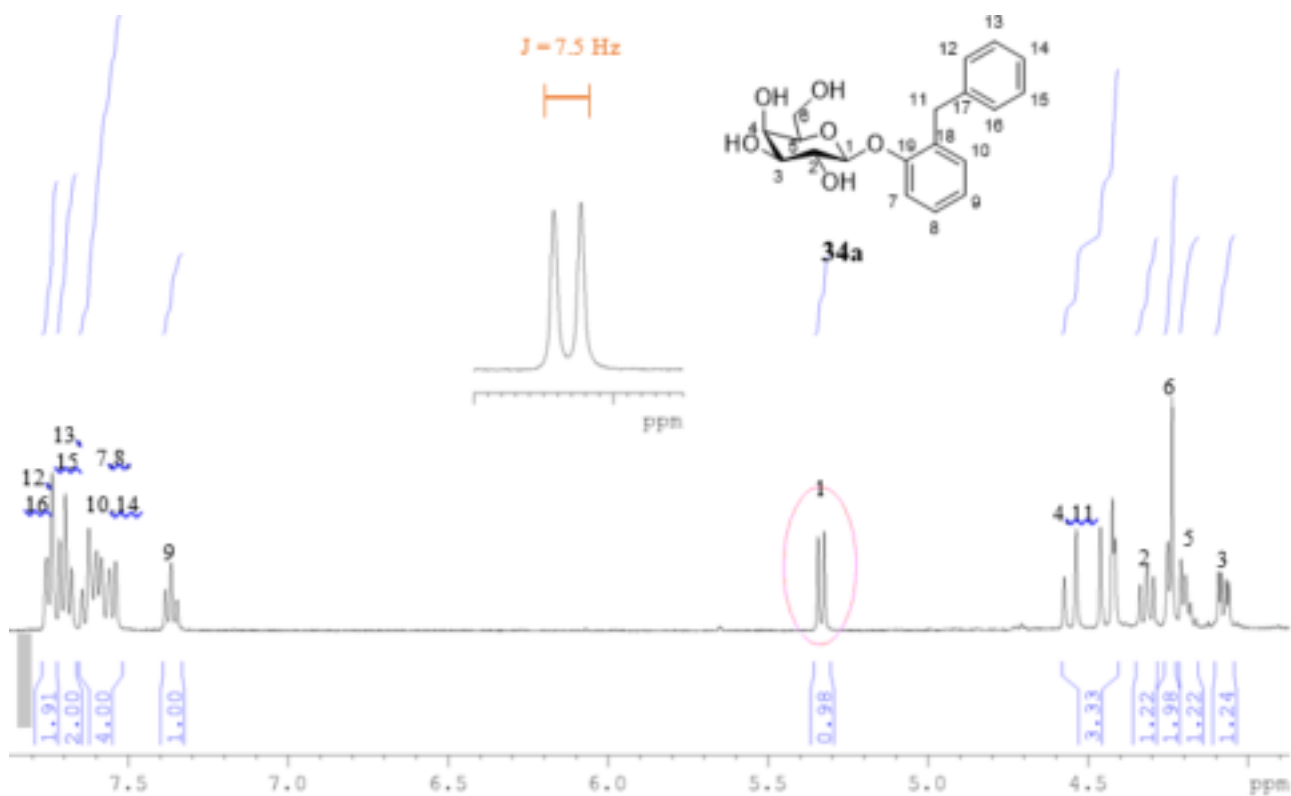
The aglycone attacked the C-1 carbon and produced the  $\beta$ -anomer. The lone pair on the oxygen in the ring activates the C-1 position, leading to the formation of the oxocarbenium ion. The oxygen in the carbonyl in the acetyl group then in turn attacks the C-1 position and pushes the electron from the double bond onto the oxygen in the ring. This reaction can be described as an  $S_N1$  mechanism, or unimolecular. The acetyl protecting group leads to the formation of the  $\beta$ -anomer due to neighbouring group participation (NGP), as seen in Scheme 7. NGP, also known as anchimeric assistance, is present in this mechanism due to acetyl groups being used as the protecting group. This phenomenon stabilises the intermediate produced by being bonded to the anomeric centre.<sup>147</sup> Due to the steric hindrance around C-1 position the deprotonated aglycone can only form the  $\beta$ -anomer.



**Scheme 7:** The mechanism for the formation of the  $\beta$ -anomer.

To ascertain which anomer was formed  $^1\text{H}$ - nuclear magnetic resonance (NMR) spectroscopy was used. The  $J$  values between these two anomers changes drastically, with  $\beta$ -anomers having

a coupling constant of  $\sim 7$  Hz and  $\alpha$ - anomers  $\sim 4$  Hz.<sup>148</sup> For the glycosides synthesised in this project, the  $\beta$ -anomers were formed. The coupling constants for the H-1, anomeric centre, were between 6.0 – 7.5 Hz. In Figure 20, the  $^1\text{H-NMR}$  spectrum of **34a** is displayed with the anomeric peak highlighted. This doublet has a  $J$  value of 7.5 Hz, indicative of the  $\beta$  glycoside. The other  $J$  values are shown in Figure 20.



Compound	$J$ value (Hz)
<b>33a</b>	7.0
<b>34a</b>	7.5
<b>33b</b>	6.0
<b>34b</b>	CBD

**Figure 20:**  $^1\text{H-NMR}$  spectrum for **34a**, the highlighted peak is the hydrogen present at the anomeric centre. The  $J$  value highlights that it's the  $\beta$ -anomer has been synthesised. The table above shows the  $J$  values (Hz) for the four compounds, **33-34**, as determined from their respective  $^1\text{H-NMR}$  spectra. CBD – cannot be determined.

The value for **34b** could not be distinguished as there was a water solvent resonance masking the anomeric peak. The anomeric effect is a term to describe the stereoelectronic effect that dictates the axial conformational preference of electronegative substituents in the C-1 position in a sugar or heterocycle; therefore it determines whether the  $\alpha$ - or  $\beta$ -anomers of the target compounds **34-35** are synthesised. It is also known as Edward-Lemieux effect and was first described in 1958.<sup>149,150</sup> There are two main models used to describe this effect: electrostatic and hyperconjugation model. The electrostatic model states that the preference for the  $\alpha$ -anomer arises from local dipole-dipole interactions. These interactions can be seen in Figure 21. In the equatorial position, the dipole moments are aligned and this gives a greater net dipole. The axial position is preferred as the dipoles oppose each other and this reduces the net dipole. This model is in agreement with experimental data, which suggests that the solvent effect influences the stabilisation of the  $\beta$ -anomer and in turn reduces the anomeric stabilisation, example of this is in tetrahydropyranosyl systems.<sup>151,152</sup>

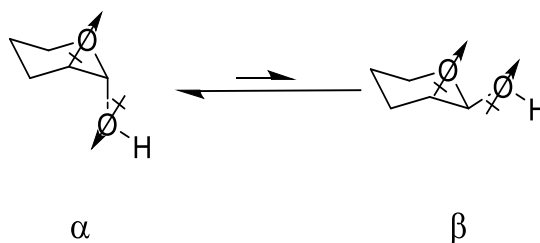


**Figure 21:** The dipole interactions shown on the  $\alpha$ - and  $\beta$ - anomers.

There is much debate, however, with the hyperconjugation model. The model suggests that there is a stabilising effect asserted between the unshared electrons on the heterocycle (in glucose and galactose these are from an oxygen) and the  $\sigma^*$  orbital in the C1 position, seen in Figure 22. In the axial position, these orbitals align which lowers the energy of the system and causes greater stability. When in the equatorial position, these orbitals do not align so this extra stability is not provided. This model is supported by the direct computations of the  $n \rightarrow \sigma^*$  and

$\sigma^* \rightarrow \sigma^*$  stabilisation energies, which are based on natural bond orbital (NBO) method.<sup>153</sup> NBO uses orthogonal orbitals to describe the localised construct, using algorithms that enable fundamental bonding concepts.<sup>154</sup>

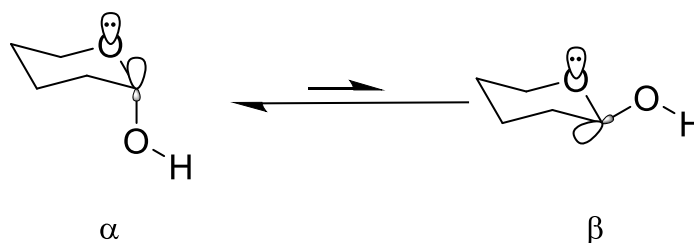


**Figure 22:** The hyperconjugation model. This shows the lone pair orbital on the oxygen and the  $\sigma^*$  orbital in C-1 position.

When using the block-localised wavefunction (BLW) method, however, the electron delocalisation slightly favoured the trans conformator of dimethoxymethane and cis for the substituted tetrahydropyrans.<sup>155</sup> This method is an *ab initio* valence bond (VB) theory: this approach combines molecular orbitals theory with VB theory.<sup>156</sup> One school of thought is that the steric effect dominates the conformation formed.<sup>155</sup>

Many conditions influence this effect, the main two conditions being substituent and solvent effect. Substituent effects can influence which anomer is formed. Alkoxy, acetoxy and halogen substituents on the anomeric centre prefer the axial position, whereas hydroxyl prefers equatorial.<sup>157</sup> The solvent effect shows that the solvent used will help dictate which anomer is formed. Computation studies have shown that the conformational preference is reduced in solution, and this increases as the polarity of the solvent increases.<sup>158</sup> When designing the synthetic pathway for compounds **34-35** the above conditions had to be taken into consideration as the  $\beta$ -anomer was the target stereochemistry.

#### 2.3.1.4 Optimisation of the purification for the target compounds

After the acetylation reaction, the compounds were partially purified using column chromatography. The product was only partially purified as the acetylated compounds and the bisphenol starting materials had very similar  $R_f$  values on thin layer chromatography (TLC), 0.46 in a solvent mixture of ethyl acetate: petrol ether (3:2), and therefore had very similar retention times on the normal phase column. The protected glycosides were partially purified using normal phase (NP) column chromatography ethyl acetate: petrol ether (3:2). The compounds were then deprotected using anh. MeOH and  $K_2CO_3$  in a process called methanolysis, with the  $K_2CO_3$  being used as a base catalyst. This crude mixture was then purified using reverse phase chromatography, using 0.1% formic acid in water: acetonitrile (3:7). When the final products were first purified it was performed using NP column chromatography, with solvent system of methanol: dichloromethane (DCM) (1:99 up to 1:9).

In NP silica, compounds with hydrophilic properties contained within the mobile phase will have a high affinity to the stationary phase, in column chromatography that is the NP silica. Hydrophobic compounds have less affinity for the stationary phase and therefore are the first to be eluted. To counteract this, methanol (a polar solvent) was used to try and elute the hydrophilic target compounds. This, however, did not work on small scale reactions. When NP silica eluted the targeted molecules, the retention time was a prolonged and there will be more interactions with the stationary phase. For these reasons, reverse phase (RP) silica column chromatography was used. The polar nature of the compounds meant that the compounds retention time on the column was drastically shortened.

### 2.3.1.5 Yields and purity of the target compounds

When synthesising these compounds there was a difference in yields between the glucosides and galactoside, as well as differences as to which bisphenol moiety was used. The compounds **33b** and **34b** contained the extra hydroxyl on the aromatic ring. It is hypothesised that the hydroxyl hydrogen bonds to the oxygen in the carbohydrate ring. This provides more stability and has caused the yield to increase when compared to no extra hydroxyl present.

The purity for these glycosides was determined using a high performance liquid chromatography (HPLC) method, using a gradient solvent system. Each compound has >99% purity, with the results seen in Table 10. A solvent system of A=0.1% formic acid in H<sub>2</sub>O and B=MeCN was used, with a flow rate = 1.0 mL/ min. Compounds were eluted with a gradient of 5% B to 80% B for 30 min. Wavelengths 254, 280, and 210 nm were used. A gradient was used to expose any compounds that are less polar than the target compound, such as hydrolysed sugars. An evaporative light scattering detector (ELSD) was used in conjunction with UV in the HPLC as some of the side products could be ultra-violet (UV) inactive, an example is the hydrolysed sugar. The yields and purities for compounds **33-34** are shown in Table 10.

**Table 10:** A table showing the yields and purity of the target compounds **33-34**.

Compound	Yields (%)	Purity (%)
<b>33a</b>	9	99
<b>33b</b>	15	99
<b>34a</b>	7	99
<b>34b</b>	11	99

## 2.3.2 Microbiology data for the bisphenol series

### 2.3.2.1 Bioscreen method

The bioscreen method is used to quantitatively measure bacterial growth in different broth mediums. The bioscreen method is described as turbidimetric. A bioscreen can measure the optical density (OD) of the bacterial cells in a broth at a certain temperature and wavelength. It allows for up to 18 bacterial organisms over 9 different concentrations to be measured. It can be applied to determine how an antibiotic may affect the growth of different bacterial cells, when compared to a control which contains no drug.

As the bacteria grow in the bioscreen plates they follow a pattern; containing four phases or stages. These are shown in Figure 23. The first phase is the lag stage, also known as the latent period. In this phase, the bacteria are thought to adapt themselves to the growth conditions. This may be due to dilution of exoenzymes and nutrients that are given out by the growing cells. The dilutions means that these cells are not close to each other, which makes sharing these materials more difficult.<sup>159</sup> They mature, with little to no cell division occurring.<sup>160</sup> They then enter the exponential stage; this is where the cells start to double. This can be expressed mathematically as:

$$\frac{dX}{dt} = \mu X$$

**Equation 2:** An equation to express the exponential stage of growth in bacteria.

Where  $X$  is the number of cells, or equally the mass of the cells,  $\mu$  is the growth rate constant (1/time) and  $t$  is the time taken for the cells to grow. The specific growth rate constant depends on its surroundings, if unchanged it is equal to the same as the constant at time = 0.<sup>159</sup>

The third stage in the growth of the bacteria is the stationary phase. There is no net growth in this stage; therefore Equation 2 is equal to zero. The cells are still dividing at the same rate that they are dying.<sup>161</sup> There are many reasons this could happen, one common reason is all the nutrients are used up. Another reason may be that the waste products which are produced when the cells grow are beginning to inhibit cell growth. Although, as stated earlier, the net growth is zero, there can sometimes be a small growth. This is caused by the dead cells lysing and providing a source of nutrients. The final phase in bacteria growth is the death stage. This is characterised as a net loss in cells. The death of cells is exponential, but often slower than cell growth. A graph of bacterial cells life cycles shown in Figure 23.

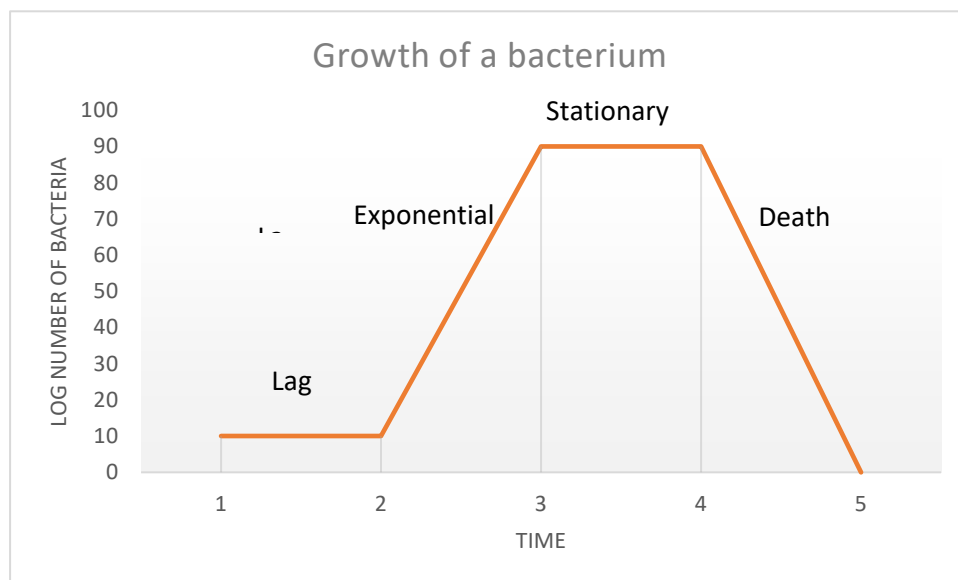


**Figure 23:** A graph showing the growth of a bacterium, in relation to time.

### 2.3.2.2 Justification for organisms used

The tables display the bacteria that were chosen for these projects. Where they are naturally found and their pathogenicity are also shown, as a justification as to why these bacteria were chosen.

#### Gram-positive bacteria

<b>Bacteria chosen</b>	<b>Naturally found</b>	<b>Pathogenicity</b>	<b>Refs.</b>
<i>Bacillus cereus</i>	Decaying organic matter. Fresh and marine waters. Vegetables and fomites. Intestinal tract of invertebrates.	Food poisoning and gastro-intestinal infections. Local and systematic infections in immunocompromised individuals, including central nervous system.	162,163
<i>Enterococcus faecium</i>	Gastro-intestinal and urinal tract in mammals.	Wound and soft tissue infections. Meningitis (post-neurosurgical). Respiratory infections. Nosocomial	164,165
<i>Enterococcus faecalis</i>			
<i>Staphylococcus aureus</i>	Skin and nasal cavities.	Adaptable to human flora conditions and can colonise easily. Sole cause of epidural abscess, acute endocarditis, botryomycosis, impetigo bullosa, pyomyositis, toxic shock syndrome and scaled skin syndrome.	166,167
<i>Staphylococcus epidermidis</i>	Skin and mucous membranes of the human body.	Colonises the skin. Predominant pathogen of sepsis in preterm infants. Major cause of Nosocomial infections.	168,169

<i>Streptococcus agalactiae</i>	Lower gastrointestinal and vaginal flora.	Affects babies, generally in the first 6 days of life. Been an increase in adults and elderly incidences (in the US), mostly pneumonia and also septicaemia.	170–172
<i>Streptococcus pyogenes</i>	Throat and skin.	Exclusively affects humans, ranging from mild skin conditions to life threatening diseases. Infections include streptococcal toxic shock syndrome, scarlet fever and mucosal.	173–175
<i>Streptococcus pneumoniae</i>	Mucosal surfaces of the human upper respiratory tract.	Human pathogen. Infections such as meningitis, bacteraemia and septicaemia.	176,177
<i>Streptococcus viridans</i>	Most prevalent in the oral cavity but also found in the upper respiratory tract, the female genital tract, and the gastrointestinal tract. Can also be found on human skin flora.	Causes endocarditis, bacteraemia, abscesses in the lungs, hearts and bones of occasional patients, and dental caries in most people.	178,179

### Gram negative bacteria

<b>Bacteria chosen</b>	<b>Naturally found</b>	<b>Pathogenicity</b>	<b>Refs.</b>
<i>Citrobacter freundii</i>	Water, soil, food, and the intestinal tracts of animals and humans.	In immunocompromised people, can lead to such diseases as sepsis and meningitis.	180,181
<i>Cronobacter sakazakii</i>	Water, soil, food and some foodborne sources including milk and meats.	(Formally known as <i>Enterobacter sakazakii</i> ) Affects neonates. Infections include bacteraemia, meningitis and endocarditis.	182,183
<i>Enterobacter cloacae</i>	Human gastro-intestinal tract. Also found in soil and sewage.	Hospital-acquired sepsis, nosocomial pneumonias, nosocomial urinary tract infections and postsurgical peritonitis.	184

<i>Escherichia coli</i>	Human colon and other warm blooded animals.	There are four types of <i>Es. coli</i> : B2 and D damage gastrointestinal barriers and cause infections such as urinary tract and gastroenteritis in humans.	185,186
<i>Klebsiella pneumoniae</i>	Transmitted by contaminated medical equipment, blood and from hospital personal.	Responsible for community acquired pneumonia.	187,188
<i>Proteus mirabilis</i>	Human intestines	Affects anyone using a catheter. Responsible for some urinary tract infections.	189,190
<i>Salmonella typhimurium</i>	Intestinal tracts of animals, including birds, and people.	Lead to gastroenteritis and easily can acquire antibiotic resistance.	191
<i>Pseudomonas aeruginosa</i>	Soil and surface water	Requires little nutrition. Infect the airway, urinary tract, burns and wounds. Also causes other blood infections	192,193
<i>Serratia marcescens</i>	Soil and water	Respiratory, urinary and wound infections. Easily can acquire antibiotic resistance.	194,195

### 2.3.2.3 Microbiological results

As discussed earlier, a bioscreen method was used to obtain the MIC<sub>100</sub> values for the compounds **33-34**. Three different broths were used: MHB, CM5, and NB. Different broths were used to see if the broth had any effect on the bacterial growth. MHB is the standard by which the European committee on antimicrobial susceptibility testing (EUCAST) and the clinical and laboratory standards institute (CLSI) use, NB is a good general medium, supports the growth of most bacteria. The control measurement for these glycosides **33-34** are the free compound 2-benzyl phenol (BP, **42**) and bis(2-hydroxyphenyl)methane) (HPM, **43**).

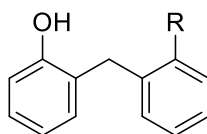
### 2.3.2.4 Microbiological results for $\beta$ -2-benzylphenol glycosides and $\beta$ -bis(2-hydroxyphenyl)methane glycosides

In Table **11**, the MIC values for the free drugs, BP **42** and HPM **43**, are shown in two different media, NB and MH. As can be seen the media has very little effect on the MIC<sub>100</sub> data for the same compound. The difference between these two compounds is an extra hydroxyl which is present in HPM in the *ortho* position on second ring. Firstly, there very little differences between the two different broths, NB and MH. Without the hydroxyl present, the MIC values were improved in *Streptococcus agalactiae*, *Streptococcus pneumoniae* and *Streptococcus pyogenes*, highlighted in yellow.

A tool used preclinically to gain information about potential toxicity is ClogP. This is the measure of lipophilicity of a given compound, with the higher the ClogP value, the more lipophilic the compound. Many lipophilic antibiotics are less active against gram-negative bacteria. This is due to the structure of the outer membrane; it is composed of lipopolysaccharide molecules that form a hydrophilic environment. This gives the gram-negative protection against hydrophobic molecules.<sup>196</sup> Lipophilic compounds are capable

of diffusing through the lipid bilayer, which is the main entry for drugs in gram-positive bacteria. In Table 11, the ClogP data is shown. When comparing these compounds, the ClogP value for BP is slightly higher than HPM. This could mean that BP is slightly more toxic than HMP, which is seen in the results against *Streptococcus agalactiae*, *Streptococcus pneumoniae* and *Streptococcus pyogenes*.

**Table 11:** The MIC<sub>100</sub> data for the underivised compounds, BP **42** and HPM **43**. The NB and MHB refer to the media used in the bioscreen. NG – No growth. The ClogP data was calculated using Chem BioDraw Ultra software version 13.0. It is highlighted in yellow where the value  $\leq 64$   $\mu\text{g/ml}$ .



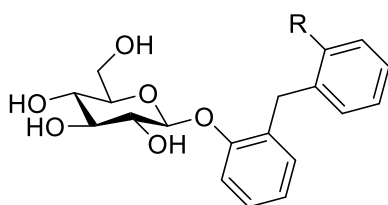
**42** R = H

**43** R = OH

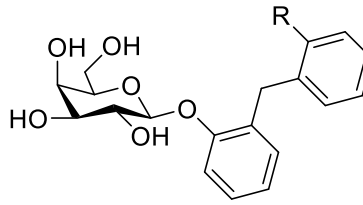
Organisms	MIC ( $\mu\text{g/ml}$ ) of various bis-phenyl parent compounds				
		NB		MHB	
	OCC	BP <b>42</b>	HPM <b>43</b>	BP <b>42</b>	HPM <b>43</b>
	ClogP	3.49	2.76	3.49	2.76
<i>B. cereus</i>	754	128	256	128	256
<i>E. faecalis</i>	640	128	>256	128	>256
<i>E. faecium</i>	220	128	>256	128	>256
<i>S. aureus</i>	100	NG	256	128	256
<i>S. epidermis</i>	691	128	256	128	256
<i>St. agalactiae</i>	182	64	128	64	256
<i>St. pneumoniae</i>		64	128	NG	256
<i>St. pyogenes</i>	163	64	128	64	256
<i>St. viridans</i>		128	256	128	256
<i>C. freundii</i>	851	128	256	128	256
<i>Cr. sakazakii</i>	1888	128	256	128	256
<i>En. cloacae</i>	760	>128	128	64	256
<i>Es. coli</i>	199	128	256	128	256
<i>K. pneumoniae</i>	758	128	256	128	256
<i>P. mirabilis</i>	2080	128	256	128	>256
<i>Ps. aeruginosa</i>	201	>128	>256	>256	>256
<i>Sa. typhimurium</i>	854	128	256	128	256
<i>Se. marcescens</i>	217	128	256	128	256

The results for the *Streptococci* bacteria could be a result from their uptake system which allows this compound **42** to be taken up when compared to the other bacteria that the bisphenolic compounds were analysed against. The glycosides, both glucosides and galactoside **33-34**, were also tested against the same bacteria species; the results are shown in Table 12.

**Table 12:** The MIC<sub>100</sub> data for the glycosidic compounds, BP and HMP. The broth is NB. NG – No growth. The ClogP data was calculated using Chem BioDraw Ultra software version 13.0. It is highlighted in yellow where the value  $\leq 64$   $\mu\text{g/ml}$



R= H **33a**  
R = OH **33b**



R= H **34a**  
R = OH **34b**

Organisms	MIC ( $\mu\text{g/ml}$ ) of various bis-phenyl moieties attached to various sugars.						
	OCC	<b>43</b>	<b>34b</b>	<b>34a</b>	<b>42</b>	<b>33b</b>	<b>33a</b>
	CLogP	2.76	1.33	1.33	3.49	2.05	2.05
<i>B. cereus</i>	754	256	>256	>256	128	>256	>256
<i>E. faecalis</i>	640	>256	>256	>256	128	>256	>256
<i>E. faecium</i>	220	>256	>256	>256	128	>256	>256
<i>S. aureus</i>	100	256	>256	>256	NG	>256	>256
<i>S. epidermis</i>	691	256	>256	>256	128	>256	>256
<i>St. agalactiae</i>	182	128	>256	>256	64	>256	>256
<i>St. pneumoniae</i>	1548	128	>256	>256	64	>256	>256
<i>St. pyogenes</i>	163	128	>256	>256	64	>256	>256
<i>St. viridans</i>	1638	256	>256	>256	128	>256	>256
<i>C. freundii</i>	851	256	>256	>256	128	>256	>256
<i>Cr. sakazakii</i>	1888	256	>256	>256	128	>256	>256
<i>En. cloacae</i>	760	128	>256	>256	>128	>256	>256
<i>Es. coli</i>	199	256	>256	>256	128	>256	>256
<i>K. pneumoniae</i>	758	256	>256	>256	128	>256	>256
<i>P. mirabilis</i>	2080	256	>256	>256	64	>256	>256
<i>Ps. aeruginosa</i>	201	>256	>256	>256	>128	>256	>256
<i>Sa. typhimurium</i>	854	256	>256	>256	128	>256	>256
<i>Se. marcescens</i>	217	256	>256	>256	128	>256	>256

The table shows the bioscreen results with the broth NB. As can be seen, the glycosides had the same MIC values. This could be due to the timescale over which the bioscreen ran, or that the concentrations used of the drug were too weak. The glycosides also had higher MIC values when compared to their underivatised counterparts when the same method was employed. This signifies that the glycosides are not as biological active against the bacteria in the same timescale as the parent compounds. This is not entirely unexpected as the cleaving of the sugar from the prodrug compound should delay the release of the drug; this in turn could make the glycosides less toxic on the same timescale as the parent compound. The ClogP values were also decreased in the glycosidic compounds when compared to their respective parent compounds. As previously described in Section 1.2.1, prodrugs are converted to the active compound at the target compound, which may take an amount of time. This hypothesis is also shown in work on carbohydrate prodrugs performed by Dr. Brierley.<sup>142</sup>

The glycosidic compounds **24-25** were also analysed in MHB and CM5. The results for these are shown in Table 13. The glycosides, again, had very high MIC values, similar values to that of them shown in NB.

**Table 13:** The MIC<sub>100</sub> data for the glycosidic compounds, **33** and **34**. The broth is MHB and CM5. NG – No growth. It is highlighted in yellow where the value ≤ 64 µg/ml

Organisms	MIC (µg/ml) of various bis-phenyl moieties with their corresponding glycosides.											
	OCC	MHB					CM5					
		43	34b	34a	42	33b	43	34b	34a	42	33b	33a
<i>B. cereus</i>	754	256	>256	>256	128	>256	256	>256	>256	128	>256	>256
<i>E. faecalis</i>	640	>256	>256	>256	128	>256	>256	>256	>256	128	>256	>256
<i>E. faecium</i>	220	>256	>256	128	128	>256	>256	>256	128	128	>256	128
<i>S. aureus</i>	100	256	>256	256	128	>256	256	>256	256	128	>256	256
<i>S. epidermis</i>	691	256	>256	>256	128	>256	256	>256	>256	128	>256	>256
<i>St. agalactiae</i>	182	256	>256	>256	64	>256	256	>256	>256	64	>256	>256
<i>St. pneumoniae</i>	1548	256	NG	NG	NG	NG	256	256	>256	64	256	>256
<i>St. pyogenes</i>	163	256	256	>256	64	256	256	>256	>256	128	>256	>256
<i>St. viridans</i>	1638	256	>256	>256	128	>256	256	>256	>256	128	>256	>256

<i>C. freundii</i>	851	256	>256	>256	128	>256	256	>256	>256	128	>256	>256
<i>Cr. sakazakii</i>	1888	256	>256	>256	128	>256	256	>256	>256	128	>256	>256
<i>En. cloacae</i>	760	256	>256	>256	64	>256	256	>256	>256	64	>256	>256
<i>Es. coli</i>	199	256	>256	>256	128	>256	256	>256	>256	128	>256	>256
<i>K. pneumoniae</i>	758	256	>256	>256	128	>256	>256	>256	>256	128	>256	>256
<i>P. mirabilis</i>	2080	>256	>256	>256	128	>256	>256	>256	>256	>256	>256	>256
<i>Ps. aeruginosa</i>	201	>256	>256	>256	>256	>256	256	>256	>256	128	>256	>256
<i>Sa. typhimurium</i>	854	256	>256	>256	128	>256	256	>256	>256	128	>256	>256
<i>Se. marcescens</i>	217	256	>256	>256	128	>256	256	>256	>256	128	>256	>256

### 2.3.3 Structure-activity relationships between the bisphenol moiety glycosides

Using the data collected in Chapter 2, SAR can be deduced. Figure 24 shows a summary of the SAR collected. The addition of the carbohydrate to one of the free hydroxyls produced lower MIC values when compared to their respective parent compounds. This is to be expected as it will require additional time to cleave the sugar from the bisphenol moiety. When referring to the prodrug approach this is one of these advantages, the carbohydrate was masking the drug producing a less toxic drug and the drug is released once enzymes cleave the sugar to produce the toxic compound. When comparing BP and HPM, the free compounds had the same MIC values in the different broths used. They also had very similar values, with BP being slightly more biologically active against *Streptococcus agalactiae*, *Streptococcus pneumoniae*, *Proteus mirabilis* and *Streptococcus pyogenes*. This is to be expected when ClogP is taken into consideration, with BP having a slightly higher ClogP value.

When the glycosides were analysed, the glucosides and galactosides of BP and HPM had the same MIC values. They all had values over  $>258 \mu\text{g/mL}$  over a 24 h time period. The compounds **33-34** and **42-43** were compared to previously synthesised compounds **35-37**, and the latter compounds had lower MIC values. In the compounds **35-37**, both the parent compounds and the glycoside had lower MIC data. The only difference between **33** and **35-37** is the amount of halogens present. The compounds **33** contained no halogens and had higher MIC values. As more halogens were added to the aromatic rings, the lower the MIC obtained, with **39**, as a parent compound, having values of  $<0.5 \mu\text{g/mL}$  for all the gram-positive bacteria tested. The glycosides of this compound, **42a** and **42b**, had similar activity to **49a** and **49b** which were higher values than their respective parent compounds.

For **33-34** there were no difference between the glucosides and galactosides, all had the same values. For **40a** and **40b**, the galactosides performed better with lower MIC values, a similar

trend was also seen in **39a** and **39b**. However in **39a** and **39b**, the glucosides had the same values as **39b** or slightly lower MIC data. This information is shown in Figure 24.

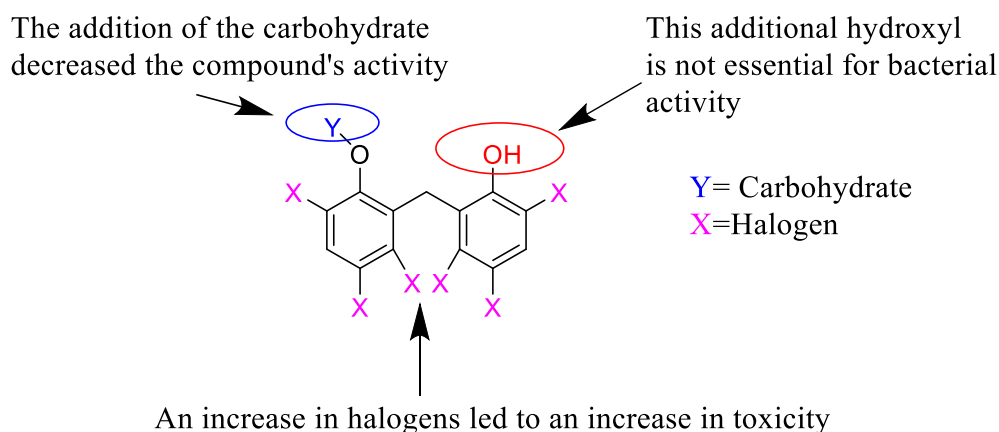
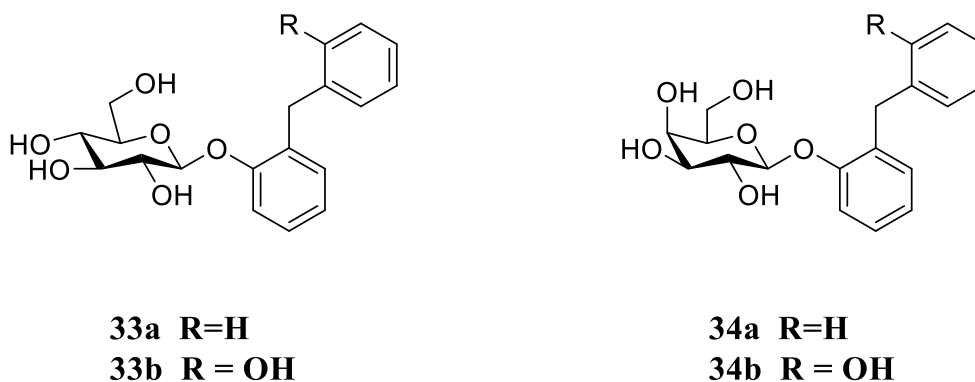


**Figure 24:** A diagram showing the SAR collected from the different bisphenol moieties attached as glucosides and galactosides.

## 2.4 Conclusion

The target compounds **33-34**, found in Figure 25, were synthesised using an aq. NaOH glycosylation method. The  $\beta$ -anomers were synthesised, as can be seen from the  $^1\text{H-NMR}$  spectra, by analysing the  $J$  values of doublet for the anomeric centre. The compounds **33-34** were analysed using a HPLC method and were found to all have >99% purity.



	<b>33a</b>	<b>33b</b>	<b>34a</b>	<b>34b</b>
Yields (%)	9	15	7	11
Purity (%)	99	99	99	99

**Figure 25:** The target structure **33-34**, with their respective yields and purities shown.

When synthesising these compounds, **33-34**, there was a slight difference between the yields. Compounds **33b** and **34b** may have had hydrogen bonding stability with the extra hydroxyl present in the aromatic ring not involved with the glycosylation. This led to slightly greater yields in **33b** and **34b**.

The MIC data was collected and compared to their respective parent compounds, as well as to previously synthesised compounds that contain various bisphenol moieties, **35-37**. Thus, SAR data could be deduced. In the underivatised compounds, **42** and **43**, there was a correlation between ClogP values and MIC data. Against the bacteria *Streptococcus agalactiae*, *Streptococcus pneumoniae* and *Streptococcus pyogenes*, **42** had MIC values of 64 µg/mL and a ClogP value of 3.49. In comparison, **43** had a ClogP value of 2.76 and observed no notable MIC values against all the bacteria tested. Once a glycoside was added to the bisphenol moiety, the MIC values for all the bacteria were >258 µg/mL.

SAR data was collected from comparisons between compounds **35-37**, **33-34** and **42-43**. The extra hydroxyl that is present in all the compounds other than **43** was shown to not be essential for biological activity. Once halogens were added to the aromatic rings, in varying amounts and what halogens were present, the MIC values decreased. Hex **39** was found to be particularly active against gram-positive bacteria, with all the ones it was tested against had MIC values of  $>0.5 \mu\text{g/mL}$ . Compared to **43**, once these chlorine groups were removed the values for the gram-positive bacteria were 128-  $>258 \mu\text{g/mL}$ .

**Chapter 3 – The synthesis and  
microbiological evaluation of triazole  
containing compounds based on  
azidothymidine**

### 3.1 Introduction

This group of compounds, structures shown in Figure 26, was designed to probe the biological activities of 1,2,3-triazoles derived from AZT, also known as Zidovudine. AZT was first marketed as an antiviral agent, but activity against gram-negative bacteria has also been reported.<sup>197</sup> As the 1,2,3-triazole functionality is also reported to enhance antibacterial activities of compounds, this work sought to determine any benefits from combining the AZT moiety with a triazole moiety for antibacterial activity.

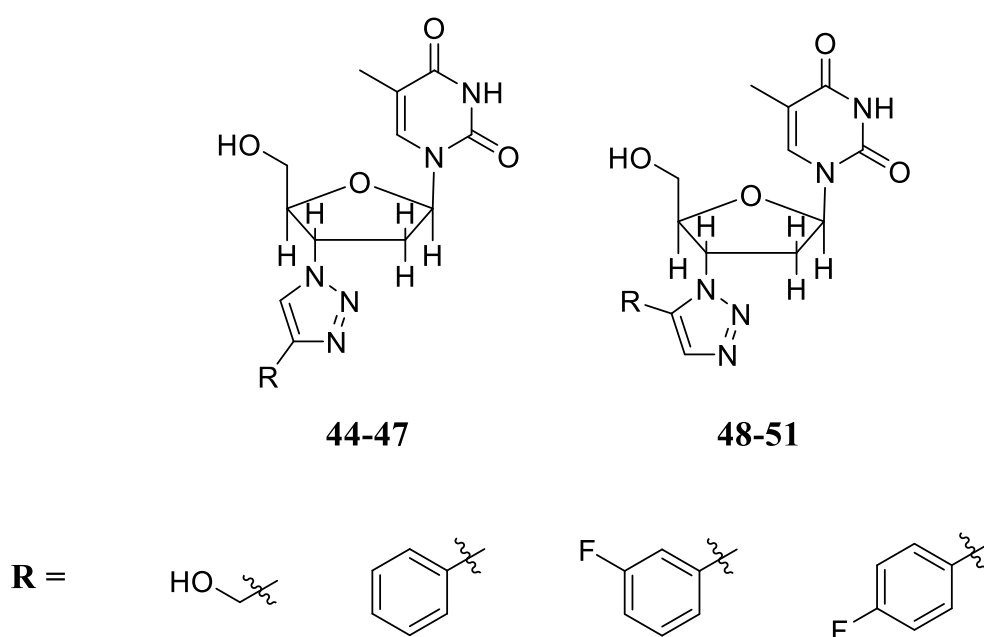


**Figure 26:** The basic structures for this series of compounds. In **44-51**, the R groups are shown below the target compounds.

#### 3.1.2 The history and further development of AZT

AZT **52** is an antiretroviral used for the prevention and treatment of human immunodeficiency virus (HIV) and acquired immune deficiency syndrome (AIDS). AZT is described as a nucleoside derived HIV reverse transcriptase drug, and is a potent inhibitor of HIV replication due to an inhibition of HIV reverse transcriptase for DNA synthesis.<sup>198</sup> There have also been

other nucleoside based drugs released, shown in Figure 27. They are shown with their ID<sub>50</sub> (infectious dose) values, AZT has the lowest values of the nucleosides tested, in both HIV type 1 and 2.<sup>148</sup> After it was released as an anti-HIV therapy, it was discovered that **52** also had antimicrobial properties.<sup>197</sup> The structure of AZT **52** is close to that of thymidine **53**, which is a DNA base. The two structures can be seen in Figure 27, the only difference between them is the functional group present in the 3' position.

Compounds	ID <sub>50</sub>	
	HIV-1	HIV-2
<b>52</b>	0.05	0.08
<b>54</b>	1.2	2.8
<b>55</b>	3	3.5
<b>56</b>	2.1	5.6
<b>57</b>	0.2	0.35
<b>58</b>	0.7	1.3
<b>59</b>	0.4	-

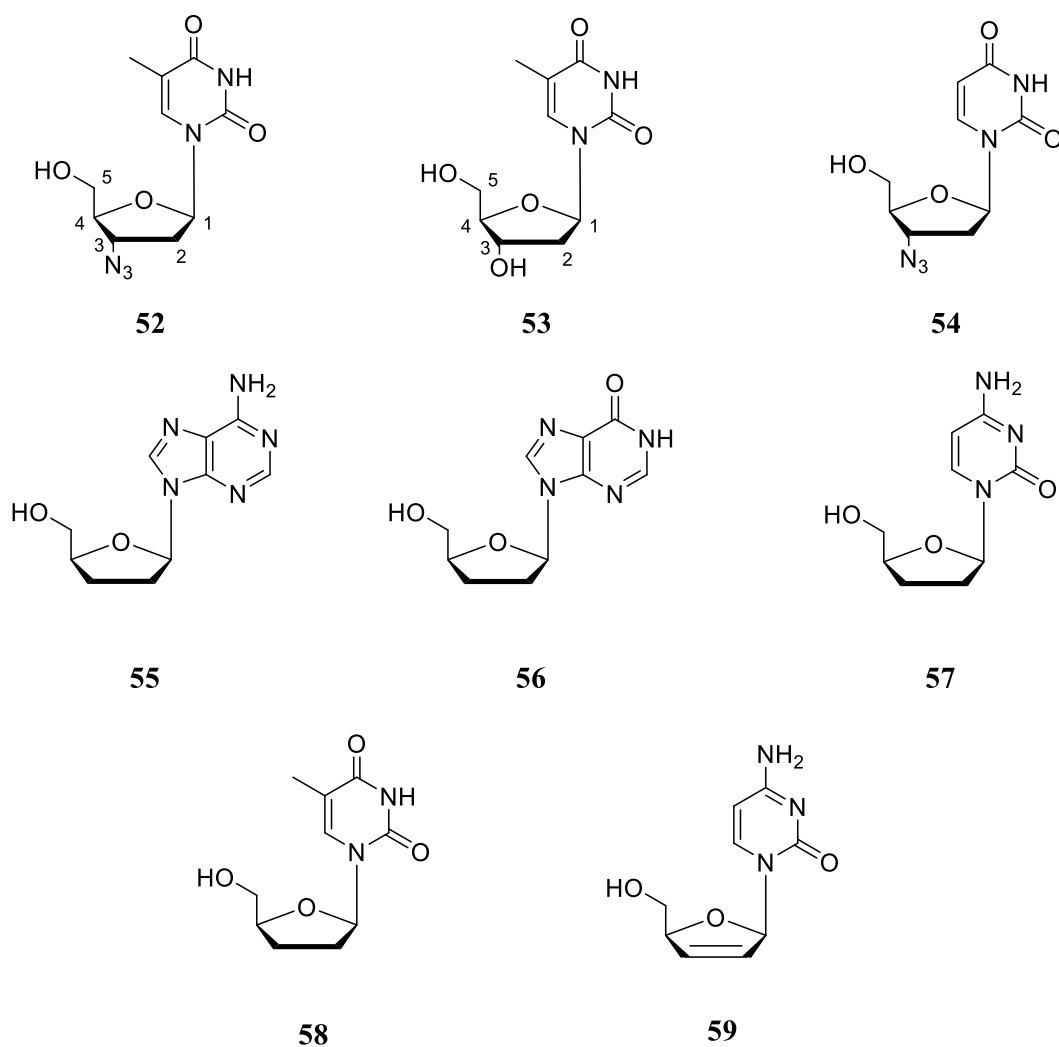


**Figure 27:** The structure of Azidothymidine **52** and thymidine **53**. The hydroxyl on the 3' position of the thymidine is replaced with an azido group in AZT **52**. The ID<sub>50</sub> is displayed for **54-59**. Adapted from ref. 146.

Whilst AZT **52** was first tested and used for the treatment of HIV and AIDS, nucleosides have also been tested for use as antibiotics.<sup>199</sup> An example of a synthetic nucleoside with antibacterial properties is 2',3' dideoxyadenosine. This has a similar structure to adenosine, with the absence of the two hydroxyls present at the 2' and 3' - positions. This was found to inhibit DNA synthesis in most gram-negative bacteria, as there is no hydrogen bond donor in the 3' position and this contributes to the compound inhibiting DNA. It was found to be lethal against *Es. coli*,<sup>200</sup> with inhibitory effects at 0.1  $\mu\text{mol/mL}$ .<sup>201</sup> This result, among others, started the interest into synthetic nucleosides as antimicrobial compounds. There was a high-throughput screen (HTS) performed on compounds for potential antimicrobial properties and AZT **52** was observed to be potent. The HTS assay was based on a screen-counterscreen approach and used *Klebsiella pneumoniae* BIDMC12A.<sup>202</sup> It was found to have bactericidal properties against various *Enterobacteraceae* members, with a MIC range of 0.3-2.0  $\mu\text{g/mL}$  against *Enterobacter aerogenes*.<sup>197</sup> Later, it was discovered that its mechanism of action involves phosphorylation at the 5' hydroxyl position. It is metabolically activated to the nucleotide, using deoxythymidine (dThd) kinases. This enzyme phosphorylates the 5' position to AZT-triphosphate **62**; this can then in turn act as a DNA chain terminator. It was discovered that the di- **61** and mono- **60** phosphate compounds were less potent.<sup>197</sup> There are several enzymes involved to create the potent AZT-triphosphate; namely dThd, thymidylate (dTMP) and nucleoside-diphosphate (NDP) kinases.<sup>203</sup> Thymidine kinases are present in many organisms, including viruses. Cellular cytoplasmic thymidine kinase 1 (TK1) catalyses the intracellular phosphorylation of AZT **52** into the corresponding monophosphate compound. Further kinases are used to catalyse the additional phosphorylations.<sup>204</sup> These enzymes are not found in gram-positive bacteria and are also not present in *Pseudomonas aeruginosa*.<sup>205</sup> AZT-triphosphate **62** is then incorporated into DNA causing it to terminate the azide in the 3'-position stops the hydrogen bonding within the DNA. The mechanism can be seen in Figure 28.<sup>203</sup>

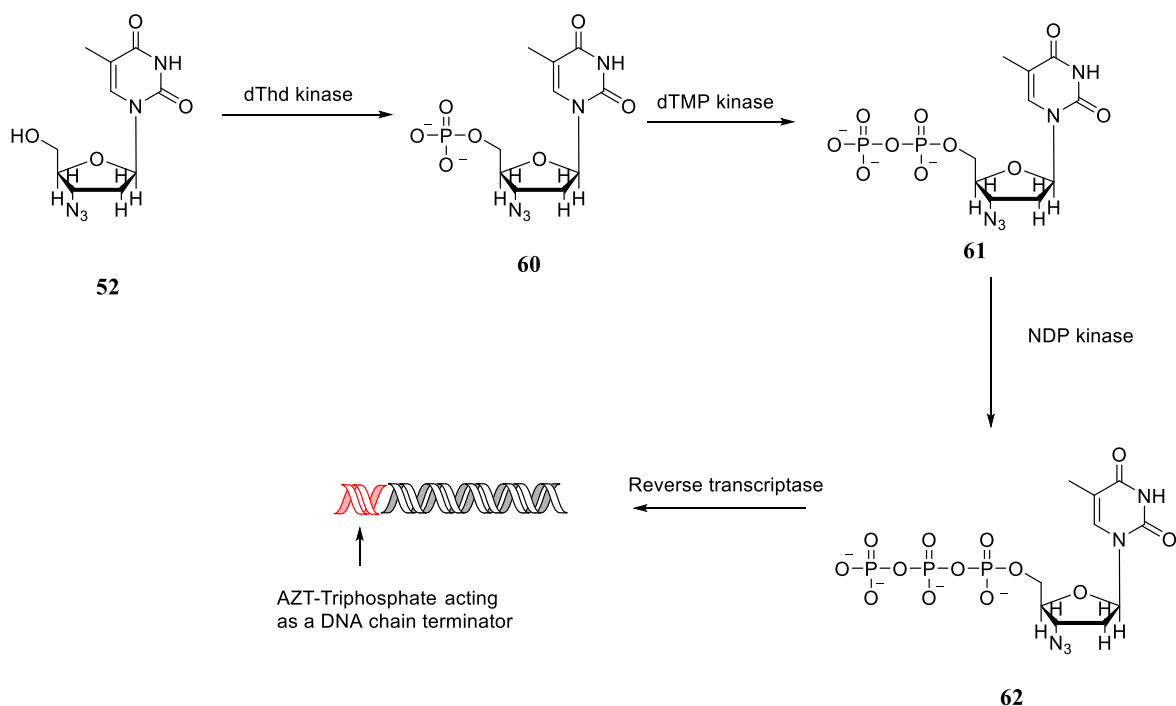


**Figure 28:** The mechanism of action for AZT **52**. The use of enzymes allows for the active metabolite (AZT-triphosphate **62**) to be synthesised and used as a DNA chain terminator. Adapted from ref. <sup>203</sup>.

Although AZT **52** is still used today for treating HIV and AIDS, there are still many side effects associated with the drug which result in limited clinical use. It is a known bone marrow suppressant, causes severe anaemia, as well as hepatic abnormalities and myopathy.<sup>206,207</sup> Along with these side effects, the drug is also limited pharmacologically.<sup>208</sup>

### 3.1.3 Nucleoside based prodrugs

Prodrugs have proven to be effective for providing more pharmacokinetically or bioavailable compounds of active drugs. The common prodrugs of **52** involve modification of the 5'

position, by using different functional groups. There are two main groups of prodrugs that have been studied: ester derivatised and masked phosphate compounds.

Ester prodrugs of AZT have been the main focus of most studies into prodrugs of AZT **52**. Esters as a functional group have ideal features, they can enhance lipophilicity and oral absorption, but can be chemically broken down in the body by uses of the enzyme esterase. These prodrugs have been tested for a variety of different biological activities; including anti-HIV, anticancer and antimicrobial. The prodrugs shown in Figure 29 have been tested against a variety of different bacteria, compounds **63-66** were tested against fifteen different bacteria and among them different strains of the same bacteria. As expected, the compounds were not active against gram-positive bacteria but were all active against *Klebsiella pneumoniae* and *Klebsiella oxytoca*. **63** performed better than the parent compound, with **64** having the same MIC value. The prodrugs present in **60** and **61** contain an antibiotic, norfloxacin and ciprofloxacin, respectively. These prodrugs performed better when compared to **67** and **68**, which did not contain an antibiotic attached to AZT. They worked well in both gram-positive and gram-negative bacteria, with **69** performing nearly as well as the parent drugs.

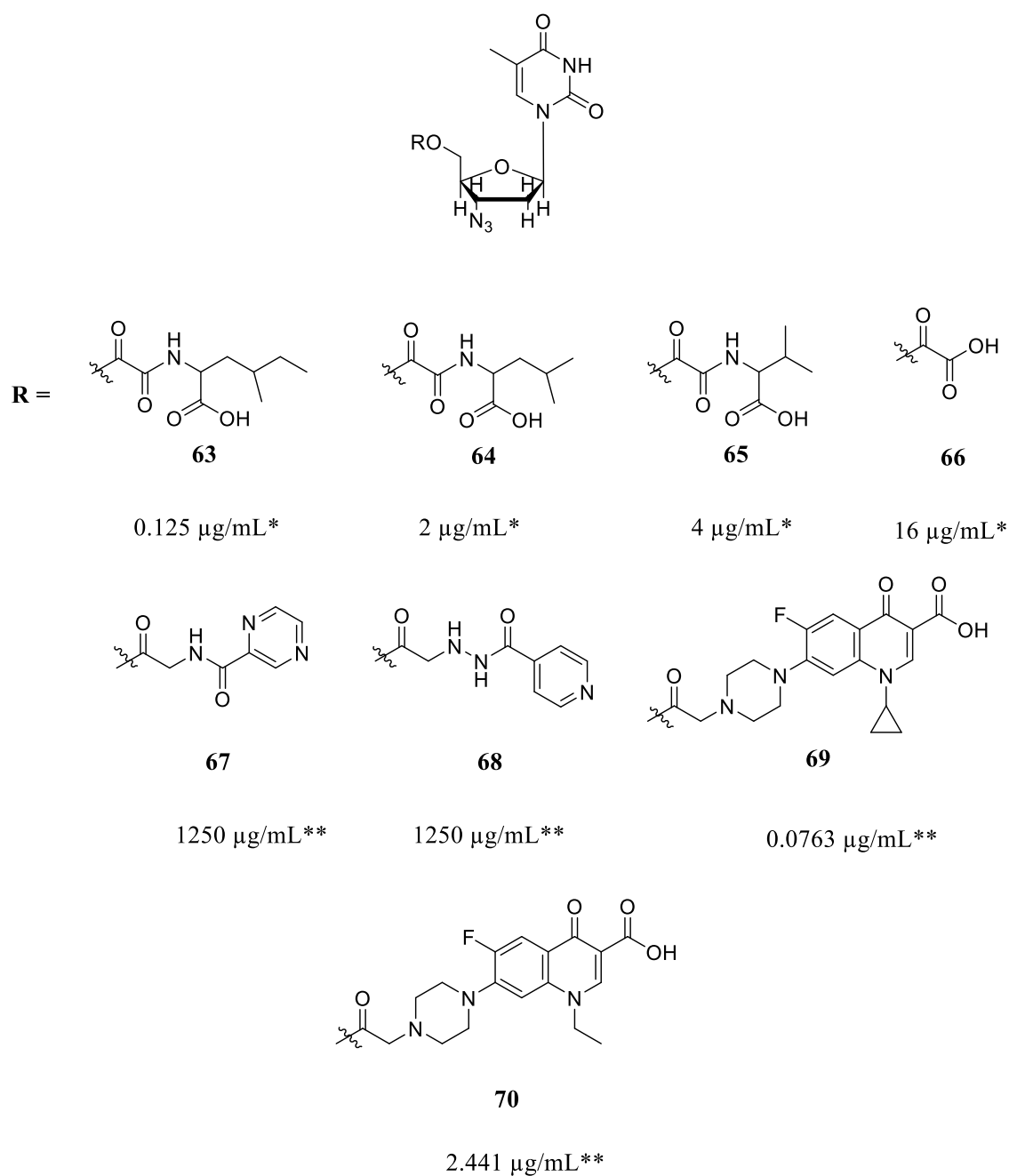


**Figure 29:** Examples of ester prodrugs of AZT. **63-70** are reported in ref. <sup>209</sup>, **67-70** in ref. <sup>210</sup>. The MIC data is presented below each compound. **63-66** MIC was assayed using MHB against *Klebsiella pneumoniae* ATCC 10031. **63-70** were assayed using Mueller-Hinton broth against *Klebsiella pneumoniae*. \* compared to the parent compound, AZT **52**, which had an MIC= 2  $\mu\text{g/mL}$ . \*\* compared to commercial antibiotics: Norfloxacin MIC = 0.0381  $\mu\text{g/mL}$  and ciprofloxacin MIC = 0.0381  $\mu\text{g/mL}$ .

### 3.1.3.1 1,2,3-Triazoles

There are many triazole containing compounds with a range of different properties: examples of these include anti-HIV,<sup>211</sup> anti-influenza agents,<sup>212</sup> anti-cancer,<sup>213</sup> and antimicrobial compounds.<sup>214-217</sup> Due to these properties, the triazole functional group is being explored as an avenue for novel antibiotics. Another avenue being explored as drug modifications for AZT is adding a 1,2,3-triazole moiety. Promising results for some 1,4-isomers are shown in Figure 30.<sup>218</sup>

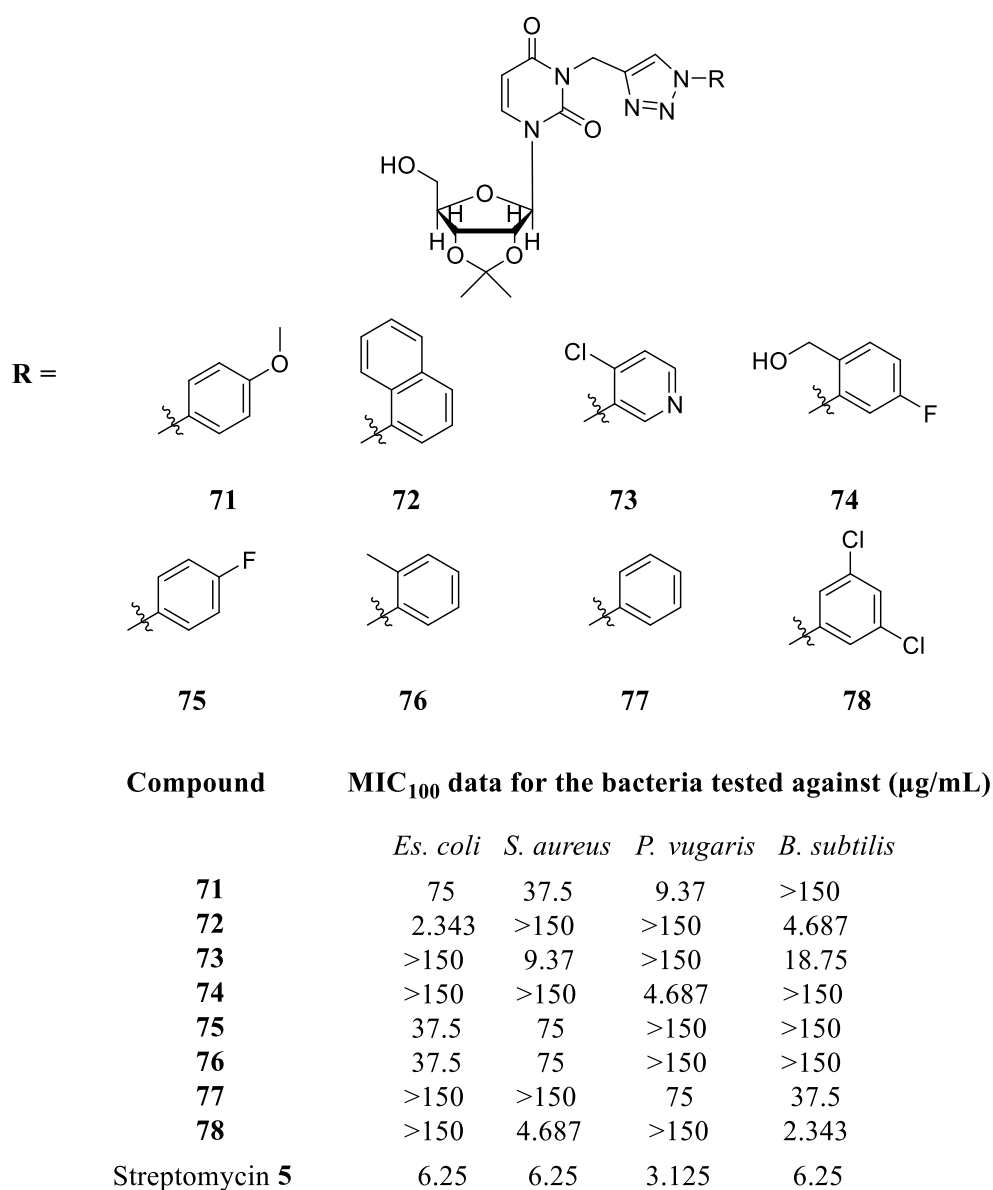


**Figure 30:** The structures **71-78** which were tested against various bacteria. These are from ref. 217. The MIC data is also displayed for compounds **71-78**.

The compounds were tested against 4 different bacteria, two gram-negative and two gram-positive. The addition of a halogen to the phenyl group increased its activity against *S. aureus*. The addition of a fluoride, **75**, also increased the activity in *Es. coli* when compared to **77**. The addition of two halogens to the phenyl group increased the activity in *B. subtilis* and performed better than the standard it was tested against, streptomycin **5**.

The prodrugs shown in Figure 31 were all tested to assess their efficiencies to inhibit *Ureaplasma parvum* thymidine kinase (*UpTK*) and human thymidine kinase 1 (hTK1). *Ureaplasma parvum* are bacteria belonging to the family *Mycoplasmataceae* found in the human urinary and genital tracts with a gram-positive shape. All the compounds **79-84** phosphorylated more efficiently with *UpTK* when compared to hTK1. Compound **80** was also 5 times more potent with *UpTK* than hTK1 *in vitro*.<sup>75</sup> The higher efficiency with *UpTK* the lower the effect on the host cells when compared to the bacterial cells.

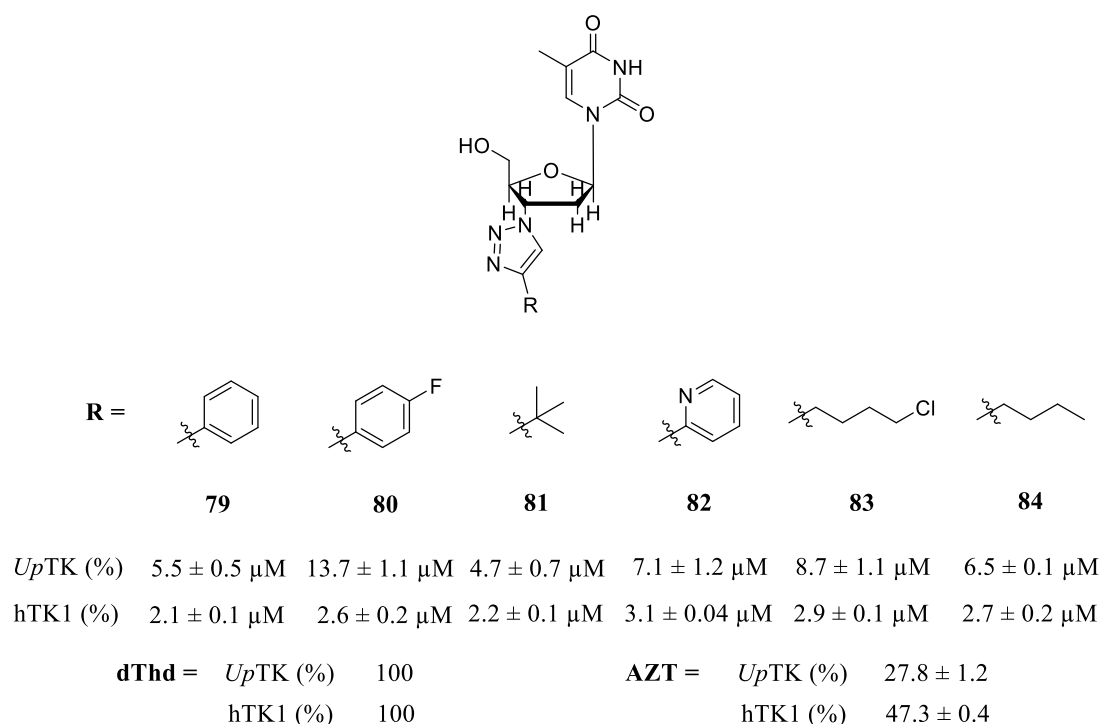
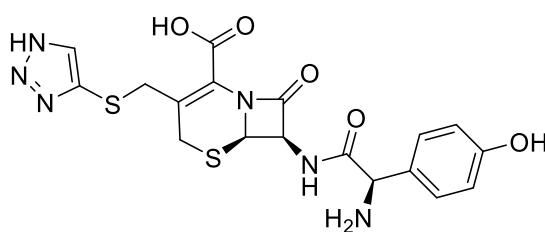


**Figure 31:** Compounds **79-84**, which all contain a 1,2,3-triazole in the 3' position. The data is showing the phosphorylation by *UpTK* and hTK1, with 100 M ATP and the nucleosides, respectively. The data is presented as relative activity (%) when compared to dThd. Data from ref.<sup>75</sup>.

In the previous section, compounds **68-84** all contained triazoles and were used to explore anti-HIV and antimicrobial activities. Cefatrizine **85** is an example of a clinically used drug that contains a triazole moiety. It is a broad spectrum antibiotic and inhibits the final cross-linking stage of peptidoglycan production, thus it is a bacterial cell wall synthesis inhibitor. It is used in some gram-positive infections, the exception being *Enterococci* bacteria. The MIC data is shown in Figure 32. The drug is well tolerated with limited toxicity being detected in the liver or renal area.<sup>219,220</sup>



**85**

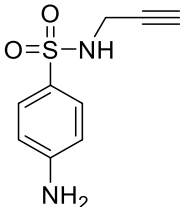
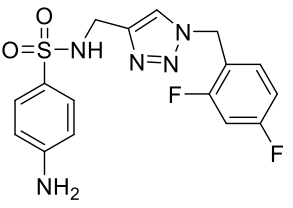
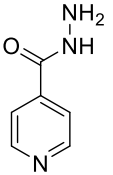
	<i>S. aureus</i>	<i>S. epidermidis</i>	<i>Es. coli</i>	<i>P. vulgaris</i>	<i>S. typhi</i>	<i>S. dysenteriae</i>
<b>MIC data</b>	1 µg/mL	1 µg/mL	4 µg/mL	32 µg/mL	8 µg/mL	2 µg/mL

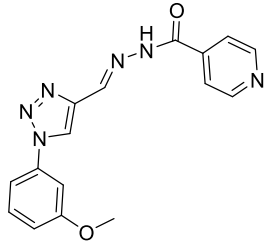
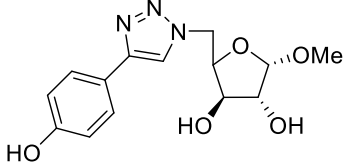
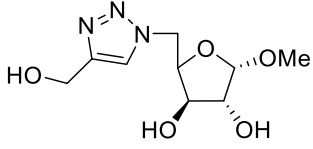
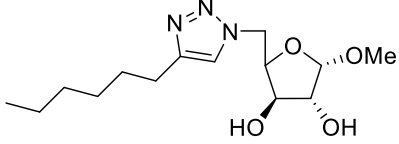
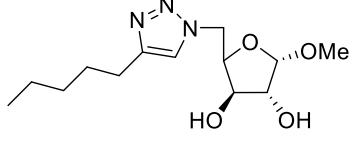
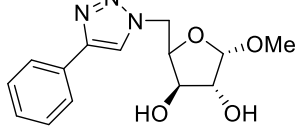
**Figure 32:** Cefatrizine **76** is a commercial drug that contains a 1,2,3,-triazole. The MIC data (µg/mL) is displayed, with good activity against the bacteria shown. Data from ref. 218.

Other examples of antimicrobial 1,2,3-triazole containing compounds are shown in Table 14. The precursor **86** was tested for its inhibitory activity and was found to have no activity. The triazole attached to an aromatic moiety drastically enhanced the activity thus providing some evidence that the triazole is of biological significance.<sup>217</sup> Isonicotinylhydrazine **88** (INH), is an active oral drug that is highly active against *Mycobacterium tuberculosis* and bacteriostatic on the *Bacillus* family. Its mechanism of action is the interference with a pathway that is responsible for cell wall synthesis. It is, however, toxic to the liver so there was a need to design a different drug. The 1,2,3-triazoles exhibited similar MIC values as INH for mycobacterial

activity. Compound **89** exhibited lower toxicity and fewer side effects compared to INH this could be because the hydrazine is protected using the triazole.<sup>214</sup> There has already been interest in carbohydrates tethered to a triazole for the purposes of antimicrobial agents. Triazole **90**, a xylose tethered to a 1,2,3-triazole, was synthesised with a multitude of alkynes to incorporate differing R<sup>1</sup> groups. Compound **90D** showed moderate activities against *M. tuberculosis*.<sup>215</sup>

**Table 14:** Antimicrobial compounds containing 1,2,3-triazole moieties. MIC ( $\mu\text{g/mL}$ ) for compounds **86** and **87** were determined by two-fold serial dilution method for microdilution plates. Compounds **90** the lowest concentration of the compound which inhibits the growth of mycobacterium >90%. n.d.= not determined

Compound	Structure	MIC <sub>100</sub> Data ( $\mu\text{g/mL}$ )							Ref.
		<i>S. aureus</i>	<i>B. subtilis</i>	<i>Es. coli</i>	MRSA	<i>P. aeruginosa</i>	<i>M. tuberculosis H37Ra</i>	<i>M. tuberculosis H37Rv</i>	
<b>86</b>		>512	>512	>512	>512	>512	n.d.	n.d.	217
<b>87</b>		64	128	16	128	16	n.d.	n.d.	
<b>88</b>		n.d.	n.d.	n.d.	n.d.	n.d.	n.d.	0.06	214

<b>89</b>		n.d.	n.d.	n.d.	n.d.	n.d.	n.d.	0.62	
<b>90A</b>		n.d.	n.d.	n.d.	n.d.	n.d.	>12.5	>12.5	
<b>90B</b>		n.d.	n.d.	n.d.	n.d.	n.d.	>12.5	>12.5	
<b>90C</b>		n.d.	n.d.	n.d.	n.d.	n.d.	>12.5	>12.5	215
<b>90D</b>		n.d.	n.d.	n.d.	n.d.	n.d.	>12.5	12.5	
<b>90E</b>		n.d.	n.d.	n.d.	n.d.	n.d.	>12.5	>12.5	

### 3.1.4 Justification for drug design

This series of compounds used ‘click’ chemistry to create a 1,2,3-triazole moiety in the 3’ position on the AZT ring. An advantage is that libraries of compounds can be quickly assembled, using a ‘click’ reaction. This allows many compounds to be generated and tested for their antimicrobial properties. From this, SARs can be defined and this can inform the synthesis of further libraries of triazoles. The proposed compounds are shown in Figure 33 . The 2 different isomers, 1,4- and 1,5-, were synthesised to explore the possibility of the position of the functional group affecting the activity.

As can be seen in Figure 33, the hydroxylated moiety was synthesised to explore whether the phosphorylation of the hydroxyl in the 5’ position on the AZT ring (blue circle) is affected if the hydroxyl on the 4- or 5-position on the 1,2,3-triazole ring (red circle) is present. Compounds **45** and **49** contain a benzyl group , it was found that a benzyl containing compounds gave lower MIC values than their alkyl counterparts.<sup>217</sup> A fluorine group attached to the benzyl group in different positions attached to the 1,2,3-triazole ring (pink circle) can interfere with its electronics and can in turn affect its metabolism and distribution.<sup>221,222</sup>

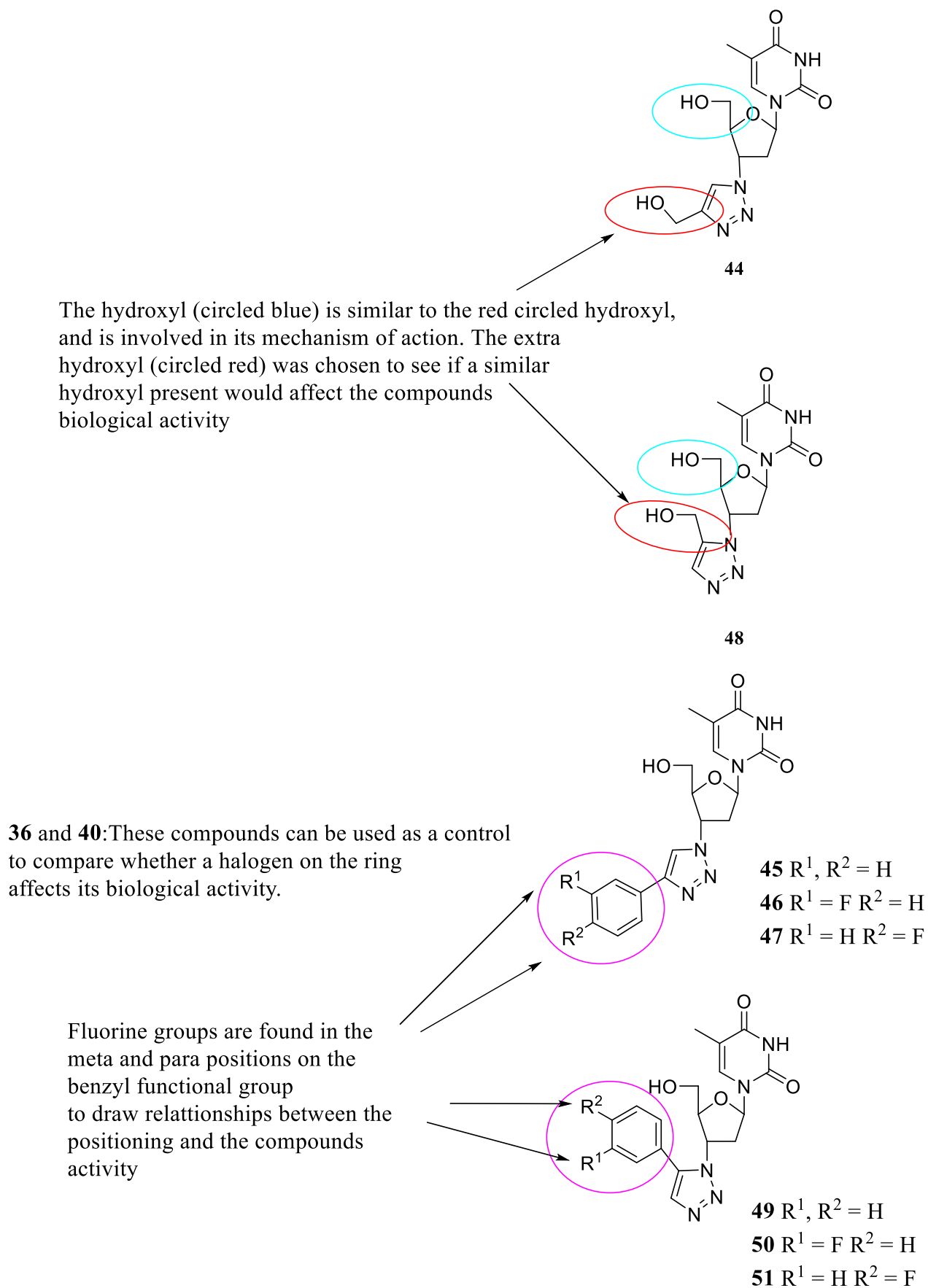


**Figure 33:** Annotated structures, **44-51**, showing the justification for their drug design.

### 3.2.1 Aims for the triazole based compounds

The aim of these triazole containing compounds was to create a family of prodrugs that contain AZT. This drug is a nucleoside based drug, whose mechanism of action involves enzymatic phosphorylation of the 5'-*O* position to produce AZT-triphosphate. This compound is then incorporated into DNA, with the azide present in the 3' position not allowing for hydrogen bonding between AZT and the DNA base pairs, hence causing DNA replication to terminate. This causes the death of the microbe as they are not able to produce DNA. There is, however, limited use of this drug as an antiviral or antimicrobial due to its severe side effects. To overcome these problems, compounds have been designed to try and mask AZT's activity until it is at the target site, to try and limit its side effects. These designed compounds **44-51** were synthesised to try and overcome the side effects by forming a triazole at the 3'-*N* position. These were then tested to see if they are viable and effective as antibacterials using various biological activity tests.

### 3.2.2 Objectives of the triazole based compounds

These aims will be achieved using synthetic methods to create the compounds **44-51**. A synthesis of the 1,2,3- triazoles was proposed using 'click' chemistry, which involves reactions between an azide and an alkyne, in a process that is expected to be high yielding, produce by-products (different by-products depending on the reactants used) which can be easily separated from the product, be stereospecific, simple to form and conducted in solvents that can be easily removed or are benign. This started to become popular after Sharpless described 'click chemistry' and its reactions.<sup>223</sup> Triazoles as an additional functional group are attractive for drug design as they are stable to metabolic degradation, improve solubility and are easy to

synthesise using the 'click chemistry' methods. The 1,4-isomer for the 1,2,3-triazole is formed by forming  $\text{Cu}^{\text{II}}$  *in situ*. The 1,5- isomer is produced by using a ruthenium catalyst. The  $\text{MIC}_{100}$  data was collected using a bioscreen method, using different media. A preliminary fitting model method was also used to probe the antiviral activities of these compounds.

### 3.3 Results and discussion

#### 3.3.1 Synthesis

##### 3.3.1.1 Synthetic route

'Click' chemistry has proven invaluable for the formation of 1,4- and 1,5- isomers of 1,2,3-triazoles using an azide, alkyne and different metal catalysts, dependant on which isomer is preferred. Originally, the 'click' reaction was performed using heat and stirring, also known as Huisgen 1,3-dipolar cycloaddition. This afforded a mixture of the 1,4- and 1,5- isomers. With the introduction of a metal catalyst either isomer can be selectively synthesised, the reaction schemes are shown in Figure 34. A copper catalyst is used in a copper-catalysed azide-alkyne cycloaddition (CuAAC) to produce the 1,4- isomer. A ruthenium catalyst is used to produce the 1,5- isomer in a ruthenium-catalysed azide-alkyne cycloaddition (RuAAC).

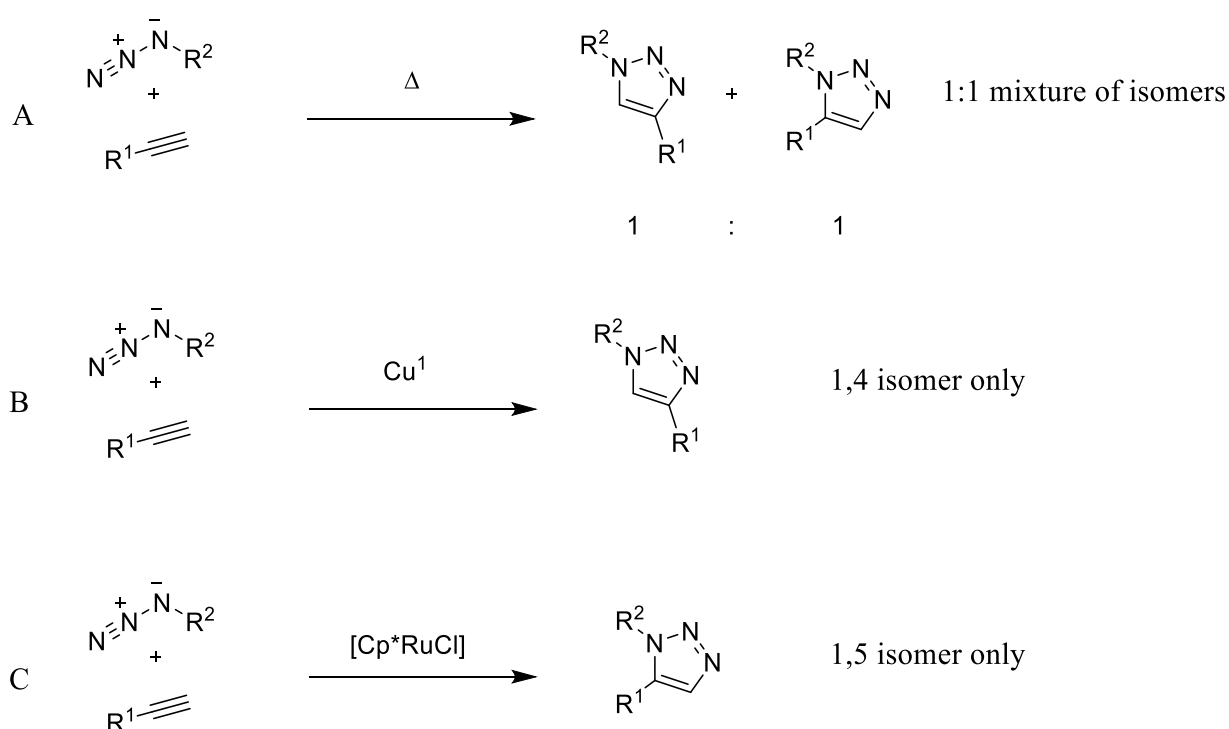


**Figure 34:** Three different 'click' reactions. (A) is the Huisgen 1, 3-Dipolar Cycloaddition, stereocontrol is achieved. (B) uses CuAAC and (C) uses RuAAC.

A general reaction scheme for the formation of the different isomers is shown in Figure 35, as well as the target compounds **44-51**.

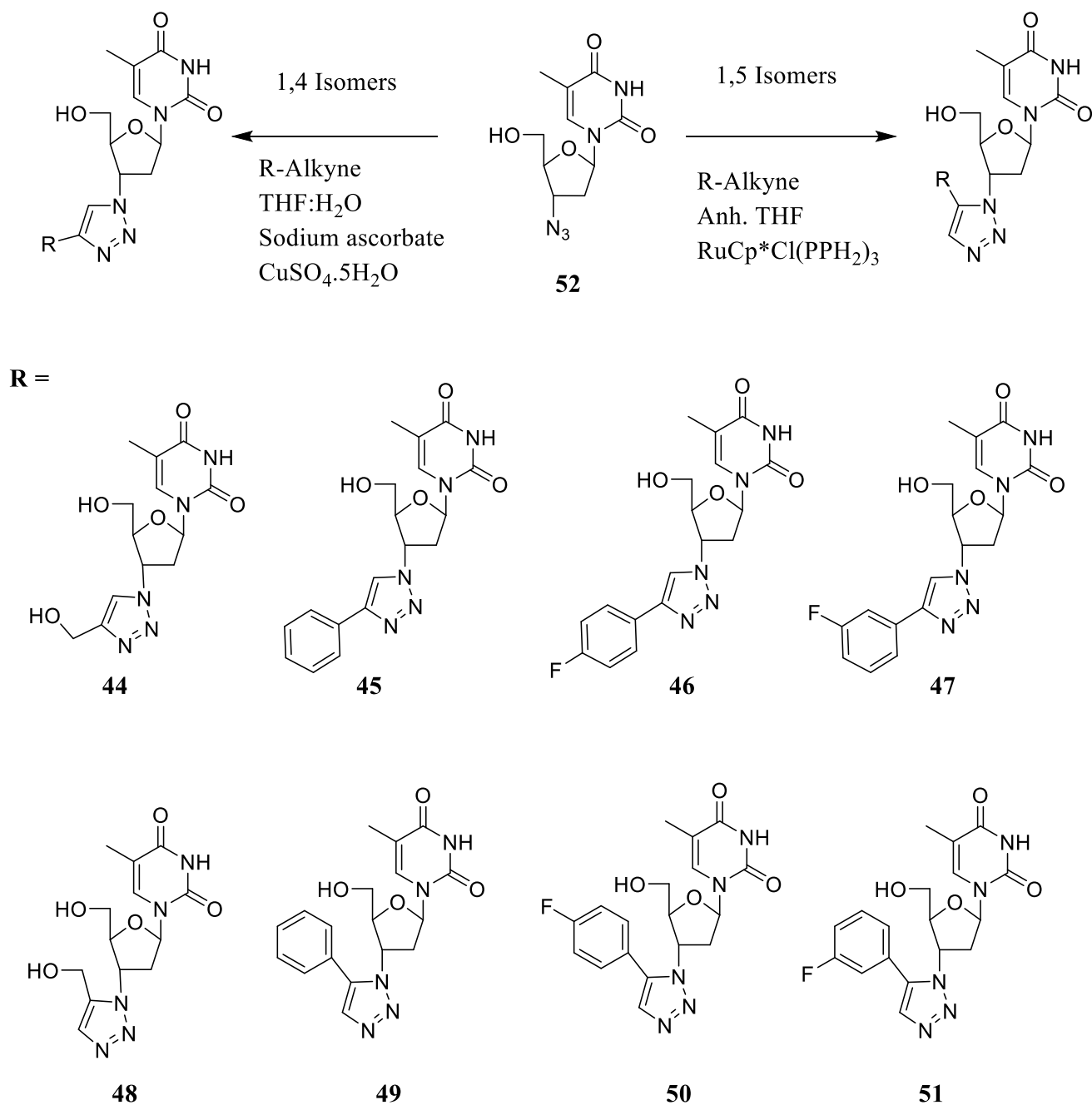


**Figure 35:** The general reaction schemes for the synthesis of the 1,4- and 1,5- isomers of the 1,2,3-triazoles. The target compounds **44-51** are shown below the general reaction

As previously mentioned, for the 1,4- isomer, a copper catalyst is used. The copper first forms a complex with the alkyne, which allows the carbon to attack the negatively charged nitrogen in the azide. In the azide, the terminal nitrogen is electrophilic, or Lewis basic, which allows it to interact with the  $\text{Cu}^{\text{I}}$ . The  $\sigma$ -bonded copper (I)-acetylide interacts with the terminal nitrogen. This complex then contracts and forms a 6-membered metallacycle, which constrains the  $\text{sp}$ -hybridised carbon present. This requires a lot of energy to activate, so there is a current theory that two copper ions are used to alleviate this constraint. This intermediate then forms the 1,4-triazole with the copper in the 5' position. This forms the final 1,4- product, and copper is then free to be reused, this can be seen in Figure 36.  $\text{Cu}^{\text{I}}$  is used as the copper catalyst; this is generally produced *in situ* with  $\text{Cu}^{\text{II}}$  salts and a reducing agent, this is usually sodium ascorbate.<sup>224</sup>

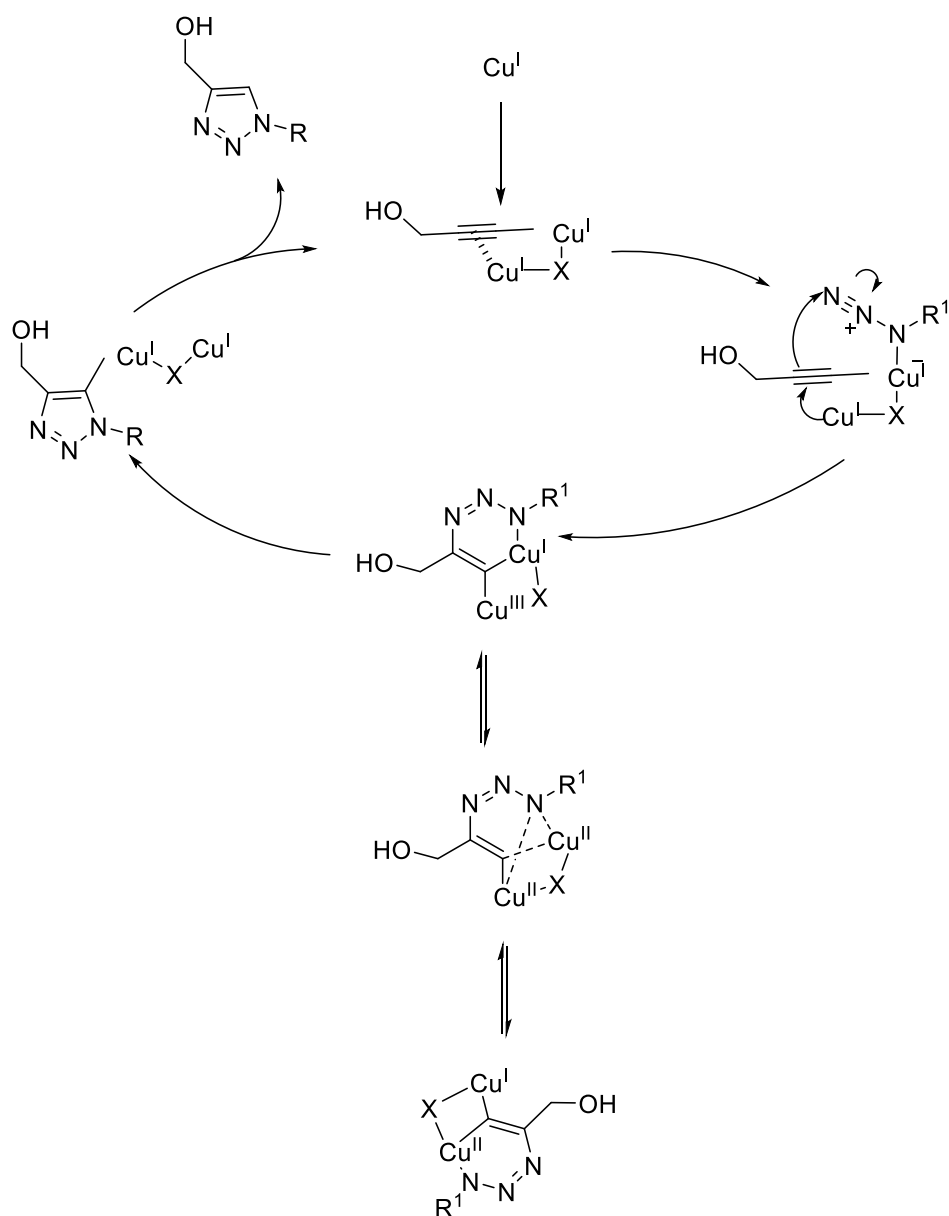


**Figure 36:** The copper catalytic cycle for the formation of a 1,4-isomer. Adapted from ref. <sup>224</sup>. R<sup>1</sup> = AZT, This shows the formation of **44**.

A different catalyst is used to create the 1,5-isomer. Commonly used catalysts for these formations contain ruthenium. In the ‘click’ reactions using RuCp\*Cl(PPh<sub>3</sub>)<sub>2</sub> it has been observed that the active component of the catalyst is [Cp\*RuCl].<sup>225</sup> The first part of this cycle starts with the alkyne and azide displacing the PPh<sub>3</sub> groups on the ruthenium, then the strained intermediate is formed using oxidative coupling of the alkyne group and the azide. Due to the

complex being bulky, the new bond is formed using the less sterically hindered carbon (containing the moiety present in the alkyne) and the terminal nitrogen in the azide. To form the triazole, the third compound undergoes reductive elimination, then the triazole is released and the catalyst regenerated. This can be seen in Figure 37.

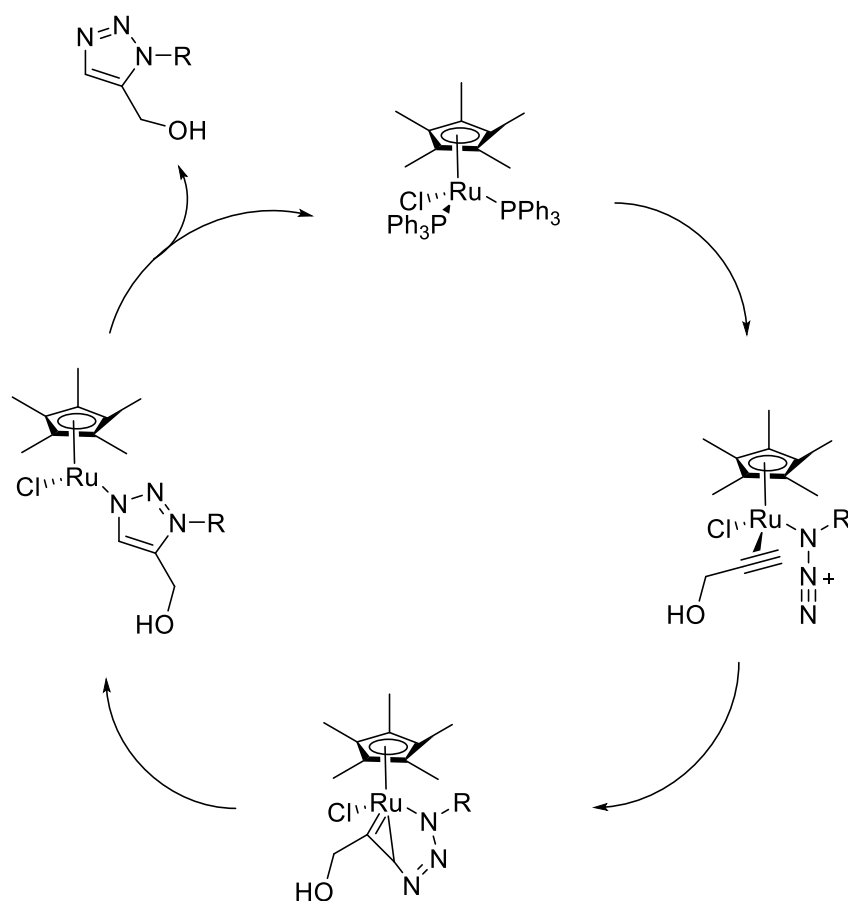
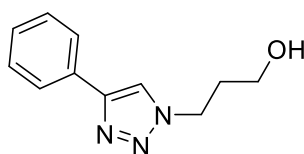


**Figure 37:** The ruthenium catalytic cycle for the formation of the 1,5-isomer. Adapted from ref. <sup>225</sup>. R = AZT. This figure displays the formation of **48**.

### 3.3.1.2 Optimisation of the formation of the 1, 4 isomer

Several experimental conditions were initially explored to synthesise the 1,4-isomer of the 1,2,3-triazole ring. Compound **91** was first synthesised for method development. It allowed to obtain which synthetic pathway was greater yielding, and therefore could be used for the AZT containing compounds, **44-51**. These conditions are summarised in Table 15. These are all an one-pot synthesis, meaning that the azides are generated *in situ*, from the sodium azide and corresponding halide (3-bromo-1-propanol).

**Table 15:** The different experimental condition used to synthesis **91**. The reaction can be seen above the table. NR = No reaction



**91**

Conditions	Materials used	Yield	Ref.
Stirring- 65 °C, 18 h, H <sub>2</sub> O:THF		77 %	226
Microwave – 125 °C, 20 mins, 100 W, H <sub>2</sub> O:THF		68 %	227
Sonication- RT, 25 mins, 20 Hz, THF		NR	228

For the sonication method, the Cu<sup>1</sup> catalyst was added to the reactions, whereas in the other two methods the Cu<sup>1</sup> was formed *in situ*. The sonication method is seen as an environmentally friendly method for chemical synthesis as it can significantly reduce the reaction time to minutes compared to traditional stirring. Ultrasound induces chemical or physical changes during cavitation, a phenomenon involving the formation, growth, and instantaneous implosive collapse of bubbles in a liquid.<sup>229</sup> There was no reaction, however, with the sonication method. This could be due to the frequency of the sonication being insufficient to allow bubbles formation and subsequent implosion to occur.

The other two methods, microwave and stirring, did afford the triazole product in very good synthetic yield. Microwave irradiation has been well-documented as a useful method for triazole synthesis, which often gives better reaction times and yields when compared to traditional heating methods. The heating in a microwave vessel is different to that of stirring. The reaction absorbs the microwave energy from the interior to the exterior of the vessel. This dielectric heating allows the reaction times to be shortened as it is a more effective way of heating. In the reaction, the polar component causes the absorption of these waves as a dipole moment is needed. The dipole is sensitive to the changes in the electric field, trying to realign once one is applied. The alternating field causes rotation in these molecules; this in turn causes heat to dissipate from these molecules. The heating directly correlates to the dielectric properties of the components. The vessel itself is not heated in the process, leading to better homogeneity and better selective heating of the polar compounds.<sup>230,231</sup>

In the reactions shown in Table 15, the stirring method afforded a higher yield when compared to the microwave. The stirring method was used in future reactions due to this method providing the best results in the method development process.

### 3.3.1.3 Chemical analysis of the triazole containing compounds 44-51

In this series of compounds there are two possible isomers of the 1,2,3-triazole that can form, specifically 1,4- and 1,5- isomers, and when analysing the product there were noticeable differences in the  $^1\text{H}$  NMR spectra between these two isomers. The VB theory approach can help explain as to why the hydrogen on the triazole, in the 5-position on the 1,4 isomer and in the 4-position on the 1,5 isomer, is shifted upfield in the 1,4 isomer, the positions are seen in Figure 38. Some of the key resonance forms are shown for both the 1,4 and 1,5 isomers, the upfield position on the  $^1\text{H}$  NMR spectra of the hydrogen in the ring, 5' position in the 1,4-isomer and 4' position in the 1,5-isomer (hydrogens coloured pink in Figure 38), can be accredited to resonance donation from the nitrogen with a function group attached. A positive charge is formed on the nitrogen which leaves the more electronegative nitrogen with a negative charge. This charge is then transferred to the hydrogen. The negative charge on that carbon causes an increase in electron density. This in turn causes a strong shielding effect for the hydrogen and hence why the resonance on the NMR spectra is upfield. The resonance peaks for the target compounds **44-51** are shown in Table 16.

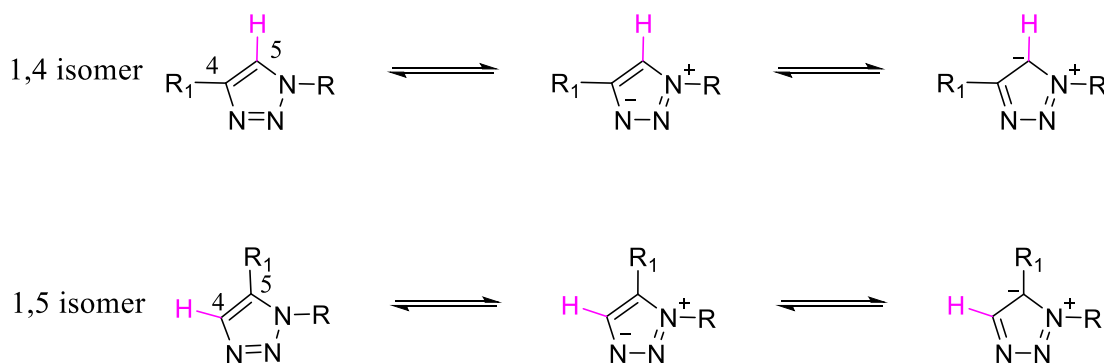


**Figure 38:** The key resonance forms on the 1,2,3-triazole ring. The 1,4 and 1,5 isomers are shown. The hydrogen coloured is the hydrogen resonance peak on the  $^1\text{H}$  NMR spectra that is being shown.

**Table 16:** A table summarising the resonance peaks for the hydrogens in the 1,2,3-triazole ring.

Compound	Resonance peak for the correspond hydrogens in the 1,2,3-triazole ring (ppm)	
	H-5	H-4
44	8.24	--
45	8.78	--
46	8.88	--
47	8.79	--
48	--	7.83
49	--	7.82
50	--	7.91
51	--	7.90

The 1,2,3-triazoles also demonstrate characteristic features that are commensurate with the formation of the triazole, and loss of the alkyne and azide functionalities. An example of a spectrometric analysis technique that can be used in determining the formation of the 1,2,3-triazole ring is Infrared spectroscopy. Phenylacetylene is the alkyne starting material for the 1,4 (**45**) and the 1,5 (**49**) isomer. There is a peak present at  $3289\text{ cm}^{-1}$ , this corresponds the CH bond present in the alkyne. This peak, however, is absent in both the spectra for **45** and **49**. This suggests that the alkyne has been removed from the products.

It was noted that there was also differences in solubilities between the two isomers. The 1, 4- isomers were only soluble in dimethyl sulfoxide (DMSO), whereas the 1,5- isomers were soluble in methanol and acetone as well as DMSO.

#### **3.3.1.4 Yields and purity of the target compounds 44-51**

There were two different catalysts used in the synthesis of these compounds. They had drastically different yields, with the copper CuAAC reactions producing the better yields. There was also a difference depending on which alkyne was used. The 1,4-isomers, **44-47**, gave a range of yields from 75-93%, whereas the RuAAC reactions that produced the 1,5-isomers **48-51** yields range from 38-50%. This could be due to the RuAAC reactions requiring the production of a strained intermediate, whereas in the CuAAC reactions the strained intermediate is alleviated using two copper ions.

In general, alkynes that contained a benzyl group afforded better yields for the 1,4- and 1,5- isomers. These aromatic groups are more electron withdrawing when compared to the alcohol on the alkyne. As previously reported in the literature the efficacy of the process depends on the electronic factors on the alkyne, with the introduction of electron withdrawing groups enhancing yields of 1,2,3-triazole formations.<sup>232</sup>

The purity of these compounds was determined using a developed HPLC method, using a gradient solvent system. Each compound was shown to have > 99% purity. A solvent system of A = H<sub>2</sub>O and B = MeCN was used, with a flow rate = 1.0 mL/min. Compounds were eluted with a gradient of 5% B to 100% B for 25 min. Detection at wavelengths of 254, 280, 210 nm was used. A gradient was used to expose any compounds that are less polar than the target compound, such as hydrolysed sugars. An ELSD was used in conjunction with UV in the HPLC

as some of the side products could be UV inactive. The yields and purities for compounds **44-51** are shown in Table 17.

**Table 17:** A table showing the yields and purity of the target compounds **44-51**.

<b>Compound</b>	<b>Yields (%)</b>	<b>Purity (%)</b>
<b>44</b>	75	>99
<b>45</b>	80	>99
<b>46</b>	93	>99
<b>47</b>	89	>99
<b>48</b>	38	>99
<b>49</b>	42	>99
<b>50</b>	50	>99
<b>51</b>	48	>99

### **3.2.1 Microbiology data for the triazole containing compounds**

#### **3.2.1.1 Microbiological results**

As previously discussed (Section 2.3.2.1), a bioscreen method was used to obtain the MIC<sub>100</sub> values for the triazole containing AZT compounds. Two different broths, MHB and NB, were used to understand whether the broth had any effect on bacterial growth. The control measurement for these compounds **44-51** is AZT **52**.

### 3.2.1.2 Microbiological results for AZT 52 using the bioscreen method

Data for the control drug, AZT 52, is shown in Table 18. As expected, the MIC values were high, >128 µg/mL, for the gram-positive bacteria and *Pseudomonas aeruginosa*.<sup>197</sup> It was shown in Section 3.1.3, that the mechanism of action for AZT needs dThd kinases to activate 52, which are not present in these bacteria. In Table 19, the dThd levels in certain bacteria are shown.<sup>205</sup> In *Klebsiella pneumoniae*, the levels are elevated which is consistent with the MIC<sub>100</sub> results as that bacterial strain had values of 0.5 µg/mL.

There was very little difference in MIC values between the two media, with *Enterobacter cloacae* and *Escherichia coli* being the only two bacteria that showed slight differences. This is to be expected as both broths ingredients should not interfere with the growth of the bacteria chosen.

**Table 18:** MIC<sub>100</sub> data for AZT 52 in two different media; MHB and NB. The values highlighted yellow show MIC<sub>100</sub> ≥64 µg/mL. NG – No growth. The bacteria in red refer to gram-positive strains.

Organisms	MIC <sub>100</sub> (µg/ml) of AZT 52 in two different broths		
	OCC	MHB	NB
<i>B. cereus</i>	754	>128	>128
<i>E. faecalis</i>	640	>128	>128
<i>E. faecium</i>	220	>128	>128
<i>S. aureus</i>	100	>128	>128
<i>S. epidermis</i>	691	>128	>128
<i>St. agalactiae</i>	182	>128	>128
<i>St. pneumoniae</i>	1548	>128	>128
<i>St. pyogenes</i>	168	>128	>128
<i>St. viridans</i>	1683	>128	>128
<i>C. freundii</i>	851	128	128
<i>Cr. sakazakii</i>	1888	8	8
<i>En. cloacae</i>	760	1	2
<i>Es. coli</i>	199	4	8
<i>K. pneumoniae</i>	758	0.5	0.5
<i>P. mirabilis</i>	2080	>128	>128
<i>Ps. aeruginosa</i>	201	>128	>128
<i>Sa. typhimurium</i>	854	NG	NG
<i>Se. marcescens</i>	217	128	128

**Table 19:** Cell extracts of the bacteria were examined for TK activity at a protein concentration of 50 pg mL<sup>-1</sup> in the reaction mixture. Adapted from data in ref. 205.

Strain of bacteria	Relative specific dThD kinase activity in cell extract (%)	Relative dThD kinase production in cell extract (%)
<i>Staphylococcus aureus</i> (209) <sup>a</sup>	83	59
<i>Streptococcus pyogenes</i> (ST1) <sup>b</sup>	29	4.6
<i>Salmonella typhimurium</i> (HKB-1) <sup>d</sup>	1130	878
<i>Escherichia coli</i> (K12) <sup>c</sup>	100	100
<i>Klebsiella pneumoniae</i> (Kasuya) <sup>c</sup>	528	329
<i>Pseudomonas aeruginosa</i> (HKB-2) <sup>d</sup>	0	0
<i>Proteus mirabilis</i> (IFO3849) <sup>c</sup>	34	39

### 3.2.1.3 Microbiological results for the 1,4-1,2,3-triazole derived compounds 44-47 using the bioscreen method

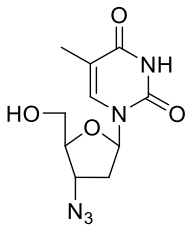
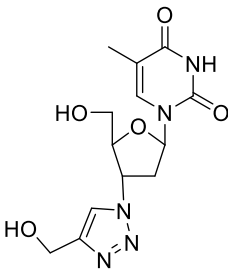
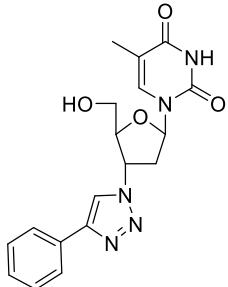
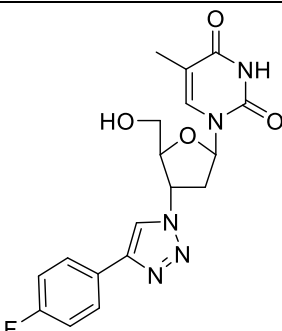
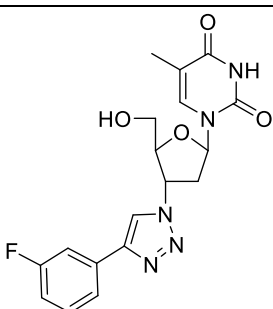
The MIC values for the 1,4-1,2,3-triazole isomers of the triazole based compounds, **44-47**, had similar MIC values to AZT **52** for the gram-positive bacteria, >128 g/mL, as well as in *Pseudomonas aeruginosa* and *Proteus mirabilis*. The broth used was NB. Compound **37** lost activity compared to the parent AZT and gave MIC values of >128 µg/mL. This was similar to **44** and **47**, where the only bacterium where MIC activity was seen was *Klebsiella pneumoniae*, with values of 64 µg/mL, respectively.

**Table 20:** The MIC<sub>100</sub> data for the underivised compound AZT and the 1,4-isomers **44-47**. The broth is NB. NG – No growth. The values highlighted yellow show MIC<sub>100</sub> ≥64 µg/mL. The ClogP data was calculated using Chem BioDraw Ultra software version 13.0.

Organisms	MIC <sub>100</sub> (µg/mL) of various 1,4-triazole moieties attached to AZT in NB.					
	OCC	AZT (52)	44	45	46	47
CLogP		0.04	-2.48	0.66	0.84	0.84
<i>B. cereus</i>	754	>128	>128	>128	>128	>128
<i>E. faecalis</i>	640	>128	>128	>128	>128	>128
<i>E. faecium</i>	220	>128	>128	>128	>128	>128
<i>S. aureus</i>	100	>128	>128	>128	>128	>128
<i>S. epidermis</i>	691	>128	>128	>128	>128	>128
<i>St. agalactiae</i>	182	>128	>128	>128	>128	>128
<i>St. pneumoniae</i>	1548	>128	>128	>128	>128	>128
<i>St. pyogenes</i>	168	>128	>128	>128	>128	>128
<i>St. viridans</i>	1683	>128	>128	>128	>128	>128
<i>C. freundii</i>	851	128	128	128	>128	128
<i>Cr. sakazakii</i>	1888	8	>128	16	>128	>128
<i>En. cloacae</i>	760	2	>128	128	>128	>128
<i>Es. coli</i>	199	8	>128	64	>128	>128
<i>K. pneumoniae</i>	758	0.5	64	4	>128	64
<i>P. mirabilis</i>	2080	>128	>128	>128	>128	>128
<i>Ps. aeruginosa</i>	201	>128	>128	>128	>128	>128
<i>Sa. typhimurium</i>	854	NG	>128	8	>128	>128
<i>Se. marcescens</i>	217	128	>128	>128	>128	>128

Compound **44** contained an extra hydroxyl handle on the triazole ring, and had a CLogP value of -2.48. This could help to explain why its MIC value was increased in certain gram-negative bacteria, as its lipophilicity is decreased and as previously mentioned this affects gram-negative bacteria in an undesirable manner. The ClogP values, however, for the other compounds do not follow the same pattern, i.e. parent compound, AZT has a lower ClogP value when compared to **45-47** but demonstrated lower MIC data for certain gram-negative bacteria. The structure **44-47** and **52** are shown in Table 21, the ClogP values and select gram-negative bacteria's MIC<sub>100</sub> values are also shown.

**Table 21:** The structure **44-47** and **52** shown with their ClogP and select gram-negative bacteria's MIC<sub>100</sub> values.

Compound	Structure	ClogP	MIC <sub>100</sub> data			
			<i>Cr. sakazakii</i>	<i>En. cloacae</i>	<i>Es. coli</i>	<i>K. pneumoniae</i>
<b>52</b>		0.04	8	2	8	0.5
<b>44</b>		-2.48	>128	>128	>128	64
<b>45</b>		0.66	16	128	64	4
<b>46</b>		0.84	>128	>128	>128	>128
<b>47</b>		0.84	>128	>128	>128	64

Of the 1,4-isomers, **45**, with the benzyl group in the 4- position on the triazole ring, still retained activity against the same bacteria as AZT **52**. It had similar MIC values in *Klebsiella pneumoniae*, 4 µg/mL when compared to 0.5 µg/mL for AZT, and *Cronobacter sakazakii*, 16 µg/mL when compared to 8 µg/mL. This compound, **45**, was also the only compound to possess activity against *Salmonella typhimurium*. No growth was detected by the control AZT, and **44-47** all displayed values >128 µg/mL. Once a fluoride atom was added to the benzyl ring on the triazole ring the values for MIC<sub>100</sub> increased.

#### **3.2.1.4 Microbiological results for the 1,5-1,2,3-triazole derived compounds 48-51 using the bioscreen method**

The 1,5-isomers, **48-51**, were also tested against the same species of bacteria. The MIC<sub>100</sub> data are shown in Table 22.

**Table 22:** The MIC<sub>100</sub> data for the underivised compound AZT and the 1,5-isomers **48-51**. The broth is NB. NG – No growth. The values highlighted yellow show MIC<sub>100</sub> ≥64 µg/mL. The ClogP data was calculated using Chem BioDraw Ultra software version 13.0.

Organisms	MIC <sub>100</sub> (µg/mL) of various 1,5-triazole moieties attached to AZT in NB.					
	OCC	AZT (52)	48	49	50	51
ClogP		0.044	-2.48	0.66	0.84	0.84
<i>B. cereus</i>	754	>128	>128	>128	>128	>128
<i>E. faecalis</i>	640	>128	>128	>128	>128	>128
<i>E. faecium</i>	220	>128	>128	>128	>128	>128
<i>S. aureus</i>	100	>128	>128	>128	>128	>128
<i>S. epidermis</i>	691	>128	>128	>128	>128	>128
<i>St. agalactiae</i>	182	>128	>128	>128	>128	>128
<i>St. pneumoniae</i>	1548	>128	>128	>128	>128	>128
<i>St. pyogenes</i>	168	>128	>128	>128	>128	>128
<i>St. viridans</i>	1683	>128	>128	>128	>128	>128
<i>C. freundii</i>	851	128	>128	128	>128	>128
<i>Cr. sakazakii</i>	1888	8	16	4	>128	>128
<i>En. cloacae</i>	760	2	4	64	>128	>128
<i>Es. coli</i>	199	8	8	32	>128	>128
<i>K. pneumoniae</i>	758	0.5	0.5	4	>128	64
<i>P. mirabilis</i>	2080	>128	>128	>128	>128	>128
<i>Ps. aeruginosa</i>	201	>128	>128	>128	>128	>128
<i>Sa. typhimurium</i>	854	NG	NG	4	>128	>128
<i>Se. marcescens</i>	217	128	128	>128	>128	>128

For these 1,5-isomers, there was no activity against gram-positive bacteria, *Pseudomonas aeruginosa* and *Proteus mirabilis*, with MIC values of >128 µg/mL for the respective bacteria. This is again due to a lack of dThd kinases in these species. Relatively high MIC<sub>100</sub> values were also found in *Citrobacter freundii* and *Serratia marcescens*, in both the parent drug and the 1,5-compounds. In all but one of the bacteria (*C. freundii*), AZT gave better activity. When compound **49** was tested against *Cronobacter sakazakii*, a MIC<sub>100</sub> of 4 µg/mL was recorded. This is similar than the MIC value obtained for AZT, 8 µg/mL. This compound was also the only compound that was found to have activity against *Salmonella typhimurium*, this was also similar to the activity of the 1,4- isomers. The compound containing the hydroxyl handle, **48**, and benzyl group, **49**, displayed similar activity against *Enterobacter cloacae* and *Escherichia coli*, which was in turn similar to **51**. The lowest MIC<sub>100</sub> values were found in *Klebsiella pneumoniae*, with compound **48** having the same MIC values as the parent drug. As previously mentioned, *K. pneumoniae* contains a high percentage of the dThd kinases, which allows the compound to be incorporated into the DNA.

When comparing the two different isomers compounds **50** and **51** gave the same activity as their 1,4-counterparts an example being the position of the fluorinated benzyl group on the triazole ring did not change the MIC<sub>100</sub> values. With four bacteria (*Cr. sakazakii*, *En. cloacae*, *Es. coli*, and *K. pneumoniae*) both the hydroxylated **48** and benzylated **49** rings gave lower MIC values with the 1,5- isomer. For compound **48**, there is a hydroxyl group at the 5, position of the triazole ring. Both the hydroxyl on the *O'*-5 membered ring and the hydroxyl attached to the triazole ring are spaced by a methyl chain. The 1,5-isomer group could be positioned closer to the active site for dThd kinases, therefore could potentially be phosphorylated. In the 1,4-isomer, this hydroxyl chain is positioned further away and this could explain why the 1,5-isomer has better MIC<sub>100</sub> values for a select gram-negative bacteria. Compound **49** demonstrated improved biological activity against *En. cloacae*, from 128 µg/mL in the 1,4-isomer **45** to 64

$\mu\text{g/mL}$  in the 1,5- isomer **49**. Overall, the 1,5-isomers gave lower  $\text{MIC}_{100}$  values for the bacteria against which the compounds were active, with a significant difference between **44** and **48**, the hydroxylated triazole rings.

The MIC values of the triazole containing compounds **44-51** were also determined in MHB. The results for these are shown in Table 23. The values are similar to those reported for the NB media.

**Table 23:** The MIC<sub>100</sub> data for the underivised compound AZT and both the 1,4- the 1,5-isomers **44-51**. The broth is MHB. NG – No growth. The values highlighted yellow show MIC<sub>100</sub> ≥64 µg/mL

Organisms	MIC <sub>100</sub> (µg/mL) of various 1,4- and 1,5- 1,2,3-triazole moieties attached to AZT.									
	OCC	MHB								
		52	44	45	46	47	48	49	50	51
<i>B. cereus</i>	754	>128	>128	>128	>128	>128	>128	>128	>128	>128
<i>E. faecalis</i>	640	>128	>128	>128	>128	>128	>128	>128	>128	>128
<i>E. faecium</i>	220	>128	>128	>128	>128	>128	>128	>128	>128	>128
<i>S. aureus</i>	100	>128	>128	>128	>128	>128	>128	>128	>128	>128
<i>S. epidermis</i>	691	>128	>128	>128	>128	>128	>128	>128	>128	>128
<i>St. agalactiae</i>	182	>128	>128	>128	>128	>128	>128	>128	>128	>128
<i>St. pneumoniae</i>	1548	>128	>128	>128	>128	>128	>128	>128	>128	>128
<i>St. pyogenes</i>	163	>128	>128	>128	>128	>128	>128	>128	>128	>128
<i>St. viridans</i>	1683	>128	>128	>128	>128	>128	>128	>128	>128	>128

<i>C. freundii</i>	851	128	128	128	>128	128	>128	128	>128	>128
<i>Cr. sakazakii</i>	1888	8	>128	16	>128	>128	16	4	>128	>128
<i>En. cloacae</i>	760	1	>128	128	>128	>128	4	64	>128	>128
<i>Es. coli</i>	199	4	>128	64	>128	>128	8	32	>128	>128
<i>K. pneumoniae</i>	758	0.5	64	4	>128	64	0.5	4	>128	64
<i>P. mirabilis</i>	2080	>128	>128	>128	>128	>128	>128	>128	>128	>128
<i>Ps. aeruginosa</i>	201	>128	>128	>128	>128	>128	>128	>128	>128	>128
<i>Sa. typhimurium</i>	854	NG	>128	8	>128	>128	NG	4	>128	>128
<i>Se. marcescens</i>	217	128	>128	>128	>128	>128	128	>128	>128	>128

### 3.3 SAR for the target compounds in the triazole containing compounds

Using the data collected in Chapter 3, SAR's can be deduced. Figure 39 shows a summary of the SAR data collected. The addition of a triazole moiety to AZT **52** saw a loss in antimicrobial activity; this is for the 3- and 4- position on the ring. The bacteria strain which was most responsive to these compounds **44-51** was *Klebsiella pneumoniae*, this bacteria is responsible for community acquired pneumonia.<sup>188</sup> This is unsurprising considering the level of dThd kinases that are found in this strain.<sup>205</sup> MIC<sub>100</sub> values collected for **48** and AZT were comparable. This was not true of the 1,4-isomer of the same product, **44**. The addition of a hydroxyl chain to the 1,5- position seemed to have very little effect on the activity of the compound, this could be due to the smaller group being able to fit in the active site of the kinases, which are needed to activate the compound to become a DNA terminator. Compounds **48** and **49** had similar activities against select gram-bacteria strains, again very similar to the values found for the parent drug AZT.

The addition of a benzyl ring to the 1,5- position gave slightly higher MIC values for the gram-negative bacteria, but **49** was the only compound which saw growth and activity of *Sa. typhimurium*. Salmonellosis is a disease in humans and animals caused by *Sa. typhimurium*, it is characterised by fever, acute intestinal inflammation, and diarrhoea within 24 h after infection.<sup>191</sup> Once a fluoride was added to the 4' or 3' position on the benzyl ring there was a loss of activity. The electronegative group had a negative effect on the MIC values.

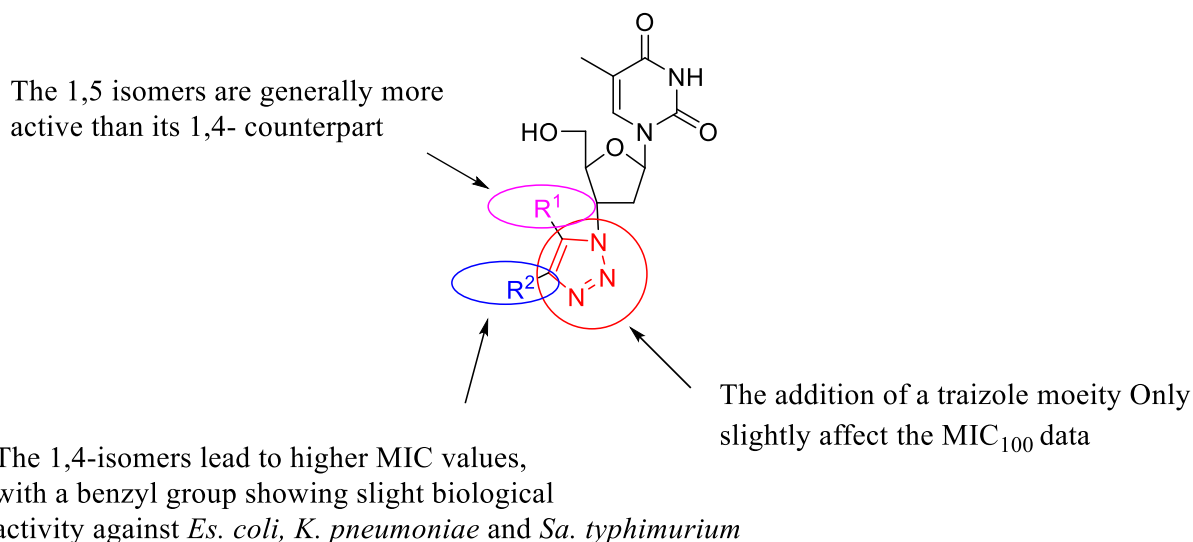


**Figure 39:** A diagram showing the SAR collected from the different triazole containing compounds.

### 3.4 Antiviral properties of AZT and its modifications

As previously mentioned, AZT **52** was first designed as an antiviral for HIV. Antiretroviral drugs are used to combat diseases caused by retroviruses, with AZT **52** being the first drug discovered and used for treating AIDS through inhibition of HIV. It was found to inhibit the HIV-1 replication *in vitro* at a concentration of  $>0.37 \mu\text{g/mL}$ .<sup>233</sup> Although this was the first drug discovered and used in the treatment of this virus, its history is unique and subject to controversy. For example, there were problems with the controls in the trials used to approve AZT, as well as issues surrounding patient confidentiality and the stocks of drugs leading to limited supply.<sup>234</sup> The compound inhibits HIV reverse transcriptase by incorporating itself into DNA and acting as a chain terminator. In order for this to occur AZT **52** has to first be phosphorylated by several kinase enzymes. The triphosphorylated chain chelates to the magnesium ion in the transcriptase enzyme active site, this can be seen in Figure 40. The figure shows AZT triphosphate being incorporated into the DNA of the HIV, causing the DNA chain

to terminate. In Figure 40, the structure is taken from the reverse transcriptase enzyme present in HIV.

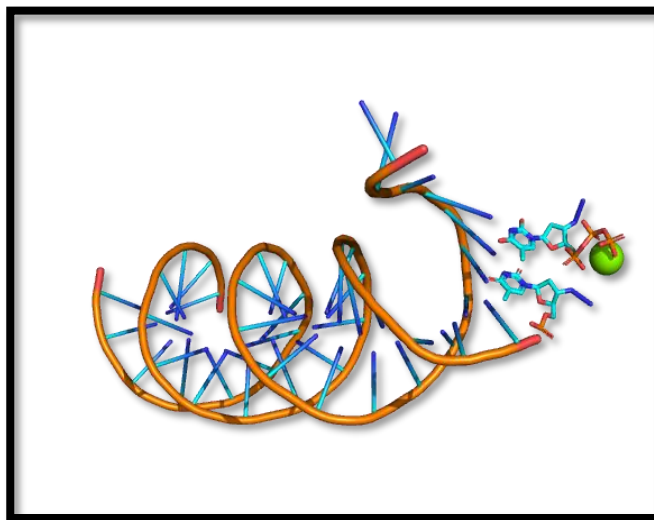


**Figure 40:** A computer model of AZT triphosphate chelating to the magnesium ion. AZT **52** is incorporated into the DNA and causes the chain to end. (Software: PyMOLWin)

To primarily investigate the potential antiviral properties of the 1,2,3-triazole containing compounds, the target compounds were fitted into the biological target (HIV reverse transcriptase) was used. This involved fitting the compounds into the HIV reverse transcriptase enzymes active site to probe their potentials as antiviral agents.

### 3.4.1 HIV reverse transcriptase

AZT inhibits DNA synthesis by acting as a chain terminator. This occurs in HIV reverse transcriptase. The compounds previously synthesised (**44-51**) were fitted into the mentioned enzyme active site to determine whether the compounds with the extra triazole ring would fit and therefore would, in theory, be able to inhibit the DNA synthesis in HIV. There were a number of assumptions that were made; the most important of these is that the original compounds would be phosphorylated with the prior enzymes (kinases).

The compounds **44-51** were fitted into the active site of the HIV reverse transcriptase, these are shown in Figure 41. The model of the new derivatised compounds were fitted to the biological structure which contained the underivatised parent compound, AZT **52**. As can be seen, the compound needs to be tri-phosphorylated to allow it to chelate to the magnesium, which in turn allows it to be incorporated into the DNA of the virus. The figures have been generated using an existing model (PDB : 3V4I) and fitting the triazole compounds in the active site using Coot,<sup>235</sup> and have been generated using PyMol.

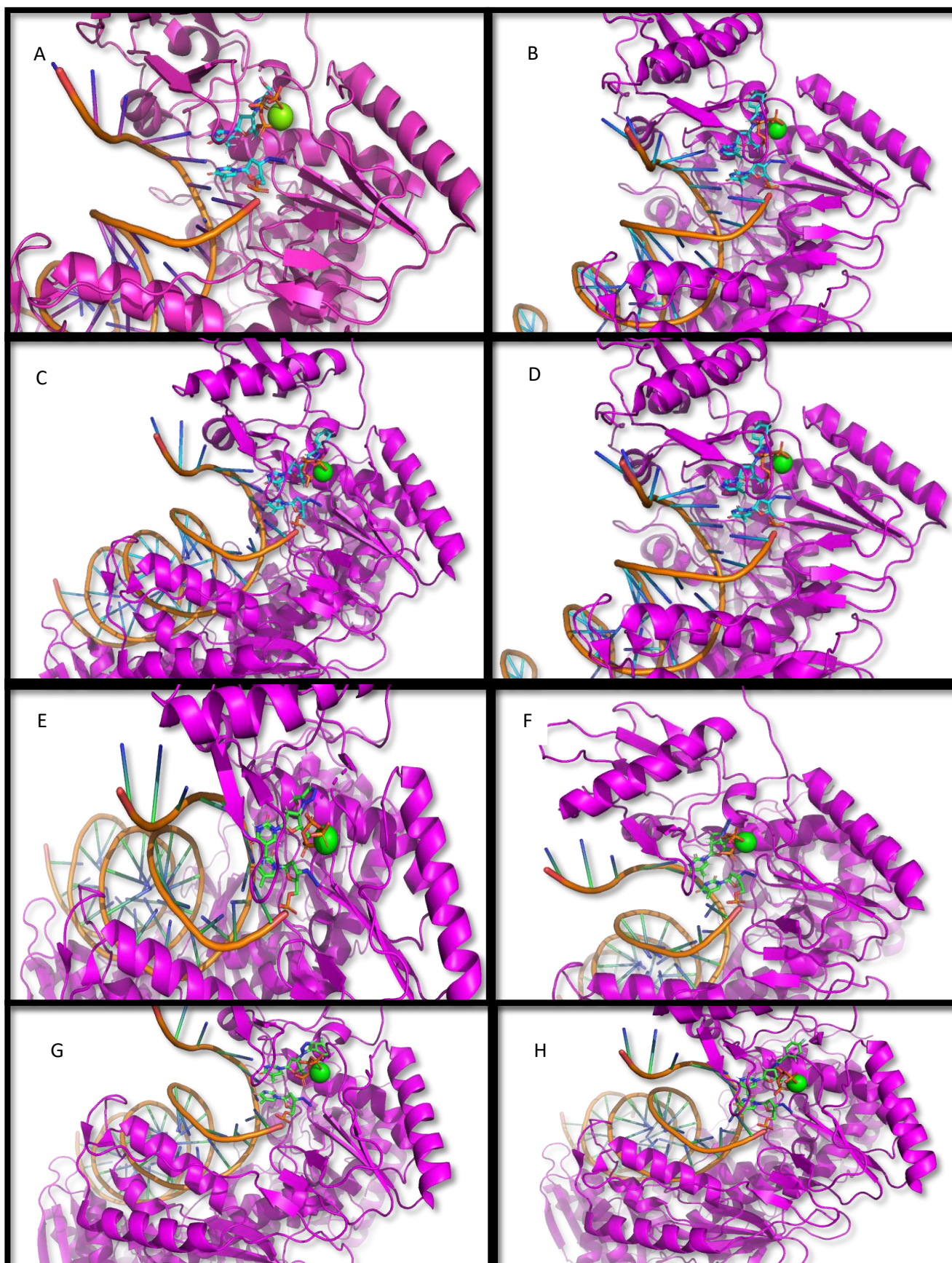


**Figure 41:** The fitting of the compounds **44-51** with the active site of HIV reverse transcriptase. A = **44**, B = **45**, C = **46**, D = **47**, E = **48**, F = **49**, G = **50**, and H = **51**.

In this model, the compounds fit in the active site. When fitting the compounds, there was space for either the 1,4- or 1,5- isomers. In Figure 42, there is an example of both isomers on the 1,2,3 triazole with a benzyl moiety attached to the ring, overlapped around the cyclic AZT core, showing the space they both occupy in the active site. As there is free rotation around the bond between nitrogen in the triazole and carbon in the AZT ring, the different isomers could in theory move around until they could fit. In the active site, the azido moiety on AZT **52** does not hydrogen bond to any residues. These models are limited, however. These are crude models and can be used to potentially indicate if any of the compounds was more likely to fit into the enzyme's active site. More experimental data is needed to say with certainty if the triazole based structures are useful as antiviral compounds.

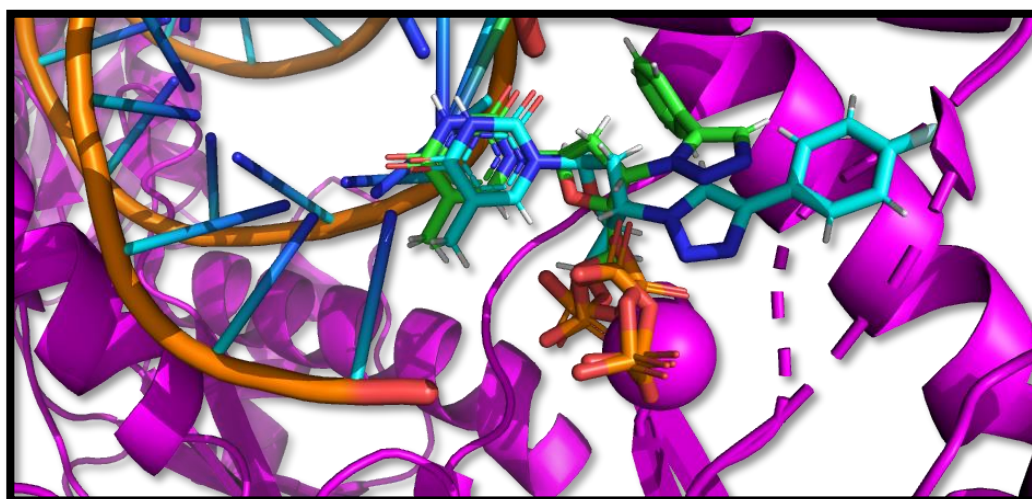


**Figure 42:** The overlapped view of **45** and **49** (**45**=blue and **49** = green) in the active site of HIV-1 reverse transcriptase.

### 3.5 Conclusion

The target compounds **44-51**, shown in Figure 43, were successfully synthesised using ‘click’ chemistry. This involved using two different metal catalysts to synthesise the two different isomers; 1,4-1,2,3-triazole isomers were synthesised using a copper catalyst and 1,5-1,2,3-triazole isomers were synthesised using a ruthenium catalyst. The 1,4-1,2,3-triazole containing compounds, **44-47**, were synthesised in greater yields when compared to the 1,5-1,2,3-triazole isomers, 75-93% for the 1,4-isomers as compared to 38-50% for the 1,5-isomers.

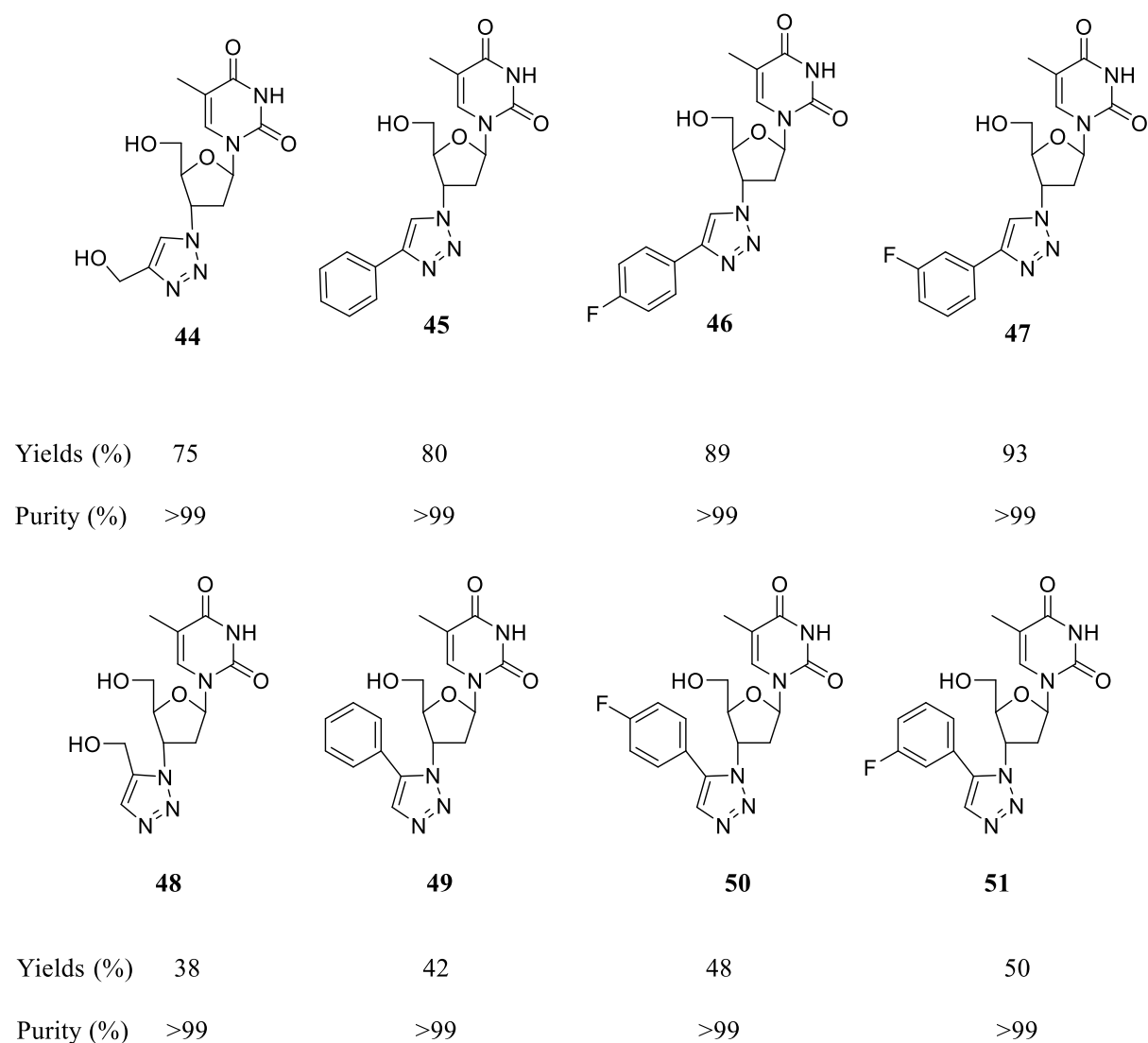


**Figure 43:** The target structure **44-51**, with their respective yields and purities shown.

These compounds were tested using a bioscreen method to obtain MIC<sub>100</sub> data. All compounds displayed no biological activity against gram-positive bacteria; this is to be expected when the parent, AZT **52**, is also inactive against these bacteria. Compounds **47** and **51**, containing a fluoride in the 4' position in the benzyl ring, had MIC values of >128 µg/mL. When the fluoride was in the 3' position on the benzyl ring, **46** and **50**, similar MIC values were recorded, with the exception of *Klebsiella pneumoniae* which the MIC value was 64 µg/mL. The 1,5-1,2,3-triazoles, **48-51**, generally had smaller MIC values when compared to their 1,4-1,2,3-triazole isomer counterparts, with compound **48** having comparable MIC values against *Escherichia coli* and *Klebsiella pneumoniae*.

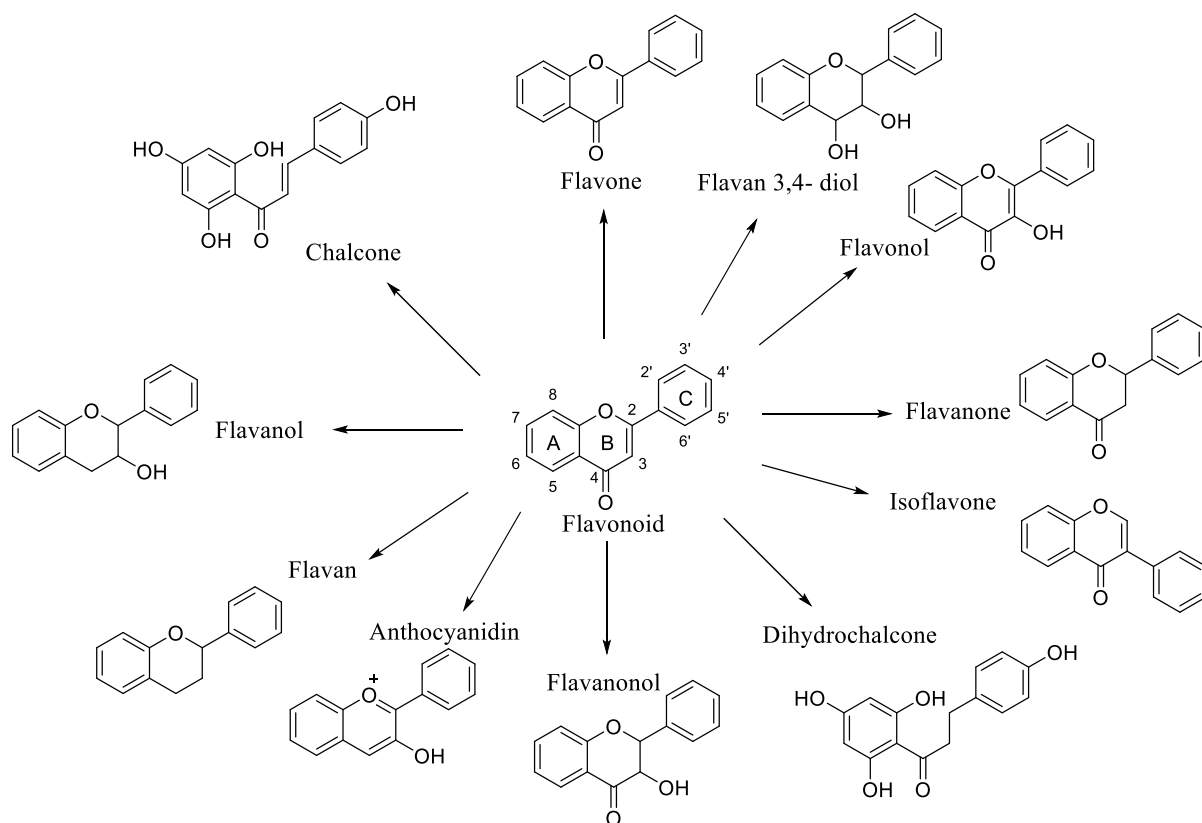
Preliminary antiviral models were performed using a fitting model, with all the compounds **44-51** found to fit in the HIV reverse transcriptase active site. *In vitro* studies will be needed to be conducted to fully evaluate their potentials as antivirals. These crude models have their limitations, as they are just an indicator as to which compounds could potentially give the greater antiviral activity.

**Chapter 4 – The synthesis and  
microbiological evaluation of carbohydrate  
prodrugs containing a flavonoid moiety to  
probe SAR's**

## 4.1 Introduction

### 4.1.1 Introduction to Flavonoids

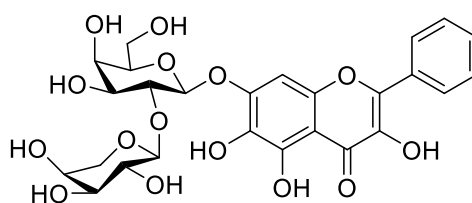
Flavonoids are a family of compounds consisting of two benzene rings linked through a heterocyclic pyrene ring.<sup>236</sup> This group of compounds can be split into further sub-groups, the most common known as flavones, isoflavones, flavonols and chalcones (structures can be seen in Figure 44). They are a naturally occurring secondary metabolite from plants, with many health benefits.<sup>237</sup>



### 4.1.2 Flavonoid as antimicrobial agents

**Figure 44:** The general structures of the different flavonoids. The general flavonoid structure is numbered and displayed in the middle.

As well as the previously discussed biological activities, some flavonoids contain antibacterial activities. Without people realising, they have been using flavonoids found in plants to improve their health. An example of this is the use of *Tagetes minuta*. This plant was used by individuals as a hot tea to treat diseases as an Argentinian folk medicine. The active compound in this tea is quercetagenin-7-arabinosyl-galactoside **98**, a glycosidic flavonoid which has good antimicrobial activity.<sup>238</sup> The structure and chloramphenicol equivalent concentrations are shown in Figure 45. Chloramphenicol equivalent concentration was used to compare how the glycoside compared to a clinically available antimicrobial compound.



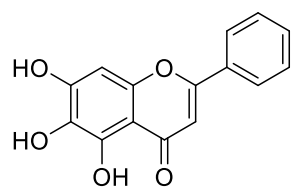
**98**

Chloramphenicol equivalent concentrations ( $\mu\text{g/mL}$ )	<b>98</b>
<i>S. aureus</i>	38
<i>Es. coli</i>	130
<i>B. subtilis</i>	69
<i>Ps. aeruginosa</i>	122
<i>S. epidermidis</i>	115

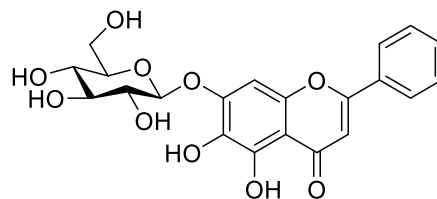
**Figure 45:** Quercetagenin-7-arabinosyl-galactoside **98** equivalent concentrations against select bacteria.

Huang qin is a herb used in Chinese medicine, it is from the *Scutellaria baicalensis* plant. It contains many flavonoids, including chrysin. Other flavonoids also present in this plant are baicalein **99** and wogonin **102**. Baicalin **101** is baicalein **89** with a glycoside, glucuronide, present at the hydroxyl on the C (7) position on the A ring. Interestingly, when the MIC data for **99** and **100** are compared there is only a slight difference, data shown in Figure 46.<sup>239</sup> This

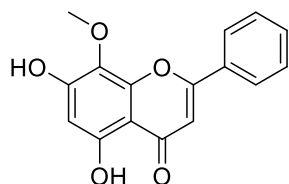
was also found true for **101** and **102**. The MIC and minimum bacterial concentration (MBC) were measured. The MBC data was defined as minimum concentration at which no growth was observed on the bacto tryptic soya agar (TSA) plates.



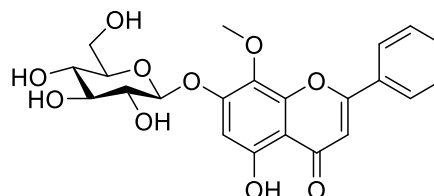
**99**



**100**



**101**



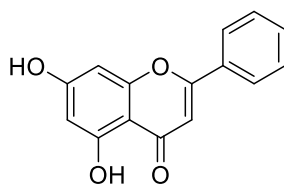
**102**

	<b>99</b>	<b>100</b>	<b>101</b>	<b>102</b>
<b>MIC (mg/mL)</b>				
<i>S. aureus</i>	0.5	0.5	1	1
<i>L. monocytogenes</i>	1	2	5	5
<i>S. enterica</i>				
-Kentucky	1	2	10	10
-Senftenberg	1	2	10	10
-Enteritidis	1	2	10	10
-Typhimurium	1	2	10	10
<b>MBC (mg/mL)</b>				
<i>S. aureus</i>	1	1	2	2
<i>L. monocytogenes</i>	2	5	10	10
<i>S. enterica</i>				
-Kentucky	2	5	20	20
-Senftenberg	2	5	20	20
-Enteritidis	2	5	20	20
-Typhimurium	2	5	20	20

**Figure 46:** The structures of the flavonoids and their glycosidic counter parts found in *Scutellaria baicalensis*. The MIC and MBC were determined using methods described by Hansen et al.<sup>312</sup> *S. aureus* (ATCC 19115), and *L. monocytogenes* (ATCC 27217). Data adapted from ref. <sup>239</sup>.

## 4.2 Chrysin

Chrysin **103** is a flavone, which is distributed in many plants. Examples of where this flavone **103** can be found include honey and honeycomb, as well as the passion flowers, *Passiflora caerulea* and *Passiflora incarnata*.<sup>240</sup> This compound **103** has a variety of different biological activities; including antiviral,<sup>241–243</sup> antiinflammatory,<sup>244,245</sup> anticancer,<sup>246,247</sup> antioxidant,<sup>248,249</sup> and antibacterial.<sup>250,251</sup> The structure of chrysin **103** and select MIC values are shown in Figure 47.<sup>252</sup>



**103**

MIC ( $\mu\text{g/mL}$ )	<b>103</b>
<i>S. aureus</i>	6.25
<i>Es. coli</i>	6.25
<i>B. subtilis</i>	12.5
<i>A. tumefaciens</i>	12.5
<i>P. lachrymans</i>	12.5
<i>X. vesicatoria</i>	6.25
<i>S. haemolyticus</i>	12.5

**Figure 47:** Chrysin **103** MIC values against selective gram-positive and gram-negative bacteria. Four gram-negative (*Agrobacterium tumefaciens* (ATCC 11158), *Escherichia coli* (ATCC 29425), *Pseudomonas lachrymans* (ATCC 11921) and *Xanthomonas vesicatoria* (ATCC 11633)) and three gram-positive (*Bacillus subtilis* (ATCC 11562), *Staphylococcus aureus* (ATCC 6538) and *Staphylococcus haemolyticus* (ATCC 29970)). The method used was a modified broth dilution-colorimetric assay. Adapted from ref. 263.

#### 4.2.1 Mechanism of action

Chrysin **103** has been reported to be a FabH inhibitor.<sup>250</sup> FabH is used to catalyse the fatty acid synthesis in bacteria and is considered one of the  $\beta$ -ketoacyl-acyl carrier protein (ACP) synthases. These catalyse the Claisen condensation of the fatty acid thioesters and malonyl-ACP, this initial elongation is performed by FabH. The fatty acid synthesis pathway has been discussed in Section 1.1.3.2, with the FabH pathway shown in Figure 48.

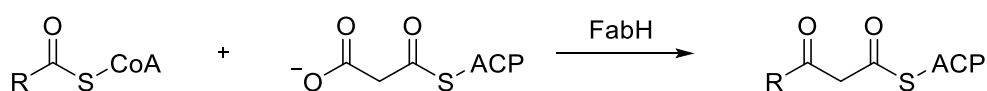


**Figure 48:** Part of the elongation stage in the fatty acid synthesis in bacteria which involved FabH.

#### 4.2.2 Derivatives of chrysin

Modifications have been made to chrysin **103** and the antibacterial properties of these derivatives were tested. One such example is shown in Figure 49.<sup>251</sup> In these compounds, the C (7) position was changed. Alkyl amines were added with varying chain lengths to enhance the compounds lipophilicity. The compounds with the lower MIC values were the compounds with a 4-carbon spacer on the alkyl chain. These compounds were effective in inhibiting gram-positive and gram-negative bacteria, and outperformed chrysin, the parent compound.



however the MIC data was only measured up to 50  $\mu\text{g/mL}$ . The molecule, **109g**, was the most potent and was a potent inhibitor of *Es. coli* FabH.<sup>250</sup>

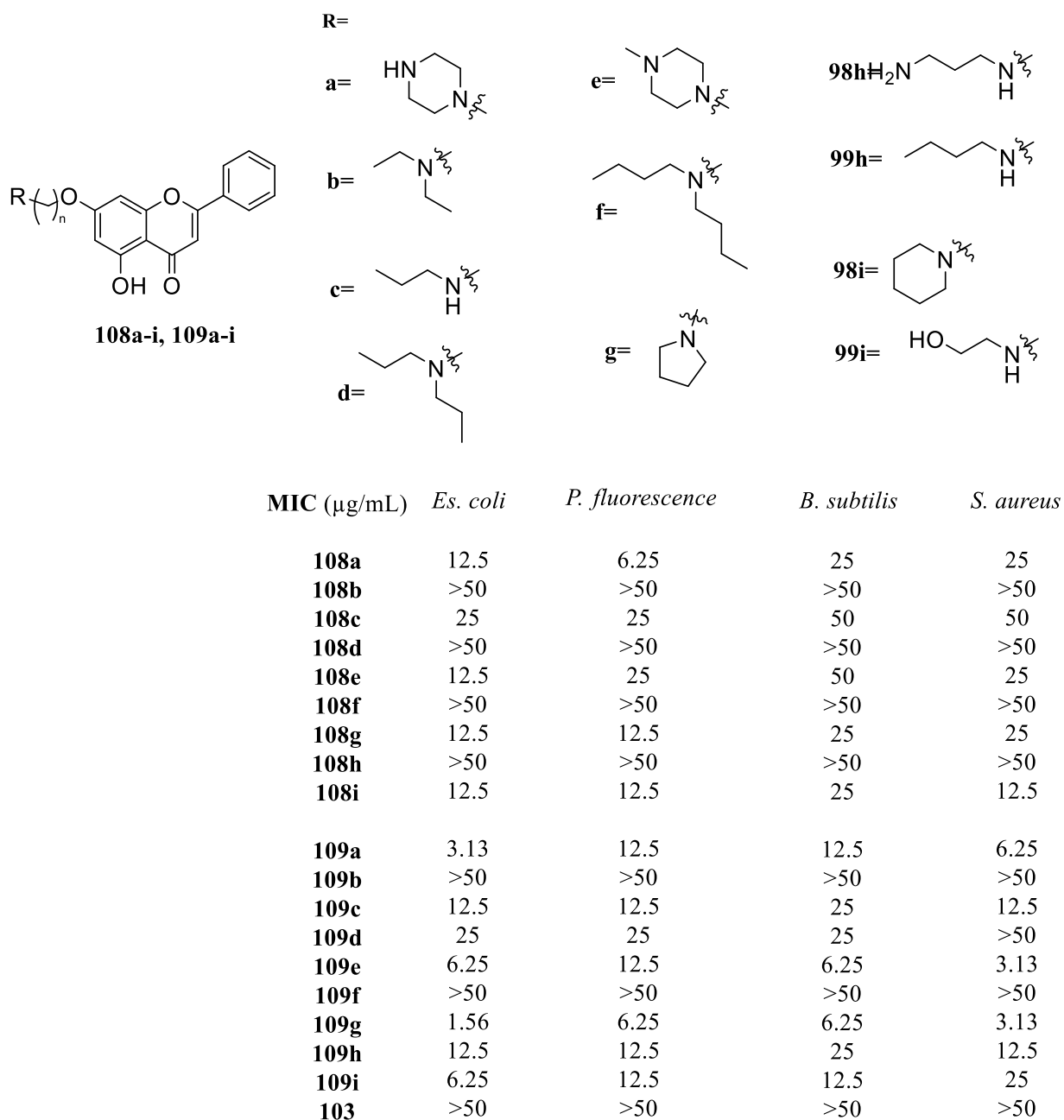


**Figure 50:** The structures of C (7) derivatives. The MIC values were determined using the MTT method in MHB. Data adapted from ref. 260.

### 4.3 Justification for design

Although chrysin **103**, and numerous other flavones, have many significant biological properties, they have poor bioavailability. Chrysin **103** is limited as a therapeutic drug as it has a compromised oral delivery.<sup>253</sup> Other flavones also suffer from modest to poor bioavailability. Phenolics, including chrysin **103**, undergo glucuronidation via UDP-glucuronosyltransferases (UGTs), which adds a glucuronide moiety to the nucleophilic hydroxyl on the phenolics. In chrysin **103** and 7,8-dihydroxyflavone **111**, the hydroxyl, which attacks the C (1) position on the glucuronide moiety, is found in the C (7) position on the A ring.<sup>254</sup> The mechanism by which this occurs is shown in Figure 51. In a previous study, it was shown that chrysin was rapidly metabolised by glucuronidation.<sup>255</sup> Sulfation and methylation in the liver also leads to the poor oral bioavailability.<sup>256</sup>

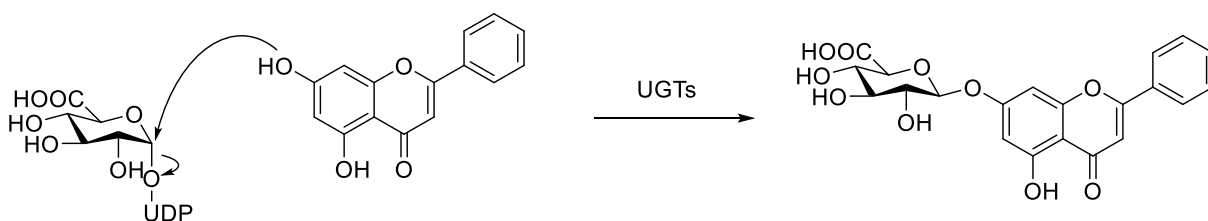


**Figure 51:** The mechanism by which chrysin **103** undergoes glucuronidation. Modified from ref. 266.

Along with glucuronidation, the solubility of flavonoids, including chrysin **103**, is an issue. These polyphenolic compounds are quite polar, however are poorly water soluble.<sup>257</sup>

The hypothesis is that attaching a glycoside to chrysin **103** and 7,8-dihydroxyflavone **111** will aid with the solubility in aq. environments of the compounds, as well as blocking the 7-*O*-position on the A ring, which should reduce the glucuronidation process, making this prodrug more bioavailable. As can be seen in Figure 52, a glucoside and galactoside have been attached to the 7 position through a glycosylation.

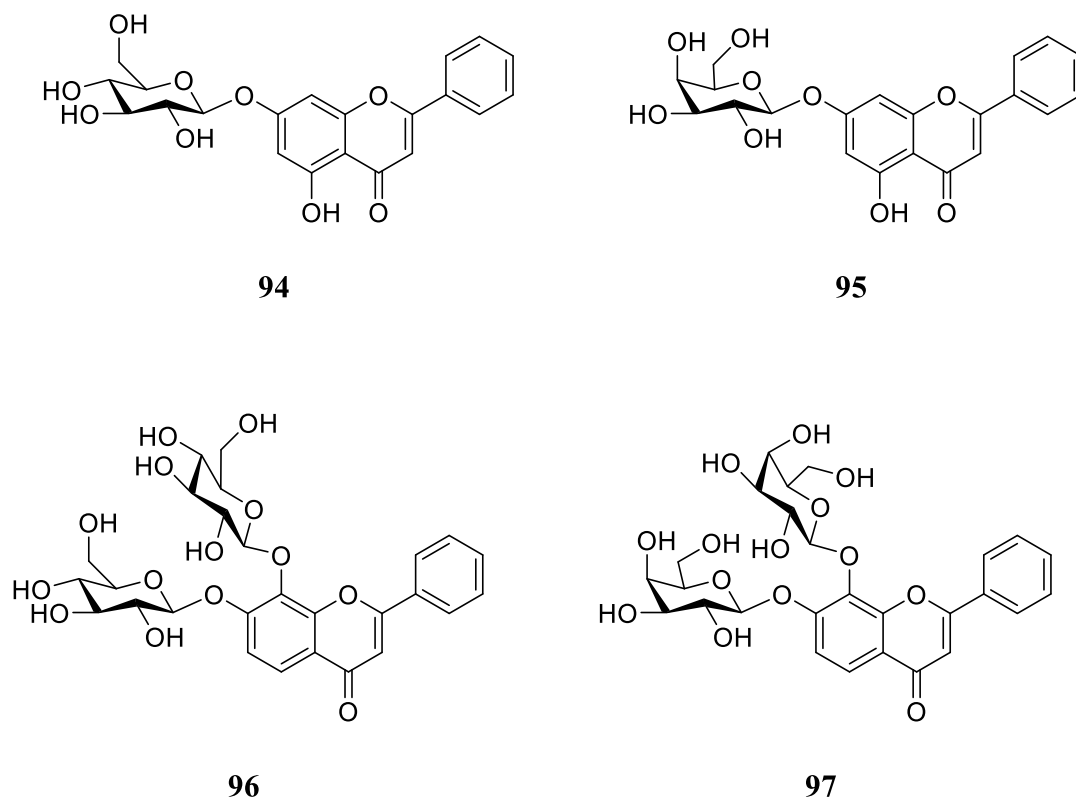


**Figure 52:** The glucosides **94** and **96** and galactosides **95** and **97** of their respective parent flavonoids.

To also gain SAR information for these flavones, with respect to their antimicrobial activity, another sub-set of compounds were selected for synthesis. These compounds contain a 7-hydroxyflavone **110** attached to either a glucose or galactose. There are no free hydroxyls present in these glycosides, whereas in **94-95** a hydroxyl is present in the C (5) position at the A ring.

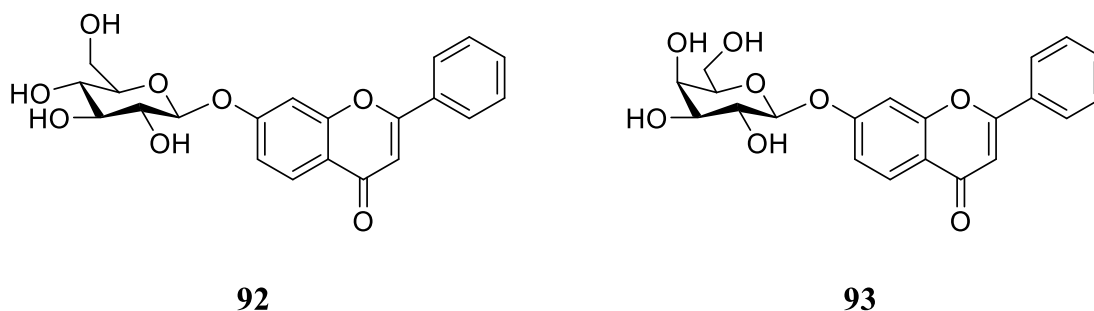


**Figure 53:** The glucosides **92** and galactosides **93** of 7-hydroxyflavone **110**.

#### 4.3.1 Aims for the glycosidic flavonoid compounds 92-97

Flavonoids are naturally occurring polyphenolic compounds which have a plethora of different biological activities; including antimicrobial,<sup>258,259</sup> anti-inflammatory,<sup>260,261,262,263</sup> antioxidant,<sup>264,265</sup> antithrombotic,<sup>266,267</sup> antiviral,<sup>268</sup> and anti-carcinogenic<sup>269,270</sup> agents.

Although flavonoids have all these beneficial biological activities, they are for the most part also insoluble in aq. solutions. The objective for this programme was to synthesise more soluble flavonoids, through the design and synthesis of glycosidic prodrugs. Glycosylating at a free hydroxyl position should allow the compounds to become more soluble in an aq. environment.<sup>271</sup> Once at the target site in the body, the glycosides in the compounds will be cleaved and this will allow the desired drug to be delivered at the active site. The target compounds are shown in Figure 54.

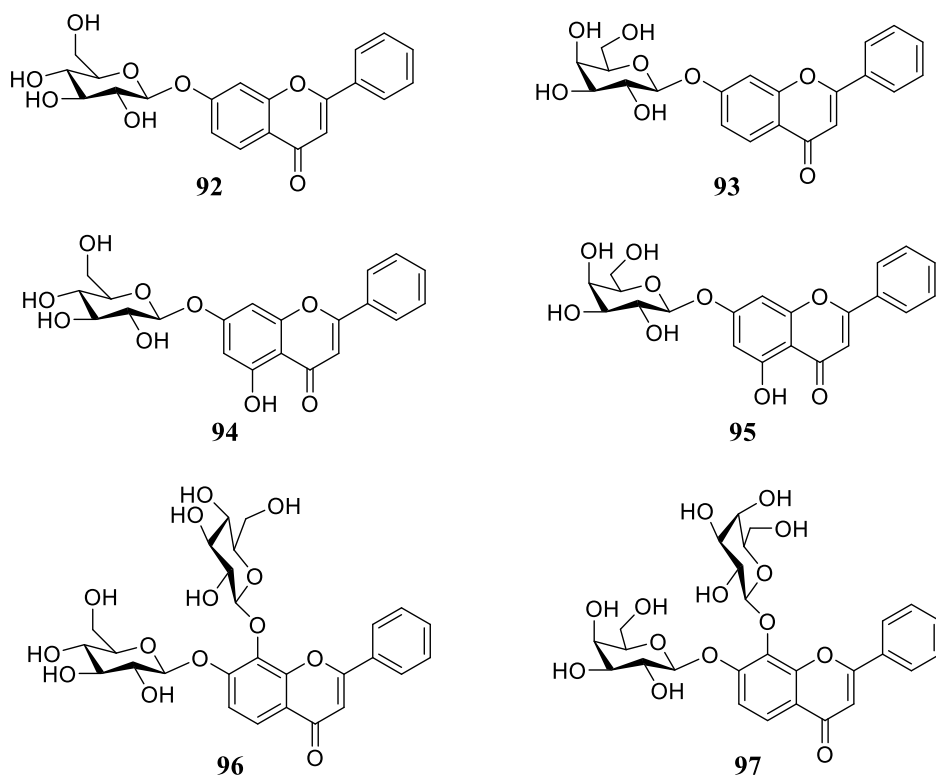


**Figure 54:** The target structures for the flavonoid series, **92-97**.

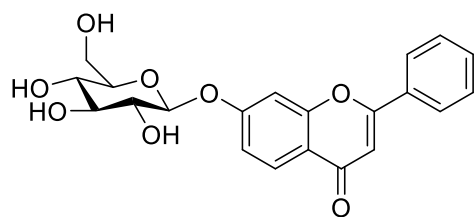
## 4.4 Results and discussion

### 4.4.1 Synthesis

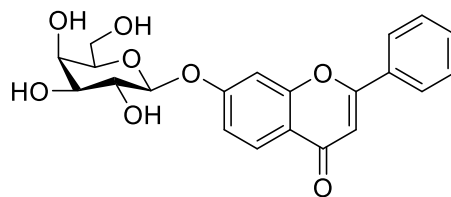
#### 4.4.1.2 Synthetic route

There are many different methods for glycosylations, for this series a different approach was used; PTC (previously mentioned in Section 2.3.1.4). This involves using a catalyst to enable the migration of a reactant from one phase to another where the reaction occurs. It was first devised to bring reactants that have incompatible solubilities together so a reaction may occur.<sup>272</sup>

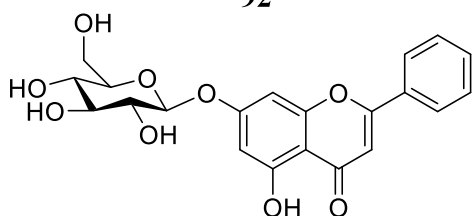
The target compounds, **102-107**, and retrosynthetic analysis are shown in Figure 55.



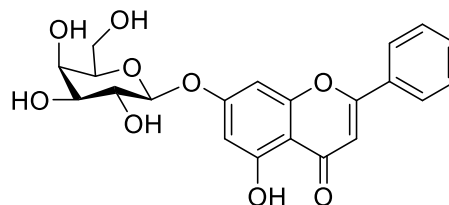
**92**



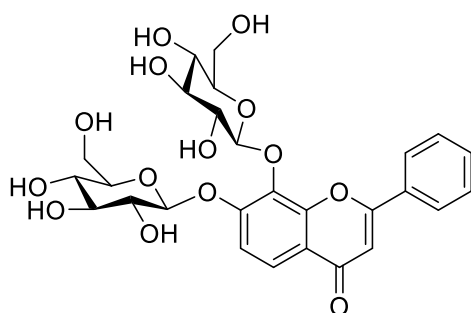
**93**



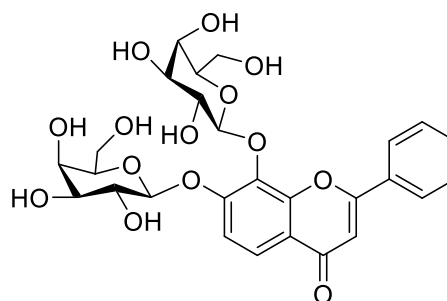
**94**



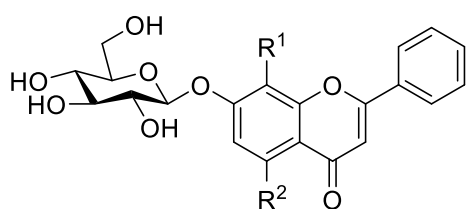
**95**



**96**



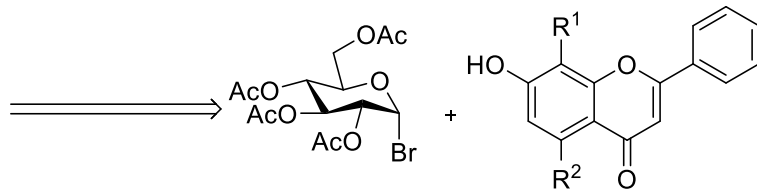
**97**



**92**  $R^1 = H, R^2 = H$

**94**  $R^1 = H, R^2 = OH$

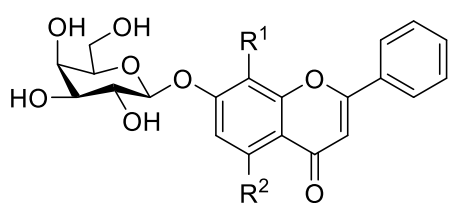
**96**  $R^1 = OH, R^2 = H$



**110**  $R^1 = H, R^2 = H$

**103**  $R^1 = H, R^2 = OH$

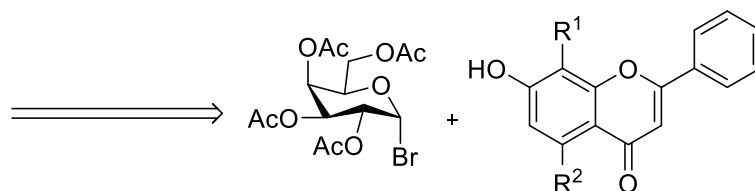
**111**  $R^1 = OH, R^2 = OH$



**93**  $R^1 = H, R^2 = H$

**95**  $R^1 = H, R^2 = OH$

**97**  $R^1 = OH, R^2 = H$



**110**  $R^1 = H, R^2 = H$

**103**  $R^1 = H, R^2 = OH$

**111**  $R^1 = OH, R^2 = OH$

**Figure 55:** The target compounds **92-97**. The retrosynthetic route is also shown beneath the target compounds.

In PTC, the reaction proceeds via an  $S_N2$  style of reaction, a transition state is formed as can be seen in Figure 56. The reaction was left for 24 h with the PTC. Methanolysis was used to deprotect the acetylated compounds. The catalyst used in this process was  $K_2CO_3$ .

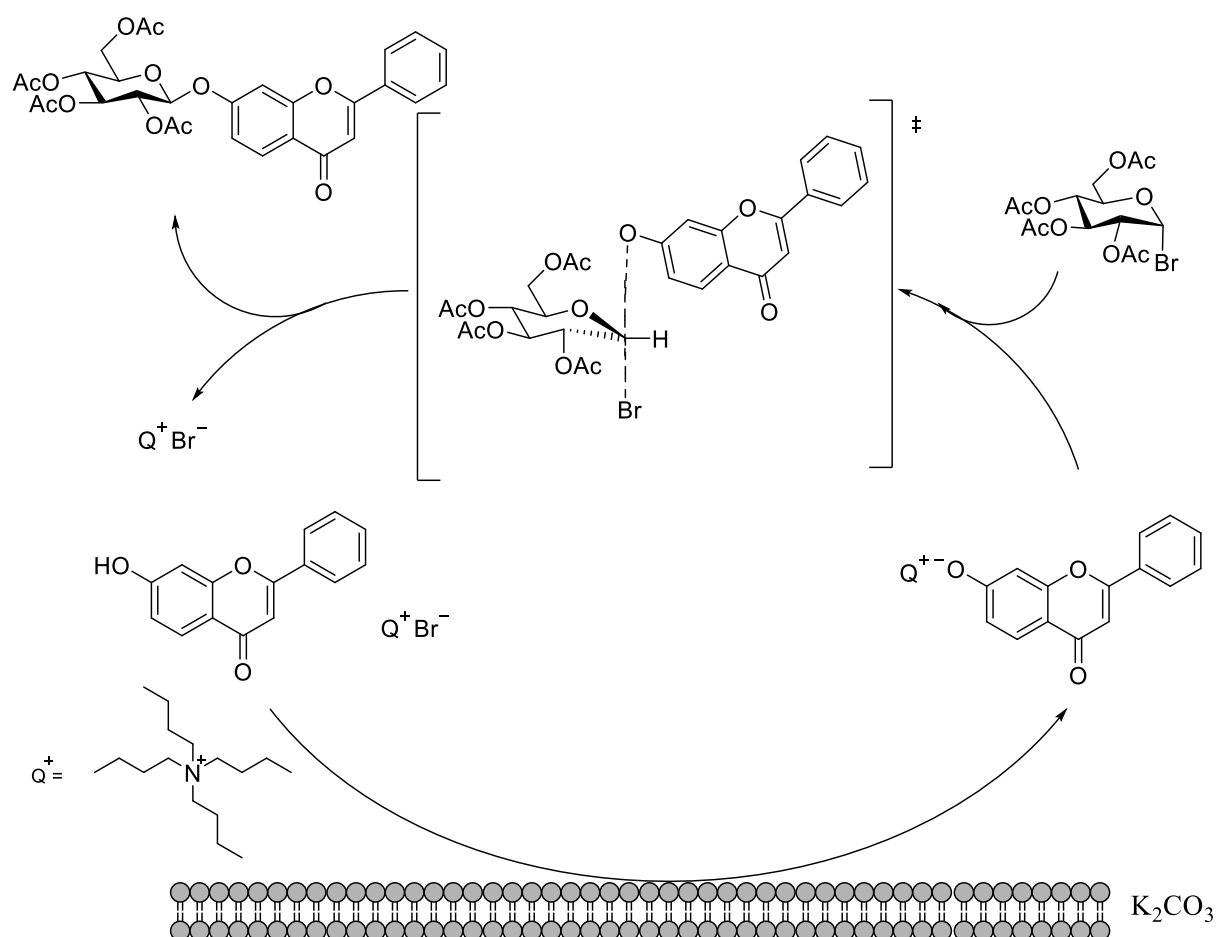


**Figure 56:** The catalytic cycle for the formation of the glycosidic flavonoids. The transition state is formed due to the reaction going through an  $S_N2$  reaction style.

When this reaction was performed on chrysin **103** to produce the per-*O*-acetylated intermediates for **114** and **115**, a mono-glycosylated compound was formed, with the *O*-glycosylation having occurred at the C (7) position. The  $^1H$ -NMR spectra for **94** is shown in Figure 57. This displays a resonance at 12.83 ppm which refers to the hydroxyl present in the A ring (C (5) labelled as

20). The free hydroxyl for the C (7) position is found further downfield (~10 ppm) due to resonance effects present at the C (20) position.

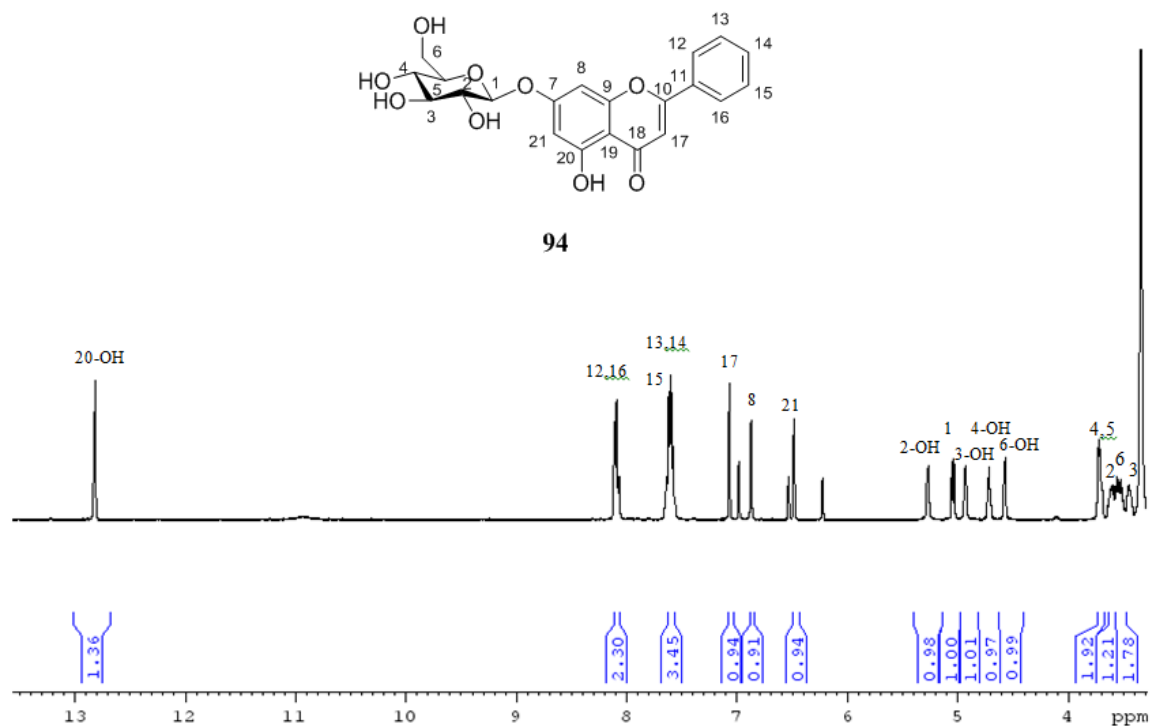


**Figure 57:** The <sup>1</sup>H-NMR spectra for compound **94**.

The acetylated intermediates are shown in Figure 58. These are first synthesised by the PTC method before deprotection to give their respective target compounds **92-97**.

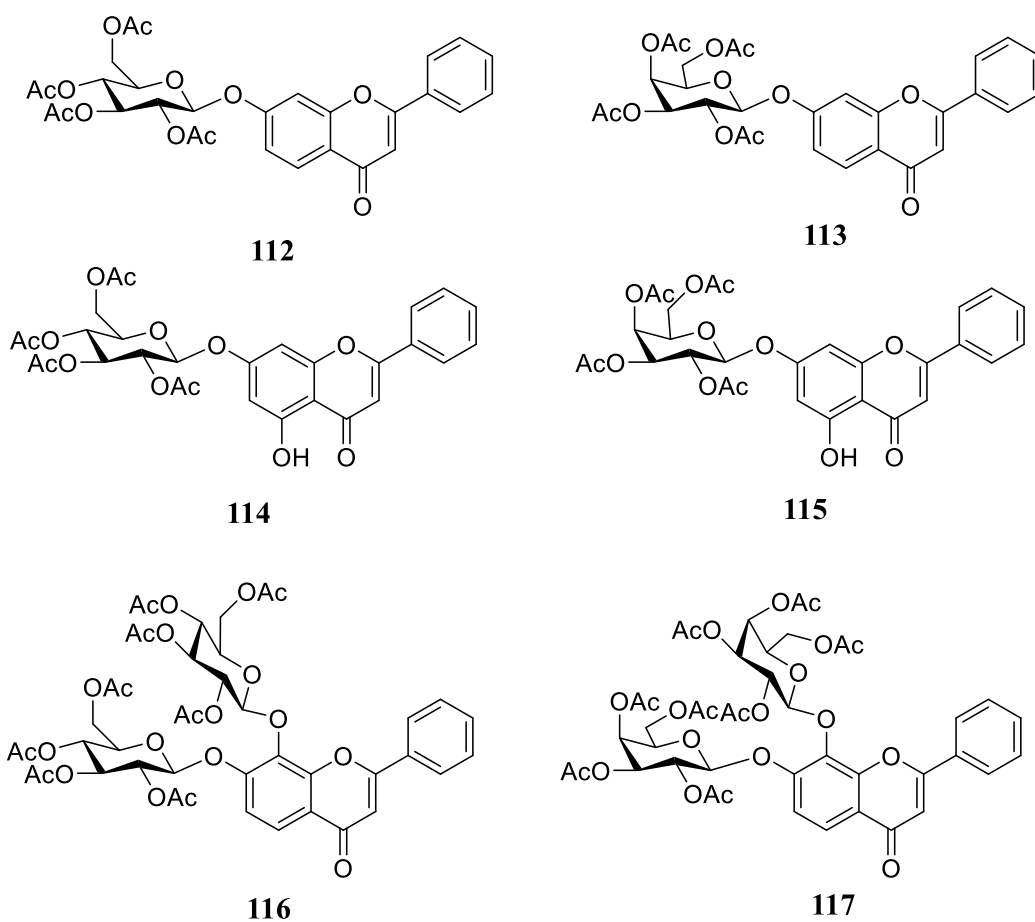


**Figure 58:** The acetylated intermediates, **112-117**, that are the products of the PTC reactions.

Only the mono-glycosylated compounds are synthesised possibly due to hydrogen bonding between the carbonyl and hydroxyl present in the C (5) position. This would hinder this position for glycosylation, therefore the glycosylations occurred in the C (7) position. This has been previously discussed in the literature, which suggests a strong hydrogen bond is present.<sup>273</sup>

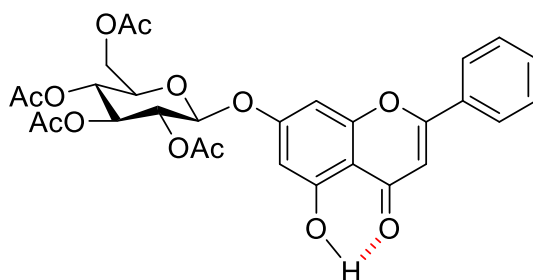


**Figure 59:** The possible hydrogen bond present in the acetylated intermediates in the synthesis for **84** and **85**.

#### 4.4.1.3 Yields and purity

Three different parent flavonoids were used to synthesise glucosides and galactosides. There was a difference in yields dependant on which carbohydrate was used, with the galactosides being produced in better yields. The parent flavonoid compound had very little impact on the yield of the glycosylation reaction as can be seen in Table 24. The di-glycosylated compounds **96** and **97** were formed in lower yields due to the mono-glycosylated product also forming.

The acetylated intermediates, **112-117**, were purified using NP-column chromatography. Following the deprotection, the products (**92-97**) were firstly filtered from the reaction mixture. This crude solid was washed with methanol and the resultant mixture was purified using RP-column chromatography. RP- silica was used to as the resultant target compounds (**92-97**) were polar.

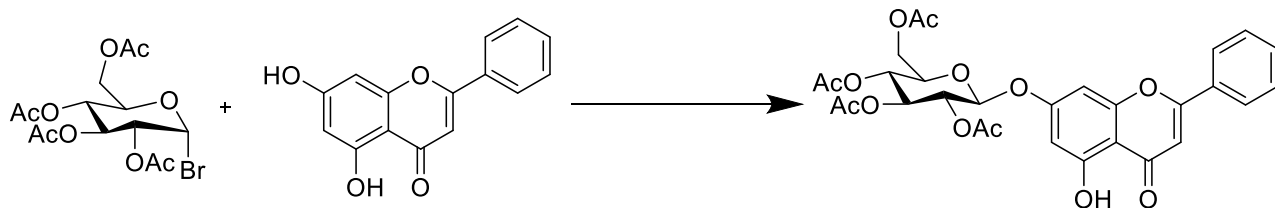
The purity of these compounds was determined using a developed HPLC method, using a gradient solvent system. Each compound was shown to have >97% purity. The chrysin based glycosides, **94** and **95**, had purities of >99%. A solvent system of A = H<sub>2</sub>O and B = MeCN was used, with a flow rate = 1.0 mL/ min. Compounds were eluted with a gradient of 10% B to 80% B for 25 min. Detection at wavelengths of 254 and 210 nm was used. A gradient was used to expose any compounds that are less polar than the target compound, such as hydrolysed sugars. An ELSD was used in conjunction with UV in the HPLC as some of the side products could be UV inactive. The yields and purities for compounds **92-97** are shown in Table 24.

**Table 24:** A table showing the yields and purity of the target compounds **92-97** and the acetylated intermediates, **112-117**.

Compound	Yields (%)		Purity (%)
	Formation of acetylated intermediates	For the deprotection	
<b>112, 92</b>	62	65	97
<b>113, 93</b>	71	68	98
<b>114, 94</b>	68	51	99
<b>115, 95</b>	69	53	99
<b>116, 96</b>	40	64	97
<b>117, 97</b>	41	62	97

#### 4.4.1.4 Optimisation of the synthetic route

There are many synthetic pathways that can be employed to *O*-glycosylate a compound. PTC is just one synthetic route that has been explored. As previously mentioned, an aq. NaOH method can be utilised to synthesise glycosidic target compounds. Both the reaction pathways for the synthesis of **114** are shown in Figure 60.



	103		114	
Glycosylation	Reactants used	Glycosyl donor used	Yield	Ref.
Aq. Michael addition	NaOH		2%	143
PTC	TBAB, K <sub>2</sub> CO <sub>3</sub>		57%	274

**Figure 60:** A table that summarizes the different conditions used for glycosylation of **114**. The scheme for the reaction is shown above the table.

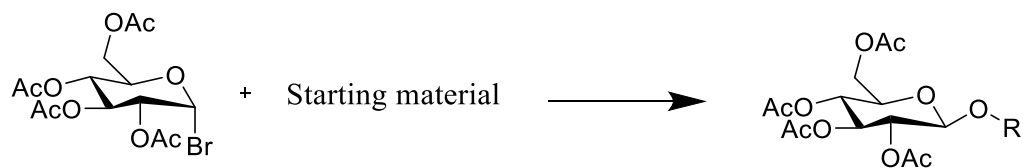
There was a big difference in yields between these two reactions. This could possibly be caused by solubility issues, chrysin **93**, the parent compound, is not soluble in aq. solutions. The solubility of chrysin is shown in Table 25. The aq. mixture was basic, with the use with NaOH, which would have aided the solubility. However, with poor solubility and the hydrolysis of the brominated carbohydrate the yield was extremely low at 2%. The solvents used in the PTC route were a mixture of anh. solvents; acetone and dimethylformamide (DMF), which are solvents in which chrysin is soluble. The use of anh. solvents also could have aided in the yield as less opportunity for the carbohydrate to hydrolyse.

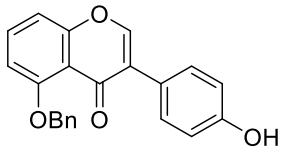
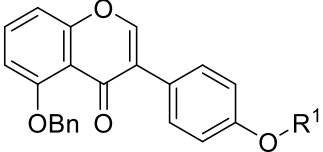
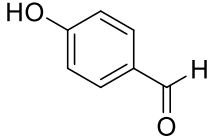
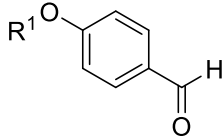
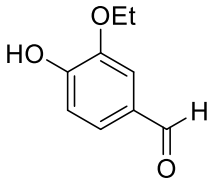
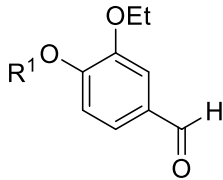
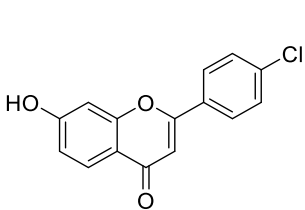
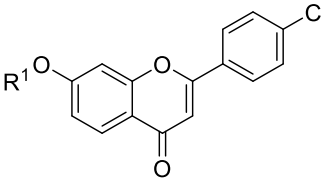
**Table 25:** A table summarising the solubility of chrysin. A concentration of 1 mg/mL was used.

<b>Solvents</b>	<b>Solubility at a concentration of 1 mg/mL</b>
DMSO	Soluble
DMF	Soluble
H <sub>2</sub> O	Insoluble
Acetone	Soluble
MeOH	Partially soluble
Chloroform	Partially soluble

There are many compounds which are classified as phase transfer catalysts. The most common catalysts used in *O*-glycosylations of aromatic compounds are tetrabutylammonium salts, with some relevant examples included within Table 26. As can be seen tetrabutylammonium bromide (TBAB), under the right conditions, can produce a greater yield when used as a phase transfer catalyst compared to benzyltriethylammonium chloride (TEBA). TBAB was therefore chosen as the phase transfer catalyst in this work, with the added advantage that the solvents used are more suitable for the sparsely soluble flavonoids.

**Table 26:** The starting material for these reactions was acetobromo- $\alpha$ -D-glucose. All produced the  $\beta$ -anomer. The R group = sugar attached to the various products. R<sup>1</sup> = sugar attached.



Catalyst used	Starting material	Product	Yield (%)	Ref.
Benzyltriethylammonium chloride (TEBA)			83	275
Tetra-n-butylammonium bromide (TBAB)			55	276
			59	277
			89	274

#### 4.4.1.5 Chemical analysis

Confirmation of the stereochemistry at the anomeric centre was determined through the use of  $^1\text{H-NMR}$  spectroscopic analysis. As previously discussed in Section 2.3.1.5., the stereochemistry at C-1 could be determined by analysing the  $J$  values for the anomeric hydrogen, H (1). The values for these are summarised in Table 27.

**Table 27:** The  $J$  values (Hz) for the six compounds **92-97**, as determined from their respective  $^1\text{H-NMR}$  spectra. CD = cannot be distinguished

Compound	$J$ value for the anomeric hydrogen (Hz)	Determined Stereochemistry
<b>92</b>	8.0	$\beta$
<b>93</b>	8.0	$\beta$
<b>94</b>	7.5	$\beta$
<b>95</b>	8.5	$\beta$
<b>96a</b>	7.5	$\beta$
<b>96b</b>	CD (cannot be distinguished)	$\beta$
<b>97a</b>	CD	$\beta$
<b>97b</b>	8.5	$\beta$

For compounds **96** and **97**, one of the anomeric H peaks for the carbohydrates are under another peak so a  $J$  value cannot be distinguished.

There is a difference in resonance shifts for the anomeric hydrogen between the acetylated intermediates and the deprotected final products. In Table 28, the anomeric H resonance peaks are shown for the acetylated intermediates and the final target compounds **92-97**, with the peaks from the acetylated intermediates being further upfield. There are also resonance peaks found between 2-3 ppm, these are not present in the final compounds.

**Table 28:** A table showing the differences between the resonance peaks using  $^1\text{H-NMR}$  spectra.  
\* = The resonance peaks are under other peaks

<b>Compound</b>	<b>Resonance peak at the anomeric H (ppm)</b>	<b>Acetylated intermediate resonance peak at the anomeric H (ppm)</b>
<b>92</b>	5.09	5.25
<b>93</b>	5.12	5.32
<b>94</b>	5.03	5.20
<b>95</b>	5.04	5.13-5.18*
<b>96a</b>	5.04	5.27-5.41*
<b>96b</b>	4.97-5.01*	5.52
<b>97a</b>	4.92-4.99*	5.27
<b>97b</b>	4.91	5.44-5.52*

#### 4.4.2 Microbiology data for the flavonoid containing compounds

##### 4.4.2.1 Microbiological results

A bioscreen method was used to obtain the MIC<sub>100</sub> values for the glycosylated flavonoid compounds **92-97**. Two different broths were used: NB and MHB.

##### 4.4.2.2 Microbiology data for the parent flavonoid compounds **103, 110 and 111** in agar

Due to the poor solubility of the parent flavonoid compounds (**103, 110 and 111**), the bioscreen method could not be used to gain MIC<sub>100</sub> information. When the compounds **103, 110 and 111** were dissolved in the maximum percentage of DMSO (3%)<sup>278</sup> in the two respective broths (NB and MHB), precipitation occurred once the aq. media was added. In Table 29, the conditions that were used to try and overcome these solubility issues are summarised.

**Table 29:** A table showing the different conditions used to try and solubilise the parent flavonoid compounds for the bioscreen method.

Method used	Result
Aq. Media, 3% DMSO	Precipitation occurred
Tween 80 (emulsifier)	Precipitation occurred
pH change to 6.5. (using aq. NaOH)	Precipitation occurred

Precipitation occurred in all the conditions, which led to an agar method being used, an example of the plates is shown in Figure 61. The agar chosen was Mueller-Hinton agar (MHA), the results are still comparable to the MIC<sub>100</sub> values collected using the bioscreen method.<sup>116,143</sup>

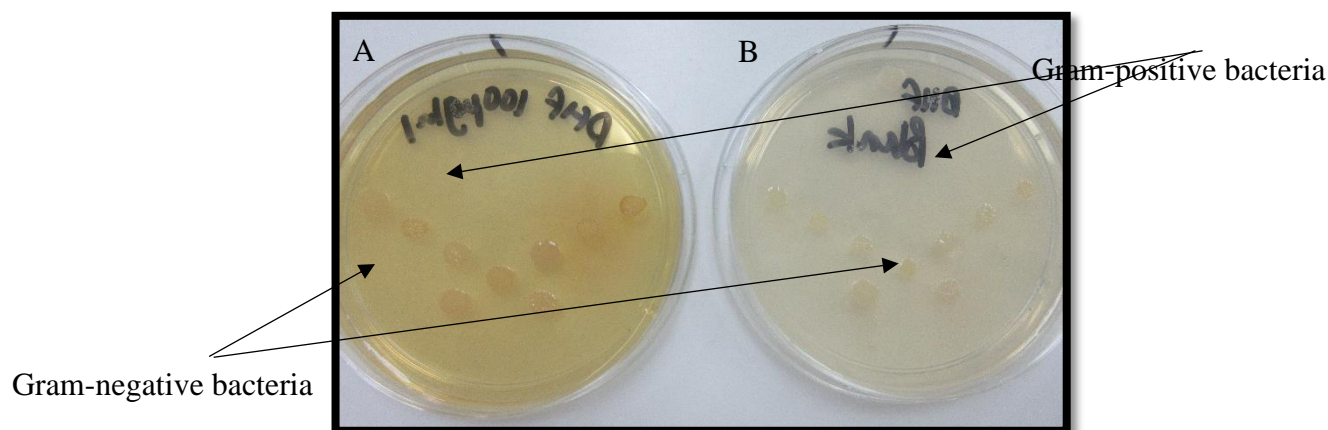


**Figure 61:** MHA with the target bacteria. A = **111** at 100 µg/mL. B = MHA control

During the agar method, different solvents were used to improve solubility in the agar. The parent flavonoid was firstly dissolved in the selected solvent. The solvents used were present in literature and would not affect the bacterial growth. These were then added to the agar and set on a plate before bacteria was added to the top of the agar. The solvents used are summarised in Table 30.

**Table 30:** A summary of the different conditions in which the agar was prepared

Solvent used	Percentage used	Result	Ref.
DMSO	0.5-1.5%	Precipitation visible in the agar	278
DMSO	2%	Precipitation visible for <b>110</b> and <b>103</b>	
Acetone	30%	Precipitation visible before adding agar	252
Methanol	10%	Precipitation visible	279

Once water was added to the acetone stock solution to create 30% concentrations, precipitation occurred. The parent flavonoids, **103**, and **110-111**, were also found not to be soluble in

methanol before the aq. media was added. In DMSO, all the flavonoids are soluble, however once the aq. media is added to **103** and **110** precipitation occurred. DMSO, at 2%, was used although precipitation still occurred at concentrations 100-50  $\mu\text{g/mL}$  for **103** and **110**. The MIC values reflect this with the maximum concentration of compound that fully dissolved into agar, 25  $\mu\text{g/mL}$ . The MIC<sub>100</sub> values for the parent flavonoids **103**, **110** and **111** are shown in Table 31.

**Table 31:** The MIC<sub>100</sub> data for the underivised parent compounds **93**, **100-101**. The agar is MH. NG – No growth. The values highlighted yellow show MIC<sub>100</sub>  $\geq 50$   $\mu\text{g/mL}$ . The ClogP data was calculated using Chem BioDraw Ultra software version 13.0.

Organisms	MIC ( $\mu\text{g/ml}$ ) of various parent flavonoids ( <b>103</b> , <b>110</b> , and <b>111</b> ).			
	OCC	<b>110</b>	<b>103</b>	<b>111</b>
	CLogP	3.21	3.56	2.73
<i>B. cereus</i>	754	>25	>25	100
<i>E. faecalis</i>	640	>25	>25	>100
<i>E. faecium</i>	220	>25	>25	>100
<i>S. aureus</i>	100	12.5	>25	50
<i>S. epidermis</i>	691	6.25	NG	25
<i>St. agalactiae</i>	182	25	>25	100
<i>St. pneumoniae</i>	1548	NG	NG	NG
<i>St. pyogenes</i>	168	NG	NG	NG
<i>St. viridans</i>	1683	NG	NG	NG
<i>C. freundii</i>	851	>25	>25	>100
<i>Cr. sakazakii</i>	1888	>25	>25	>100
<i>En. cloacae</i>	760	>25	>25	>100
<i>Es. coli</i>	199	>25	>25	>100
<i>K. pneumoniae</i>	758	>25	>25	>100
<i>P. mirabilis</i>	2080	>25	>25	>100
<i>Ps. aeruginosa</i>	201	>25	>25	>100
<i>Sa. typhimurium</i>	854	>25	>25	>100
<i>Se. marcescens</i>	217	>25	>25	>100

As to be expected, the MIC values for the gram-negative bacteria were all high, >25  $\mu\text{g/mL}$  for **103** and **110** and >100  $\mu\text{g/mL}$  for **111**. For the compound **110**, with one hydroxyl present in the

C (7) position, there were MIC values collected for *Staphylococcus aureus*, *Staphylococcus epidermidis* and *Streptococcus agalactiae*, 12.5, 6.25, and 25  $\mu\text{g/mL}$  respectively. *Staphylococcus epidermidis*, when present in blood, can lead to sepsis especially in preterm infants. In 2010, sepsis accounted for 5.1% of deaths in England.<sup>280</sup> *Staphylococcus aureus* is a sole contributor to toxic shock syndrome, acute endocarditis and botryomycosis. This bacteria also acquires resistance to produce MRSA, which recently has gained a lot of media attention as named as the superbug. A potential mechanism of action, as seen with various other flavonoids, for these compounds could involve inhibiting *Staphylococcus aureus*  $\beta$ -Ketoacyl acyl carrier protein synthase III (saKASIII). The enzyme saKASIII is responsible for initiating the fatty acid synthesis in bacteria, and is seen as a key target enzyme to overcome the antibiotic resistance problem. The hydroxyl present in the C (7) position can participate in hydrogen bond interactions with the backbone oxygen of Phe298 and Ser152.<sup>281</sup>

The flavone **111** has hydroxyls present in the C (7) and (8) positions. Against *Staphylococcus aureus* and *Staphylococcus epidermidis* was found to have MIC values of 50  $\mu\text{g/mL}$  and 25  $\mu\text{g/mL}$ , respectively. These values are less than those recorded for **110**, suggesting the hydroxyl present in the C (8) position may slightly affect the MIC values. When a hydroxyl was added to the C (5) position in **103**, the values were higher at  $>25 \mu\text{g/mL}$ .

There was no growth shown for *Streptococcus pneumoniae*, *Streptococcus pyogenes* and *Streptococcus viridians*. There were difficulties when culturing these strains of bacteria, with little growth in the cultures overnight.

#### **4.4.2.3 Microbiology data for the parent flavonoid compounds (103, 110 and 111) and their respective glycosides 92-97**

The glycosides, **92-97**, of the various parent flavonoids (**103,110** and **111**) were tested using the bioscreen method in two different broths, NB and MHB. These results were then compared

to the agar results for their respective flavonoid parent compounds. All the glycosylated flavonoid compounds, **92-97**, could be analysed using an aq. media broth method. The solubilities of flavonoids increased when glycosylated to either glucose or galactose. DMSO, at 3%, was used to solubilise the glycosylated compounds, **92-97**, during the bioscreen technique. Precipitation did not occur during the testing unlike their parent counterparts.

The glycosides **92** and **93** of 7-hydroxyflavone **110** were tested against gram-negative and gram-positive bacteria; the MIC values are shown in Table 32.

**Table 32:** The MIC<sub>100</sub> data for the underivised parent compounds **110** and its respective glycosides **92** and **93**. The agar is MHB; with the broth shown NB (**92-93**). NG – No growth. The values highlighted yellow show MIC<sub>100</sub> ≥ 50 µg/mL. The ClogP data was calculated using Chem BioDraw Ultra software version 13.0.

Organisms	MIC (µg/ml) of the 110 moiety attached to various sugars.			
	OCC	110	92	93
	CLogP	3.21	1.51	1.51
<i>B. cereus</i>	754	>25	>128	>128
<i>E. faecalis</i>	640	>25	>128	>128
<i>E. faecium</i>	220	>25	>128	>128
<i>S. aureus</i>	100	12.5	>128	>128
<i>S. epidermis</i>	691	6.25	>128	>128
<i>St. agalactiae</i>	182	25	>128	>128
<i>St. pneumoniae</i>	1548	NG	>128	>128
<i>St. pyogenes</i>	168	NG	>128	>128
<i>St. viridans</i>	1683	NG	>128	>128
<i>C. freundii</i>	851	>25	>128	>128
<i>Cr. sakazakii</i>	1888	>25	>128	>128
<i>En. cloacae</i>	760	>25	>128	>128
<i>Es. coli</i>	199	>25	>128	>128
<i>K. pneumoniae</i>	758	>25	>128	>128
<i>P. mirabilis</i>	2080	>25	>128	>128
<i>Ps. aeruginosa</i>	201	>25	>128	>128
<i>Sa. typhimurium</i>	854	>25	>128	>128
<i>Se. marcescens</i>	217	>25	>128	>128

The glycosides, **92** and **93**, had values of >128 µg/ml for all bacteria strains tested against in NB. The glycosides also had higher MIC values when compared to their parent compound, **110**.

The glycosides **94** and **95** of chrysin **103** MIC values were compared and are shown in Table 33.

**Table 33:** The MIC<sub>100</sub> data for the underivised parent compounds **93** and its respective glycosides **84** and **85**. The agar is MHB; with the broth shown NB (**94-95**). NG – No growth. The values highlighted yellow show MIC<sub>100</sub> ≥ 50 µg/mL. The ClogP data was calculated using Chem BioDraw Ultra software version 13.0.

Organisms	MIC (µg/ml) of the 103 moiety attached to various sugars.			
	OCC	103	94	95
	CLogP	3.56	2.07	2.07
<i>B. cereus</i>	754	>25	>128	>128
<i>E. faecalis</i>	640	>25	>128	>128
<i>E. faecium</i>	220	>25	>128	>128
<i>S. aureus</i>	100	>25	>128	>128
<i>S. epidermis</i>	691	NG	>128	>128
<i>St. agalactiae</i>	182	>25	>128	>128
<i>St. pneumoniae</i>	1548	NG	>128	>128
<i>St. pyogenes</i>	168	NG	>128	>128
<i>St. viridans</i>	1683	NG	>128	>128
<i>C. freundii</i>	851	>25	>128	>128
<i>Cr. sakazakii</i>	1888	>25	>128	>128
<i>En. cloacae</i>	760	>25	>128	>128
<i>Es. coli</i>	199	>25	>128	>128
<i>K. pneumoniae</i>	758	>25	>128	>128
<i>P. mirabilis</i>	2080	>25	>128	>128
<i>Ps. aeruginosa</i>	201	>25	>128	>128
<i>Sa. typhimurium</i>	854	>25	>128	>128
<i>Se. marcescens</i>	217	>25	>128	>128

The results shown above are results in NB. Similar to **92-93**, the glycosides **94** and **95** had values of >128 µg/ml. When compared the **103**, the parent compound, they all had values that exceeded the limits of the experiment.

The glycosides **96** and **97** of 7,8-dihydroxyflavone **111** were tested against gram-negative and gram-positive bacteria, the MIC values are shown in Table 34.

**Table 34:** The MIC<sub>100</sub> data for the underivised parent compounds **111** and its respective glycosides **96** and **97**. The agar is MHB; with the broth shown NB (**96-97**). NG – No growth. The values highlighted yellow show MIC<sub>100</sub> ≥ 50 µg/mL. The ClogP data was calculated using Chem BioDraw Ultra software version 13.0.

Organisms	MIC (µg/ml) of the 111 moiety attached to various sugars.			
	OCC	101	96	97
	CLogP	2.73	-0.89	-0.89
<i>B. cereus</i>	754	100	>128	>128
<i>E. faecalis</i>	640	>100	>128	>128
<i>E. faecium</i>	220	>100	>128	>128
<i>S. aureus</i>	100	50	>128	>128
<i>S. epidermis</i>	691	25	>128	>128
<i>St. agalactiae</i>	182	100	>128	>128
<i>St. pneumoniae</i>		NG	>128	>128
<i>St. pyogenes</i>	163	NG	>128	>128
<i>St. viridans</i>		NG	>128	>128
<i>C. freundii</i>	851	>100	>128	>128
<i>Cr. sakazakii</i>	1888	>100	>128	>128
<i>En. cloacae</i>	760	>100	>128	>128
<i>Es. coli</i>	199	>100	>128	>128
<i>K. pneumoniae</i>	758	>100	>128	>128
<i>P. mirabilis</i>	2080	>100	>128	>128
<i>Ps. aeruginosa</i>	201	>100	>128	>128
<i>Sa. typhimurium</i>	854	>100	>128	>128
<i>Se. marcescens</i>	217	>100	>128	>128

The results from **96-97** are  $>128 \mu\text{g/mL}$  for all bacteria tested in NB. Similarly to **92-93**, **96-97** had higher MIC values for *Staphylococcus aureus* and *Staphylococcus epidermis*.

For all the glycosides tested, **92-97**, had values of  $>128 \mu\text{g/mL}$ . This could be due to many factors; including transport issues and enzyme issues. Further testing is needed to exploring the kinetics of the enzyme cleaving the glycoside to release the drug.

For all the measured  $\text{MIC}_{100}$  values using the bioscreen method, **92-97**, there were no differences between the two different media employed during the bioscreen method (NB and MHB). The results for the MHB are shown in Table 35.

**Table 35:** The MIC<sub>100</sub> data for the glycosidic flavonoid compound **92-97**. The broth is MHB. NG – No growth.

Organisms	MIC <sub>100</sub> (µg/mL) of various flavonoid moieties attached to glycosides, 92-97.						
	OCC	MHB					
		92	93	94	95	96	97
<i>B. cereus</i>	754	>128	>128	>128	>128	>128	>128
<i>E. faecalis</i>	640	>128	>128	>128	>128	>128	>128
<i>E. faecium</i>	220	>128	>128	>128	>128	>128	>128
<i>S. aureus</i>	100	>128	>128	>128	>128	>128	>128
<i>S. epidermis</i>	691	>128	>128	>128	>128	>128	>128
<i>St. agalactiae</i>	182	>128	>128	>128	>128	>128	>128
<i>St. pneumoniae</i>	1548	>128	>128	>128	>128	>128	>128
<i>St. pyogenes</i>	168	>128	>128	>128	>128	>128	>128
<i>St. viridans</i>	1683	>128	>128	>128	>128	>128	>128
<i>C. freundii</i>	851	>128	>128	>128	>128	>128	>128
<i>Cr. sakazakii</i>	1888	>128	>128	>128	>128	>128	>128
<i>En. cloacae</i>	760	>128	>128	>128	>128	>128	>128
<i>Es. coli</i>	199	>128	>128	>128	>128	>128	>128
<i>K. pneumoniae</i>	758	>128	>128	>128	>128	>128	>128
<i>P. mirabilis</i>	2080	>128	>128	>128	>128	>128	>128
<i>Ps. aeruginosa</i>	201	>128	>128	>128	>128	>128	>128
<i>Sa. typhimurium</i>	854	>128	>128	>128	>128	>128	>128
<i>Se. marcescens</i>	217	>128	>128	>128	>128	>128	>128

#### 4.4.3 SAR of the target compounds **103**, **110** and **111** and their respective glycosides **92-97**

Using the data collected in Chapter 4, SAR can be deduced. Figure 62 summarises the SAR collected. The addition of the carbohydrate produced lowered MIC values when compared to their respective parent compounds, with the exception of **103** and **96-97**. Chrysin **103** and its glycosides (**96-97**) had values that could not be determined using the concentrations used, >128 µg/mL for **96-97** and >25 µg/mL for **103**. For the double glycosylated compounds, **94-95**, they had the same values as the mono-glycosidic compounds. When the glycosides were analysed, the glucosides and galactosides of **103**, **110** and **111** had the same MIC values, >128 µg/mL over a 24 h time period. When applying the prodrug approach to the glycosides synthesised, the carbohydrate was masking the drug producing a less toxic drug. Further kinetic analysis is needed to determine whether the sugar is cleaved or if the compound remains as a glycoside. The glycosides had better solubility in aq. media, so therefore were analysed using a bioscreen method. Whereas the parent compounds an agar method was utilised.

For the parent flavonoid **110** and **111**, there were lower MIC values recorded for *Staphylococcus aureus* and *Staphylococcus epidermis*. Both of these bacteria can lead to death, sepsis from *S. epidermis* and toxic shock syndrome, acute endocarditis, and epidural abscesses to name a few for *S. aureus*. The ‘superbug’ (MRSA) is also associated with *S. aureus*. For compound **103**, the MIC values were >25 µg/mL for all bacteria tested. The hydroxyl present in the C (5) position hindered antimicrobial activity when compared to **110**. The extra hydroxyl present in the C (8) position in **111** slightly affected the MIC values.

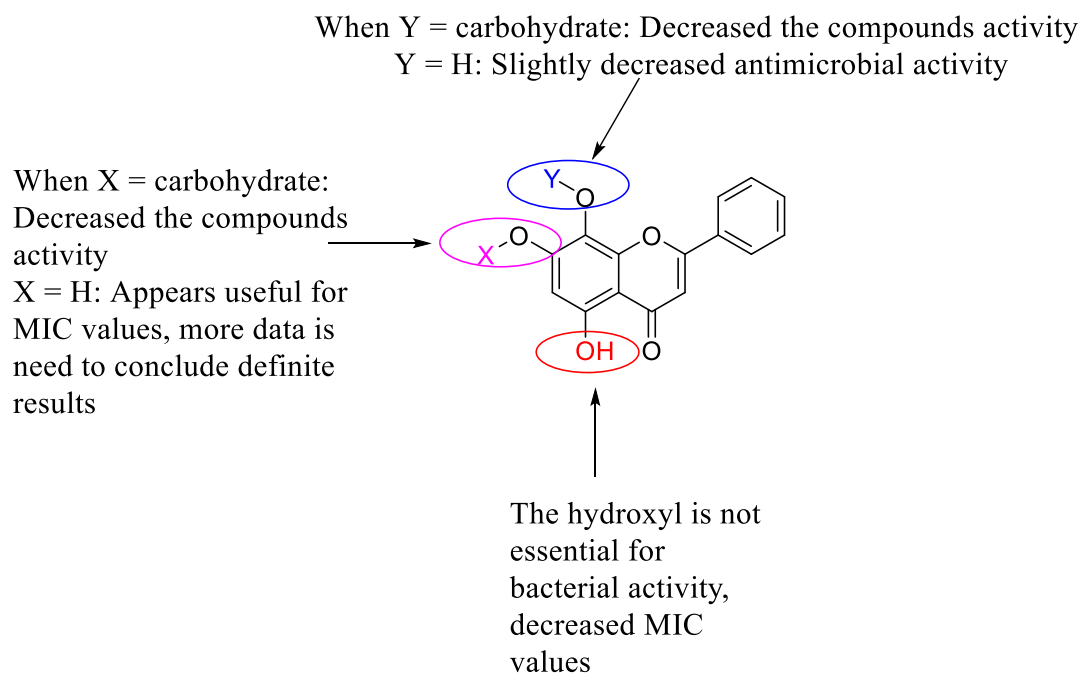
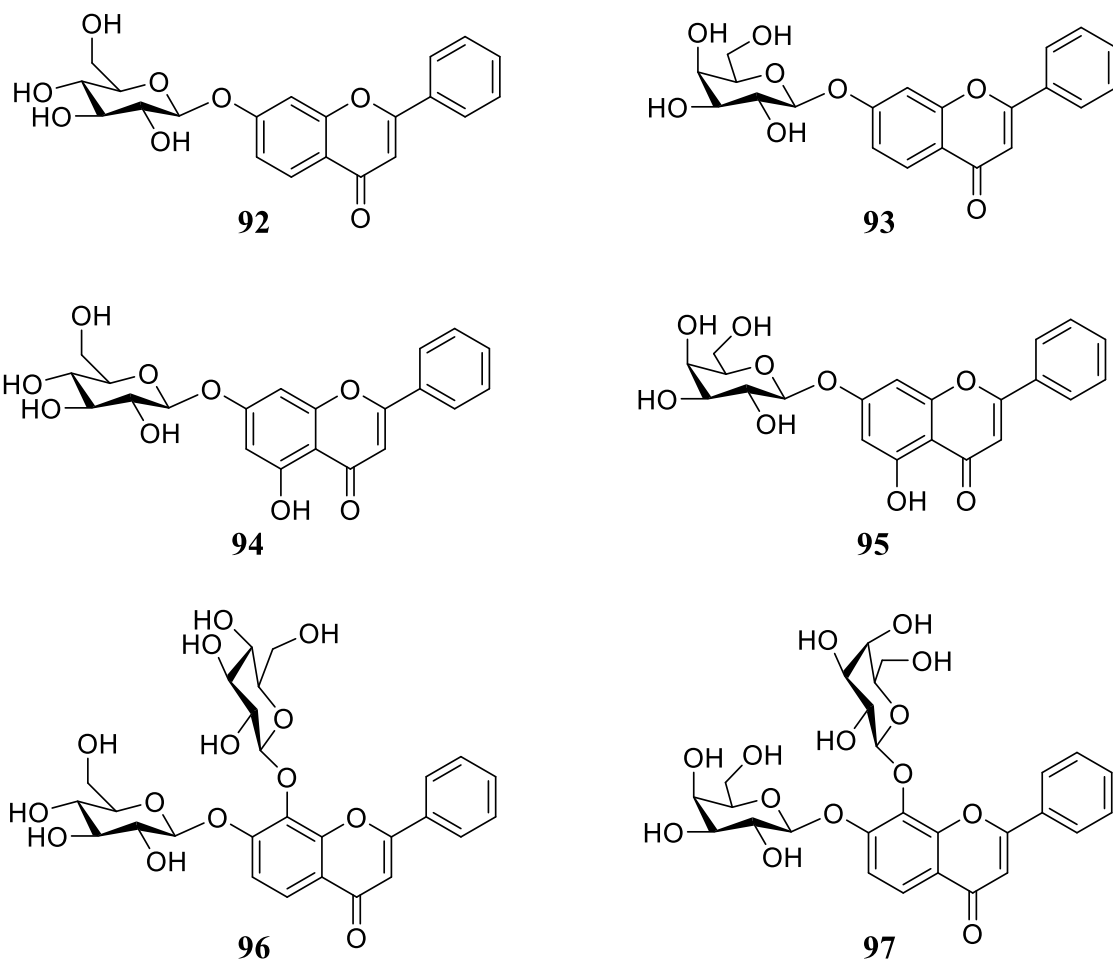


**Figure 62:** A diagram showing the SAR collected from the different flavonoid moieties attached as glucosides and galactosides.

#### 4.5 Conclusion

The target compounds **92-97**, found in Figure 63, were successful synthesised using a PTC method. The  $\beta$ -anomers were synthesised, as can be seen for the  $^1\text{H-NMR}$  spectra, using  $J$  values of the doublet present for the anomeric centre.



	112	92	113	93	114	94	115	95	116	96	117	97
Yield:	62	65	71	68	68	51	69	53	40	64	41	62
Purity:	--	97	--	98	--	99	--	99	--	97	--	97

**Figure 63:** The target structures **92-97**, with their respective yields and purities shown. The yields of their respective intermediates are also displayed.

There were slight differences in the yields for the acetylated intermediate compounds, **112-117**, with lower yields recorded for the double glycosylated compounds **116-117**. PTC was utilised for the glycosylation as the parent compounds, **103**, **110** and **111**, were soluble in the solvents used, DMF and acetone. The deprotection of the acetylated compounds was performed using  $K_2CO_3$  in anh. methanol.

The MIC data for the parent compounds were collected using an agar method, due to solubility issues. For compounds **103** and **110**, precipitation still occurred at 2% DMSO in aq. media, therefore the results recorded were limited to 25 µg/mL. Against the bacteria *Staphylococcus aureus* and *Staphylococcus epidermis*, **110** and **111** had MIC values of 12.5 and 50 µg/mL for *S. aureus* and 6.25 and 25 µg/mL for *S. epidermis*, respectively. Compound **110** also had an MIC value of 25 µg/mL for *St. agalactiae*, which is comparable to fusidic acid which has a MIC value of 32 µg/mL.<sup>282</sup> Fusidic acid is used as a topical cream and eye drops for *Staphylococci* and *Streptococci* infections. The glycosides of the respective flavonoid parent compounds were more soluble in the 3% DMSO in aq. media, therefore a bioscreen method was used to analyse these compounds for MIC values. The MIC values collected for all the glycosides, **92-97**, were >128 µg/mL.

SAR data was collected from comparisons between compounds **92-97**, **103**, **110**, and **111**. The hydroxyl present in the C (7) position appears to be essential for antimicrobial activity against *Staphylococci*. This is in agreement with literature, which suggests that this hydroxyl hydrogen bonds to inhibit the enzyme saKASIII. The hydroxyl present in the C (5) position is not essential for antimicrobial activity, **103** had MIC values of >25 µg/mL for all bacteria tested against. The hydroxyl present in the C (8) position seemed to increase the MIC values slightly, as seen in compound **111** when compared to **110**.

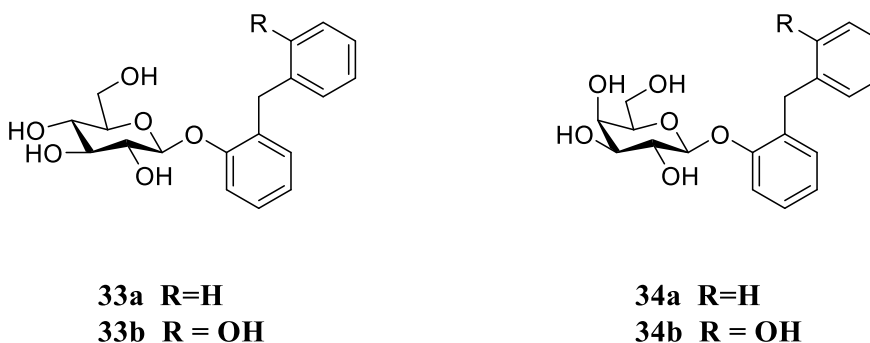
## **Chapter 5 – Conclusions and Future work**

## 5.1 Overall summary of this project

The research presented in this project concentrated on the design, synthesis, and biological testing of novel antimicrobials. The moieties were all selected to probe SAR of the various classes of compounds. The target compounds were synthesised using various synthetic methods; namely glycosylations or ‘click’ chemistry. These were then screened against various bacteria that are seen as a threat to human and animal health to ascertain their antimicrobial properties. In Chapter 3, the triazole containing compounds were fitted in the HIV reverse transcriptase enzyme active site to probe the compounds **44-51** antiviral properties. In Chapter 4, the flavonoid containing compounds were also tested to explore their anticancer properties. All the glycosides tested had MIC values above that of their respective parent compounds.

## 5.2 The carbohydrate prodrugs containing a bisphenol moiety

Four novel  $\beta$ -glycoside containing compounds, **33-34** (Figure 64), were synthesised. This route used the corresponding per-*O*-acetylated carbohydrate and NaOH to create the acetylated glycoside intermediates. These were then deprotected using  $K_2CO_3$  in anhydrous methanol. All compounds had >99% purity as determined by HPLC.



The MIC<sub>100</sub> data for these compounds were then determined using a bioscreen method. There was a correlation between the ClogP values and the MIC<sub>100</sub> values; the higher the ClogP value

the lower the MIC<sub>100</sub> value. The addition of a glycoside to the parent compounds led to higher MIC values when compared to their respective parent compounds. In *Streptococcus agalactiae*, BP **42**, the parent compound, had a MIC value of 64 µg/mL whereas the glucoside **33a** and the galactoside **34a** had MIC values of >256 µg/mL.

When compared with other data in the literature,<sup>142,283</sup> SAR could be found. The additional hydroxyl which is present in **43**, the underivised compound for **33b** and **34b**, was not required to improve the MIC values. BP **42** had MIC values of 64 µg/mL for *Streptococcus agalactiae* and *Streptococcus pyogenes*, whereas HMP **43** had MIC values of >256 µg/mL for the respective bacteria. There was also a positive correlation between an increase in halogens present and an increase in MIC values, the MIC values for the underivised compounds are shown in Table 36.

**Table 36:** The MIC values (µg/mL) for *St. agalactiae* and *Es. coli* the underivised compounds. Compounds **39-41** data was adapted from ref. 103.

Compound	Halogens present	Hydroxyls present	MIC <sub>100</sub> values (µg/mL)	
			<i>St. agalactiae</i>	<i>Es. coli</i>
Hex <b>39</b>	6 x Cl	2	<0.5	8
BCP <b>40</b>	2 x Br 2 x Cl	2	<0.5	>128
DP <b>41</b>	2 x Cl	2	1	64
BP <b>42</b>	0	1	64	128
HMP <b>43</b>	0	2	128	256

A summary of the MIC values for clinically available antimicrobial compounds is shown in Table 37. There is also a comparison shown with the MIC values collected for the parent

bisphenol compounds (**42** and **43**) and their respective glycosides (**33-34**). BP (**42**) had similar MIC values as cefaclor and cefadroxil in *Streptococcus pneumoniae*.

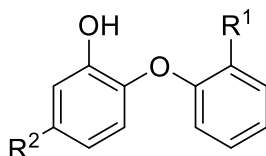
**Table 37:** A comparison of clinically available antimicrobials MIC values with the bisphenol parent compounds **42** and **43** and their respective glycosides **33-34** MIC values. The values are reported by EUCAST for the clinically used compounds.

Compound	Bacterial strain MIC ( $\mu\text{g/mL}$ )
	<i>St. pneumoniae</i>
amoxicillin	0.004-2
ampicillin	0.004-4
azithromycin	0.03-32
cefaclor	0.06-64
cefadroxil	1-64
daptomycin	0.06-0.5
ertapenem	0.008-0.5
fosfomicin	4-32
levofloxacin	0.5-2
linezolid	0.5-2
minocycline	0.03-0.5
2-benzyl phenol ( <b>42</b> )	64
bis(2-hydroxyphenyl)methane ( <b>43</b> )	128
2-benzyl phenol- $\beta$ -D-glucofuranoside ( <b>33a</b> )	>256
2-benzyl phenol- $\beta$ -D-galactofuranoside ( <b>33b</b> )	>256
bis(2-hydroxyphenyl)methane- $\beta$ -D-glucofuranoside ( <b>34a</b> )	>256
bis(2-hydroxyphenyl)methane- $\beta$ -D-galactofuranoside ( <b>34b</b> )	>256

The MIC values collected for the glycosides **33-34** were all higher than that of the antimicrobials already available.

### 5.2.1 Future work for the carbohydrate prodrugs containing a bisphenol moiety

As previously mentioned in Section 2.2.3, other bisphenols have been previously studied to determine their MIC against *Es. coli* (wild type). These compounds could also be converted to carbohydrate prodrugs to draw more SAR data. The compounds are shown in Figure 65.<sup>283</sup>



Compound	R <sup>1</sup>	R <sup>2</sup>	MIC (µg/mL) <i>Es. coli</i>
<b>118</b>	H	H	3.7
<b>119</b>	H	Cl	0.07
<b>120</b>	H	F	0.6
<b>121</b>	H	Me	1.0
<b>122</b>	OH	H	2.0

**Figure 65:** The MIC<sub>100</sub> values for compounds **118-122**. The work was performed by ref. 284.

The β-glycosides derivatives of these compounds could be synthesised and their MIC<sub>100</sub> determined. These can then be compared to **33-34** and **35-37** to gain SAR information. In the compounds presented above, **118-122**, there is an oxygen present in the bridge between the two aromatic rings. SAR data can be collected when compared to **33-34** and **35-37** where it is a methyl bridge. The analysis of the SAR data could enable the determination of the chemical group responsible for evoking a target biological effect in the organism. This in turn allows for the modification of the effect or the potency of a bioactive compound by changing its chemical structure.

### 5.3 The triazole containing compounds based on azidothymidine

Eight novel 1,2,3-triazole containing compounds, **44-51**, were synthesised using ‘click’ chemistry methods, the compounds are shown in Figure 66. Different metal catalysts were used to synthesis the two different isomers; the 1,4-1,2,3-triazole isomers were synthesised using a copper catalyst and the 1,5-1,2,3-triazole isomers were synthesised using a ruthenium catalyst. The 1,4-1,2,3-triazole containing compounds, **44-47**, were synthesised in greater yields when compared to the 1,5-1,2,3-triazole isomers, **48-51**. All compounds had >99% purity as determined by HPLC.

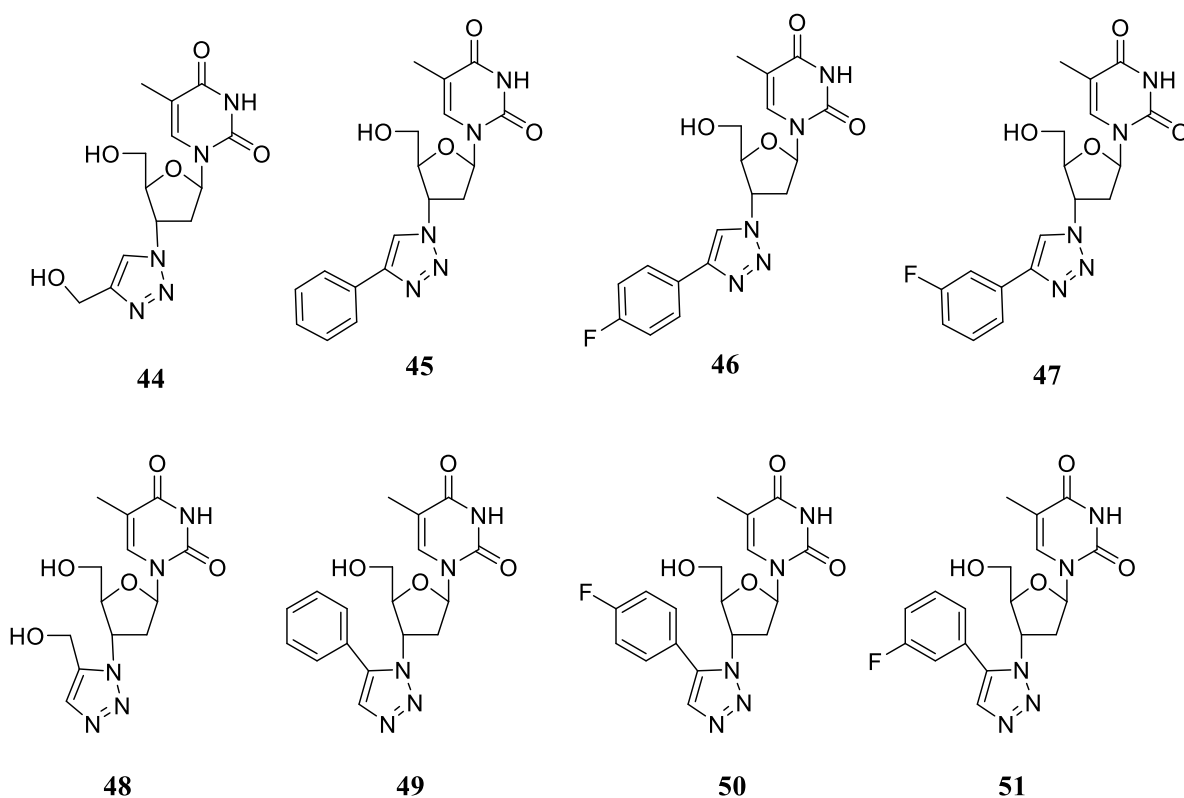


**Figure 66:** The target compounds, **44-51**, for the 1,2,3-triazole containing compounds.

These compounds' MIC<sub>100</sub> values were obtained using the bioscreen method. Compounds **44-51** all displayed no biological activity against gram-positive bacteria. The

1,5-1,2,3-triazoles, **44-47**, generally had lower MIC values when compared to their 1,4-1,2,3-triazole isomer counterparts, with compound **48** having comparable MIC values to AZT **52** against *Escherichia coli*, 8 µg/mL, and *Klebsiella pneumoniae*, 0.5 µg/mL. The compounds AZT (**52**) and 3'-deoxy-3'-(5-Hydroxymethyl-1,2,3-triazol-1-yl)-β-D-thymidine (**48**) had comparable MIC values when compared to clinically used antimicrobials, summarised in Table 38. Compounds **45** and **49** also had comparable MIC values, 4 µg/mL, when compared to chloramphenicol, 1-16 µg/mL.

**Table 38:** A comparison of clinically available antimicrobials MIC values with the AZT **52** and its triazole containing compounds **44-51** MIC values. The values are reported by EUCAST for the clinically used compounds.

Compound	Bacterial strain MIC values ( $\mu\text{g/mL}$ )
	<i>K. pneumoniae</i>
amoxicillin	32->512
ampicillin	4-256
azteonam	0.5-32
chloroamphenicol	1-16
colistin	0.12-2
doxycycline	0.5-4
ertapenem	0.08-0.25
gentamycin	0.12-2
levofloxacin	0.03-0.25
mecillinam	0.06-1
minocycline	0.5-8
<b>AZT (52)</b>	0.5
3'-deoxy-3'-(4-hydroxymethyl-1,2,3-triazol-1-yl)- $\beta$ -D-thymidine ( <b>44</b> )	64
3'-deoxy-3'-(4-benzyl-1,2,3-triazol-1-yl)- $\beta$ -D-thymidine ( <b>45</b> )	4
3'-deoxy-3'-(4-4''-fluoro-benzyl-1,2,3-triazol-1-yl)- $\beta$ -D-thymidine ( <b>46</b> )	>128
3'-deoxy-3'-(4-3''-fluoro-benzyl-1,2,3-triazol-1-yl)- $\beta$ -D-thymidine ( <b>47</b> )	64
3'-deoxy-3'-(5-Hydroxymethyl-1,2,3-triazol-1-yl)- $\beta$ -D-thymidine ( <b>48</b> )	0.5
3'-deoxy-3'-(5-benzyl-1,2,3-triazol-1-yl)- $\beta$ -D-thymidine ( <b>49</b> )	4
3'-deoxy-3'-(5-4''-fluoro-benzyl-1,2,3-triazol-1-yl)- $\beta$ -D-thymidine ( <b>50</b> )	>128
3'-deoxy-3'-(5-3''-fluoro-benzyl-1,2,3-triazol-1-yl)- $\beta$ -D-thymidine ( <b>51</b> )	64

Preliminary antiviral studies were performed using a fitting model. All the compounds **44-51** were found to potentially fit in the HIV reverse transcriptase active site. This could lead to further viral studies on HIV to further explore their potentials as antivirals.

### 5.3.1 Future work for the triazole containing compounds based on azidothymidine

The mechanism of action for AZT involves phosphorylating at the 5'-O position to allow the compound to be integrated into DNA and causes the DNA replication to terminate. To mask the active hydroxyl, a carbohydrate could be used. This would provide target specificity, the bacterial cell wall recognises the carbohydrate; it acts as a guidance mechanism for certain bacteria, so allows the drug to arrive there precisely. Enzymes within the bacterial cell will cleave the sugar before the kinases can phosphorylate the hydroxyl present in the 5' position. These potential target compounds are shown in Figure 67.

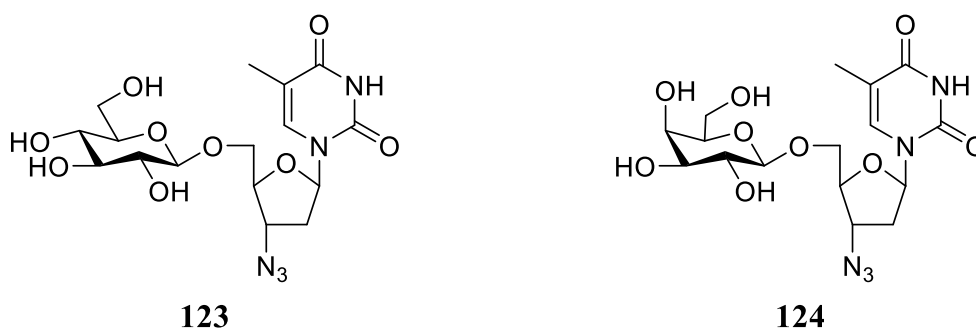


**Figure 67:** Potential carbohydrate prodrugs, **123** (Glu) and **124** (Gal), of AZT.

The  $\beta$ -glycosides **123** and **124** could be synthesised using a glycosylation method such as Koenings-Knorr. This synthetic pathway uses acetylated sugar with a good leaving group on the anomeric centre, usually a chloride or bromide, a promoter such as silver triflate or silver carbonate and an acid scavenger. The acid scavenger, an example being tetramethyl urea, ensures that the acid that is produced in the last step of the mechanism does not cleave the new glycosidic bond that has just formed. Their MIC<sub>100</sub> values would also be determined. Then kinetic studies could be performed to determine whether the sugar is cleaved, to determine their value as prodrug compounds.

To further investigate the antiviral properties for compounds **44-51**, further computer fitting models could be used. These could ascertain as to whether the compounds fit in the active site for the enzymes responsible for phosphorylations (dThd's). Antiviral assays can also be performed. These could use tissue culture lines infected with HIV-1 and a control being healthy cells. This would help determine which compounds possess antiviral properties against HIV-1.<sup>284,285</sup>

#### **5.4 The carbohydrate prodrugs containing flavonoids**

Six novel compounds, **92-97**, were synthesised using a PTC synthesis method to create per-*O*-acetylated  $\beta$ -glycosidic flavonoids. These acetylated glycosides were then deprotected using  $K_2CO_3$  and anh. methanol. These compounds are shown in Figure 68.

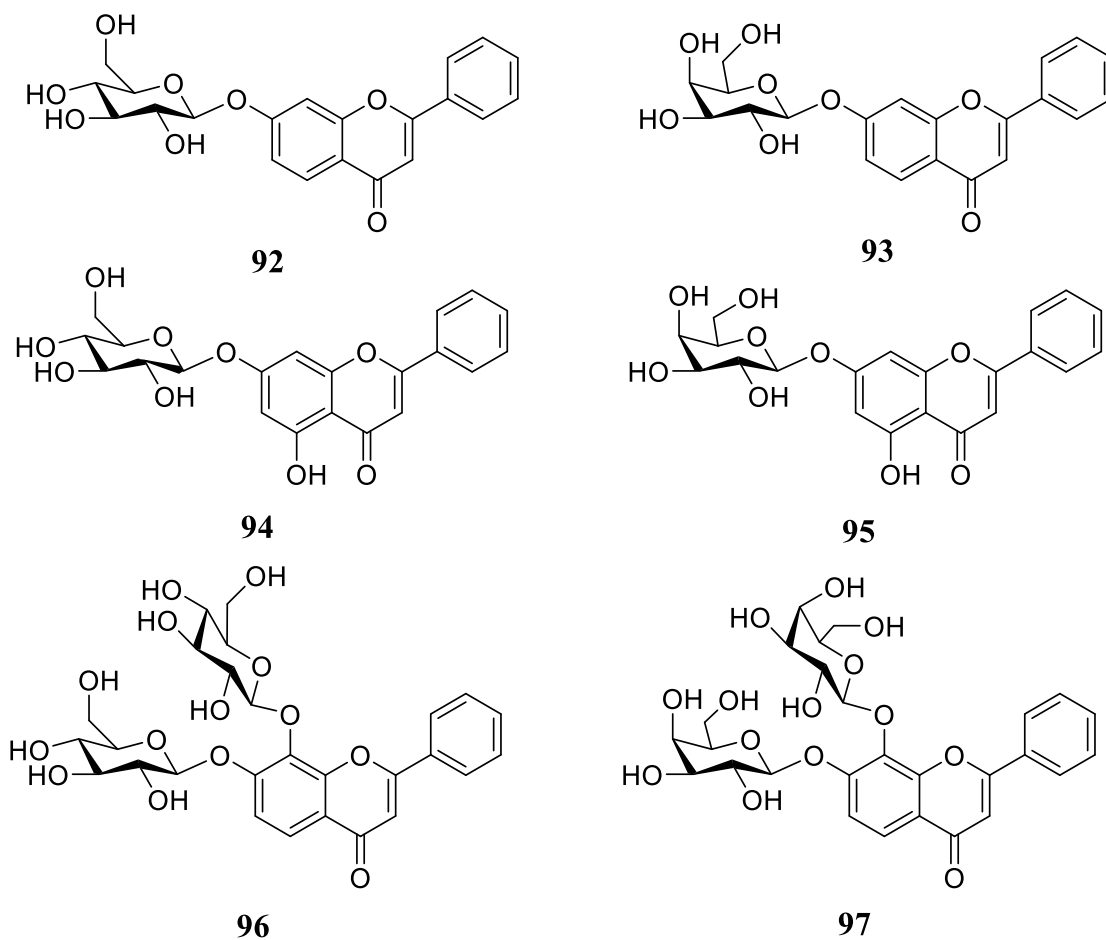


**Figure 68:** The target compounds, **92-97**, for the flavonoid containing glycosides.

The bioscreen method was used for compounds **92-97** to collect the MIC<sub>100</sub> values against various gram-positive and gram-negative bacteria. This method, however, could not be used for the parent compounds (**103**, **110** and **111**) due to solubility issues, so an agar method was used to gain MIC<sub>100</sub> values for the parent compounds. The addition of a glycoside to the parent flavonoid led to higher MIC values when compared to their respective parent compounds. In Table 39, the MIC values for the underivatized flavonoid compounds are shown. This displays how the positioning of the hydroxyls on the A ring on the flavonoid affect the MIC values.

**Table 39:** The MIC values ( $\mu\text{g/mL}$ ) for *S. aureus*, *S. epidermidis*, *St. agalactiae* for the underivised compounds.

Compound	Hydroxyls present	Position of hydroxyls on A ring	MIC <sub>100</sub> values ( $\mu\text{g/mL}$ )		
			<i>S. aureus</i>	<i>S. epidermidis</i>	<i>St. agalactiae</i>
7-hydroxyflavone <b>110</b>	1	C (7)	12.5	6.25	25
chrysin <b>103</b>	2	C (7), C (5)	>25	NG	>25
7,8-dihydroxyflavone <b>111</b>	2	C (7), C (8)	50	25	100

The MIC values collected for the glycosides **92-97** were all higher than that of the antimicrobials already available, shown in Table 40. The compound 7-hydroxyflavone, **110**, had lower MIC for both *S. aureus* and *S. epidermidis* when compared to chloramphenicol and fosfomycin, commercially available treatments for bacterial infections.

**Table 40:** A comparison of clinically available antimicrobials MIC values with the parent flavonoids (**103**, **110-111**) and their glycoside derivatives **92-97** MIC values. The values are reported by EUCAST for the clinically used compounds. NG – no growth

Compound	Bacterial strain MIC values ( $\mu\text{g/mL}$ )	
	<i>S. aureus</i>	<i>S. epidermidis</i>
amikacin	8	0.5-32
ampicillin	0.12-32	0.12-32
benzylpenicillin	0.125	0.03-32
cefepime	8	--
cefotaxime	4	2
chloramphenicol	16	16
ciprofloxacin	--	1
erythromycin	1	1
fosfomycin	32	--
gentamycin	2	0.5
linezolid	4	2
7-hydroflavone ( <b>110</b> )	12.5	6.25
chrysin ( <b>103</b> )	>25	NG
7,8-dihydroxyflavone ( <b>111</b> )	50	25
7-hydroxyflavone- $\beta$ -D-glucopyranoside ( <b>92</b> )	>128	>128
7-hydroxyflavone- $\beta$ -D-galactopyranoside ( <b>93</b> )	>128	>128
chrysin- $\beta$ -D-glucopyranoside ( <b>94</b> )	>128	>128
chrysin- $\beta$ -D-galactopyranoside ( <b>95</b> )	>128	>128
7,8-dihydroxyflavone- $\beta$ -D-glucopyranoside ( <b>96</b> )	>128	>128
7,8-dihydroxyflavone- $\beta$ -D-galactopyranoside ( <b>97</b> )	>128	>128

### 5.4.1 Future work for the carbohydrate prodrugs containing flavonoids

For the parent flavonoids, **103**, **110-111**, different methods need to be used to try and solubilise the compounds therefore allowing their MIC values can be tested at over 25 µg/mL. There has been reported in literatures the synergistic effect flavonoids have with different flavonoids. Combination therapies are used in many situations, an example being in immunocompromised patients. In these patients, identification of the pathogen is more difficult so a combination therapy allows the pathogen to be treated without exactly knowing what bacteria are causing the problem.<sup>286</sup> This therapy is also used in polymicrobial infection, to cover all potential pathogenic bacteria.<sup>287,288</sup> The combination of two different classes may result in a greater bacterial activity than either agent used alone, this is described a synergistic.<sup>289</sup> Most importantly, this therapy prevents emergence of resistance.<sup>290,291</sup>

Flavonoids have been studied for their synergetic properties with various antibiotics. An example investigates three flavonoids (rutin, morin and quercetin) in synergy with various antibiotics to see how their MIC values against *S. aureus* and MRSA were affected. The results are shown in Table 41.<sup>292</sup> The activity of flavonoids was further enhanced against *S. aureus* (ATCC 43300) and clinical isolates (MRSA), when rutin, morin and quercetin were used in combination.

**Table 41:** A table showing the MIC values as a result of using combination therapy against *S. aureus* and MRSA. R – rutin, M – morin, Q - quercetin

Compound	MIC values ( $\mu\text{g/mL}$ )							
	<i>S. aureus</i>				MRSA			
	Alone	With Q	With M+R	With M+R+Q	Alone	With Q	With M+R	With M+R+Q
Amoxicillin	256	256	64	8	128-256	128-256	32-64	2-8
Ampicillin	128	16	128	4	64-256	8-32	64-256	2-8
Cephadrine	256	32	64	8	128-256	16-32	32-64	4-8
Imipenem	32	4	8	1	32-256	4-32	8-64	1-4
Methicillin	64	8	16	2	64-256	8-32	16-64	2-8
Ceftriaxone	64	16	16	2	32-128	4-16	8-64	1-4

The flavonoids, both the parent (**103, 110-111**) and the glycosides (**92-97**), could be explored as potential synergy compounds with various antibiotics and various bacterial strains, both gram-positive and gram-negative.

#### 5.4.1.2 Anticancer and *in vitro* toxicity for the glycosidic flavonoids 92-97

As previously mentioned flavonoids possess many biological activities, including anti-cancer.<sup>246,247,269,270</sup> Cancer is defined as a group of diseases that involve the abnormal growth in cells, with the potential to invade and spread to other parts of the body other than its original site. It can affect anyone, with an estimated 2.5 million people living with cancer in 2015, projected to rise to 4 million by 2030. The number of people with cancer in 2015 has

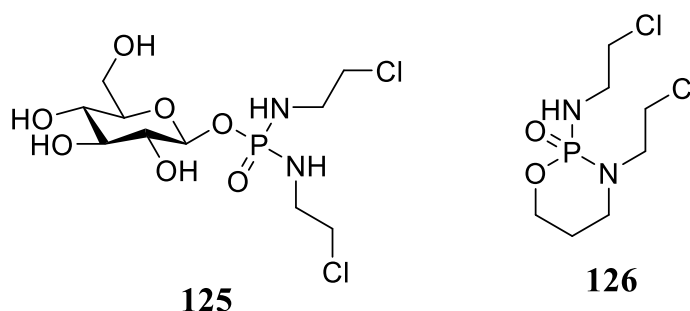
increased by almost half a million people within 5 years.<sup>293</sup> The most prevalent cancers in the UK in 2015 were breast (female), prostate, lung, bowel and skin cancers.<sup>294</sup> There are many factors which affect the risk of developing cancer; lifestyle factors include age, smoking, alcohol consumption, diet, obesity and sunlight as well as genetic factors.

There is a need to develop new therapies to try and overcome challenges presented in treatment of the diseases. The problem with treating cancers is that cancer is complex with many pathways that could potentially cause the mutation in cells to allow them to grow uncontrollably. It is also the host's own DNA which mutates. There is also an added complexity as the tumour can metastasize and move around the body. The current treatments that could be used, namely radiotherapy and chemotherapy, often have toxic side effects.

#### **5.4.1.3 Glycosidic compounds used in cancer therapy**

As the tumour mass grows they require more nutrients to survive and expand. Cancer cells alter themselves to allow for a greater uptake in glucose and fermentation into lactate. To transport the glucose, glucose transporters (GLUTs) are utilised, with cancer cells having an elevated level of these proteins, in particular GLUT1 when compared to normal human cells.<sup>295</sup> Glycoconjugate compounds are therefore an interesting class of compounds to explore for cancer therapies. In one study, radio-labelled 2-deoxy-2-(<sup>18</sup>F)-D-glucose was used to further study as to what categories of cancers would be possibly effected by carbohydrate prodrugs. Using PET screening, with the radio-labelled sugar, preferential uptake of this radiolabelled glucose analogue compared to non-cancerous cells was seen with lung, breast, colorectal, and endometrial carcinomas, as well as bone and soft tissue sarcomas and Hodgkin's and non-Hodgkin's lymphomas.<sup>296</sup>

There are examples of carbohydrate prodrugs being used clinically in cancer treatments. An early example is glufosfamide **125**. The compound **125** was designed as a cancer targeting agent, to decrease the toxicity and increase the selectivity to cancer cells of its aglycone, ifosfamide **126**. The LD<sub>50</sub> data collected from these compounds are shown in Figure 69.<sup>297</sup>



LD <sub>50</sub> (mg/Kg)		Rats	Mice
<b>125</b>	I.V	1575	1575
	P.O	1470	1470
<b>126</b>	I.V	350	370
	P.O	370	1000

**Figure 69:** The structures of glufosfamide **125** and ifosfamide **126** with their LD<sub>50</sub> data for rats and mice. Adapted from ref. 283.

#### 5.4.1.4 *In vitro* toxicity experiment

*In vitro* testing offers long-term safety data for drugs in their early stages of development. Specific properties can be identified including carcinogenic and mutagenic effects. It allows for an initial determination of toxicity before *in vivo* studies. It can be problematic as the translation between *in vitro* and *in vivo* can be difficult. The compound maybe toxic *in vitro* but due to different pathways being used it can have very little to no effect *in vivo*. First pass metabolism, also referred to as first pass effect, is an example of a pathway in which drugs can be inactivated and excreted.

The breast cancer cell line MCF-7, was chosen as it contains  $\beta$ -glycosidases which are needed to cleave the sugar from the aglycone.<sup>298</sup> Breast cancer is a prevalent cancer; in 2015 it was the most predominant cancer in females in the UK. Males are also affected by this cancer. The MCF-7 cell line was first isolated in the 1970's, and became the first hormone receptor-positive breast cancer.<sup>299</sup> It is also estrogen receptor positive, therefore it is a useful cell line when reviewing the toxicity of compounds that may interact with this receptor. The cell line MDA-MB231 was also selected for study and this cell line does not have the estrogen receptors that are present in MCF-7.

The 3-(4,5-dimethylthiazol-2-yl)-2,5-diphenyltetrazolium bromide (MTT) assay is a metabolic assay which can be used to elude to the toxicity of the compounds **92-97** and their parent compounds. This method is a colorimetric assay that assesses the cell metabolic activity. Firstly, the cell lines, MCF-7 and MDA-MB231, were incubated at 37 °C in RPMI 1640 media. The compounds were prepared in DMSO to a concentration of 2 mM. This made the stock solution. From this, a fraction was taken and added to complete media to make a final concentration of 20  $\mu$ M. The cell suspension was added to 96-well plate and then the compounds were added. These were incubated for 48 h. MTT was then added to the wells and the plate was further incubated for 4 h. The MTT is reduced in living cells with the use of NAD (P) H-dependant cellular oxidoreductase enzymes. The yellow compound MTT is reduced to its insoluble form formazan, which is purple. A solubilising solution, DMSO, is added to the formazan and the absorption is measured at 570 nm by a spectrophotometer.<sup>300</sup>

The IC<sub>50</sub> values for the parent compounds **103**, **110** and **111** were studied and these have been compared to their respective glycosidic compounds, **92-97**. This allowed the cell viabilities to be compared and determine their anticancer activities.

The graph shown in Figure 70 was produced using cell assay techniques by Az Natji (University of Reading). It summarises the % cell viability for compounds **110-111**, **92-97**. The MCF-7 cell lines were performed in duplicate and the MDA-MB231 was performed once. Further work includes performing these cell assay analyses in triplicate. Error bars show whether the data is statically significant.

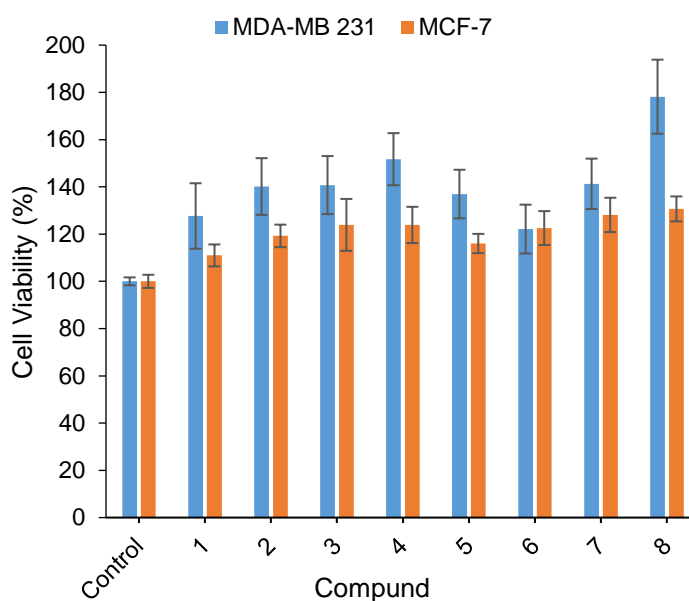


**Figure 70:** The graph summarising the % cell viability of the target compounds against cell lines MCF-7 and MDA-MB231. 1 - **111**, 2 - **96**, 3 - **97**, 4 - **110**, 5 - **92**, 6 - **93**, 7 - **95**, 8 - **96**. n=2 for MCF-7, and n=2 for MDA-MB. Control sample was the cells with no compound present.

The cells were still viable (MCF-7 and MDA-MB231 cell lines). Further investigation is needed to draw any conclusions. The assay was only performed at one concentration so would need to be performed at varying concentrations when performed again.

## 5.5 Future work

### 5.5.1 Kinetic studies

To further investigate the SAR of the compounds containing the bisphenol or flavonoid moiety, kinetic studies could be performed. The Michaelis-Menton equation could be used to determine the mechanism of the enzymatic release of the parent compound. This would be useful to ascertain, as the design of the prodrugs relies on the glycoside being cleaved to release the target drug. A double reciprocal plot, Lineweaver-burke plot, could be used as a representation of enzyme kinetics; this is based on a rearrangement of the Michaelis-Menton equation, shown in Equation 3.

$$\frac{1}{v} = \frac{K_M}{V_{max}} \frac{1}{[S]} + \frac{1}{V_{max}}$$

$$Y = M \kappa + C$$

**Equation 3:** The Lineweaver-burke rearrangement and how it relationship to  $Y=M\kappa+C$

Where  $v$  is the reaction rate,  $[S]$  is the substrate concentration and  $K_{max}$  is the Michaelis constant. Various concentrations of the target compound could be measured to obtain the initial rate.  $K_{max}$  is the measure of the affinity of the enzyme for the substrate; a smaller  $K_{max}$  indicates an increased affinity of the enzyme for a certain substrate.

### 5.5.2 Analysis with resistant bacteria

The glycosides and 1,2,3-triazole compounds that were synthesised could also be analysed against resistance strains of bacteria, an example could be MRSA. As well as analysis against

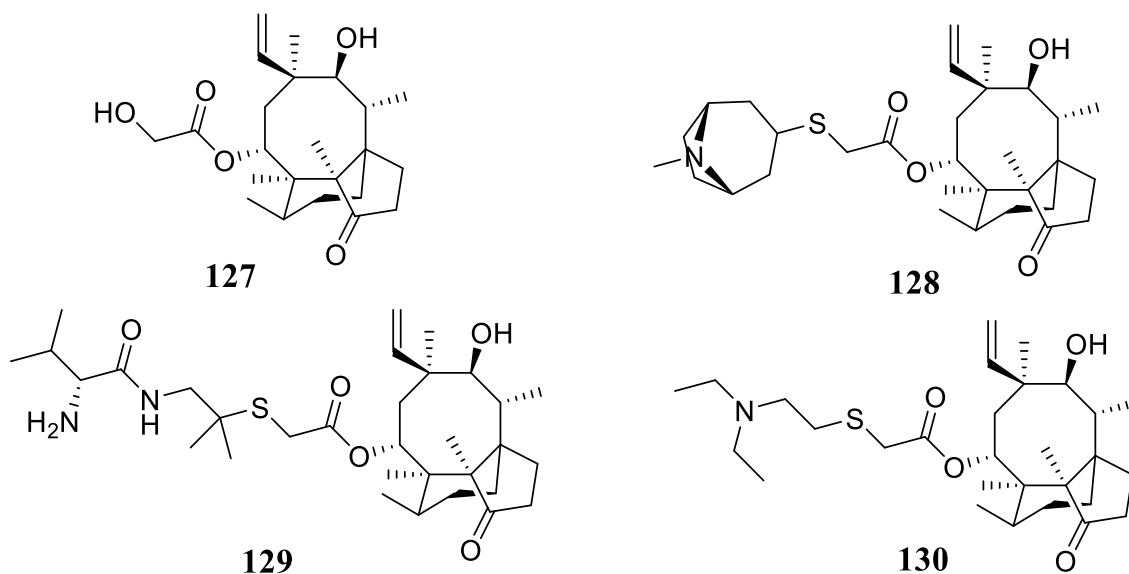
resistant strains further studies could be performed using combination therapies. Different antimicrobial compounds could be used with the synthesised glycosides to discover whether they have synergetic properties.

### **5.5.3 Possible future glycoside strategies**

There are many antimicrobials that possess a free hydroxyl which could undergo a glycosylation reaction to synthesise carbohydrate prodrugs.

#### **5.5.3.1 Pleuromutilin compounds**

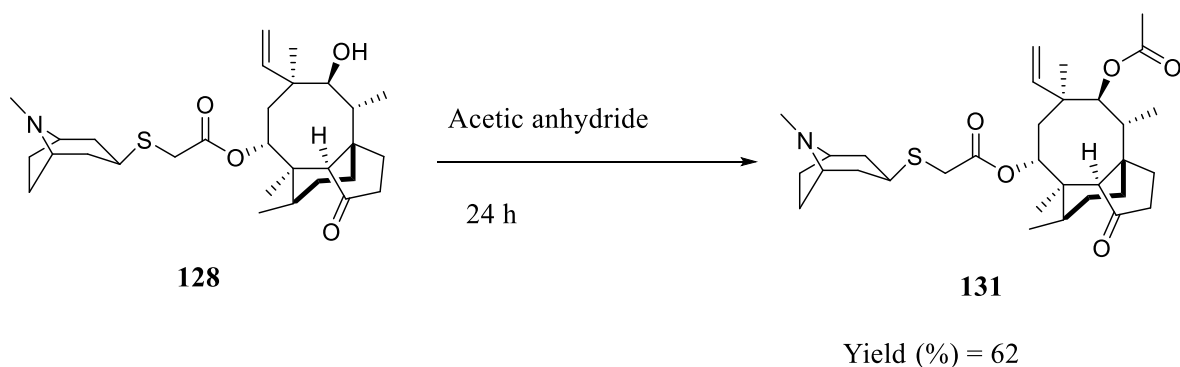
This class of antibiotics was first isolated in 1951 from *Pleurotus mutilus* (Fr.) Sacc. and *P. passeckerianus* pilat.<sup>301</sup> Pleuromutilin **127** was extracted from the fungi and was found to have excellent activity against *Staphylococcus aureus*. Many derivatives have been designed, synthesised and tested using the pleuromutilin backbone. Retapamulin **128**, valnemulin **129** and tiamulin **130** are examples of some of these derivatives; their structures are shown in Figure 13. Retapamulin **128** was first developed by GlaxoSmithKline and is the only one of this family to be approved for human use, while **129** and **130** are for animal use only. These compounds were found to be active against a selection of gram-positive and gram-negative bacteria, shown in Figure 71.<sup>302,303</sup>



Compound	MIC <sub>100</sub> data for the bacteria tested against (µg/mL)			
	<i>S. agalactiae</i>	<i>S. aureus</i>	<i>S. pyogenes</i>	<i>Es. coli</i>
<b>127</b>	32	0.5	32	32
<b>128</b>	0.008-0.03	0.016-0.12	<0.004-0.12	-
<b>129</b>	64	> 0.125	64	16
<b>130</b>	32	0.125	>64	32

**Figure 71:** The MIC<sub>100</sub> data for four compounds in the pleuromutilin class: Pleuromutilin **127**, retapamulin **128**, valnemulin **129** and tiamulin **130**. Data was collected using a liquid both method.

This family of compounds is of interest as it is stated in the literature that the free hydroxyl on the pleuromutilin backbone is needed for its antibacterial activity.<sup>304,305</sup> Masking the hydroxyl with an acetate functionality decreased the MIC data for the bacteria shown in Figure 72. The results shown in Figure 72 were collected using NB in a bioscreen method.



Organisms	OCC	<b>128</b>	<b>131</b>
<i>B. cereus</i>	754	32	256
<i>E. faecalis</i>	640	128	128
<i>E. faecium</i>	220	16	16
<i>S. aureus</i>	100	<1	16
<i>St. epidermis</i>	691	<1	16
<i>St. agalactiae</i>	182	<1	16
<i>St. pneumoniae</i>	1548	<1	16
<i>St. pyogenes</i>	168	NG	NG
<i>St. viridans</i>	1681	<1	16
<i>C. freundii</i>	851	16	>256
<i>Cr. sakazakii</i>	1888	8	>256
<i>En. cloacae</i>	760	<1	>256
<i>Es. coli</i>	199	NG	NG
<i>K. pneumoniae</i>	758	NG	NG
<i>P. mirabilis</i>	2080	128	>256
<i>Ps. aeruginosa</i>	201	128	>256
<i>Sa. typhimurium</i>	853	8	>256
<i>Se. marcescens</i>	217	8	>256

**Figure 72:** The MIC<sub>100</sub> values for **128** and **131**, displaying how masking the hydroxyl moiety lowers the biological activity. The reaction scheme and yield for the reaction is also shown.

Synthesising  $\beta$ -glycosides of **127-130** would mask the free hydroxyl functionality and would potentially allow a non-toxic prodrug to be created, with a more targeted release of the drug.

### 5.5.3.2 Carvacrol compounds

Monoterpenes are a class of terpenes which consist of two isoprene units. Carvacrol **132** is a compound which belongs to this class. This monoterpenic phenol is isomeric to thymol and is found in a plethora of different plants; including *Thymus vulgaris* and *Thymus zygis* (thyme), *Thymus serpyllum* (white thyme), and *Satureja montana* (winter savoury).<sup>306</sup> This natural compound **132** possesses a hydroxyl which is vital for its mechanism of action. This phenolic hydroxyl potentially could decrease the pH of the bacterial membrane, which could cause the destabilisation of the bacterial membrane and decrease the membrane potential.<sup>307</sup> In Figure 73, the MIC<sub>100</sub> data for carvacrol **132** and carvacrol acetate **133** is shown. There was a decrease in biological activity once the hydroxyl is masked.<sup>308</sup>



**MIC<sub>100</sub> data for the bacteria tested against (µg/mL)**

	<b>132</b>	<b>133</b>
<i>Saccharomyces cerevisiae</i>	0.25	>3
<i>S. aureus</i>	0.25	>3
<i>Es. coli</i>	0.25	>3
<i>Pseudomonas fluorescens</i>	1	>3
<i>Bacillus cereus</i>	0.25	>3
<i>Lactobacillus plantarum</i>	>3	>3

**Figure 73:** The MIC<sub>100</sub> data for **132** and **133**. The data was collected using a liquid broth method. This work was performed by 305.

A carbohydrate could be used to mask the hydroxyl and would allow the glycoside to be cleaved in the bacteria by glycosidase enzymes. This will also provide a more targeted approach to using **132** as an antimicrobial.

### 5.5.3.3 Azido moiety containing antimicrobials

Azidamfenicol **134** is a phenicol antibiotic, under the same class as chloramphenicol **135**, structures are shown in Figure 74. Compound **134** is a water soluble compound and found in eye drops.<sup>309</sup> It has the same mechanism of action as chloramphenicol, inhibiting peptide synthesis by interacting with the 23S RNA of the 50S ribosomal subunit in bacteria. As previously described, antibiotic resistance is an emerging problem amongst antibiotics, with the phenicol antibiotics being no exception. Chloramphenicol acetyltransferases are able to inactivate chloramphenicol **135** but also azidamfenicol **136**.<sup>310</sup> To try and overcome this problem the azido moiety could be used in a ‘click’ style reaction to create 1,2,3-triazoles. As previously mentioned, the 1,2,3-triazole is a pharmacophore and could potentially enhance the MIC values of the compound, as well as masking the parent compound from resistance mechanisms.

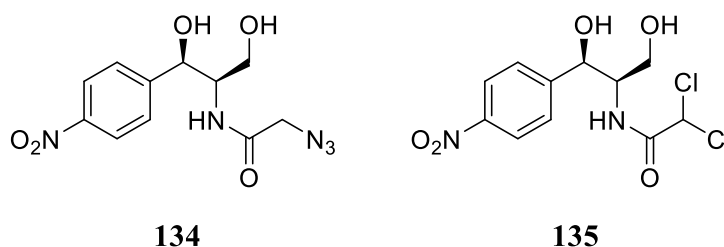


**Figure 74:** The structures of azidamfenicol **134** and chloramphenicol **135**.

### 5.5.4 Further biological analysis

With the compounds suggested previously, **127-135**, further analysis could be performed to ascertain their potentials as other biological relevant compounds, such as antiviral and anticancer. There has been a study previously into monoterpenes and their antiviral activity against herpes simplex virus type 1 (HSV-1).<sup>311</sup> The glycosidic compounds of the monoterpenes

could be investigated for their antiviral potential. All newly synthesised glycosidic compounds could also be used in a tissue cell assay, to evaluate their cytotoxicity and potential as anticancer molecules.

## **Chapter 6 – Experimental**

## **6.1 Equipment and Materials**

### **6.1.1 NMR Spectroscopy**

The NMR spectra were measured in either MeOD, CDCl<sub>3</sub> or DMSO at room temperature on the Nano400 which is a two-channel NMR instrument running ICON NMR 4.2 under TOPSPIN 2.4. It incorporates a 9.39 T Ultrashield Plus Long Hold Time Magnet and is equipped with a 5mm indirect observation z-gradient inverse (<sup>1</sup>H/<sup>13</sup>C)- BBI probe and a 60-position BACS sample changer. δ units are ppm relative to the internal standard, trimethylsilane. All coupling constants are quoted to the nearest 0.5 Hz.

### **6.1.2 Mass Spectrometry**

The mass spectra were measured using fourier transform mass spectroscopy (FTMS) on a Thermo Scientific LTQ Orbitrap XL and was run in positive ion mode. The detector used was the Orbitrap (this mass spectrometer has two detectors), an Orbitrap which is very high resolution and mass accuracy, and an LTQ ion trap. The sample dissolved in methanol to give a concentration of 1 mg/mL, each sample was then diluted 30 fold in 0.1% formic acid in methanol (LCMS grade). The scan range was 150-2000 m/z and resolution level was 30,000.

### **6.1.3 HPLC**

High Performance Liquid Chromatography (HPLC) was performed on an Agilent 1100 series machine using a Hypersil Gold aQ column (150mm x 4.6 μm x 5), unless otherwise stated. Each of the chromatography conditions for each individual experiments are listed accordingly.

### **6.1.4 Infrared Spectroscopy**

The IR spectra were recorded on a Thermo Scientific Nicolet iS5 FT-IR spectrophotometer equipped with a Thermo Scientific™ iD5 ATR Accessory. The method used a sample loaded onto a diamond sensor.

### **6.1.5 Polarimetry**

The optical rotations were recorded on a Perkins Elmer 341 polarimeter. They were recorded using the Na lamp in Methanol.

### **6.1.6 Thin layer Chromatography**

These were performed using Merck TLC silica gel 60 plates. Spots were visualised using UV light ( $\lambda_{\text{max}}$  254 nm) and staining with either 5% H<sub>2</sub>SO<sub>4</sub> in ethanol, or ninhydrin with 3% acetic acid in n-BuOH.

### **6.1.7 Column Chromatography**

For normal phase chromatography Sigma Aldrich silica gel (particle size 35-79  $\mu\text{m}$ ) was used. For reverse phase chromatography, the Reveleris X2 flash chromatography system was used. The different conditions and columns used are stated for the individual experiments.

### **6.1.8 Melting points**

The melting points were recorded using a Gallenkamp melting point machine and are uncorrected.

### **6.1.9 Chemicals**

2-Benzyl phenol, zidovudine (AZT), and 7-hydroxyl flavone were purchased from Alfa Aesar, Heysham, UK. Bis(2-hydroxyphenyl)methane and chrysin were purchased from Sigma Aldrich, Dorset, UK. 7,8-Dihydroxyflavone hydrate was purchased from TCI, Oxford, UK. The anhydrous solvents were all Sureseal from Sigma Aldrich. The other chemicals used were purchased from Sigma Aldrich, Fisher Scientific or Acros.

### **6.1.10 Microorganism strain list**

The bacteria in red indicate gram-positive bacteria strains.

Organism name	Oxoid culture collection number (OCC)	Other Culture Collection References			Isolation
		NCTC	ATCC	NCIMB	
<i>Bacillus cereus</i>	754	2599	14579	9373	
<i>Enterococcus faecalis</i>	640	12697	29212		Urine
<i>Enterococcus faecium</i>	220	7171	19434	11508	
<i>Staphylococcus aureus V. Oxford</i>	100	6571	9144		
<i>Streptococcus epidermis</i>	691	11047	14990	12721	Nose
<i>Streptococcus agalactiae</i>	182				
<i>Streptococcus pneumoniae</i>	1548		6305		
<i>Streptococcus pyogenes</i>	163				
<i>Streptococcus viridans</i>	234				
<i>Citrobacter freundii</i>	851				
<i>Cronobacter sakazakii</i>	1888	11467	29544		Childrens throat
<i>Enterobacter cloacae</i>	760	10005	13047		Cerebrospinal fluid
<i>Escherichia coli</i>	199		25922	12210	
<i>Klebsiella pneumoniae</i>	758	9633	13883		
<i>Proteus mirabilis</i>	2080		12453		
<i>Pseudomonas aeruginosa</i>	201		27853		
<i>Salmonella typhimurium</i>	854				
<i>Serratia marcescens</i>	217				

#### **6.1.11 Preparation of bacteria**

The organisms were inoculated from a stock plate into 10 mL of the desired broth (NB, MHB, and CM5). The cultures were grown for 18 h at 37 °C. The overnight cultures were the diluted in maximum recovery diluent (MRD) (Thermofisher, UK) (1 mL culture into 9 mL MRD).

#### **6.1.12 Preparation of broths**

All the broths were prepared in accordance to the manufacturer's instructions and autoclaved. The broths were all cooled to room temperature before use.

#### **6.1.13 Preparation of plate media**

Mueller Hinton agar (Thermofisher, UK) was prepared as per the manufacturing protocol.

#### **6.1.14 Determination of MIC of desired compounds using the bioscreen method**

A stock solution of the desired compound was made using 3 % DMSO in the desired broth (NB, MHB, and CM5) to a concentration of either 128 µg/mL or 256 µg/mL. These stock solutions were filtered and sterilised before use.

The stock solutions were then diluted down to give final concentrations of 256, 128, 64, 32, 16, 8, 4, 2, and 1 µg/mL or 128, 64, 32, 16, 8, 4, 2, 2, 1 and 0.5 µg/mL. Each concentration of the compound (300 µL) was added to the wells of the bioscreen plates. This was followed by the culture in broth (30 µL).

The optical density (OD) for each well was measured every 15 min for 24 h. It was read at 600 nm wavelength in an automatic bioscreen reader machine at 37 °C.

#### **6.1.15 Determination of MIC of desired compounds using the agar method.**

A stock of the desired compounds was prepared to a final concentration of 100,000 µg/mL in DMSO. The solutions was sterilised filtered prior to use.

The Mueller Hinton agar was prepared as described in Section 6.1.13. The required concentration of compound was added to the agar to give final concentrations of 100, 50, 25, 12.5, 6.25, 3.125, 1.5625 and 0.78125  $\mu\text{g/mL}$ . A plate containing no compound was poured and used as a control. The plates were poured and dried for 20 min at 37°C prior to use.

A 36 pin multipoint inoculator (Thermofisher, UK) was utilised to seed the plates with bacteria. Each bacterial strain was incubated overnight, and then these strains were diluted in MRD, to about  $10^4$  CFU. These were applied to each well. The organisms were inoculated onto the plates and incubated for 24 h at 37°C. The MIC were determined as whether growth occurred on the plate, this was determined as to whether the growth was viable upon examination.

#### **6.1.16 Cell culture**

All techniques were performed in a biological safety cabinet under sterile conditions. The MCF-7 cells were cultured in RPMI 1640 media (Fisher, UK) supplemented with 5% bovine serum, MDA-MB231 cells were cultured in DMEM media (Fisher, UK) and supplemented with 10% bovine serum (heat inactivated). Both were incubated at 37°C under 5% CO<sub>2</sub> atmosphere. The cells were grown until 75% confluent.

ATCC code: MCF-7 (ATCCâ HTB-22™), MDA-MB-231 7 (ATCCâ HTB-26™).

ECACC code: MCF-7 (MCF7 (ECACC 86012803)), MDA-MB-231 (MDA-MB-231 (ECACC 92020424))

MCF-7, provided by Tenovus centre for Cancer research (Cardiff, UK), the triple negative breast cancer cell line MDA-MB-231 was purchased as a frozen stock from the European Collection of Cell Cultures (ECACC).

Cells below passage-30 were used in your experiment. All cell lines were free of mycoplasma

For media, for MCF-7: RPMI (with L-glutamine) REF: 21875-034 (supplied by Gibco), and 5% FBS, REF: 10270-106 (supplied by Gibco). For MDA-MB-231: DMEM (with L-glutamine, low glucose, pyruvate) REF: 31885-023 (supplied by Gibco), and 10% FBS, REF: 10270-106 (supplied by Gibco). For trypsin: Trypsin-EDTA (0.25%), Phenol red, REF: 25200-056 (supplied by Gibco). Gibco can be found in Fisher.

#### **6.1.17 Cell sub-culturing**

Once the cells were 70-80% confluent, the growth medium for the cultured cells was removed from the cell culture flask and washed with 10 mL phosphate-buffered saline (PBS). Trypsin (2-3 mL) was then added and the flask was incubated at 37 °C for 5 min. The complete growth media (7-8 mL) was added to the flask, and the cell suspension was centrifuged at 215 xg for 5 min. The media was removed and the pellet was resuspended in 10 mL fresh complete growth media. 0.5 mL of the suspension was transferred to 5 mL complete growth media. To each suspension, 4 or 8 mL of the corresponding media was added, these were then incubated at 37 °C

#### **6.1.18 Preparation of MTT**

The MTT (Sigma-Aldrich, UK) was prepared. Briefly, the MTT was dissolved in PBS at a concentration of 5 mg/mL. The solution was sonicated for 30 min under dark conditions, and then filtered through a sterile filter and stored in a fridge until use.

For MTT, MTT solution was prepared in at 5 mg/mL in PBS pH 7.4. The code of MTT: M2128-1G Thiazolyl Blue Tetrazolium Bromide 98% (Sigma Aldrich)

The seeding densities of the cells: For MCF-7:  $4 \times 10^4$  cells/mL, for MDA-MB-231:  $2 \times 10^4$  cells/mL, both seeding densities were optimised by our group.

### **6.1.19 MTT assay**

A stock solution of 2 mM of the desired compound in DMSO was prepared. These were further diluted in complete growth media so that the concentration of DMSO is 1% (as to not affect the cell growth).

The cell suspension (100  $\mu$ L) was added to 96-well plate and the cells were grown for 24 h. Then the compounds were added to make the final concentration (10  $\mu$ M). Controls were employed also. These were incubated at 37  $^{\circ}$ C in a 5% CO<sub>2</sub> atmosphere for 67 h. The plates were then treated with MTT and further incubated for 5 h. The MTT and media were then removed and the formazan crystals were dissolved in DMSO. The plates were further incubated for 30 min to ensure that all the formazan had dissolved. The OD was then measured. The absorbance was used to determine cell viability.

## **6.2 The glycosidic compounds with a bis-phenol moiety 33-34**

### **6.2.1 General procedure for the synthesis of 33-34**

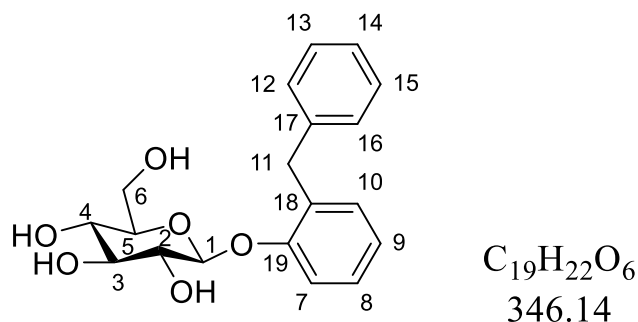
The bis-phenol (1 eq.) was suspended in deionised H<sub>2</sub>O (30 mL), and NaOH (1 eq.) was added and the solution was left to stir for 20 min. Anhyd. acetone (21 mL) was added to the flask. In a separate flask, the acetobromosugar (1 eq.) was dissolved in acetone (26 mL) and added dropwise to the stirred bis-phenol solution and the solution was left to stir at room temperature (RT) for 2 h. The progress of the reaction was monitored using TLC (ethyl acetate: petrol ether (3:2)).

The crude mixture was extracted using DCM (3 x 70 mL). The organic layers were combined and the solvent removed *in vacuo*. The crude compound was partially purified by column chromatography using silica (ethyl acetate: petrol ether (3:2)). The partially purified product was then dissolved in anhydrous methanol (30 mL) and K<sub>2</sub>CO<sub>3</sub> (90 mg) was added and the

suspension was stirred for 20 h. The reaction was concentrated and chloroform was added. The crude filtrate was filtered using a sintered funnel and the solid was purified using reverse phase column chromatography. (0.1% formic acid in water: acetonitrile (3:7)).

The purity of these compounds was measured using a HPLC method. A solvent system of A=0.1% formic acid in H<sub>2</sub>O and B=MeCN was used, with a flow rate = 1.0 mL/ min. Compounds were eluted with a gradient of 5% B to 80% B for 30 min. Wavelengths 254, 280, and 210 nm were used. A hypersil column (Thermofisher, Hypersil GOLD, 5 $\mu$ m, 150  $\times$  4.6mm, 30 °C) was used.

### 6.1.2.1 Synthesis of 2-benzyl phenol- $\beta$ -D-glucoopyranoside (**33a**)

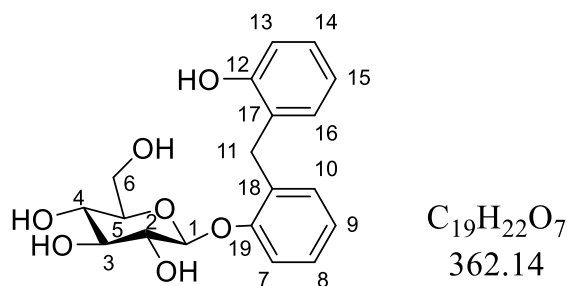


**33a**

Following the general method outlined in Section 6.2.1: 2-benzylphenol (0.66 g, 3.57 mmol) was suspended in water (30 mL) and 1 M NaOH (0.14 g, 3.57 mmol, 3.57 mL) along with anh. acetone (21 mL) was added. Acetobromo- $\alpha$ -D-glucose (1.47 g, 3.57 mmol) was dissolved in acetone (26 mL) and added dropwise to the bis-phenyl solution and left to stir at RT for 2 h. The crude mixture was partially purified using silica (ethyl acetate: petrol ether (3:2)). The crude product was dissolved in anh. methanol (30 mL) and  $K_2CO_3$  (90 mg) was added and stirred for 20 h. The reaction was concentrated and purified using column chromatography to obtain the desired product **33a** (Yield: 9%, white powder, Purity: >99%).

**$^1H$ -NMR** (400 MHz, MeOD):  $\delta$  = 3.87-4.02 (4H, m, H-2, H-3, H-4, H-5), 4.15 (1H, dd,  $J$  = 5.5 Hz,  $J$  = 12.0 Hz, Ha-6), 4.33 (1H, app.d,  $J$  = 12.0 Hz, Hb-6), 4.43 (1H, d,  $J$  = 14.5 Hz, Ha-11), 4.55 (1H, d,  $J$  = 14.5 Hz, Ha-11), 5.39 (1H, d,  $J$  = 7.0 Hz, H-1), 7.39 (1H, t,  $J$  = 7.0 Hz, H-9), 7.55-7.64 (4H, m, H-7, H-8, H-10, H-14), 7.70 (2H, t,  $J$  = 7.5 Hz, H-13, H-15), 7.76 (2H, d,  $J$  = 7.5 Hz, H-16, H-12) ppm.  **$^{13}C$ -NMR** (100 MHz, MeOD):  $\delta$  = 38.4 (C-11), 64.4 (C-6), 73.3 (C-4), 76.6 (C-2), 79.6 (C-3, C-5), 104.2 (C-1), 117.4 (C-14), 125.0 (C-9), 130.1 (C-7, C-8), 130.8 (C-13), 131.7 (C-12, C-16), 132.9 (C-10), 133.4 (C-18), 144.1 (C-17), 158.5 (C-19) ppm. **FTMS (ESI)  $m/z$** : 369.1416 ( $[M+Na]^+$ , 99%), found 396.1315  $[M+Na]^+$ . **Melting point**: 132-35 °C. **FT-IR (ATR)**: 3307 (O-H, br),  $cm^{-1}$ .

### 6.1.2.2 Synthesis of Bis(2-hydroxyphenyl)methane- $\beta$ -D-glucopyranoside (**33b**)



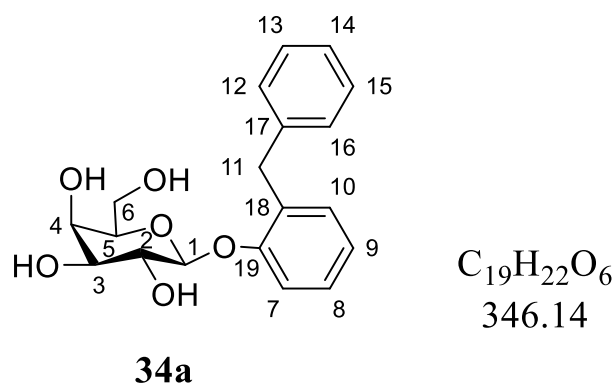
#### **33b**

Following the general method outlined in Section 6.2.1: Bis (2-hydroxyphenyl) methane (0.7 g, 3.57 mmol) was suspended in water (30 mL) and 1 M NaOH (0.14 g, 3.57 mmol, 3.57 mL) along with anh. acetone (21 mL) was added. Acetobromo- $\beta$ -D-glucose (1.47 g, 3.57 mmol) was dissolved in acetone (26 mL) and added dropwise to the bis-phenyl solution and left to stir at RT for 2 h. The crude mixture was partially purified using silica (ethyl acetate: petrol ether (3:2)). The crude product was dissolved in anh. methanol (30 mL) and  $K_2CO_3$  (90 mg) was added and stirred for 20 h. The reaction was concentrated and purified using column chromatography to obtain the desired product **33b** (Yield: 15%, white powder, purity: >99%).

**$^1H$ -NMR** (400 MHz, MeOD):  $\delta$  = 3.86-3.99 (4H, m, H-2, H-3, H-4, H-5), 4.14 (1H, dd,  $J$  = 5.0 Hz,  $J$  = 12.0 Hz, Ha-6), 4.32 (1H, dd,  $J$  = 2.0 Hz,  $J$  = 12.0 Hz, Hb-6), 4.43 (1H, d,  $J$  = 15.0 Hz, Ha-11), 4.50 (1H, d,  $J$  = 15.5 Hz, Hb-11), 5.37 (1H, d,  $J$  = 6.0 Hz, H-1), 7.20 (1H, t,  $J$  = 7.5 Hz, H-9), 7.31 (1H, d,  $J$  = 8.0 Hz, H-7), 7.35 (1H, t,  $J$  = 7.5 Hz, H-15), 7.47 (1H, t,  $J$  = 8.0 Hz, H-8), 7.56 (3H, d,  $J$  = 8.5 Hz, H-10, H-13, H-16), 7.60 (1H, t,  $J$  = 8.0 Hz, H-14) ppm.  **$^{13}C$ -NMR** (100 MHz, MeOD):  $\delta$  = 31.6 (C-11), 64.5 (C-6), 73.1 (C-4), 77.0 (C-2), 79.9 (C-3, C-5), 105.1 (C-1), 117.8 (C-7), 118.0 (C-13), 122.3 (C-9), 124.7 (C-8, C-15), 129.8 (C-14), 132.7 (C-16), 133.1 (C-10), 144.3 (C-17, C-18), 157.5 (C-19), 158.5 (C-

12) ppm. **FTMS (ESI)**  $m/z$  : 385.1263 ( $[M+Na]^+$ , 99%), found 384.1259  $[M + Na]^+$ . **Melting point:** 145-47 °C. **FT-IR (ATR):** 34344 (O-H, br),  $cm^{-1}$ .

### 6.1.2.3 Synthesis of 2-benzyl phenol- $\beta$ -D-galactopyranoside (**34a**)



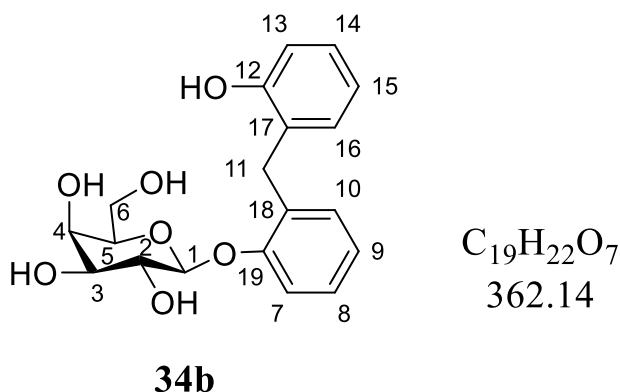
Following the general method outlined in Section 6.2.1: 2-benzylphenol (0.66 g, 3.57 mmol) was suspended in water (30 mL) and 1 M NaOH (0.14 g, 3.57 mmol, 3.57 mL) along with anh. acetone (21 mL) was added. Acetobromo- $\beta$ -D-galactose (1.47 g, 3.57 mmol) was dissolved in acetone (26 mL) and added dropwise to the bis-phenyl solution and left to stir at RT for 2 h. The crude mixture was partially purified using silica (ethyl acetate: petrol ether (3:2)). The crude product was dissolved in anh. methanol (30 mL) and  $K_2CO_3$  (90 mg) was added and stirred for 20 h. The reaction was concentrated and purified using column chromatography to obtain the desired product **34a** (Yield: 7%, white powder, purity: >99%).

**$^1H$ -NMR** (400 MHz, MeOD):  $\delta$  = 4.07 (1H, dd,  $J$  = 3.5 Hz,  $J$  = 9.5 Hz, H-3), 4.16-4.22 (1H, m, H-5), 4.23-4.27 (2H, m, H-6), 4.31 (1H, t,  $J$  = 8.5 Hz, H-2), 4.41-4.58 (3H, m, H-4, H-11), 5.33 (1H, d,  $J$  = 7.5 Hz, H-1), 7.37 (1H, t,  $J$  = 7.5 Hz, H-9), 7.52-7.65 (4H, m, H-7, H-8, H-10, H-14), 7.70 (2H, d,  $J$  = 7.5 Hz, H-13, H-15), 7.75 (2H, t,  $J$  = 7.5 Hz, H-12, H-16) ppm.

**$^{13}C$ -NMR** (100 MHz, MeOD):  $\delta$  = 38.1 (C-11), 64.0 (C-6), 71.8 (C-4), 74.3 (C-2), 76.6 (C-3), 78.4 (C-5), 105.2 (C-1), 118.3 (C-7, C-8, C-14), 124.9 (C-9), 129.4 (C-18), 130.9 (C-12, C-16), 132.0 (C-13, C-15), 133.1 (C-10), 133.3 (C-17), 158.3 (C-19) ppm. **FTMS (ESI)**

$m/z$  : 369.1416 ( $[M+Na]^+$ , 99%), found 369.1318  $[M + 2Na]^+$ . **Melting point:** 142-47 °C. **FT-IR (ATR):** 3364 (O-H, br)  $cm^{-1}$ .

#### 6.1.2.4 Synthesis of Bis(2-hydroxyphenyl)methane- $\beta$ -D-galactopyranoside (**34b**)



Following the general method outlined in Section 6.2.1: Bis (2-hydroxyphenyl) methane (0.7 g, 3.57 mmol) was suspended in water (30 mL) and 1 M NaOH (0.14 g, 3.57 mmol, 3.57 mL) along with anh. acetone (21 mL) was added. Acetobromo- $\beta$ -D-glucose (1.47 g, 3.57 mmol) was dissolved in acetone (26 mL) and added dropwise to the bis-phenyl solution and left to stir at RT for 2 h. The crude mixture was partially purified using silica (ethyl acetate: petrol ether (3:2)). The crude product was dissolved in anh. methanol (30 mL) and  $K_2CO_3$  (90 mg) was added and stirred for 20 h. The reaction was concentrated and purified using column chromatography to obtain the desired product **34b** (Yield: 11%, white powder, Purity: >99%).

**$^1H$ -NMR** (400 MHz, MeOD):  $\delta$  = 3.58 (1H, dd,  $J$  = 3.5 Hz,  $J$  = 9.5 Hz, H-3), 3.67 (1H, t,  $J$  = 6.5 Hz, H-5), 3.72-3.79 (2H, m, H-6), 3.83 (1H, app. t,  $J$  = 9.0 Hz, H-2), 3.90 (1H, d,  $J$  = 4.0 Hz, H-4), 4.02 (2H, app. t,  $J$  = 17.0, H-11), 5.40 (1H, d,  $J$  = 7.5 Hz, H-1), 7.25 (1H, t,  $J$  = 7.0 Hz, H-9), 7.31 (1H, d,  $J$  = 8.0 Hz, H-7), 7.43 (1H, t,  $J$  = 7.5 Hz, H-15), 7.51-7.59 (3H, m, H-8, H-10, H-16), 7.67 (1H, t,  $J$  = 8.0 Hz, H-14), 7.72 (1H, t,  $J$  = 8.0 Hz, H-13) ppm.

**$^{13}C$ -NMR** (100 MHz, MeOD):  $\delta$  = 30.1 (C-11), 62.5 (C-6), 70.4 (C-4), 72.5 (C-2), 75.0 (C-3),

76.5 (C-5), 104.1 (C-1), 116.0 (C-7), 116.5 (C-13), 120.8 (C-9), 123.4 (C-15), 128.3 (C-14), 128.6 (C-8), 131.3 (C-16), 131.8 (C-10), 144.3 (C-17, C-18), 157.5 (C-19), 158.5 (C-12) ppm.

**FTMS (ESI)  $m/z$**  : 384.1259 [M + Na]<sup>+</sup>. found 384.1257 [M + Na]<sup>+</sup>. **FT-IR (ATR):** 3253

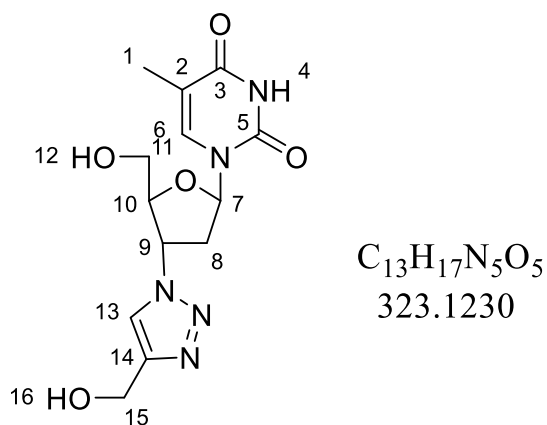
(O-H, br) cm<sup>-1</sup>. **Melting point:** 156-59°C.

### 6.3 The compounds based on azidothymidine containing a triazole moiety 41-48

#### 6.3.1 General Procedure for synthesis of 1,4 triazoles via click reactions

3'-Azido-3'-deoxythymidine (AZT) (1 equivalence (eq.)) and the alkyne (1 eq.) were added to a solution of THF: water (3:1). Freshly prepared sodium ascorbate (1M, 0.1 eq., in H<sub>2</sub>O) was then added followed by CuSO<sub>4</sub>·5H<sub>2</sub>O (1M, 0.06 eq., in H<sub>2</sub>O). The reaction was left to stir for 18 h at room temperature, monitored using TLC. The mixture was then evaporated *in vacuo*. Water was then added to the crude mixture and filtered through a sintered funnel. The solid precipitate was then purified as described for the individual compounds.

### 6.3.1.1 Synthesis of 3'-Deoxy-3'-(4-hydroxymethyl-1,2,3-triazol-1-yl)- $\beta$ -D-thymidine (**44**)

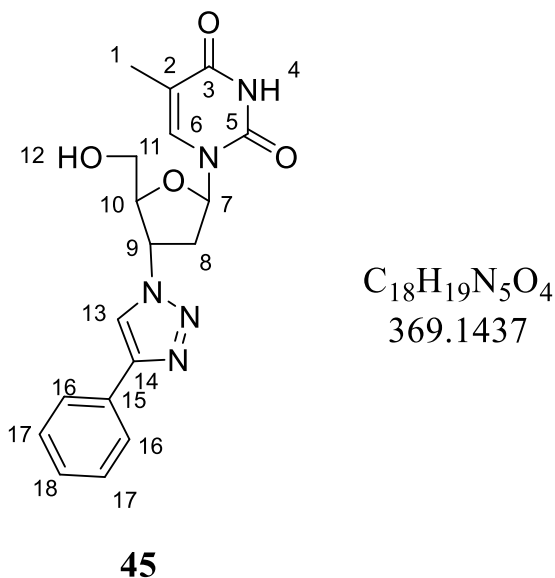


Following the general method outlined in Section 6.3.1: AZT (0.3 g, 1.12 mmol) and propargyl alcohol (0.066 mL, 1.12 mmol) were added to a solution of THF: water (3:1, 12 mL). Freshly prepared sodium ascorbate (0.112 mL, 1 M, 0.112 mmol) was then added followed by  $\text{CuSO}_4 \cdot 5\text{H}_2\text{O}$  (0.067 mL, 1 M, 0.067 mmol). The reaction was left to stir for 18 h at room temperature, monitored using TLC. The mixture was then evaporated to dryness. Water (20 mL) was then added to the crude mixture and filtered. The precipitate was then purified using reverse phase chromatography (0.1% Formic acid: MeCN, starting at 9:1, until 7:3) to produce **44** (Yield: 56%, white powder, Purity: >99%).

**$^1\text{H-NMR}$**  (400 MHz,  $(\text{CD}_3)_2\text{SO}$ ):  $\delta$  = 1.88 (3H, s, H-1), 2.66-2.83 (2H, m, H-8), 3.68 (1H, dt,  $J$  = 12.5 Hz,  $J$  = 4.5 Hz, Ha-11), 3.76 (1H, dt,  $J$  = 12.5 Hz,  $J$  = 4.5 Hz, Hb-11), 4.24-4.29 (1H, m, H-10), 4.60 (2H, d,  $J$  = 6.5 Hz, H-15), 5.30 (1H, t,  $J$  = 5.5 Hz, H-12), 5.36 (1H, t,  $J$  = 5.5 Hz, H-16), 5.45 (1H, dt,  $J$  = 6.0 Hz,  $J$  = 8.5 Hz, H-9), 6.48 (1H, t,  $J$  = 6.5 Hz, H-7), 7.89 (1H, s, H-6), 8.24 (1H, s, H-13), 11.44 (1H, s, H-4), ppm.  **$^{13}\text{C-NMR}$**  (100 MHz,  $(\text{CD}_3)_2\text{SO}$ ):  $\delta$  = 12.5 (C-1), 37.1 (C-8), 55.9 (C-15), 58.8 (C-9), 60.9 (C-11), 83.9 (C-7), 84.4 (C-10), 109.8 (C-2), 122.7 (C-13), 136.1 (C-6), 149.7 (C-3), 163.6 (C-5) ppm. **FTMS (ESI)**

$m/z$  : 346.1126  $[M + Na]^+$ , found 346.1120  $[M + Na]^+$ . **Melting point:** 179-183 °C. **FT-IR**  
(**ATR**): 3673 (O-H, br), 3469 (O-H, br), 1670 (C=O)  $\text{cm}^{-1}$ .

### 6.3.1.2 Synthesis of 3'-Deoxy-3'-(4-benzyl-1,2,3-triazol-1-yl)- $\beta$ -D-thymidine (**45**)

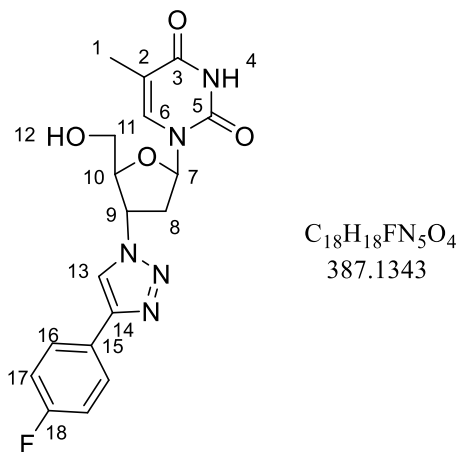


Following the general method outlined in Section 6.3.1: AZT (0.5 g, 1.8 mmol) and phenylacetylene (0.2 mL, 1.8 mmol) were added to a solution of THF: water (3:1, 12 ml). Freshly prepared sodium ascorbate (0.18 mL, 1 M, 0.18 mmol) was then added followed by  $\text{CuSO}_4 \cdot 5\text{H}_2\text{O}$  (0.108 mL, 1 M, 0.108 mmol). The reaction was left to stir for 18 h at room temperature, monitored using TLC. The mixture was then evaporated to dryness. Water (20 mL) was then added to the crude mixture and filtered. . The precipitate was then purified using reverse phase chromatography (0.1% Formic acid: MeCN , starting at 9:1, until 7:3) to produce **45** (Yield: 62%, white powder, Purity: >99%).

**$^1\text{H-NMR}$**  (400 MHz,  $(\text{CD}_3)_2\text{SO}$ ):  $\delta$  = 1.83 (3H, s, H-1), 2.64-2.88 (2H, m, H-8), 3.64-3.79 (2H, m, H-11), 4.26-4.36 (1H, m, H-10), 5.40-5.46 (1H, m, H-9), 5.36 (1H, at,  $J = 3.5$  Hz, 8.5 Hz, H-12), 6.47 (1H, t,  $J = 7.0$  Hz, H-7), 7.36 (1H, at,  $J = 7.5$  Hz, H-18), 7.47 (2H, t,  $J = 7.5$  Hz, H-17), 7.86 (1H, s, H-6), 7.87 (2H, d,  $J = 8.0$  Hz, H-16), 8.78 (1H, s, H-13), 11.41

(1H, s, H-4), ppm. <sup>13</sup>C-NMR (100 MHz, (CD<sub>3</sub>)<sub>2</sub>SO): δ = 12.4 (C-1), 37.1 (C-8), 54.9 (C-9), 60.8 (C-11), 83.3 (C-7), 84.4 (C-10), 110.7.8 (C-2), 121.1 (C-13), 124.8 (C-16), 128.0 (C-18), 128.9 (C-17), 129.2 (C-15), 136.3 (C-6), 147.0 (C-14), 151.7 (C-5), 165.2 (C-3) ppm. **FTMS (ESI) m/z:** 370.1437 [M + H]<sup>+</sup>, found 370.1515 [M + H]<sup>+</sup>. 392.1437 [M + Na]<sup>+</sup>, found 392.1327 [M + Na]<sup>+</sup>. **Melting point:** 218-221 °C. **FT-IR (ATR):** 3418 (O-H, br), 3029 (C-H), 1685 (C=O) cm<sup>-1</sup>.

### 6.3.1.3 Synthesis of 3'-Deoxy-3'-(4-4''-fluoro-benzyl-1,2,3-triazol-1-yl)-β-D-thymidine (46)



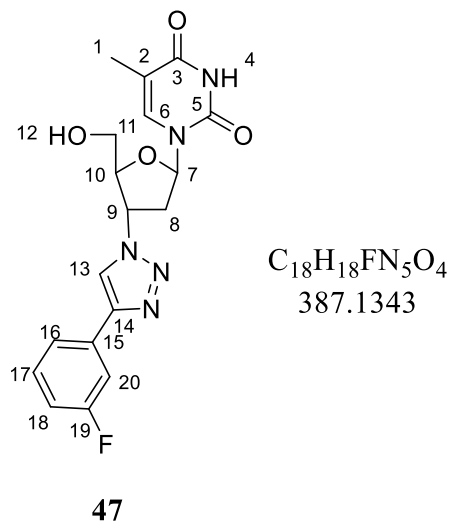
#### 46

Following the general method outlined in Section 6.3.1: AZT (0.5 g, 1.8 mmol) and 1-ethynyl-3-fluorobenzene (0.21 mL, 1.8 mmol) were added to a solution of THF: water (3:1, 16 mL). Freshly prepared sodium ascorbate (0.18 mL, 1 M, 0.18 mmol) was then added followed by CuSO<sub>4</sub>·5H<sub>2</sub>O (0.108 mL, 1 M, 0.108 mmol). The reaction was left to stir for 18 h at room temperature, monitored using TLC. The mixture was then evaporated to dryness. Water (30 mL) was then added to the crude mixture and filtered to produce **46** (93%, Yellow powder, Purity: >99%).

**<sup>1</sup>H-NMR** (400 MHz, (CD<sub>3</sub>)<sub>2</sub>SO): δ = 1.83 (3H, s, H-1), 2.66-2.87 (2H, m, H-8), 3.72 (2H, q, *J* = 12.5 Hz, H-11), 4.24-4.35 (1H, m, H-10), 5.32-5.36 (1H, m, H-12), 5.38-5.46 (1H, m, H-9), 6.45 (1H, t, *J* = 7.0 Hz, H-7), 7.20 (1H, t, *J* = 8.0 Hz, H-18), 7.53 (2H, q, *J* = 7.5 Hz, H-16), 7.73 (2H, d, *J* = 7.5 Hz, H-17), 7.85 (1H, s, H-6), 8.88 (1H, s, H-13), 11.41 (1H, s, H-4) ppm. **<sup>13</sup>C-NMR** (100 MHz, (CD<sub>3</sub>)<sub>2</sub>SO): δ = 12.3 (C-1), 37.2 (C-8), 59.6 (C-9), 60.8 (C-11), 83.9 (C-7), 84.4 (C-10), 109.8 (C-2), 111.7 (C-20), 114.6 (C-18), 121.2 (C-16), 121.7 (C-13), 131.2 (C-17), 133.2 (C-15), 136.3 (C-6), 145.6 (C-14), 150.5 (C-5), 161.9 (C-19), 164.0 (C-3) ppm. **FTMS (ESI) *m/z***: 388.1343 [M + H]<sup>+</sup>, found 388.1417 [M + H]<sup>+</sup>. 410.1343 [M + Na]<sup>+</sup>, found 410.1230 [M + Na]<sup>+</sup>. **Melting point**: 230-233 °C. **FT-IR (ATR)**: 3431 (O-H, br), 1692 (C=O), 1278 (C-F) cm<sup>-1</sup>.

#### 6.3.1.4 Synthesis of 3'-Deoxy-3'-(4-3''-fluoro-benzyl-1,2,3-triazol-1-yl)-β-D-thymidine

(47)



Following the general method outlined in Section 6.3.1: AZT (0.5 g, 1.8 mmol) and 1-ethynyl-3-fluorobenzene (0.21 mL, 1.8 mmol) were added to a solution of THF: water (3:1, 16 mL). Freshly prepared sodium ascorbate (0.18 mL, 1 M, 0.18 mmol) was then added followed by CuSO<sub>4</sub>·5H<sub>2</sub>O (0.108 mL, 1 M, 0.108 mmol). The reaction was left to stir for 18 h

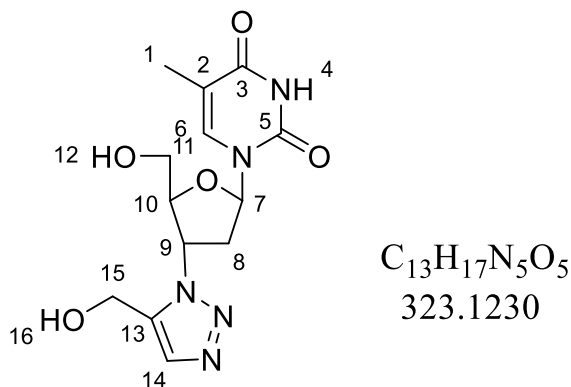
at room temperature, monitored using TLC. The mixture was then evaporated to dryness. Water (30 mL) was then added to the crude mixture and filtered to produce **47** (89%, white powder, Purity: >99%).

**<sup>1</sup>H-NMR** (400 MHz, (CD<sub>3</sub>)<sub>2</sub>SO):  $\delta$  = 1.82 (3H, s, H-1), 2.65-2.84 (2H, m, H-8), 3.63-3.77 (2H, m, H-11), 3.28 (1H, q,  $J$  = 4.0 Hz, H-10), 5.33 (1H, t,  $J$  = 5.0 Hz, H-12), 5.42 (1H, dt,  $J$  = 9.0 Hz,  $J$  = 5.5 Hz, H-9), 6.47 (1H, t,  $J$  = 8.0 Hz, H-7), 7.32 (2H, t,  $J$  = 9.0 Hz, H-6, H-17), 7.85 (1H, s, H-20), 7.89 (1H, d,  $J$  = 7.0 Hz, H-16), 7.92 (1H, d,  $J$  = 7.0 Hz, H-18), 8.79 (1H, s, H-13), 11.39 (1H, s, H-4), ppm. **<sup>13</sup>C-NMR** (100 MHz, (CD<sub>3</sub>)<sub>2</sub>SO):  $\delta$  = 12.2 (C-1), 37.3 (C-8), 59.4 (C-9), 60.7 (C-11), 83.8 (C-7), 84.4 (C-10), 109.9 (C-2), 115.9 (C-17), 120.91 (C-13), 127.2 (C-16), 127.5 (C-15), 136.2 (C-6), 146.4 (C-14), 150.4 (C-5), 164.0 (C-3) ppm. **FTMS (ESI)  $m/z$** : 388.1343 [M + H]<sup>+</sup>, found 388.1421 [M + H]<sup>+</sup>. 410.1343 [M + Na]<sup>+</sup>, found 410.1232 [M + Na]<sup>+</sup>. **Melting point**: 241-243 °C. **FT-IR (ATR)**: 3472 (O-H), 1676 (C=O), 1266 (C-F) cm<sup>-1</sup>.

### **6.3.2 General Procedure for synthesis of 1,5 triazoles via click reactions**

3'-Azido-3'-deoxythymidine (AZT) (1 eq.) and the alkyne (1 eq.) were added to anh. THF. A catalytic amount of  $\text{RuCl} \cdot \text{Cp}(\text{PH}_3)_2$  (0.05 eq.) was added and the mixture was stirred for 1-2 days at 60°C. The reaction was monitored using TLC. Upon completion, the reaction was evaporated to dryness. The precipitate is then purified as describe for the individual compounds.

### 6.3.2.1 Synthesis of 3'-Deoxy-3'-(5-Hydroxymethyl-1,2,3-triazol-1-yl)- $\beta$ -D-thymidine (**48**)

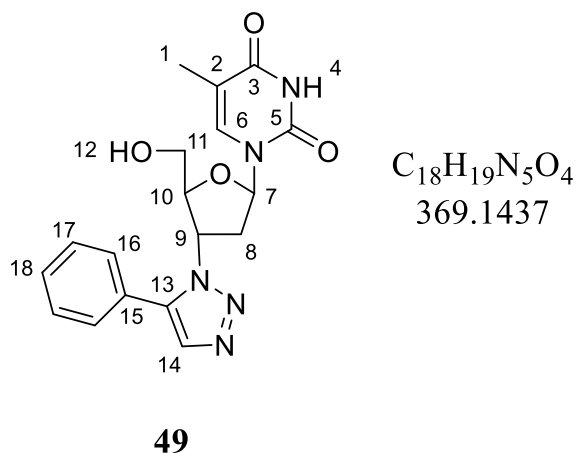


## **48**

Following the general method outlined in Section 6.3.2: AZT (0.15 g, 0.5 mmol) was added to stirred anh. THF (20 mL). Propargyl alcohol (0.48 mL, 0.05 g, 0.84 mmol) and  $RuCp^*Cl(PPH_2)_3$  (20.3 mg, 0.028 mmol) were added to the solution. The reaction was left to stir for 2 days at 60 °C, monitored using TLC. The mixture was then evaporated to dryness. The precipitate is then purified using reverse phase chromatography (0.1% Formic acid: MeCN, starting at 9:1, until 7:3) to produce **48** (38%, white powder, Purity: >99%).

**$^1H$ -NMR** (400 MHz, MeOD):  $\delta$  = 1.84 (3H, s, H-1), 2.68-2.88 (2H, m, H-8), 3.75 (1H, dd,  $J$  = 12.5 Hz,  $J$  = 3.5 Hz, Ha-11), 3.76 (1H, dd,  $J$  = 12.5 Hz,  $J$  = 3.5 Hz, Hb-11), 4.44-4.45 (1H, m, H-10), 5.25 (2H, s, H-15), 5.40-5.45 (1H, m, H-12), 6.06 (1H, t,  $J$  = 6.0 Hz, H-16), 6.69-7.02 (2H, m, H-6, H-9, H-7), 7.29 (1H, t,  $J$  = 7.0 Hz, H-7), 7.83 (1H, s, H-14) ppm.  **$^{13}C$ -NMR** (100 MHz, MeOD):  $\delta$  = 12.4 (C-1), 39.2 (C-8), 58.6 (C-15), 59.9 (C-9), 62.1 (C-11), 85.8 (C-7), 87.2 (C-10), 123.2 (C-2), 135.6 (C-13), 138.6 (C-6), 152.4 (C-14), 160.2 (C-5), 166.6 (C-3) ppm. **FTMS (ESI)  $m/z$** : 346.1230.  $[M + Na]^+$ , found 346.1120  $[M + Na]^+$ . **Melting point**: 162-164 °C. **FT-IR (ATR)**: 3459 (O-H), 1676 (C=O)  $cm^{-1}$ .

### 6.3.2.2 Synthesis of 3'-Deoxy-3'-(5-benzyl-1,2,3-triazol-1-yl)- $\beta$ -D-thymidine (**49**)

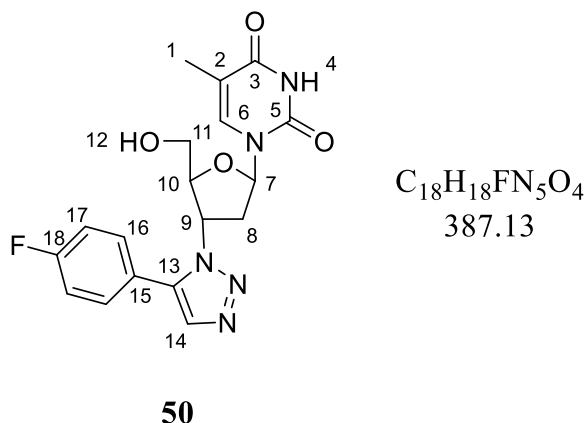


Following the general method outlined in Section 6.3.2: AZT (0.3 g, 1.12 mmol) was added to stirred anhydrous THF (20 mL). Phenylacetylene (1.8 mL, 16.5 mmol) and  $\text{RuCp}^*\text{Cl}(\text{PPh}_2)_3$  (0.04 g, 0.055 mmol) were added to the solution. The reaction was left to stir for 2 days at  $60^\circ\text{C}$ , monitored using TLC. The mixture was then evaporated to dryness. The precipitate is then purified using reverse phase chromatography (0.1% Formic acid: MeCN, starting at 9:1, until 7:3) to produce **49** (42%, white solid, Purity: >99%).

**$^1\text{H-NMR}$**  (400 MHz, (MeOD)):  $\delta$  = 1.83 (3H, s, H-1), 2.53- 2.64 (1H, m, Ha-8), 2.73- 2.81 (1H, m, Hb-8), 3.54 (1H, dd,  $J$  = 12.0 Hz,  $J$  = 3.0 Hz, Ha-11), 3.73 (1H, dd,  $J$  = 12.5 Hz,  $J$  = 3.5 Hz, Hb-11), 4.46 (1H, q,  $J$  = 3.5 Hz, H-10), 5.26-5.31 (1H, m, H-9), 6.61 (1H, t,  $J$  = 7.5 Hz, H-7), 7.45-7.54 (5H, m, H-16, H-17, H-18), 7.78 (1H, s, H-6), 7.82 (1H, s, H-14) ppm.  **$^{13}\text{C-NMR}$**  (100 MHz, (MeOD)):  $\delta$  = 12.5 (C-1), 39.9 (C-8), 59.9 (C-9), 62.8 (C-11), 86.8 (C-10), 86.8 (C-7), 130.4-131.1 (C-16, C-17, C-18), 133.9 (C-6), 138.3 (C-14), 152.7 (C-3), 166.4 (C-5) ppm. **FTMS (ESI)  $m/z$** : 370.1437  $[\text{M} + \text{H}]^+$ , found 370.1520  $[\text{M} + \text{H}]^+$ . 392.1437  $[\text{M} + \text{Na}]^+$ , found 392.1332  $[\text{M} + \text{Na}]^+$ . **Melting point**:  $216\text{-}219^\circ\text{C}$ . **FT-IR (ATR)**: 3462 (O-H), 3030 (C-H, aromatic), 1679 (C=O)  $\text{cm}^{-1}$ .

### 6.3.2.3 Synthesis of 3'-Deoxy-3'-(5-4''-fluoro-benzyl-1,2,3-triazol-1-yl)-β-D-thymidine

(50)

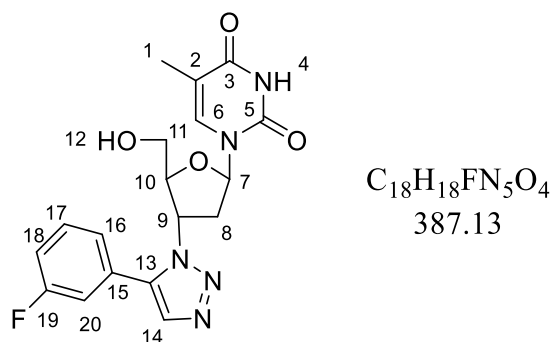


Following the general method outlined in Section 6.3.2: AZT (0.3 g, 1.1 mmol) was added to stirred anhydrous THF (20 mL). 1-ethynyl-3-fluorobenzene (1.91 mL, 1.98 g, 16.5 mmol) and  $\text{RuCp}^*\text{Cl}(\text{PPH}_2)_3$  (39 mg, 0.06 mmol) were added to the solution. The reaction was left to stir for 2 days at 60 °C, monitored using TLC. The mixture was then evaporated to dryness. The precipitate is then purified using reverse phase chromatography (0.1% Formic acid: MeCN, starting at 9:1, until 7:3) to produce **50** (50%, white solid, Purity: >99%).

**$^1\text{H-NMR}$**  (400 MHz, MeOD):  $\delta = 1.77$  (3H, s, H-1), 2.49-2.59 (2H, m, H-8), 3.68 (1H, dd,  $J = 3.0$  Hz, 12.0 Hz, Ha-11), 3.75 (1H, dd,  $J = 3.0$  Hz, 12.0 Hz, Hb-11), 4.40 (1H, m, H-10), 5.34-5.39 (1H, m, H-9), 6.52 (1H, t,  $J = 6.5$  Hz, H-7), 7.16-7.27 (2H, m, H-16), 7.42-7.47 (2H, m, H-17), 7.87 (1H, s, H-6), 7.91 (1H, s, H-14) ppm.  **$^{13}\text{C-NMR}$**  (100 MHz, MeOD):  $\delta = 12.3$  (C-1), 37.2 (C-8), 59.4 (C-9), 61.8 (C-11), 83.2 (C-7), 88.4 (C-10), 115.8 (C-2), 115.0 (Ca-16), 115.2 (Ca-16), 121.2 (C-15), 130.5 (Ca-17), 131.2 (Cb-17), 134.7 (C-6), 136.5 (C-14), 145.6 (C-14), 151.2 (C-5), 161.8 (C-18), 167.1 (C-3) ppm. **FTMS (ESI)  $m/z$** : 388.1343  $[\text{M} + \text{H}]^+$ , found 388.1442  $[\text{M} + \text{H}]^+$ . 410.1343  $[\text{M} + \text{Na}]^+$ , found 410.1430  $[\text{M} + \text{Na}]^+$ . **Melting point**: 221-223 °C. **FT-IR (ATR)**: 3337 (O-H, br), 1652 (C=O)  $\text{cm}^{-1}$ .

### 6.3.2.4 Synthesis of 3'-Deoxy-3'-(5-3''-fluoro-benzyl-1,2,3-triazol-1-yl)-β-D-thymidine

(51)



**51**

Following the general method outlined in Section 6.3.2: AZT (0.3 g, 1.1 mmol) was added to stirred anh. THF (20 mL). 1-ethynyl-4-fluorobenzene (1.91 mL, 1.98 g, 16.5 mmol) and  $RuCp^*Cl(PPh_2)_3$  (39 mg, 0.06 mmol) were added to the solution. The reaction was left to stir for 2 days at 60 °C, monitored using TLC. The mixture was then evaporated to dryness. The precipitate is then purified using reverse phase chromatography (0.1% Formic acid: MeCN, starting at 9:1, until 7:3) to produce **51** (48%, white powder, Purity: >99%).

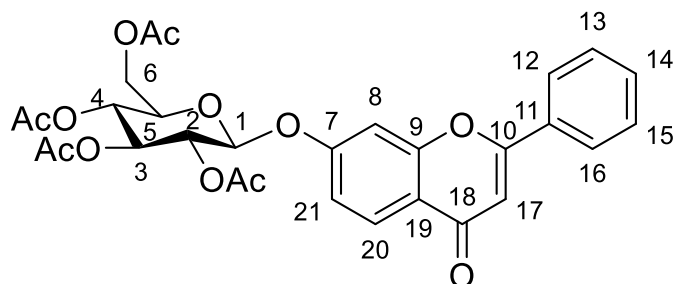
**$^1H$ -NMR** (400 MHz, MeOD):  $\delta$  = 1.79 (3H, s, H-1), 2.48-2.62 (2H, m, H-8), 3.47 (1H, dd,  $J$  = 3.0 Hz, 12.0 Hz, Ha-11), 3.59 (1H, dd,  $J$  = 3.0 Hz, 12.0 Hz, Hb-11), 4.28 (1H, q,  $J$  = 3.5 Hz, H-10), 5.36 (1H, dt,  $J$  = 4.0 Hz, 8.5 Hz H-9), 6.51 (1H, t,  $J$  = 7.5 Hz, H-7), 7.10 (1H, t,  $J$  = 8.5 Hz, H-17), 7.35 (1H, s, H-6), 7.70 (1H, s, H-14), 7.82 (1H, s, H-20), 7.92-7.99 (2H, m, H-16, H-18) ppm.  **$^{13}C$ -NMR** (100 MHz, MeOD):  $\delta$  = 12.2 (C-1), 39.6 (C-8), 59.7 (C-9), 62.5 (C-11), 86.7 (C-10), 87.3 (C-7), 111.7 (C-2), 117.3 (Ca-16), 117.5 (Cb-16), 123.7 (C-15), 132.9 (Ca-17), 133.0 (Cb-17), 134.0 (C-14), 138.3 (C-6), 139.4 (C-13), 152.6 (C-5), 163.7 (C-18), 166.3 (C-13) ppm. **FTMS (ESI)  $m/z$** : 388.1343  $[M + H]^+$ , found 388.1366  $[M + H]^+$ . 410.1343  $[M + Na]^+$ , found 410.1326  $[M + Na]^+$ . **Melting point**: 236-239 °C. **FT-IR (ATR)**: 3301 (O-H, br), 1641 (C=O)  $cm^{-1}$ .

## 6.4 The glycosidic flavonoid containing compounds 92-97 and 112-117

### 6.4.1 General Procedure for synthesis of *O*-acetylated flavonoid glycosides 112-117

To a mixture of DMF: acetone (5:3), K<sub>2</sub>CO<sub>3</sub> (21 eq.) was added. This was followed by the addition of the flavonoid (1 eq.), tetrabutylammonium bromide (TBAB) and the sugar (10 eq.). The reaction was stirred for 18 h at room temperature. Upon completion, the acetone was removed *in vacuo* and the remaining solution was washed with a saturated LiCl solution. Ethyl acetate was added and the organic layers were separated and combined. The organic layer was dried with MgSO<sub>4</sub> and the solvent was removed *in vacuo*. The precipitate was then purified using column chromatography to produce the desired *O*-acetylated product.

#### 6.4.1.1 Synthesis of 7-hydroxyflavone- $\beta$ -D-2,3,4,6-tetra-*O*-acetate glucopyranoside (**112**)



### **112**

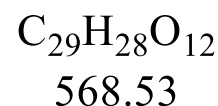
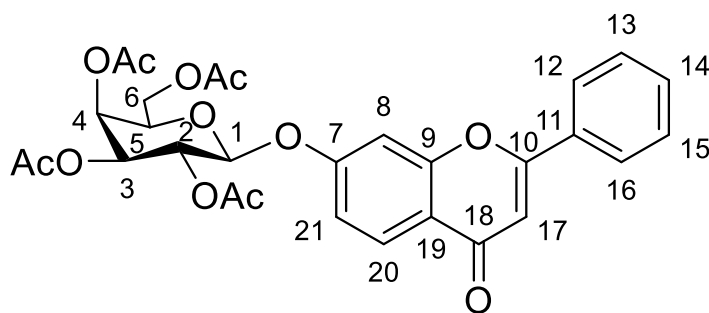
Following the general method outlined in Section 6.4.1: To a mixture of DMF: acetone (100:60 mL),  $K_2CO_3$  (11.5 g, 84.0 mmol) was added. This was followed by the addition of 7-hydroxyflavone (0.952 g, 4.0 mmol), TBAB (100 mg) and the acetobromoglucose (10 g, 20.0 mmol). The reaction was stirred for 18 h at room temperature. Upon completion, the acetone was removed *in vacuo* and remaining solvent washed with a saturated LiCl solution. Ethyl acetate ( $3 \times 70$  mL) was added and the organic layers were separated and combined. The organic layer was dried with  $MgSO_4$  and the solvent was removed *in vacuo*. The precipitate is then purified using column chromatography (ethyl acetate: petrol ether (3:2)) to produce **112** (62%, clear oil)

$\delta = ^1H-NMR$  (400 MHz,  $CDCl_3$ ):  $\delta = 2.05$  (3H, s, H- $OCOCH_3$ ), 2.07 (3H, s, H- $OCOCH_3$ ), 2.10 (3H, s, H- $OCOCH_3$ ), 2.21 (3H, s, H- $OCOCH_3$ ), 4.21-4.27 (3H, m, H-5, H-6), 5.19 (1H, dd,  $J = 3.5$  Hz,  $J = 10.5$  Hz, H-3), 5.25 (1H, d,  $J = 8.0$  Hz, H-1), 5.52 (1H, d,  $J = 3.5$  Hz, H-2), 5.56 (1H, dd,  $J = 8.0$  Hz,  $J = 10.5$  Hz, H-4), 6.78 (1H, s, H-17), 7.07 (1H, dd,  $J = 2.5$  Hz,  $J = 9.0$  Hz, H-21), 7.16 (1H, d,  $J = 2.0$  Hz, H-8), 7.49-7.57 (3H, m, H-13, H-14, H-15), 7.87-7.92 (2 H, add,  $J = 2.0$  Hz,  $J = 7.0$  Hz, H-12, H-16), 8.17 (1H, d,  $J = 9.0$  Hz, H-20) ppm.  $^{13}C-NMR$  (100 MHz,  $CDCl_3$ ):  $\delta = 20.5$  (C- $OCOCH_3$ ), 20.6 (C- $OCOCH_3$ ), 20.7 (C- $OCOCH_3$ ), 21.0 (C- $OCOCH_3$ ), 61.7 (C-6), 66.7 (C-2), 68.3 (C-4), 70.7 (C-3), 71.7 (C-5), 99.1 (C-1), 104.6 (C-8), 1

07.6 (C-17), 115.3 (C-21), 119.6 (C-19), 126.2 (C-12, C-16), 127.4 (C-20), 129.0 (C-13, C-15), 131.8 (C-11, C-14), 156.6 (C-9), 160.2 (C-7), 163.2 (C-10), 170.0 (C-OCOCH<sub>3</sub>), 170.2 (C-OCOCH<sub>3</sub>), 170.3 (C-OCOCH<sub>3</sub>), 171.1 (C-OCOCH<sub>3</sub>), 177.6 (C-18) ppm.

**FTMS (ESI)** *m/z*: 591.5192 [M + Na]<sup>+</sup>, found 591.1462 [M + Na]<sup>+</sup>. **FT-IR (ATR)**: 1685 (C=O), 1035 (C-O) cm<sup>-1</sup>.

#### 6.4.1.2 Synthesis of 7-hydroxyflavone-β-D-2,3,4,6-tetra-O-acetate galactopyranoside (**113**)

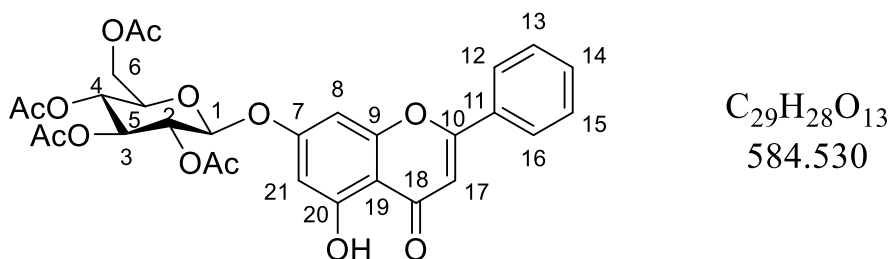


### **113**

Following the general method outlined in Section 6.4.1: To a mixture of DMF: acetone (100:60 mL), K<sub>2</sub>CO<sub>3</sub> (11.50 g, 84.00 mmol) was added. This was followed by the addition of 7-hydroxyflavone (0.95 g, 4.00 mmol), TBAB (100 mg) and the acetobromogalactose (10.00 g, 20.00 mmol). The reaction was stirred for 18 h at room temperature. Upon completion, the acetone was removed *in vacuo* and remaining solvent washed with a saturated LiCl solution. Ethyl acetate (3 × 70 mL) was added and the organic layers were separated and combined. The organic layer was dried with MgSO<sub>4</sub> and the solvent was removed *in vacuo*. The precipitate is then purified using column chromatography (ethyl acetate: petrol ether (3:2)) to produce **113** (71%, clear oil).

**<sup>1</sup>H-NMR** (400 MHz, CDCl<sub>3</sub>): δ = 2.05 (3H, s, H-OCOCH<sub>3</sub>), 2.08 (3H, s, H-OCOCH<sub>3</sub>), 2.11 (3H, s, H-OCOCH<sub>3</sub>), 2.12 (3H, s, H-OCOCH<sub>3</sub>), 4.26-4.31 (3H, m, H-5, H-6), 5.24 (1H, dd, *J* = 3.5 Hz, *J* = 10.5 Hz, H-3), 5.32 (1H, d, *J* = 8.0 Hz, H-1), 5.54 (1H, d, *J* = 3.5 Hz, H-2), 5.57 (1H, dd, *J* = 8.0 Hz, *J* = 11.0 Hz, H-4), 6.75 (1H, s, H-17), 7.08 (1H, dd, *J* = 2.5 Hz, *J* = 9.0 Hz, H-21), 7.18 (1H, d, *J* = 2.5 Hz, H-8), 7.49-7.57 (3H, m, H-13, H-14, H-15), 7.87-7.92 (2H, m, H-12, H-16), 8.16 (1H, d, *J* = 9.0 Hz, H-20) ppm. **<sup>13</sup>C-NMR** (100 MHz, CDCl<sub>3</sub>): δ = 20.4 (C-OCOCH<sub>3</sub>), 20.5 (C-OCOCH<sub>3</sub>), 20.6 (C-OCOCH<sub>3</sub>), 20.9 (C-OCOCH<sub>3</sub>), 61.6 (C-6), 67.0 (C-2), 68.4 (C-4), 70.6 (C-3), 71.5 (C-5), 98.7 (C-1), 104.2 (C-8), 107.5 (C-17), 115.1 (C-21), 115.4 (C-19), 125.9 (C-12, C-16), 127.5 (C-20), 129.1 (C-13, C-15), 131.4 (C-11), 132.6 (C-14), 157.7 (C-9), 160.9 (C-7), 163.6 (C-10), 169.9 (C-OCOCH<sub>3</sub>), 170.1 (C-OCOCH<sub>3</sub>), 170.3 (C-OCOCH<sub>3</sub>), 171.1 (C-OCOCH<sub>3</sub>), 177.5 (C-18) ppm. **FTMS (ESI) *m/z***: 591.5192 [M + Na]<sup>+</sup>, found 591.0245 [M + Na]<sup>+</sup>. **FT-IR (ATR)**: 1741 (C=O), 998 (C-O) cm<sup>-1</sup>.

#### 6.4.1.3 Synthesis of chrysin-β-D-2,3,4,6-tetra-*O*-acetate glucopyranoside (114)



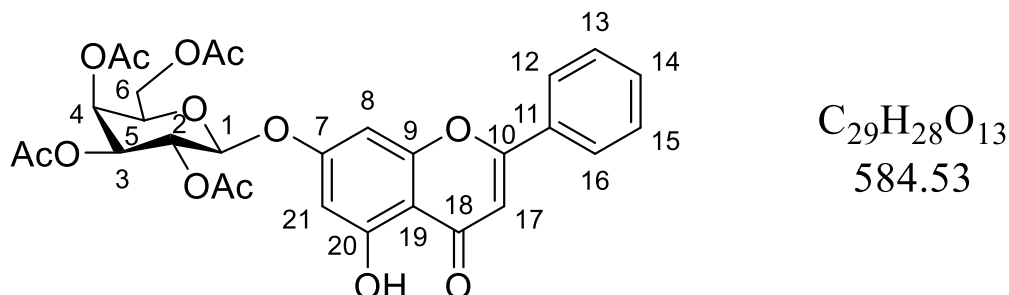
### 114

Following the general method outlined in Section 6.4.1: To a mixture of DMF: acetone (100:60 mL), K<sub>2</sub>CO<sub>3</sub> (11.50 g, 84.0 mmol) was added. This was followed by the addition of chrysin (1.02 g, 4 mmol), TBAB (100 mg) and the acetobromoglucose (10.00 g, 20.00 mmol). The reaction was stirred for 18 h at room temperature. Upon completion, the acetone was

removed *in vacuo* and remaining solvent washed with a saturated LiCl solution. Ethyl acetate (3 × 70 mL) was added and the organic layers were separated and combined. The organic layer was dried with MgSO<sub>4</sub> and the solvent was removed *in vacuo*. The precipitate is then purified using column chromatography (ethyl acetate: petrol ether (3:2)) to produce **114** (68%, clear oil).

**<sup>1</sup>H-NMR** (400 MHz, CDCl<sub>3</sub>): δ = 2.05 (3H, s, H-OCOCH<sub>3</sub>), 2.07 (3H, s, H-OCOCH<sub>3</sub>), 2.09 (3H, s, H-OCOCH<sub>3</sub>), 2.11 (3H, s, H-OCOCH<sub>3</sub>), 3.96 (1H, dq, *J* = 3.0 Hz, *J* = 6.0 Hz, H-5), 4.21 (1H, dd, Ha-6), 4.30 (1H, dd, Hb-6), 5.16 (1H, d, *J* = 9.0 Hz, H-4), 5.20 (1H, d, *J* = 7.5 Hz, H-1), 5.32 (2H, aquin, *J* = 7.5 Hz, *J* = 9.0 Hz, H-2, H-3), 6.45 (1H, d, *J* = 2.0 Hz, H-8), 6.60 (1H, d, *J* = 2.0 Hz, H-21), 6.69 (1H, s, H-17), 7.50-7.60 (3H, m, H-13, H-14, H-15), 7.50-7.88 (2H, m, H-12, H-16), 12.74 (1H, s, H-OH) ppm. **<sup>13</sup>C-NMR** (100 MHz, CDCl<sub>3</sub>): δ = 20.6 (C-OCOCH<sub>3</sub>), 20.7 (C-OCOCH<sub>3</sub>), 61.9 (C-6), 68.2 (C-4), 70.8 (C-2), 72.5 (C-3), 72.6 (C-5), 95.7 (C-21), 98.1 (C-1), 99.9 (C-8), 106.1 (C-17), 126.4 (C-12, C-16), 129.2 (C-13, C-15), 132.2 (C-14), 157.1 (C-9), 159.2 (C-7), 162.2 (C-19), 162.4 (C-20), 164.4 (C-10, C-11), 169.2 (C-OCOCH<sub>3</sub>), 169.4 (C-OCOCH<sub>3</sub>), 170.2 (C-OCOCH<sub>3</sub>), 170.6 (C-OCOCH<sub>3</sub>), 182.5 (C-18) ppm. **FTMS (ESI) *m/z***: 607.5192 [M + Na]<sup>+</sup>, found 607.1397 [M + Na]<sup>+</sup>. **FT-IR (ATR)**: 1741 (C=O) cm<sup>-1</sup>.

#### 6.4.1.4 Synthesis of chrysin- $\beta$ -D-2,3,4,6-tetra-*O*-acetate galactopyranoside (**115**)



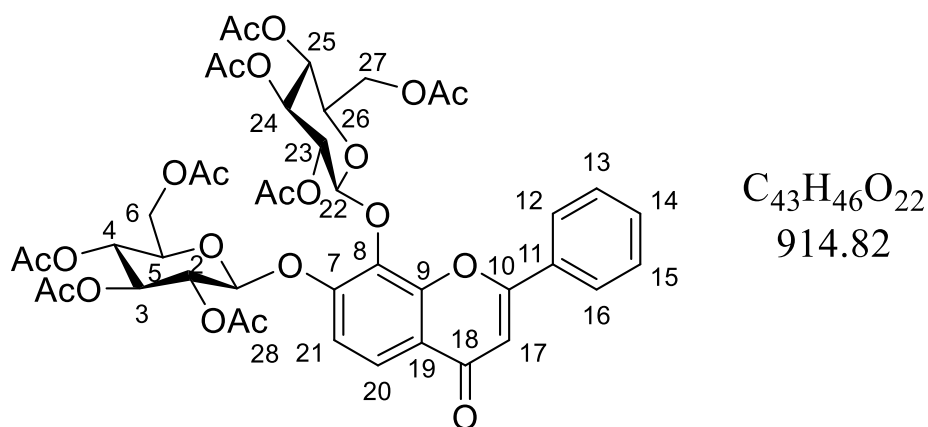
### **115**

Following the general method outlined in Section 6.4.1: To a mixture of DMF: acetone (100:60 mL),  $K_2CO_3$  (11.50 g, 84.0 mmol) was added. This was followed by the addition of chrysin (1.02 g, 4 mmol), TBAB (100 mg) and the acetobromogalactose (10.00 g, 20.00 mmol). The reaction was stirred for 18 h at room temperature. Upon completion, the acetone was removed *in vacuo* and remaining solvent washed with a saturated LiCl solution. Ethyl acetate ( $3 \times 70$  mL) was added and the organic layers were separated and combined. The organic layer was dried with  $MgSO_4$  and the solvent was removed *in vacuo*. The precipitate is then purified using column chromatography (ethyl acetate: petrol ether (3:2)) to produce **115** (69%, clear oil).

$^1H$ -NMR (400 MHz,  $CDCl_3$ ):  $\delta$  = 2.03 (3H, s, H- $OCOCH_3$ ), 2.09 (3H, s, H- $OCOCH_3$ ), 2.10 (3H, s, H- $OCOCH_3$ ), 2.20 (3H, s, H- $OCOCH_3$ ), 4.07-4.30 (3H, m, H-5, H-6), 5.13-5.18 (2H, m, H-1, H-3), 5.47-5.56 (2H, m, H-2, H-4), 6.48 (1H, d,  $J$  = 2.5 Hz, H-8), 6.63 (1H, d,  $J$  = 2.5 Hz, H-21), 6.69 (1H, s, H-17), 7.50-7.60 (3H, m, H-13, H-14, H-15), 7.86-7.91 (2H, m, H-12, H-16), 12.73 (1H, s, H-20OH) ppm.  $^{13}C$ -NMR (100 MHz,  $CDCl_3$ ):  $\delta$  = 20.6 (C- $OCOCH_3$ ), 20.7 (C- $OCOCH_3$ ), 21.0 (C- $OCOCH_3$ ), 62.0 (C-6), 66.7 (C-4), 69.1 (C-2), 71.0 (C-3), 72.4 (C-5), 95.5 (C-21), 98.7 (C-1), 99.9 (C-8), 106.1 (C-17), 126.2 (C-12, C-16), 129.2 (C-13, C-15), 132.1 (C-14), 157.1 (C-9), 162.2 (C-19), 162.4 (C-7, C-20), 164.4 (C-10, C-11), 169.3 (C-OC

OCH<sub>3</sub>), 170.0 (C-OCOCH<sub>3</sub>), 170.2(C-OCOCH<sub>3</sub>), 170.5 (C-OCOCH<sub>3</sub>), 183.1 (C-18) ppm. FT MS (ESI) *m/z*: 607.5192 [M + Na]<sup>+</sup>, found 607.2563 [M + Na]<sup>+</sup>. FT-IR (ATR): 1675 (C=O) cm<sup>-1</sup>.

#### 6.4.1.5 Synthesis of 7,8-dihydroxyflavone-β-D-2,3,4,6-tetra-O-acetate glucopyranoside (116)

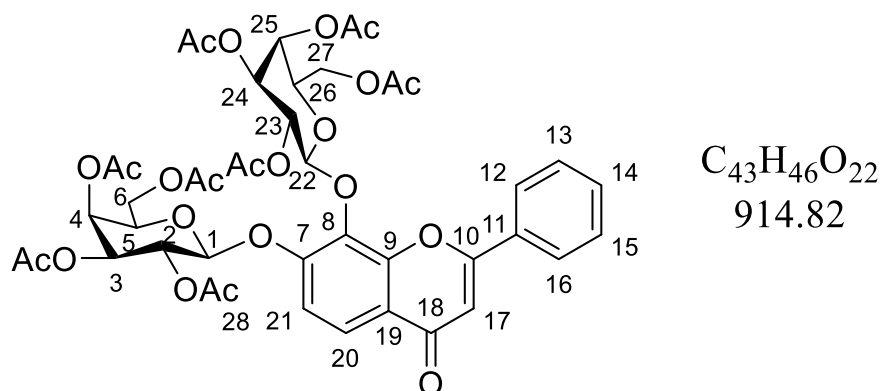


### 116

Following the general method outlined in Section 6.4.1: To a mixture of DMF: acetone (100:60 mL), K<sub>2</sub>CO<sub>3</sub> (11.50 g, 84.0 mmol) was added. This was followed by the addition of 7,8-dihydroxyflavone (1.02 g, 4 mmol), TBAB (100 mg) and the acetobromoglucose (10.00 g, 20.00 mmol). The reaction was stirred for 18 h at room temperature. Upon completion, the acetone was removed *in vacuo* and remaining solvent washed with a saturated LiCl solution. Ethyl acetate (3 × 70 mL) was added and the organic layers were separated and combined. The organic layer was dried with MgSO<sub>4</sub> and the solvent was removed *in vacuo*. The precipitate is then purified using a column chromatography (9:1 to 2:8 petrol ether: ethyl acetate) to produce **116** (40%, orange oil) product.

**<sup>1</sup>H-NMR** (400 MHz, CDCl<sub>3</sub>): δ = 1.80 (3H, s, H-OCOCH<sub>3</sub>), 1.99 (3H, s, H-OCOCH<sub>3</sub>), 2.02-2.05 (9H, m, H-OCOCH<sub>3</sub>), 2.06 (3H, s, H-OCOCH<sub>3</sub>), 2.07 (3H, s, H-OCOCH<sub>3</sub>), 2.10 (3H, s, H-OCOCH<sub>3</sub>), 3.71-3.78 (1H, m, H-5), 3.85-3.91 (2H, m, H-26), 3.94 (1H, ad, *J* = 12.5 Hz, Ha-6), 4.14 (1H, ad, *J* = 13.0 Hz, Ha-27), 4.20 (1H, dd, *J* = 5.0 Hz, *J* = 13.0 Hz, Hb-6), 4.31 (1H, dd, *J* = 5.5 Hz, *J* = 13.0 Hz, Hb-27), 5.20 (2H, aq, *J* = 10.0 Hz, H-4, H-25), 5.27-5.41 (5H, m, H-1, H-2, H-3, H-23, H-24), 5.52 (1H, d, *J* = 7.5 Hz, H-22), 6.80 (1H, s, H-17), 7.16 (1H, d, *J* = 9.0 Hz, H-21), 7.51-7.58 (3H, m, H-13, H-14, H-15), 7.94 (1H, d, *J* = 9.0 Hz, H-20), 7.98-8.03 (2H, m, H-12, H-16) ppm. **<sup>13</sup>C-NMR** (100 MHz, CDCl<sub>3</sub>): δ = 20.4 (C-OCOCH<sub>3</sub> H<sub>3</sub>), 20.6 (C-OCOCH<sub>3</sub>), 20.7 (C-OCOCH<sub>3</sub>), 20.8 (C-OCOCH<sub>3</sub>), 61.5 (C-6, C-27), 67.9 (C-4), 68.3 (C-25), 71.3 (C-2, C-23), 72.5 (C-5), 72.5 (C-3, C-26), 72.8 (C-24), 99.4 (C-1), 99.9 (C-22), 106.9 (C-17), 114.5 (C-19), 114.8 (C-21), 121.6 (C-20), 126.4 (C-12, C-16), 129.2 (C-13, C-15), 131.3 (C-11), 132.0 (C-14), 134.3 (C-8), 150.5 (C-9), 152.8 (C-7), 163.8 (C-10), 169.4 (C-OCOCH<sub>3</sub>), 170.2 (C-OCOCH<sub>3</sub>), 170.4 (C-OCOCH<sub>3</sub>), 178.0 (C-18) ppm. **FTMS (ESI) *m/z***: 937.8092 [M + Na]<sup>+</sup>, found 936.9584 [M + Na]<sup>+</sup>. **FT-IR (ATR)**: 1784 (C=O) cm<sup>-1</sup>.

#### 6.4.1.6 Synthesis of 7,8-dihydroxyflavone-β-D-2,3,4,6-tetra-*O*-acetate galactopyranoside (117)



**117**

Following the general method outlined in Section 6.4.1: To a mixture of DMF: acetone (100:60 mL), K<sub>2</sub>CO<sub>3</sub> (11.50 g, 84.0 mmol) was added. This was followed by the addition of 7,8-dihydroxyflavone (1.02 g, 4 mmol), TBAB (100 mg) and the acetobromogalactose (10.00 g, 20.00 mmol). The reaction was stirred for 18 h at room temperature. Upon completion, the acetone was removed *in vacuo* and remaining solvent washed with a saturated LiCl solution. Ethyl acetate (3 × 70 mL) was added and the organic layers were separated and combined. The organic layer was dried with MgSO<sub>4</sub> and the solvent was removed *in vacuo*. The precipitate is then purified using a column chromatography (9:1 to 2:8 petrol ether: ethyl acetate) to produce **117** (41%, clear oil).

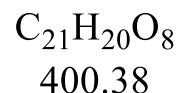
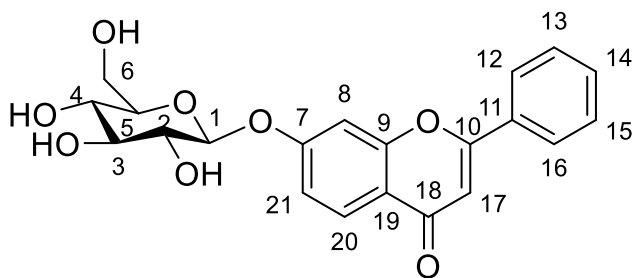
**<sup>1</sup>H-NMR** (400 MHz, CDCl<sub>3</sub>): δ = 1.86 (3H, s, H-OCOCH<sub>3</sub>), 2.01 (9H, s, H-OCOCH<sub>3</sub>), 2.10 (3H, s, H-OCOCH<sub>3</sub>), 2.14 (3H, s, H-OCOCH<sub>3</sub>), 2.21 (3H, s, H-OCOCH<sub>3</sub>), 3.95-4.07 (4H, m, H-5, H-6, H-26), 4.14-4.22 (2H, m, H-27), 5.12-5.19 (2H, m, H-3, H-24), 5.27 (1H, d, *J* = 8.0 Hz, H-1), 5.40 (1H, d, *J* = 4.0 Hz, H-4), 5.44-5.52 (3H, m, H-2, H-22, H-25), 5.58 (1H, at, *J* = 9.0 Hz, H-23), 6.81 (1H, s, H-17), 7.18 (1H, d, *J* = 9.0 Hz, H-21), 7.50-7.56 (3H, m, H-13, H-14, H-15), 7.93 (1H, d, *J* = 9.0 Hz, H-20), 8.01-8.05 (2H, m, H-12, H-16) ppm.

**<sup>13</sup>C-NMR** (100 MHz, CDCl<sub>3</sub>): δ = 20.5 (C-OCOCH<sub>3</sub>), 20.6 (C-OCOCH<sub>3</sub>), 20.8 (C-OCOCH<sub>3</sub>), 60.6 (C-6), 61.4 (C-27), 66.8 (C-4), 67.1 (C-25), 68.7 (C-2), 69.6 (C-23), 70.6 (C-3), 70.9 (C-24), 71.2 (C-5), 71.6 (C-26), 100.0 (C-1), 100.3 (C-22), 106.8 (C-17), 114.7 (C-21), 114.9 (C-19), 121.4 (C-20), 126.6 (C-12, C-16), 129.1 (C-13, C-15), 131.8 (C-11), 131.9 (C-14), 133.8 (C-8), 150.6 (C-9), 152.5 (C-7), 163.4 (C-10), 169.4 (C-OCOCH<sub>3</sub>), 169.5 (C-OCOCH<sub>3</sub>), 170.0 (C-OCOCH<sub>3</sub>), 170.1 (C-OCOCH<sub>3</sub>), 170.2 (C-OCOCH<sub>3</sub>), 170.3 (C-OCOCH<sub>3</sub>), 178.3 (C-18) ppm. **FTMS (ESI) *m/z***: 937.8092 [M + Na]<sup>+</sup>, found 937.2543[M + Na]<sup>+</sup>. **FT-IR (ATR)**: 1645 (C=O) cm<sup>-1</sup>.

#### **6.4.2 General procedure for deprotection of the flavonoid glycosides 92-97**

The product was dissolved in anh. methanol (30 mL) and  $K_2CO_3$  (90 mg) was added and stirred for 20 h. The reaction was neutralised to pH 7 using 1.0 M HCl. The filtrate was filtered through a sintered funnel and the solid was collected. The crude solid was purified using RP-column chromatography (0.1% formic acid in water: MeCN)

#### 6.4.2.1 Synthesis of 7 hydroxyflavone- $\beta$ -D-glucopyranoside (**92**)

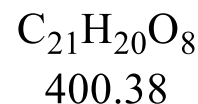
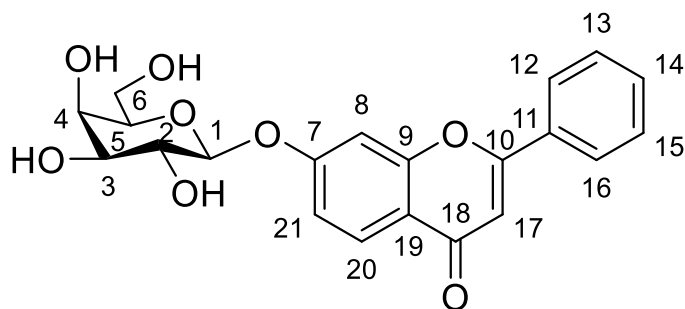


### **92**

Following the general method outlined in Section 6.4.2: The acetylated product **112** was dissolved in anh. methanol (30 mL) and  $\text{K}_2\text{CO}_3$  (90 mg) was added. This reaction was left to stir for 20 h at room temperature. The reaction was neutralised to pH 7 using 1.0 M HCl. The filtrate was filtered and the solid was collected to produce **92** (65%, white solid, Purity: 97%).

**$^1\text{H-NMR}$**  (400 MHz,  $(\text{CD}_3)_2\text{SO}$ ):  $\delta$  = 3.43-3.48 (1H, m, H-3), 3.49-3.60 (2H, m, H-6), 3.60-3.67 (1H, m, H-2), 3.69-3.70 (2H, m, H-4, H-5), 4.57 (1H, d,  $J$  = 4.5 Hz, H-4OH), 4.72 (1H, t,  $J$  = 5.5 Hz, H-6OH), 4.94 (1H, d,  $J$  = 5.5 Hz, H-3OH), 5.09 (1H, d,  $J$  = 8.0 Hz, H-1), 5.29 (1H, d,  $J$  = 5.5 Hz, H-2OH), 6.98 (1H, s, H-17), 7.15 (1H, dd,  $J$  = 2.5 Hz,  $J$  = 9.0 Hz, H-21), 7.39 (1H, d,  $J$  = 2.0 Hz, H-8), 7.56-7.62 (3H, m, H-13, H-14, H-15), 7.97 (1H, d,  $J$  = 9.0 Hz, H-20), 8.07-8.11 (2H, m, H-12, H-16) ppm.  **$^{13}\text{C-NMR}$**  (100 MHz,  $(\text{CD}_3)_2\text{SO}$ ):  $\delta$  = 61.3 (C-6), 68.0 (C-4), 70.2 (C-2), 73.5 (C-3), 75.9 (C-5), 101.3 (C-1), 103.8 (C-8), 107.0 (C-17), 115.8 (C-21), 118.4 (C-19), 126.8 (C-12, C-16, C-20), 129.2 (C-13, C-15), 131.5 (C-11), 132.0 (C-14), 157.7 (C-9), 157.8 (C-7), 161.9 (C-10), 176.2 (C-18) ppm. **FTMS (ESI)**  $m/z$  : 417.1186  $[\text{M} + \text{OH}]^+$ , found 417.1186  $[\text{M} + \text{OH}]^+$ . **Melting point**: 275-277 °C. **FT-IR (ATR)**: 3923 (O-H), 1035 (C-O)  $\text{cm}^{-1}$ .

#### 6.4.2.2 Synthesis of 7 hydroxyflavone- $\beta$ -D-galactopyranoside (**93**)



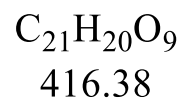
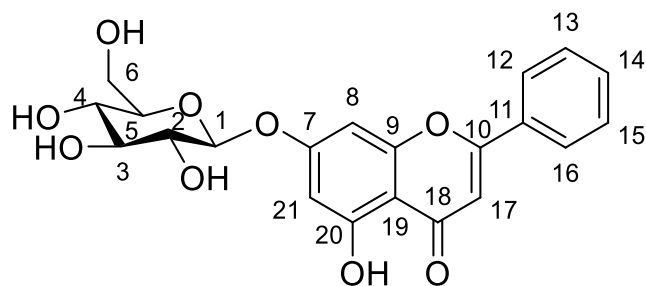
### **93**

Following the general method outlined in Section 6.4.2: The acetylated product **113** was dissolved in anh. methanol (30 mL) and  $\text{K}_2\text{CO}_3$  (90 mg) was added. This reaction was left to stir for 20 h at room temperature. The reaction was neutralised to pH 7 using 1.0 M HCl. The filtrate was filtered and the solid was collected to produce **93** (68%, white solid, Purity: 98%).

**$^1\text{H-NMR}$**  (400 MHz,  $(\text{CD}_3)_2\text{SO}$ ):  $\delta$  = 3.43-3.48 (1H, m, H-3), 3.49-3.60 (2H, m, H-6), 3.60-3.67 (1H, m, H-2), 3.69-3.70 (2H, m, H-4, H-5), 4.57 (1H, d,  $J$  = 4.5 Hz, H-4OH), 4.72 (1H, t,  $J$  = 5.5 Hz, H-6OH), 4.94 (1H, d,  $J$  = 5.5 Hz, H-3OH), 5.09 (1H, d,  $J$  = 8.0 Hz, H-1), 5.29 (1H, d,  $J$  = 5.5 Hz, H-2OH), 6.98 (1H, s, H-17), 7.15 (1H, dd,  $J$  = 2.5 Hz,  $J$  = 9.0 Hz, H-21), 7.39 (1H, d,  $J$  = 2.0 Hz, H-8), 7.56-7.62 (3H, m, H-13, H-14, H-15), 7.97 (1H, d,  $J$  = 9.0 Hz, H-20), 8.07-8.11 (2H, m, H-12, H-16) ppm.  **$^{13}\text{C-NMR}$**  (100 MHz,  $(\text{CD}_3)_2\text{SO}$ ):  $\delta$  = 61.3 (C-6), 68.0 (C-4), 70.2 (C-2), 73.5 (C-3), 75.9 (C-5), 101.3 (C-1), 103.8 (C-8), 107.0 (C-17), 115.8 (C-21), 118.4 (C-19), 126.8 (C-12, C-16, C-20), 129.2 (C-13, C-15), 131.5 (C-11), 132.0 (C-14), 157.7 (C-9), 157.8 (C-7), 161.9 (C-10), 176.2 (C-18) ppm

**FTMS (ESI)  $m/z$** : 417.1186  $[\text{M} + \text{OH}]^+$ , found 417.1176  $[\text{M} + \text{OH}]^+$ . **Melting point**: 264-268 °C. **FT-IR (ATR)**: 2923 (O-H), 1035 (C-O)  $\text{cm}^{-1}$ .

### 6.4.2.3 Synthesis of chrysin- $\beta$ -D-glucopyranoside (**94**)

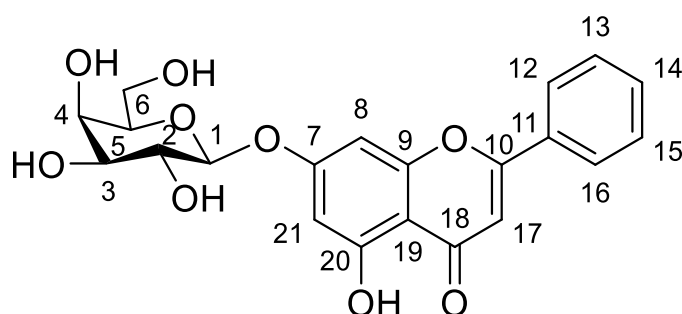


## 94

Following the general method outlined in Section 6.4.2: The acetylated product **114** was dissolved in anh. methanol (30 mL) and  $\text{K}_2\text{CO}_3$  (90 mg) was added. This reaction was left to stir for 20 h at room temperature. The reaction was neutralised to pH 7 using 1.0 M HCl. The filtrate was filtered and the solid was collected to produce **94** (51%, yellow solid, Purity: 99%).

$^1\text{H-NMR}$  (400 MHz,  $(\text{CD}_3)_2\text{SO}$ ):  $\delta$  = 3.39-3.47 (1H, m, H-3), 3.49-3.57 (2H, m, H-6), 3.57-3.64 (1H, m, H-2), 3.67-3.73 (2H, m, H-4, H-5), 4.57 (1H, d,  $J$  = 4.0 Hz, H-4OH), 4.71 (1H, t,  $J$  = 5.5 Hz, H-6OH), 4.93 (1H, d,  $J$  = 6.0 Hz, H-3OH), 5.03 (1H, d,  $J$  = 7.5 Hz, H-1), 5.27 (1H, d,  $J$  = 5.0 Hz, H-2OH), 6.48 (1H, as, H-21), 6.87 (1H, as, H-8), 7.05 (1H, s, H-17), 7.54-7.65 (3H, m, H-13, H-14, H-15), 8.05-8.12 (2H, m, H-12, H-16) ppm.  $^{13}\text{C-NMR}$  (100 MHz,  $(\text{CD}_3)_2\text{SO}$ ):  $\delta$  = 60.3 (C-6), 68.1 (C-4), 69.7 (C-2), 73.2 (C-3), 75.7 (C-5), 94.1 (C-8), 100.2 (C-21), 100.4 (C-1), 105.4 (C-17), 105.9 (C-19), 126.6 (C-12, C-16), 129.2 (C-13, C-15), 130.3 (C-11), 132.2 (C-14), 156.5 (C-9), 163.7 (C-7, C-10), 182.1 (C-18) ppm. **FTMS (ESI)  $m/z$**  : 417.3820  $[\text{M} + \text{H}]^+$ , found 417.1175  $[\text{M} + \text{H}]^+$ . 439.3718  $[\text{M} + \text{Na}]^+$ , found 439.0996  $[\text{M} + \text{H}]^+$ . **Melting point**: 208-210°C. **FT-IR (ATR)**: 3312 (O-H), 1343 (O-H, phenolic), 1032 (C-O)  $\text{cm}^{-1}$ .

#### 6.4.2.4 Synthesis of chrysin- $\beta$ -D-glucopyranoside (**95**)



### **95**

Following the general method outlined in Section 6.4.2: The acetylated product **115** was dissolved in anh. methanol (30 mL) and  $K_2CO_3$  (90 mg) was added. This reaction was left to stir for 20 h at room temperature. The reaction was neutralised to pH 7 using 1.0 M HCl. The filtrate was filtered and the solid was collected to produce **95** (53%, yellow solid, Purity: 99%).

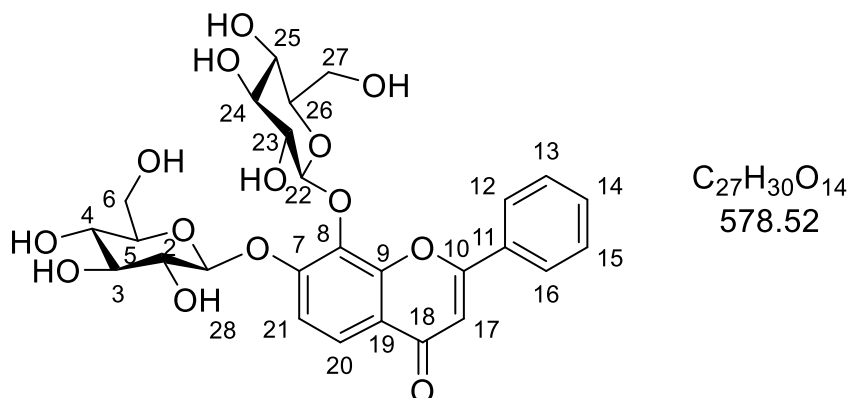
**$^1H$ -NMR** (400 MHz,  $(CD_3)_2SO$ ):  $\delta$  = 3.41-3.46 (1H, m, H-3), 3.48-3.57 (2H, m, H-6), 3.58-3.64 (1H, m, H-2), 3.67-3.74 (2H, m, H-4, H-5), 4.50 (1H, d,  $J$  = 4.5 Hz, H-4OH), 4.72 (1H, t,  $J$  = 5.0 Hz, H-6OH), 4.94 (1H, d,  $J$  = 6.0 Hz, H-3OH), 5.04 (1H, d,  $J$  = 8.0 Hz, H-1), 5.27 (1H, d,  $J$  = 5.0 Hz, H-2OH), 6.47 (1H, d,  $J$  = 2.0 Hz, H-21), 6.87 (1H, d,  $J$  = 2.0 Hz, H-8), 7.07 (1H, s, H-17), 7.54-7.66 (3H, m, H-13, H-14, H-15), 8.10 (2H, d,  $J$  = 8.5 Hz, H-12, H-16) ppm.

**$^{13}C$ -NMR** (100 MHz,  $(CD_3)_2SO$ ):  $\delta$  = 61.3 (C-6), 68.9 (C-4), 69.7 (C-2), 73.1 (C-3), 77.7 (C-5), 92.6 (C-8), 101.0 (C-21), 101.5 (C-1), 105.8 (C-17), 107.5 (C-19), 127.2 (C-12, C-16), 130.6 (C-13, C-15), 135.7 (C-11), 137.2 (C-14), 156.5 (C-9), 161.6 (C-7, C-10), 182.1 (C-18) ppm.

**FTMS (ESI)  $m/z$**  : 417.3820  $[M + H]^+$ , found 417.1175  $[M + H]^+$ . 439.3718  $[M + Na]^+$ , found 439.0996  $[M + H]^+$ . **Melting point**: 208-210°C. **FT-IR (ATR)**: 3312 (O-H), 1343

(O-H, phenolic), 1032 (C-O)  $cm^{-1}$ .

#### 6.4.2.6 Synthesis of 7,8-dihydroxyflavone- $\beta$ -D-glucopyranoside (**96**)



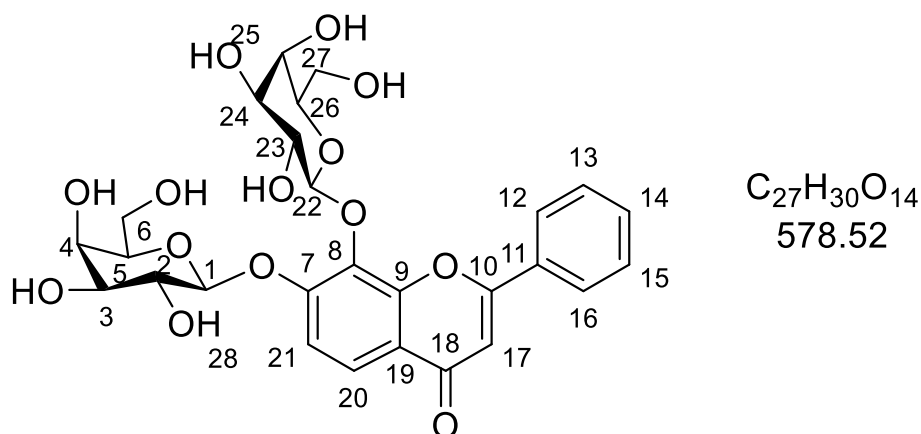
### 96

Following the general method outlined in Section 6.4.2: The acetylated product **116** was dissolved in anh. methanol (30 mL) and  $K_2CO_3$  (90 mg) was added. This reaction was left to stir for 20 h at room temperature. The reaction was neutralised to pH 7 using 1.0 M HCl. The filtrate was filtered and the solid was collected to produce **96** (64%, white solid, Purity: 97%).

$^1H$ -NMR (400 MHz,  $(CD_3)_2SO$ ):  $\delta$  = 3.13-3.24 (3H, m, H-24, H-25, H-26), 3.25-3.33 (2H, m, H-5, H-23), 3.39-3.49 (4H, m, H-2, H-3, H-4, Ha-27), 3.46-3.54 (1H, m, Ha-6), 3.61 (1H, dd,  $J$  = 5.0 Hz,  $J$  = 11.0 Hz, Hb-27), 3.73 (1H, dd,  $J$  = 5.0 Hz,  $J$  = 11.0 Hz, Hb-6), 4.32 (1H, t,  $J$  = 6.0 Hz, H-27OH), 4.63 (1H, t,  $J$  = 5.5 Hz, H-6OH), 4.97-5.01 (2H, m, H-22, H-24OH), 5.04 (1H, d,  $J$  = 7.5 Hz, H-1), 5.07-5.13 (1H, m, H-3OH, H-25OH), 5.16 (2H, d,  $J$  = 5.5 Hz, H-4OH, H-23OH), 5.43 (1H, d,  $J$  = 4.0 Hz, H-2OH), 6.98 (1H, s, H-17), 7.39 (1H, d,  $J$  = 9.5 Hz, H-21), 7.77 (1H, d,  $J$  = 9.0 Hz, H-20), 7.54-7.63 (3H, m, H-13, H-14, H-15), 8.22 (2H, d,  $J$  = 8.0 Hz, H-12, H-16) ppm.  $^{13}C$ -NMR (100 MHz,  $(CD_3)_2SO$ ):  $\delta$  = 61.1 (C-6), 61.4 (C-27), 69.6 (C-4), 69.9 (C-25), 73.4 (C-2), 74.4 (C-23), 75.9 (C-3), 76.2 (C-24), 77.2 (C-5), 77.3 (C-26), 101.2 (C-1), 104.3 (C-22), 107.0 (C-17), 114.1 (C-21), 119.8 (C-19), 120.5 (C-20), 126.9 (C-12, C-16), 129.1 (C-13, C-15), 131.6 (C-14), 131.8 (C-11), 134.5 (C-8), 150.4 (C-9), 154.7 (C-

-7), 163.3 (C-10), 177.7 (C-18) ppm. **FTMS (ESI)  $m/z$**  : 579.5230  $[M + H]^+$ , found 579.1701  $[M + H]^+$ . 601.5128  $[M + Na]^+$ , found 601.1520  $[M + Na]^+$ . **Melting point**: 245-246 °C.  
**FT-IR (ATR)**: 3329 (O-H), 1341 (O-H, phenolic), 1032 (C-O)  $cm^{-1}$ .

#### 6.4.2.8 Synthesis of 7,8-dihydroxyflavone- $\beta$ -D-galactopyranoside (**97**)



### 97

Following the general method outlined in Section 6.4.2: The acetylated product **117** was dissolved in anh. methanol (30 mL) and  $K_2CO_3$  (90 mg) was added. This reaction was left to stir for 20 h at room temperature. The reaction was neutralised to pH 7 using 1.0 M HCl. The filtrate was filtered and the solid was collected to produce **97** (62%, white solid Purity: 97%).

**$^1H$ -NMR** (400 MHz,  $(CD_3)_2SO$ ):  $\delta$  = 3.26-3.32 (1H, m, Ha-6), 3.37-3.40 (1H, m, H-26), 3.42-3.49 (2H, m, H-3, H-4, H-24), 3.51-3.61 (3H, m, Hb-6, H-27), 3.64-3.69 (1H, m, H-5), 3.69-3.75 (3H, m, H-2, H-4, H-25), 3.77-3.85 (1H, m, H-23), 4.44 (1H, t,  $J$  = 6.0 Hz, H-27OH), 4.67 (1H, d,  $J$  = 4.5 Hz, H-25OH), 4.70 (1H, d,  $J$  = 5.0 Hz, H-4OH), 4.76 (1H, t,  $J$  = 5.5 Hz, H-6OH), 4.91 (1H, d,  $J$  = 8.5 Hz, H-22), 4.92-4.99 (4H, m, H-1, H-3OH, H-23OH, H-24OH), 5.29 (1H, d,  $J$  = 4.0 Hz, H-2OH), 6.97 (1H, s, H-17), 7.38 (1H, d,  $J$  = 9.5 Hz, H-21), 7.54-7.62 (3H, m, H-13, H-14, H-15), 7.78 (1H, d,  $J$  = 9.5 Hz, H-20), 8.23 (2H, d,  $J$  = 8.0 Hz, H-12, H-1

6) ppm. **<sup>13</sup>C-NMR** (100 MHz, (CD<sub>3</sub>)<sub>2</sub>SO):  $\delta$  = 59.9 (C-6), 60.3 (C-27), 67.8 (C-4), 68.0 (C-25), 70.9 (C-2), 72.2 (C-23), 72.8 (C-3, C-24), 75.5 (C-5), 75.9 (C-26), 102.3 (C-1), 105.0 (C-22), 106.2 (C-17), 114.2 (C-21), 119.1 (C-19), 120.7 (C-20), 127.1 (C-12, C-16), 127.6 (C-11), 129.1 (C-13, C-15), 131.8 (C-14), 134.2 (C-8), 150.3 (C-9), 154.3 (C-7), 162.5 (C-10), 176.8 (C-18) ppm. **FTMS (ESI)**  $m/z$  : 579.5230 [M + H]<sup>+</sup>, found 579.7021 [M + H]<sup>+</sup>. 601.5128 [M + Na]<sup>+</sup>, found 601.1522 [M + Na]<sup>+</sup>. **Melting point:** 231-232 °C.

**FT-IR (ATR):** 3329 (O-H), 1340 (O-H, phenolic), 1032 (C-O) cm<sup>-1</sup>.

## **Chapter 7 – References**

1. Gallo, G. G., Lancini, G. & Parenti, F. *Antibiotics: A Multidisciplinary Approach*. (Springer US, 2013). doi:10.1007/s13398-014-0173-7.2
2. Drlica, K. & Perlin, D. S. *Antibiotic Resistance Understanding and Responding to an Emerging Crisis*. (2011).
3. Ravina, E. *Evolution of drug discovery: From traditional medicines to modern drugs*. (2011).
4. Gottfried, R. S. *Black Death*. (1983).
5. Lewis, K. Platforms for antibiotic discovery. *Nat. Publ. Gr.* **12**, (2013).
6. Kingston, W. Irish contributions to the origins of antibiotics. *Ir. J. Med. Sci.* **177**, 87–92 (2008).
7. Schillaci, D. & Cascioferro, S. Microbial & Biochemical Technology The Future of Antibiotic: From the Magic Bullet to the Smart Bullet. *J Microb Biochem Technol* **6**, (2014).
8. Fleming, A. On the antibacterial action of cultures of a penicillium, with special reference to their use in the isolation of B. influenzae. 1929. *Bull. World Health Organ.* (2001). doi:10.1038/146837a0
9. Coates, A. R., Halls, G. & Hu, Y. Novel classes of antibiotics or more of the same? *British Journal of Pharmacology* (2011). doi:10.1111/j.1476-5381.2011.01250.x
10. Yocum, R. R., Rasmussen, J. R. & Strominger, J. L. The mechanism of action of penicillin. Penicillin acylates the active site of Bacillus stearothermophilus D-alanine carboxypeptidase. *J. Biol. Chem.* (1980).
11. Konaklieva, M. Molecular Targets of  $\beta$ -Lactam-Based Antimicrobials: Beyond the Usual Suspects. *Antibiotics* (2014). doi:10.3390/antibiotics3020128
12. Henry, R. J. The Mode of Action of Sulfonamides. *Bacteriol Rev.* **7**, 175–262 (1943).
13. Davis, B. D. Mechanism of Bactericidal Action of Aminoglycosides. *Microbiol. Rev.*

- Sept* 341–350 (1987).
14. Burns, J. L. Mechanisms of bacterial resistance. *Pediatric Clinics of North America* **42**, 497–507 (1995).
  15. Chopra, I. & Roberts, M. Epidemiology of Bacterial Resistance Applications, Molecular Biology, and Tetracycline Antibiotics: Mode of Action, Applications, Molecular Biology, and Epidemiology of Bacterial Resistance. *Mol. Biol. Rev* **65**, 232–232 (2001).
  16. Bo, G. Giuseppe Brotzu and the Discovery of Cephalosporins. *Clin. Microbiol. Infect.* **6**, 6–8 (2000).
  17. Ghuysen, J. *et al.* Use of model enzymes in the determination of the mode of action of penicillins and 3-cephalosporins. *Annu. Rev. Biochem.* **48**, 48–73 (1979).
  18. Tenson, T., Lovmar, M. & Ehrenberg, M. The mechanism of action of macrolides, lincosamides and streptogramin B reveals the nascent peptide exit path in the ribosome. *J. Mol. Biol.* (2003). doi:10.1016/S0022-2836(03)00662-4
  19. Wu, Y.-J. & Su, W.-G. Recent Developments on Ketolides and Macrolides. *Curr. Med. Chem.* **8**, 1727–1758 (2001).
  20. Corpe, W. A. A study of the wide spread distribution of *Chromobacterium* species in soil by a simple technique. *J. Bacteriol.* **62**, 515–517 (1951).
  21. Reynolds, P. E. Structure, Biochemistry and Mechanism of Action of Glycopeptide Antibiotics. *Rev. J. Clin. Microbiol. Infect. Dis* **8**, 943–950 (1989).
  22. Shinabarger, D. L. *et al.* Mechanism of action of oxazolidinones: Effects of linezolid and eperezolid on translation reactions. *Antimicrob. Agents Chemother.* (1997).
  23. Aldred, K. J., Kerns, R. J. & Osheroff, N. Mechanism of quinolone action and resistance. *Biochemistry* (2014). doi:10.1021/bi5000564
  24. Vannuffel, P. & Cocito, C. Mechanism of Action of Streptogramins and Macrolides.

- Drugs* (1996). doi:10.2165/00003495-199600511-00006
25. Hoeksema, H. *et al.* Chemical Studies on Lincomycin. I. The Structure of Lincomycin. *J. Am. Chem. Soc.* **86**, 4223–4224 (1964).
  26. Krisztina, C., Papp-Wallace, M., Endimiani, A., Taracila, M. A. & Bonomo, R. A. Carbapenems: Past, Present, and Future. *Antimicrob. Agents Chemother.* **55**, 4943–4960 (2011).
  27. Norrby, S. R. Carbapenems. *Med. Clin. North Am.* **79**, 745–759 (1995).
  28. Nicolau, D. P. Carbapenems: a potent class of antibiotics. *Expert Opin. Pharmacother* **9**, 23–37 (2008).
  29. Straus, S. K. & Hancock, R. E. W. Mode of action of the new antibiotic for gram-positive pathogens daptomycin: Comparison with cationic antimicrobial peptides and lipopeptides. *Biochimica et Biophysica Acta - Biomembranes* (2006).  
doi:10.1016/j.bbamem.2006.02.009
  30. Avrahami, D. & Shai, Y. A New Group of Antifungal and Antibacterial Lipopeptides Derived from Non-membrane Active Peptides Conjugated to Palmitic Acid. *J. Biol. Chem.* (2004). doi:10.1074/jbc.M312260200
  31. Champney, W. S. & Tober, C. L. Structure-activity relationships for six ketolide antibiotics. *Curr. Microbiol.* (2001). doi:10.1007/s002840010205
  32. Champney, W. S. & Tober, C. L. Inhibition of Translation and 50S Ribosomal Subunit Formation in *Staphylococcus aureus* Cells by 11 Different Ketolide Antibiotics.
  33. Golan, D. E., Armstrong, E. J. & Armstrong, A. W. *Principles of Pharmacology*. (2006).
  34. Pankey, G. A. & Sabath, L. D. Clinical Relevance of Bacteriostatic versus Bactericidal Mechanisms of Action in the Treatment of Gram-Positive Bacterial Infections. *Clin. Infect. Dis.* (2004). doi:10.1086/381972

35. Liwa, A. C. & Jaka, H. in *The Battle Against Microbial Pathogens: Basic Science, Technological Advances and Educational Programs* 876–885 (2015).
36. Sigma Aldrich. Glycobiology Analysis Manual.
37. Scheffers, D.-J. & Pinho, M. G. Bacterial Cell Wall Synthesis: New Insights from Localization Studies. *Microbiol. Mol. Biol. Rev.* **69**, 585–607 (2005).
38. Bugg, T. D. H. & Walsh, C. T. Intracellular Steps of Bacterial Cell Wall Peptidoglycan Biosynthesis : Enzymology, Antibiotics, and Antibiotic Resistance.
39. Liu, Y. & Breukink, E. The Membrane Steps of Bacterial Cell Wall Synthesis as Antibiotic Targets. doi:10.3390/antibiotics5030028
40. Tomasz, A. How the Beta-Lactam Antibiotics Kill and Lyse Bacteria. *Ann. Rev. Microbiol* **33**, 113–37 (1979).
41. Berger-Buchi, B. Mini-review resistance mechanisms of gram-positive bacteria. *Int. J. Med. Microbiol* **292**, (2002).
42. Weinstein, M. P., Klugman, K. P. & Jones, R. N. Rationale for Revised Penicillin Susceptibility Breakpoints versus *Streptococcus pneumoniae*: Coping with Antimicrobial Susceptibility in an Era of Resistance. *Clin. Infect. Dis.* **48**, 1596–1600 (2009).
43. Ji Zheng, C. *et al.* Fatty acid synthesis is a target for antibacterial activity of unsaturated fatty acids. (2005). doi:10.1016/j.febslet.2005.08.028
44. Campbell, J. W. & Cronan, J. E. Bacterial fatty acid biosynthesis: targets for antibacterial drug discovery. *Annu. Rev. Microbiol.* **55**, 305–32 (2001).
45. Magnuson, K., Jackowski, S., Rock, C. & Cronan, J. E. Regulation of fatty acid biosynthesis in *Escherichia coli*. *Microbiol. Rev.* **57**, 522–542 (1993).
46. Heath, R. J. *et al.* Mechanism of Triclosan Inhibition of Bacterial Fatty Acid Synthesis. *J. Biol. Chem.* **16**, 11110–11114 (1999).

47. Baldock, C., De Boer, G. J., Rafferty, J. B., Stuitje, A. R. & Rice, D. W. Mechanism of action of diazaborines. *Biochemical Pharmacology* (1998). doi:10.1016/S0006-2952(97)00684-9
48. Syed, H. C. & Ravaoarinoro, M. LiF reduces MICs of antibiotics against clinical isolates of gram-positive and gram-negative bacteria. *Int. J. Microbiol.* **2012**, (2012).
49. Andrews, J. M. & Andrews, J. M. Determination of minimum inhibitory concentrations. *J. Antimicrob. Chemother.* **48**, 5–16 (2001).
50. Menninger, J. R. & Otto, D. P. Erythromycin, carbomycin, and spiramycin inhibit protein synthesis by stimulating the dissociation of peptidyl-tRNA from ribosomes. *Antimicrob. Agents Chemother.* (1982). doi:10.1128/AAC.21.5.811
51. Chopra, I. & Roberts, M. Tetracycline Antibiotics: Mode of Action, Applications, Molecular Biology, and Epidemiology of Bacterial Resistance. **65**, 232–260 (2001).
52. Engelberg-Kulka, H., Sat, B., Reches, M., Amitai, S. & Hazan, R. Bacterial programmed cell death systems as targets for antibiotics. *Trends in Microbiology* (2004). doi:10.1016/j.tim.2003.12.008
53. Bussiere, D. E. & Bastia, D. Termination of DNA replication of bacterial and plasmid chromosomes.
54. Watt, P. M. & Hickson, I. D. Structure and function of type 11 DNA topoisomerases. *Biochem. J* **303**, 681–695 (1994).
55. Power, E. Impact of antibiotic restrictions: The pharmaceutical perspective. *Clinical Microbiology and Infection* (2006). doi:10.1111/j.1469-0691.2006.01528.x
56. Spellberg, B. *et al.* The Epidemic of Antibiotic-Resistant Infections: A Call to Action for the Medical Community from the Infectious Diseases Society of America. *Clin. Infect. Dis.* (2008). doi:10.1086/524891
57. FDA. FDA approved Drugs.

58. Founou, R. C., Founou, L. L. & Essack, S. Y. Clinical and economic impact of antibiotic resistance in developing countries : A systematic review and meta-analysis. 1–18 (2017). doi:10.1371/journal.pone.0189621
59. Bhattacharya, A., Nsonwu, O., Johnson, A. & Hope, R. Thirty-day all-cause fatality subsequent to MRSA, MSSA and E. coli bacteraemia and C. difficile infection: 2016 to 2017. 29 (2017). doi:10.13140/RG.2.2.10020.58244
60. WHO regional office for Europe: Data and statistics.
61. Ventola, C. L. The antibiotic resistance crisis: part 1: causes and threats. *P T A peer-reviewed J. Formul. Manag.* **40**, 277–83 (2015).
62. Smith, J. T., Hamilton-Miller, J. M. T. & Knox, R. Bacterial resistance to penicillins and cephalosporins. *Journal of Pharmacy and Pharmacology* (1969). doi:10.1111/j.2042-7158.1969.tb08267.x
63. Kohanski, M. A., Dwyer, D. J. & Collins, J. J. How antibiotics kill bacteria: from targets to networks. *Nat. Publ. Gr.* **8**, (2010).
64. Marianne, F., Kumar, K. & Boutin, A. Antibiotic resistance. *J. Infect. Public Health* **10**, 369–378 (2017).
65. Lambert, P. A. Cellular impermeability and uptake of biocides and antibiotics in Gram-positive bacteria and mycobacteria. *J. Appl. Microbiol.* (2002). doi:10.1046/j.1365-2672.92.5s1.7.x
66. Denyer, S. P. Mechanisms of action of antibacterial biocides. *Int. Biodeterior. Biodegrad.* (1995). doi:10.1016/0964-8305(96)00015-7
67. Russell, A. D. Introduction of biocides into clinical practice and the impact on antibiotic-resistant bacteria. *J. Appl. Microbiol.* (2002). doi:10.1046/j.1365-2672.92.5s1.12.x
68. Aldrich, S. Tryptic Soy Broth. (2018).

69. Aldrich, S. Microbiology Theory: Media Preparation. (2018).
70. Lapage, S. P., Efstratiou, A. & Hill, L. R. The ortho-nitrophenol (ONPG) test and acid from lactose in Gram-negative genera. *J. clin. Path* **26**, 821–825 (1973).
71. Yu, Y., Mizanur, R. M. & Pohl, N. L. Glycosidase activity profiling for bacterial identification by a chemical proteomics approach. *Biocatal. Biotransformation* **26**, 25–31 (2008).
72. Hitchins, A. D. & Duvall, R. E. Feasibility of a defined microflora challenge method for evaluating the efficacy of foodborne *Listeria monocytogenes* selective enrichments. *J. Food Prot.* **63**, 1064–1070 (2000).
73. Perry, J. D. *et al.* Recovery of antimicrobial-resistant *Pseudomonas aeruginosa* from sputa of cystic fibrosis patients by culture on selective media. *J. Antimicrob. Chemother.* **61**, 1057–1061 (2008).
74. Vandeplassche, E., Coenye, T. & Crabbé, A. Developing selective media for quantification of multispecies biofilms following antibiotic treatment. *PLoS One* **12**, 1–15 (2017).
75. Lin, J. *et al.* 3-(1,2,3-Triazol-1-yl)-3-deoxythymidine analogs as substrates for human and *Ureaplasma parvum* thymidine kinase for structure-activity investigations. *Bioorganic Med. Chem.* **18**, 3261–3269 (2010).
76. Neamatallah, a. a. N., Dewar, S. J. & Austin, B. An improved selective isolation medium for the recovery of *Listeria monocytogenes* from smoked fish. *Lett. Appl. Microbiol.* **36**, 230–233 (2003).
77. al-Zoreky, N. & Sandine, W. E. Highly selective medium for isolation of *Listeria monocytogenes* from food. *Appl. Envir. Microbiol.* **56**, 3154–3157 (1990).
78. Kim, H.-J. & Oh, S.-W. Performance comparison of 5 selective media used to detect *Staphylococcus aureus* in foods. *Food Sci. Biotechnol.* **19**, 1097–1101 (2010).

79. Baird, R. M. & Lee, W. H. Media used in the detection and enumeration of *Staphylococcus aureus*. *Int. J. Food Microbiol.* **26**, 15–24 (1995).
80. Waite, R. D., Wareham, D. W., Gardiner, S. & Whiley, R. A. A simple, semiselective medium for anaerobic isolation of anginosus group streptococci from patients with chronic lung disease. *J. Clin. Microbiol.* **50**, 1430–1432 (2012).
81. Amoureux, L. *et al.* Detection of *Achromobacter xylosoxidans* in hospital, domestic, and outdoor environmental samples and comparison with human clinical isolates. *Appl. Environ. Microbiol.* **79**, 7142–7149 (2013).
82. Yabuuchi, E. & Ohyama, A. *Achromobacter xylosoxidans* n. sp. from Human Ear Discharge. *Japan J. Microbiol* **15**, 477–481 (1971).
83. Kobayashi, T., Uchibori, S., Tsuzukibashi, O., Goto, H. & Aida, M. A selective medium for *Rothia mucilaginosa* and its distribution in oral cavities. *J. Microbiol. Methods* **91**, 364–365 (2012).
84. Fang, H. & Hedin, G. Use of Cefoxitin-Based Selective Broth for Improved Detection of Methicillin-Resistant *Staphylococcus aureus* Use of Cefoxitin-Based Selective Broth for Improved Detection of Methicillin-Resistant *Staphylococcus aureus*. **44**, 2–5 (2006).
85. Ehrmann, E., Jolivet-Gougeon, A., Bonnaure-Mallet, M. & Fosse, T. Antibiotic content of selective culture media for isolation of *Capnocytophaga* species from oral polymicrobial samples. *Lett. Appl. Microbiol.* **57**, 303–309 (2013).
86. Stevenson, T. H., Lucia, L. M. & Acuff, G. R. Development of a selective medium for isolation of *Helicobacter pylori* from cattle and beef samples. *Appl. Environ. Microbiol.* **66**, 723–727 (2000).
87. Gould, W. D., Hagedorn, C., Bardinelli, T. R. & Zablutowicz, R. M. New Selective Media for Enumeration and Recovery of Fluorescent *Pseudomonads* from Various

- Habitats New Selective Media for Enumeration and Recovery of Fluorescent Pseudomonads from Various Habitats. **49**, 28–32 (1985).
88. Hayakawa, M., Yoshida, Y. & Iimura, Y. Selective isolation of bioactive soil actinomycetes belonging to the *Streptomyces violaceusniger* phenotypic cluster. *J. Appl. Microbiol.* **96**, 973–981 (2004).
89. Hirasawa, M. & Takada, K. Susceptibility of *Streptococcus mutans* and *Streptococcus sobrinus* to cell wall inhibitors and development of a novel selective medium for *S. sobrinus*. *Caries Res.* **36**, 155–160 (2002).
90. Aparoy, P., Reddy, K. K. & Reddanna, P. Structure and Ligand Based Drug Design Strategies in the Development of Novel 5- LOX Inhibitors. *Curr. Med. Chem.* **19**, 3763–3778 (2012).
91. Butler, M. S., Newman, D. . J., Petersen, F. & Amstutz, R. *Natural Compounds as Drugs*. (2008).
92. Hartenfeller, M. & Schneider, G. in *Chemoinformatics and Computational Chemical Biology* (ed. Bajorath, J.) 299–323 (Humana Press, 2011). doi:10.1007/978-1-60761-839-3\_12
93. Abu-jaish, A., Jumaa, S. & Karaman, R. *Prodrug design- A new era*. (2014).
94. Huttunen, K. M., Raunio, H. & Rautio, J. Prodrugs—from Serendipity to Rational Design. doi:10.1124/pr.110.003459
95. Zawilska, J. B., Wojcieszak, J. & Olejniczak, A. B. Prodrugs: A challenge for the drug development. *Pharmacological Reports* (2013). doi:10.1016/S1734-1140(13)70959-9
96. Berry, G. T. *Classic Galactosemia and Clinical Variant Galactosemia*. *GeneReviews* (2000).
97. Reitter, J. N., Means, R. E. & Desrosiers, R. C. A role for carbohydrates in immune evasion in AIDS. *Nat. Med.* **4**, 679–684 (1998).

98. Pais-Chanfrou, J. M. & Trujillo-Toledo, L. E. Optimization of culture medium for large-scale production of heterologous proteins in *Pichia pastoris* to be used in nanoscience and other biotechnological fields. *Biol. Med.* **8**, (2016).
99. Zhang, Y. & Wang, F. Carbohydrate drugs: current status and development prospect. *Drug discoveries & therapeutics* (2015). doi:10.5582/ddt.2015.01028
100. Saleem, M. *et al.* Antimicrobial natural products: an update on future antibiotic drug candidates. *Nat. Prod. Rep.* (2010). doi:10.1039/B916096E
101. Zhu, X. & Schmidt, R. R. New principles for glycoside-bond formation. *Angew. Chemie - Int. Ed.* **48**, 1900–1934 (2009).
102. JM, B., JL, T. & L, S. in *Biochemistry* (W H Freeman, 2002).
103. P, S., N, T. & M., A. in *Essentials of Glycobiology* (Cold Spring Harbor Laboratory Press, 2017). doi:10.1101/glycobiology.3e.009
104. Cummings, R. D. in *Encyclopedia of Genetics, Genomics, Proteomics and Bioinformatics* (American Cancer Society, 2005). doi:10.1002/047001153X.g305106
105. Taylor, M. E. & Drickamer, K. Structure-function analysis of C-type animal lectins. *Methods Enzymol.* **363**, 3–16 (2003).
106. Sharon, N. & Lis, H. History of lectins: From hemagglutinins to biological recognition molecules. *Glycobiology* **14**, 53–62 (2004).
107. Kundig, W., Ghosh, S. & Roseman, S. Phosphate bound to Histidine in a protein as an intermediate in a novel phospho-transferase system. *Proc Natl Acad Sci USA* **52**, 1067–1074 (1964).
108. Kotrba, P., Inui, M. & Yukawa, H. Bacterial Phosphotransferase System (PTS) in Carbohydrate Uptake and Control of Carbon Metabolism. *Biosci. bioengineering* **92**, 502–517 (2001).
109. Saier, M. H. MicroReview Families of transmembrane sugar transport proteins. **35**,

- (2000).
110. Reizer, J. & Jr, M. H. S. Modular multidomain phosphoryl transfer proteins of bacteria. *Curr. Opin. Struct. Biol.* **7**, 407–415 (1997).
  111. Reizer, J. & Jr, M. H. S. A voyage along the bases : novel phosphotransferase genes revealed by in silico analyses of the Escherichia coli genome. *Res. Microbiol.* **147**, 458–471 (1996).
  112. Müller, M. *Molecular Medical Parasitology Chapter 7 – Energy metabolism: Part I: Anaerobic protozoa.* (Academic press, 2003).
  113. Entner, N. & Doudoroff, M. Glucose and gluconic acid oxidation of Pseudomonas saccharophila. *J. Biol. Chem.* **196**, 853–862 (1952).
  114. Hu, H. Further Observations on Carbohydrate Metabolism and its Regulation in Azotobacter beijerinckii. 89–96 (2017).
  115. Milner, S. J. *et al.* Probing bacterial uptake of glycosylated ciprofloxacin conjugates. *ChemBioChem* **15**, 466–471 (2014).
  116. Hutchins, M. Thesis - The Synthesis and Microbiological Analysis of Nadifloxacin Glycosides. (2016).
  117. Assadian, O. *et al.* Minimum inhibitory (MIC) and minimum microbicidal concentration (MMC) of polihexanide and triclosan against antibiotic sensitiv1. Assadian, O. *et al.* Minimum inhibitory (MIC) and minimum microbicidal concentration (MMC) of polihexanide and triclosan again. *GMS Krankenhhyg. Interdiszip.* **6**, Doc06 (2011).
  118. Regos, J., Zak, O., Solf, R., Vischer, W. A. & Weirich, E. G. Antimicrobial spectrum of triclosan, a broad-spectrum antimicrobial agent for topical application. II. Comparison with some other antimicrobial agents. *Dermatologica* **158**, 72–79 (1979).
  119. Jones, R. D. *et al.* Triclosan: a review of effectiveness and safety in health care

- settings. *Am. J. Infect. Control* **28**, 184–96 (2000).
120. DeSalva, S. J., Kong, B. M. & Lin, Y. J. Triclosan: a safety profile. *Am. J. Dent.* **2**, 185—196 (1989).
121. Dann, A. B. & Hontela, A. Triclosan: Environmental exposure, toxicity and mechanisms of action. *J. Appl. Toxicol.* **31**, 285–311 (2011).
122. Paul, K. B., Hedge, J. M., Devito, M. J. & Crofton, K. M. Short-term exposure to triclosan decreases thyroxine in vivo via upregulation of hepatic catabolism in young long-evans rats. *Toxicol. Sci.* **113**, 367–379 (2009).
123. Russell, A. D. Whither triclosan? *J. Antimicrob. Chemother.* **53**, 693–695 (2004).
124. McMurry, L. Overexpression of *marA*, *soxS*, or *acrAB* produces resistance to triclosan in laboratory and clinical strains of *Escherichia coli*. *FEMS Microbiol. Lett.* **166**, 305–309 (1998).
125. McMurry, L. M., Oethinger, M. & Levy, S. B. Triclosan targets lipid synthesis. *Nature* **394**, 531–532 (1998).
126. Heath, R. J. *et al.* Broad Spectrum Antimicrobial Biocides Target the FabI Component of Fatty Acid Synthesis. *Biol. Chem.* **273**, 30316–30320 (1998).
127. Hoang, T. T. & Schweizer, H. P. Characterization of *Pseudomonas aeruginosa* enoyl-acyl carrier protein reductase (FabI): A target for the antimicrobial triclosan and its role in acylated homoserine lactone synthesis. *J. Bacteriol.* **181**, 5489–5497 (1999).
128. Chuanchuen, R. *et al.* Cross-Resistance between Triclosan and Antibiotics in. *Society* **45**, 428–432 (2001).
129. Heath, R. J., Li, J., Roland, G. E. & Rock, C. O. Inhibition of the *Staphylococcus aureus* NADPH-dependent enoyl-acyl carrier protein reductase by triclosan and hexachlorophene. *J. Biol. Chem.* **275**, 4654–4659 (2000).
130. Slayden, R. A. & Barry, C. E. The genetics and biochemistry of isoniazid resistance in

- Mycobacterium tuberculosis. *Microbes Infect.* **2**, 659–669 (2000).
131. Mdluli, K. *et al.* Biochemical and genetic data suggest that InhA is not the primary target for activated isoniazid in Mycobacterium tuberculosis. *J. Infect. Dis.* **174**, 1085–90 (1996).
  132. Place, C., Food, P. & Same, P. United States Patent Office .. 29–30 (1919).
  133. Frederick, J. J., Corner, T. R. & Gerhardt, P. Antimicrobial actions of hexachlorophene: inhibition of respiration in Bacillus megaterium. *Antimicrob. Agents Chemother.* **6**, 712–721 (1974).
  134. Corner, T. R., Joswick, H. L., Silvernale, J. N. & Gerhardt, P. Antimicrobial actions of hexachlorophene: lysis and fixation of bacterial protoplasts. *J. Bacteriol.* **108**, 501–507 (1971).
  135. Silvernale, J. N., Joswick, H. L., Corner, T. R. & Gerhardt, P. Antimicrobial actions of hexachlorophene: cytological manifestations. *J. Bacteriol.* **108**, 482–491 (1971).
  136. Nakaue, H. S., Dost, F. N. & Buhler, D. R. Studies on the Toxicity of Hexachlorophene in the Rat. 239–249 (1973).
  137. Choonara, I. & Rieder, M. J. Drug toxicity and adverse drug reactions in children - A brief historical review. *Paediatr. Perinat. Drug Ther.* **5**, 12–18 (2002).
  138. Hexachlorophene tied to infant deaths. *Chem. Eng. News* **53**, 8 (1975).
  139. Ruth, B. & Walter, C. W. The Surgical Scrub - Practical Consideration. *Arch. Surg* **107**, (1973).
  140. Dewar, N. E. & Gravens, D. L. Effectiveness of septisol antiseptic foam as a surgical scrub agent. *Appl. Microbiol.* **26**, 544–549 (1973).
  141. Pauluws, W. *Microcides for the protection of materials: A handbook.* (Springer Science & Business Media, 2012).
  142. Laura-Beth Brierley. *Thesis.* (2014). doi:10.1002/ejoc.201200111

143. Laura-Beth Brierley. *Thesis - Development of Targeted Antibacterial strategies and Relevance to the Food and Pharm industries*. (2014). doi:10.1002/ejoc.201200111
144. Jacobsson, M., Malmberg, J. & Ellervik, U. Aromatic O-glycosylation. *Carbohydr. Res.* **341**, 1266–1281 (2006).
145. Gervay-Hague, J. Taming the Reactivity of Glycosyl Iodides to Achieve Stereoselective Glycosidation. *Acc. Chem. Res.* **49**, 35–47 (2016).
146. Böttcher, S., Hederos, M., Champion, E., Dékány, G. & Thiem, J. Novel efficient routes to indoxyl glycosides for monitoring glycosidase activities. *Org. Lett.* **15**, 3766–3769 (2013).
147. Capon, B. Neighbouring Group Participation. *Chem. Soc. Rev.* **4**, 44–105 (1971).
148. Gurst, J. E. NMR and the structure of D-glucose. *J. Chem. Educ.* **68**, 1003 (1991).
149. Lemieux, R. U. Abstract of Papers. *133rd Natl. Meet. Am. Chem. Soc.* (1958).
150. Edward, J. T. Stability of glycosides to acid hydrolysis. *Chem. Ind. Eng.* 1102–1104 (1955).
151. Cramer, C. J. Anomeric and Reverse Anomeric Effects in the Gas Phase and Aqueous Solution. *J. Org. Chem.* **57**, 7034–7043 (1992).
152. Ha, S., Gao, J., Tidor, B., Brady, J. W. & Karplus, M. Solvent Effect on the Anomeric Equilibrium in D-Glucose: A Free Energy Simulation Analysis. *J. Am. Chem. Soc.* **113**, 1553–1557 (1991).
153. Reed, A. E., Curtiss, L. a & Weinhold, F. Intermolecular interactions from a natural bond orbital, donor-acceptor viewpoint. *Chem. Rev. (Washington, DC, United States)* **88**, 899–926 (1988).
154. Glendening, E. D., Landis, C. R. & Weinhold, F. Natural bond orbital methods. *Wiley Interdiscip. Rev. Comput. Mol. Sci.* **2**, 1–42 (2012).
155. Mo, Y. Computational evidence that hyperconjugative interactions are not responsible

- for the anomeric effect. *Nat. Chem.* **2**, 666–671 (2010).
156. Mo, Y., Song, L. & Lin, Y. Block-localized wavefunction (BLW) method at the density functional theory (DFT) level. *J. Phys. Chem. A* **111**, 8291–8301 (2007).
157. Tvaroska, I. & Bleha, T. Anomeric and exo-anomeric effects in carbohydrate chemistry. *Adv. Carbohydr. Chem. Biochem.* **47**, 45–123 (1989).
158. Wang, C., Ying, F., Wu, W. & Mo, Y. How solvent influences the anomeric effect: Roles of hyperconjugative versus steric interactions on the conformational preference. *J. Org. Chem.* **79**, 1571–1581 (2014).
159. Maier, R. M. Bacterial Growth. *Environ. Microbiol.* 37–54 (2009). doi:10.1016/B978-0-12-370519-8.00003-1
160. Monod, J. The growth of bacterial cultures. *Annu. Rev. Microbiol.* **3**, 371–394 (1949).
161. Kolter, R. The Stationary Phase of the Bacterial Life Cycle. *Annu. Rev. Microbiol.* **47**, 855–874 (1993).
162. Bottone, E. J. *Bacillus cereus*, a volatile human pathogen. *Clin. Microbiol. Rev.* **23**, 382–398 (2010).
163. Jensen, G. B., Hansen, B. M., Eilenberg, J. & Mahillon, J. The hidden lifestyles of *Bacillus cereus* and relatives. *Environ. Microbiol.* **5**, 631–640 (2003).
164. Castillo-Rojas, G. *et al.* Comparison of *Enterococcus faecium* and *Enterococcus faecalis* Strains Isolated from Water and Clinical Samples: Antimicrobial Susceptibility and Genetic Relationships. *PLoS One* **8**, 1–10 (2013).
165. Emori, T. G. & Gaynes, R. P. An overview of nosocomial infections, including the role of the microbiology laboratory. *Clin. Microbiol. Rev.* **6**, 428–442 (1993).
166. Herbst, A., Ulfelder, H. & Poskanzer, D. The New England Journal of Medicine  
Downloaded from nejm.org at SAN DIEGO (UCSD) on June 9, 2015. For personal use only. No other uses without permission. From the NEJM Archive. Copyright © 2010

- Massachusetts Medical Society. All rights reserved. *N. Engl. J. Med.* **284**, 878–881 (1971).
167. Archer, G. L. Staphylococcus aureus : A Well–Armed Pathogen. *Clin. Infect. Dis.* **26**, 1179–1181 (1998).
168. Dong, Y., Speer, C. P. & Glaser, K. Beyond sepsis: *Staphylococcus epidermidis* is an underestimated but significant contributor to neonatal morbidity. *Virulence* **5594**, 00–00 (2018).
169. Vuong, C. & Otto, M. Staphylococcus epidermidis infections. *Microbes Infect.* **4**, 481–489 (2002).
170. Edwards, M. S. & Baker, C. J. in *Principles and practice of infectious diseases* 2655–2667 (2010).
171. Phares, C. R. *et al.* Epidemiology of Invasive Group B Streptococcal Disease in the United States ,. **299**, 1999–2005 (2015).
172. Lindahl, G., Stålhammar-Carlemalm, M. & Areschoug, T. Surface Proteins of Streptococcus agalactiae and Related Proteins in Other Bacterial Pathogens. *Clin. Microbiol. Rev.* **18**, 102–127 (2005).
173. Ryan KJ, R. C. *Sherris Medical Microbiology: An Introduction to Infectious Diseases.* (2004).
174. Efstratiou, A. & Lamagni, T. in *Streptococcus pyogenes : Basic Biology to Clinical Manifestations* (eds. JJ, F., DL, S. & VA, F.) 1–27 (Oklahoma City (OK): University of Oklahoma Health Sciences Center, 2016).
175. Wong, S. S. & Yuen, K.-Y. Streptococcus pyogenes and re-emergence of scarlet fever as a public health problem. *Emerg. Microbes Infect.* **1**, e2 (2012).
176. Henriques-Normark, B. & Tuomanen, E. I. The pneumococcus: Epidemiology, microbiology, and pathogenesis. *Cold Spring Harb. Perspect. Med.* **3**, 1–15 (2013).

177. Weiser, J. N., Ferreira, D. M. & Paton, J. C. Streptococcus pneumoniae: transmission, colonization and invasion. *Nat. Rev. Microbiol.* **16**, 1–13 (2018).
178. Bochud, P. Y., Calandra, T. & Francioli, P. Bacteremia due to viridans streptococci in neutropenic patients: A review. *Am. J. Med.* **97**, 256–264 (1994).
179. Bao, P. *et al.* Time Trends and Characteristics of Childhood Cancer Among Children Age 0 – 14 in Shanghai. *Pediatr. Blood Cancer* **53**, 13–16 (2009).
180. Winn, W., Allen, S., Janda, W., Koneman, E. & Procop, G. Schreckenberger, P. Woods, G. *Koneman's Color Atlas and Textbook of Diagnostic Microbiology.* (2006).
181. Lipsky, B. A., Hook, E. W., Smith, A. A. & Plorde, J. J. Citrobacter infections in humans: experience at the Seattle Veterans Administration Medical Center and a review of the literature. *Rev. Infect. Dis.* **2**, 746–760 (1980).
182. Healy, B., Cooney, S., Brien, S. O., Iversen, C. & Whyte, P. No Title. **7**, (2010).
183. Iversen, C. & Forsythe, S. Risk profile of Enterobacter sakazakii, an emergent pathogen associated with infant milk formula. *Trends Food Sci. Technol.* **14**, 443–454 (2003).
184. Mezzatesta, M. L., Gona, F. & Stefani, S. Enterobacter cloacae complex: clinical impact and emerging antibiotic resistance. *Futur. Microbiol* **7**, 887–902 (2012).
185. Olsvik, Ø., Wasteson, Y., Lund, A. & Hornes, E. Pathogenic Escherichia coli found in food. *Int. J. Food Microbiol.* **12**, 103–113 (1991).
186. Katouli, M. Population structure of gut Escherichia coli and its role in development of extra-intestinal infections. *Iran. J. Microbiol.* **2**, 59–72 (2010).
187. Paczosa, M. K. & Mecsas, J. Klebsiella pneumoniae: Going on the Offense with a Strong Defense. *Microbiol. Mol. Biol. Rev.* **80**, 629–661 (2016).
188. Rammaert, B. *et al.* Klebsiella pneumoniae related community-acquired acute lower respiratory infections in Cambodia: Clinical characteristics and treatment. *BMC Infect.*

- Dis.* **12**, 3 (2012).
189. Armbruster, C. E. *et al.* Pathogenesis of *Proteus mirabilis* Infection. **8**, 1–123 (2018).
  190. Schaffer, J. N. & Pearson, M. M. *Proteus mirabilis* and Urinary Tract Infections. *Microbiol Spectr.* **3**, 1–66 (2015).
  191. Gart, E. V. *et al.* *Salmonella typhimurium* and multidirectional communication in the gut. *Front. Microbiol.* **7**, 1–18 (2016).
  192. Lyczak, J. B., Cannon, C. L. & Pier, G. B. Establishment of *Pseudomonas aeruginosa* infection : lessons from a versatile opportunist. 1051–1060 (2000).
  193. Gellatly, S. L. & Hancock, R. E. W. *Pseudomonas aeruginosa* : new insights into pathogenesis and host defenses. 159–173 (2018). doi:10.1111/2049-632X.12033
  194. YU, V. L. *Serratia Marcescens* historical prespective and clinical review. *N Engl J Med* **300**, 887–893 (1979).
  195. Sleight, J. D. Antibiotic resistance in *Serratia marcescens*. *Br. Med. J.* **287**, 1651–1653 (1983).
  196. Hancock, R. E. W. The bacterial outer membrane as a drug barrier. *Trends microbiol.* 37–42 (1997).
  197. Elwell, L. P. *et al.* Antibacterial activity and mechanism of action of 3'-azido-3'-deoxythymidine (BW A509U). *Antimicrob. Agents Chemother.* (1987). doi:10.1128/AAC.31.2.274
  198. Yarchoan, R. *et al.* Administration of 3'-Azido-3'-Deoxythymidine, an Inhibitor of Htlv-Iii/Lav Replication, To Patients With Aids or Aids-Related Complex. *Lancet* **327**, 575–580 (1986).
  199. Suhadolnik, R. J. *Nucleoside antibiotics*. (John Wiley and sons, 1970).
  200. Toji, L. & Cohen, S. S. Termination of Deoxyribonucleic Acid in *Escherichia coli* by 2', 3' -Dideoxyadenosine. **103**, 323–328 (1970).

201. Doering, A. M., Jansen, M. & Cohen, S. S. Polymer synthesis in killed bacteria: lethality of 2',3'-dideoxyadenosine. *J. Bacteriol.* **92**, 565–574 (1966).
202. Smith, K. P. & Kirby, J. E. Validation of a High-Throughput Screening Assay for Identification of Adjunctive and Directly Acting Antimicrobials Targeting Carbapenem-Resistant Enterobacteriaceae. *Assay Drug Dev Technol.* **14**, 194–206 (2016).
203. Müller, B. & Kräusslich, H. G. *Antiviral strategies. Handbook of Experimental Pharmacology* **189**, (2009).
204. Arnersj, E. S. J., Valentinll, A. & Erikssons, S. Thymidine and 3'-Azido-3'-deoxythymidine Metabolism in Human Peripheral Blood Lymphocytes and Monocyte-derived Macrophages. *Biochemistry* **267**, 10968–10975 (1992).
205. Saito, H. & Tomioka, H. Thymidine kinase of bacteria: activity of the enzyme in actinomycetes and related organisms. *J. Gen. Microbiol.* **130**, 1863–70 (1984).
206. Inoue, T. *et al.* In vitro bone marrow toxicity of nucleoside analogs against human immunodeficiency virus. *Antimicrob. Agents Chemother.* **33**, 576–579 (1989).
207. Eyster, E. *et al.* Pharmacokinetics and bioavailability of zidovudine and its glucuronidated metabolite in patients with human immunodeficiency virus infection and hepatic disease ( AIDS Clinical Trials Group protocol 062 ). Pharmacokinetics and Bioavailability of Zidovudin. *Microbiology* **39**, 2732–2737 (1995).
208. Papadopulos-eleopulos, E. *et al.* A Critical Analysis of the Pharmacology of AZT and its Use in AIDS. *Curr. Med. Res. Opin.* **15**, s1–s45 (1999).
209. Moroni, G. N., Bogdanov, P. M. & Briñón, M. C. Synthesis and in Vitro Antibacterial Activity of Novel 5'-O-Analog Derivatives of Zidovudine As Potential Prodrugs. *Nucleosides, Nucleotides and Nucleic Acids* **21**, 231–241 (2002).
210. Sriram, D., Srichakravarthy, N., Bal, T. R. & Yogeewari, P. Synthesis of zidovudine

- prodrugs with broad-spectrum chemotherapeutic properties for the effective treatment of HIV/AIDS. *Biomed. Pharmacother.* **59**, 452–455 (2005).
211. Whiting, M. *et al.* Rapid Discovery and Structure-Activity Profiling of Novel Inhibitors of Human Immunodeficiency Virus Type 1 Protease Enabled by the Copper ( I ) - Catalyzed Synthesis of 1 , 2 , 3-Triazoles and Their Further Functionalization. 7697–7710 (2006).
212. Cheng, H. *et al.* Design, Synthesis, and in Vitro Biological Evaluation of 1 H -1,2,3-Triazole-4-carboxamide Derivatives as New Anti-influenza A Agents Targeting Virus Nucleoprotein. *J. Med. Chem.* **55**, 2144–2153 (2012).
213. Kamal, A. *et al.* Synthesis and biological evaluation of 1,2,3-triazole linked aminocombretastatin conjugates as mitochondrial mediated apoptosis inducers. *Bioorg. Med. Chem.* **22**, 5155–5167 (2014).
214. Boechat, N. *et al.* Novel 1,2,3-triazole derivatives for use against mycobacterium tuberculosis H37Rv (ATCC 27294) strain. *J. Med. Chem.* **54**, 5988–5999 (2011).
215. Singh, B. K. *et al.* Preparation and reactions of sugar azides with alkynes: synthesis of sugar triazoles as antitubercular agents. *Carbohydr. Res.* **343**, 1153–1162 (2008).
216. Liqiang, C. *et al.* Triazole-linked Inhibitors of Inosine Monophosphate Dehydrogenase from Human and Mycobacterium Tuberculosis. *J. Med. Chem.* **53**, 612–624 (2011).
217. Wang, X.-L., Wan, K. & Zhou, C.-H. Synthesis of novel sulfanilamide-derived 1,2,3-triazoles and their evaluation for antibacterial and antifungal activities. *Eur. J. Med. Chem.* **45**, 4631–4639 (2010).
218. Thatipamula, R. kumar *et al.* Synthesis, anticancer and antibacterial evaluation of novel (isopropylidene) uridine-[1,2,3]triazole hybrids. *J. Saudi Chem. Soc.* **21**, 795–802 (2017).
219. Sultana, N. & Arayne, M. S. In vitro activity of cefadroxil, cephalixin, cefatrizine and

- cefpirome in presence of essential and trace elements. *Pak. J. Pharm. Sci.* **20**, 305–310 (2007).
220. Del Busto, R., Haas, E. & Madhavam, T. In vitro studies and clinical studies of cefatrizine, a new semisynthetic cephalosporin. *Antimicrob. Agents Chemother.* **9**, 397–405 (1976).
221. El Akri, K., Bougrin, K., Balzarini, J., Faraj, A. & Benhida, R. Efficient synthesis and in vitro cytostatic activity of 4-substituted triazolyl-nucleosides. *Bioorganic Med. Chem. Lett.* **17**, 6656–6659 (2007).
222. Karthikeyan, M. S., Holla, B. S. & Kumari, N. S. Synthesis and antimicrobial studies on novel chloro-fluorine containing hydroxy pyrazolines. *Eur. J. Med. Chem.* **42**, 30–36 (2007).
223. Kolb, H. C., Finn, M. G. & Sharpless, K. B. Sharpless Click Chemistry- Diverse Chemical Function from a Few Good Reactions.
224. Díez-González, S. Well-defined copper(I) complexes for click azide–alkyne cycloaddition reactions: one click beyond. *Catal. Sci. Technol.* **1**, 166 (2011).
225. Boren, B. C. *et al.* Ruthenium-Catalyzed Azide–Alkyne Cycloaddition: scope and mechanism. *J. Am. Chem. Soc.* **130**, 8923–8930 (2008).
226. Fletcher, J. T., Keeney, M. E. & Walz, S. E. 1-Allyl- and 1-benzyl-3-methyl-1,2,3-triazolium salts via tandem click transformations. *Synthesis (Stuttg.)*. 3339–3345 (2010). doi:10.1055/s-0030-1257909
227. Appukkuttan, P., Dehaen, W., Fokin, V. V. & Van Der Eycken, E. A microwave-assisted click chemistry synthesis of 1,4-disubstituted 1,2,3-triazoles via a copper(I)-catalyzed three-component reaction. *Org. Lett.* **6**, 4223–4225 (2004).
228. Sreedhar, B. & Reddy, P. S. Sonochemical synthesis of 1,4-disubstituted 1,2,3-triazoles in aqueous medium. *Synth. Commun.* **37**, 805–812 (2007).

229. Baldev, R., Rajendran, V. & Palanichamy, P. *Science and Technology of Ultrasounds*. (Narosa Publishing House Pvt. Ltd., 2006).
230. Galema, S. A. Microwave chemistry. *Chem. Soc. Rev.* **26**, 233 (1997).
231. Gavin Whittaker. Microwave chemistry. *Sch. Sci. Rev.* **85**, 87–94 (2004).
232. Cheng, Z. Y., Li, W. J., He, F., Zhou, J. M. & Zhu, X. F. Synthesis and biological evaluation of 4-aryl-5-cyano-2H-1,2,3-triazoles as inhibitor of HER2 tyrosine kinase. *Bioorganic Med. Chem.* **15**, 1533–1538 (2007).
233. Hirsch, M. S. & Hirsch, M. S. Aids commentary azidothymidine. *J. Infect. Dis.* (1988). doi:10.1093/infdis/157.3.427
234. Simoni-Wastila, L. & Lasagne, L. The history of zidovudine (AZT). *J. Clin. Res. Pharmacoevidemiol.* **4**, 25–37 (1990).
235. Emsley, P. & Lohkamp, B. Features and development of Coot. *Acta Crystallogr.* 486–501 (2010). doi:10.1107/S0907444910007493
236. Brown, J. P. Mutation Research, 75 (1980) 243--277 ©. *Mutat. Res. Genet. Toxicol.* **75**, 243–277 (1980).
237. Ballard, C. R. & Maróstica, M. R. *Health Benefits of Flavonoids. Bioactive Compounds* (Elsevier Inc., 2019). doi:10.1016/b978-0-12-814774-0.00010-4
238. Tereschuk, M. L., Riera, M. V. Q., Castro, G. R. & Abdala, L. R. Antimicrobial activity of flavonoids from leaves of *Tagetes minuta*. *J. Ethnopharmacol.* **56**, 227–232 (1997).
239. Lu, Y., Joerger, R. & Wu, C. Study of the chemical composition and antimicrobial activities of ethanolic extracts from roots of *Scutellaria baicalensis* Georgi. *J. Agric. Food Chem.* **59**, 10934–10942 (2011).
240. Brahmachari, G. *Discovery and Development of Neuroprotective Agents from Natural Products*. (Elsevier, 2017).

241. Song, J. H. *et al.* Antiviral activity of chrysin derivatives against coxsackievirus B3 in vitro and in vivo. *Biomol. Ther.* **23**, 465–470 (2015).
242. Sánchez, I., Gómez-Garibay, F., Taboada, J. & Ruiz, B. H. Antiviral effect of flavonoids on the dengue virus. *Phyther. Res.* **14**, 89–92 (2000).
243. Brinkworth, R. I., Stoermer, M. J. & Fairlie, D. P. Flavones are inhibitors of HIV-1 proteinase. *Biochem BIOPH RES CO* **188**, 631–637 (1992).
244. Xiao, J. *et al.* Chrysin attenuates experimental autoimmune neuritis by suppressing immuno-inflammatory responses. *Neuroscience* **262**, 156–164 (2014).
245. Rauf, A. *et al.* Suppression of inflammatory response by chrysin, a flavone isolated from *Potentilla evestita* Th. Wolf. in silico predictive study on its mechanistic effect. *Fitoterapia* **103**, 129–135 (2015).
246. Khoo, B. Y., Chua, S. L. & Balaram, P. Apoptotic effects of chrysin in human cancer cell lines. *Int. J. Mol. Sci.* **11**, 2188–2199 (2010).
247. Salimi, A. *et al.* Chrysin as an Anti-Cancer Agent Exerts Selective Toxicity by Directly Inhibiting Mitochondrial Complex II and V in CLL B-lymphocytes. *Cancer Invest.* **35**, 174–186 (2017).
248. Pushpavalli, G., Kalaiarasi, P., Veeramani, C. & Pugalendi, K. V. Effect of chrysin on hepatoprotective and antioxidant status in d-galactosamine-induced hepatitis in rats. *Eur. J. Pharmacol.* **631**, 36–41 (2010).
249. Anitha, T. A. & Rajadurai, M. Antioxidative potential of chrysin, a flavone in streptozotocin-nicotinamide-induced diabetic rats. *Biomed. Prev. Nutr.* **4**, 511–517 (2014).
250. Li, H. Q. *et al.* Synthesis of C(7) modified chrysin derivatives designing to inhibit ketoacyl-acyl carrier protein synthase III (FabH) as antibiotics. *Bioorganic Med. Chem.* (2009). doi:10.1016/j.bmc.2009.07.046

251. Suresh Babu, K. *et al.* Synthesis and biological evaluation of novel C (7) modified chrysin analogues as antibacterial agents. *Bioorganic Med. Chem. Lett.* **16**, 221–224 (2006).
252. Liu, H. *et al.* Flavonoids from halostachys caspica and their antimicrobial and antioxidant activities. *Molecules* **15**, 7933–7945 (2010).
253. Lin, C. H., Chen, C. H., Lin, Z. C. & Fang, J. Y. Recent advances in oral delivery of drugs and bioactive natural products using solid lipid nanoparticles as the carriers. *J. Food Drug Anal.* **25**, 219–234 (2017).
254. Baojian Wu, Kaustubh Kulkarni, Basu, S., Zhang, S. & Hu, M. First-pass metabolism via UDP-glucuronosyltransferase: a barrier to oral bioavailability of phenolics. *J Pharm Sci.* **100**, 3655–3681 (2012).
255. Bonzo, J. A., Bélanger, A. & Tukey, R. H. The role of chrysin and the Ah receptor in induction of the human UGT1A1 gene in vitro and in transgenic UGT1 mice. *Hepatology* **45**, 349–360 (2007).
256. Liu, X. *et al.* O-Methylated Metabolite of 7,8-Dihydroxyflavone Activates TrkB Receptor and Displays Antidepressant Activity. *Pharmacology* **91**, 185–200 (2013).
257. Havsteen, B. H. *The biochemistry and medical significance of the flavonoids.* *Pharmacology and Therapeutics* **96**, (2002).
258. Cushnie, T. P. T. & Lamb, A. J. Recent advances in understanding the antibacterial properties of flavonoids. *International Journal of Antimicrobial Agents* (2011). doi:10.1016/j.ijantimicag.2011.02.014
259. Bylka, W., Matlawska, I., Pilewski, N. A. & Hall, M. Natural Flavonoids as Antimicrobial Agents. *JANA* **7**, (2004).
260. Rathee, P. *et al.* Mechanism of Action of Flavonoids as Anti-inflammatory Agents: A Review. *Inflamm. Allergy - Drug Targets* **8**, 229–235 (2009).

261. García-Lafuente, A., Guillamón, E., Villares, A., Rostagno, M. A. & Martínez, J. A. Flavonoids as anti-inflammatory agents: Implications in cancer and cardiovascular disease. *Inflamm. Res.* **58**, 537–552 (2009).
262. Mutoh, M. *et al.* Suppression of cyclooxygenase-2 promoter-dependent transcriptional activity in colon cancer cells by chemopreventive agents with a resorcin-type structure. *Carcinogenesis* **21**, 959–63 (2000).
263. Raso, G. M., Meli, R., Di Carlo, G., Pacilio, M. & Di Carlo, R. Inhibition of inducible nitric oxide synthase and cyclooxygenase-2 expression by flavonoids in macrophage J774A.1. *Life Sci.* **68**, 921–931 (2001).
264. Russo, A. *et al.* Bioflavonoids as antiradicals, antioxidants and DNA cleavage protectors. *Cell Biol. Toxicol.* **16**, 91–98 (2000).
265. S, M. & K, B. *Principles and Practice of Phytotherapy – Modern Herbal Medicine.* (2000).
266. Keevil, J. G., Osman, H. E., Reed, J. D. & Folts, J. D. Grape juice, But not orange juice or grapefruit juice, inhibits human platelet aggregation. *Hum. Nutr. Metab. Res. Commun.* 53–56 (2000).
267. Lou, F. Q., Zhang, M. F., Zhang, X. G., Liu, J. M. & Yuan, W. L. A study on tea-pigment in prevention of atherosclerosis. *Chin. Med. J. (Engl.)* **102**, 579–583 (1989).
268. Kaul, T. N., Middleton, E. & Ogra, P. L. Antiviral effect of flavonoids on human viruses. *J. Med. Virol.* **15**, 71–79 (1985).
269. Batra, P. & Sharma, A. K. Anti-cancer potential of flavonoids: recent trends and future perspectives. *3 Biotech* **3**, 439–459 (2013).
270. Romagnolo, D. F. & Selmin, O. I. Flavonoids and Cancer Prevention: A Review of the Evidence. *J. Nutr. Gerontol. Geriatr.* **31**, 206–238 (2012).
271. Chebil, L. *et al.* Solubility of flavonoids in organic solvents. *J. Chem. Eng. Data* **52**,

- 1552–1556 (2007).
272. Starks.C.M., Liotta.C.L. & Halpern.M.E. in *Phase-Transfer Catalysis* 23–47 (1994).
273. Alluis, B. & Dangles, O. Acylated flavone glucosides: Synthesis, conformational investigation, and complexation properties. *Helv. Chim. Acta* **82**, 2201–2212 (1999).
274. Wu, Z., Jiang, L., Chen, H. & Wang, Q.-A. Synthesis of flavonoid 7-D-3-D-glycosides by phase transfer catalysis. *J. Chem. Res.* 195–197 (2009).
275. Jung, S. H. *et al.* Structural requirement of isoflavonones for the inhibitory activity of interleukin-5. *Eur. J. Med. Chem.* **38**, 537–545 (2003).
276. Bao, C. *et al.* Synthesis, self-assembly and characterization of a new glucoside-type hydrogel having a Schiff base on the aglycon. *Carbohydr. Res.* **339**, 1311–1316 (2004).
277. Kröger, L. & Thiem, J. Convenient multigram scale glycosylations of scented alcohols employing phase-transfer reactions. *J. Carbohydr. Chem.* **22**, 9–23 (2003).
278. Wadhvani, T. *et al.* Effect of various solvents on bacterial growth in context of determining MIC of various antimicrobials. *Internet J. Microbiol.* **7**, 1–6 (2008).
279. Ristivojević, P. *et al.* Antimicrobial activity of Serbian propolis evaluated by means of MIC, HPTLC, bioautography and chemometrics. *PLoS One* **11**, 1–15 (2016).
280. McPherson, D. *et al.* Sepsis-associated mortality in England: An analysis of multiple cause of death data from 2001 to 2010. *BMJ Open* **3**, 1–7 (2013).
281. Lee, J. Y., Lee, J., Jeong, K. W., Lee, E. & Kim, Y. Flavonoid inhibitors of beta-Ketoacyl acyl carrier protein synthase III against methicillin-resistant staphylococcus aureus. *Bull. Korean Chem. Soc.* **32**, 2695–2699 (2011).
282. The European Committee on Antimicrobial Susceptibility Testing. *Breakpoint tables for interpretation of MICs and zone diameters. Version 8.0.* (2018). at [http://www.eucast.org/clinical\\_breakpoints/](http://www.eucast.org/clinical_breakpoints/)
283. Sivaraman, S. *et al.* Inhibition of the Bacterial Enoyl Reductase FabI by Triclosan: A

- Structure-Reactivity Analysis of FabI Inhibition by Triclosan Analogues. *J. Med. Chem.* **47**, 509–518 (2004).
284. Devine, D., Mathews, N. & Kinchington, D. Testing compounds for antiviral activity in cell cultures infected with HIV. *Methods Mol. Med. Vol 24* **24**, (2000).
285. Krowicka, H. *et al.* Use of Tissue Culture Cell Lines to Evaluate HIV Antiviral Resistance. *AIDS Res. Hum. Retroviruses* **24**, 957–967 (2008).
286. Schimpff, S. . Therapy of infection in patients with granulocytopenia. *Med Clin North Am* **61**, 1101–1108 (1978).
287. Moellering, R. C. in *Principals and practice of infectious diseases* 206–218 (1990).
288. Freifeld, A. G. in *Infectious complications in the immunocompromised host I: Hematology/Oncology Clinics of North America* 813–839 (1993).
289. Lorian, V. *Antibiotics in laboratory medicine. Laboratory methods used to assess the activity of antimicrobial combinations.* (1991).
290. Bushby, S. R. . Trimethoprim-sulfamethoxazole: in vitro microbiologic aspects. *J Infect Dis* **128**, S442-4462 (1973).
291. Hitchings, G. . in *Trimethoprim-sulfamethoxazole in bacterial infections* 7–16 (1973).
292. Amin, M. U., Khurram, M., Khattak, B. & Khan, J. Antibiotic additive and synergistic action of rutin, morin and quercetin against methicillin resistant *Staphylococcus aureus*. *BMC Complement. Altern. Med.* **15**, 1–12 (2015).
293. Maddams, J., Utley, M. & Møller, H. Projections of cancer prevalence in the United Kingdom, 2010–2040. *Br. J. Cancer* **107**, 1195–1202 (2012).
294. Cancer research UK. The Twenty Most Common Cancers: 2015.
295. Oh, S., Kim, H., Nam, K. & Shin, I. Glut1 promotes cell proliferation, migration and invasion by regulating epidermal growth factor receptor and integrin signaling in triple-negative breast cancer cells. *BMB Rep.* **50**, 132–137 (2017).

296. Bensinger, S. J. & Christofk, H. R. Seminars in Cell & Developmental Biology New aspects of the Warburg effect in cancer cell biology. *Semin. Cell Dev. Biol.* **23**, 352–361 (2012).
297. Bertram, J. P. B., Nowrousian, P. H. M. R. & Wieller, J. S. M. D-19575 — a sugar-linked isophosphoramidate mustard derivative exploiting transmembrane glucose transport. *Cancer Chemother Pharmacol* 364–370 (1995).
298. Moon, J.-Y. *et al.* Inhibition of cell growth and down-regulation of telomerase activity by amygdalin in human cancer cell lines Inhibition of cell growth and down-regulation of telomerase activity by amygdalin in human cancer cell lines. *Animal Cells Syst. (Seoul)*. (2015). doi:10.1080/19768354.2015.1060261
299. Lee, A. V., Oesterreich, S. & Davidson, N. E. MCF-7 Cells - Changing the Course of Breast Cancer Research and Care for 45 Years. *J. Natl. Cancer Inst.* **107**, 2–5 (2015).
300. Plumb, J. A., Milroy, R. & Kaye, S. B. Effects of the pH Dependence of 3-(4,5-Dimethylthiazol-2-yl) -2,5-diphenyl- tetrazolium Bromide-Formazan Absorption on Chemosensitivity Determined by a Novel Tetrazolium-based Assay<sup>1</sup>. 4435–4440 (1989).
301. Kavanagh, F., Hervey, A. & Robbins, W. J. Antibiotic substances from basidiomycetes. VIII. *Pleurotus multilus* (Fr.) Sacc. and *Pleurotus passeckerianus* Pilat. *Proc. Natl. Acad. Sci.* **37**, 570–574 (1950).
302. Rittenhouse, S. *et al.* Selection of Retapamulin , a Novel Pleuromutilin for Topical Use. *Antimicrob. Agents Chemother.* **50**, 3882–3885 (2006).
303. Tang, Y. *et al.* Synthesis and in vitro antibacterial activity of four novel pleuromutilin derivatives. *J. Chil. Chem. Soc.* **58**, 1537–1540 (2013).
304. Egger, H. & Reinshagen, H. New pleuromutilin derivatives with enhanced antimicrobial activity II. structure-activity correlations. *J. Antibiot. (Tokyo)*. **29**, 923–

- 927 (1976).
305. Tang, Y.-Z., Liu, Y.-H. & Chen, J.-X. Pleuromutilin and its Derivatives-The Lead Compounds for Novel Antibiotics. *Mini-Reviews Med. Chem.* **12**, 53–61 (2012).
306. Park, A. B., Choi, W., Kim, J., Kim, K. & Lee, S. Monoterpenes from Thyme (*Thymus vulgaris*) as potential mosquito repellents. *J. Am. Mosq. Control Assoc.* **21**, 80–83 (2005).
307. Ultee, A., Bennik, M. H. J. & Moezelaar, R. The Phenolic Hydroxyl Group of Carvacrol Is Essential for Action against the Food-Borne Pathogen *Bacillus cereus* The Phenolic Hydroxyl Group of Carvacrol Is Essential for Action against the Food-Borne Pathogen *Bacillus cereus*. *Appl. Environ. Microbiol.* **68**, 1561–1568 (2002).
308. Ben Arfa, A., Combes, S., Preziosi-Belloy, L., Gontard, N. & Chalier, P. Antimicrobial activity of carvacrol related to its chemical structure. *Lett. Appl. Microbiol.* **43**, 149–154 (2006).
309. Schwarz, S., Kehrenberg, C. & Cloeckert, A. Molecular basis of bacterial resistance to chloramphenicol and florfenicol. **28**, 519–542 (2017).
310. Madhavan, H. & Bagyalakshmi, R. Farewell, Chloramphenicol? Is this True?: A Review. *J. Microbiol. Biotechnol.* **3**, 13–26 (2014).
311. Astani, A., Reichling, J. & Schnitzler, P. Comparative study on the antiviral activity of selected monoterpenes derived from essential oils. *Phytother. Res* **24**, 673–679 (2010).
312. Truelstrup Hansen, L., Austin, J. W. & Gill, T. A. Antibacterial effect of protamine in combination with EDTA and refrigeration. *Int. J. Food Microbiol.* **66**, 149–161 (2001).

# Appendix

**A(1): Nutrient broth 2**

<b>Component description</b>	<b>g/L</b>
'Lab-Lemco' powder	10
Peptone	10
Sodium chloride	5
pH 7.5 ± 0.2	

**A(2): Mueller Hinton Broth**

<b>Component description</b>	<b>g/L</b>
Beef, dehydrated infusion	300
Caesein hydrolysate	17.5
Starch	1.5
pH 7.3 ± 0.1 @ 25 °C	

**A(3): Mueller Hinton Agar**

<b>Component description</b>	<b>g/L</b>
Beef, dehydrated infusion	300
Caesein hydrolysate	17.5
Starch	1.5
Agar	17
pH 7.3 ± 0.1 @ 25 °C	

**A(4):**  
**CM5**

<b>Component Description</b>	<b>g/l</b>	<b>Component Description</b>	<b>g/l</b>
Adenine	0.01	Nicotinamide	0.01
Ammonium sulfate	1	4-aminobenzoic acid (PABA)	0.1
ATP	0.07	Dibasic phosphate buffer	7
Biotin	0.01	Dipotassium hydrogen phosphate	7
Calcium chloride	0.1	Folic acid	0.01
Calcium pantothenate	0.05	Glucose	2.5
Choline chloride	0.01	Iso sensitest peptone	3
Cytosine	0.01	Ketoglutaric acid	0.1
Glycine	0.1	L-asparagine	0.1
Guanine	0.01	L-glutamine	0.1
L-arginine	0.1	L-ornithine monohydrochloride	0.1
L-aspartic acid	0.1	Monobasic phosphate buffer	2
L-cysteine	0.1	NAD	0.07
L-cystine	0.1	Potassium dihydrogen phosphate	2
L-glutamate	0.1	Pyridoxal hydrochloride	0.01
L-histidine	0.1	Pyridoxamine	0.01
L-isoleucine	0.1	Pyridoxine	0.01
L-leucine	0.1	Riboflavin	0.01
L-lysine HCL	0.1	Sodium citrate	0.5
L-methionine	0.1	Sodium pyruvate	2.5
L-phenylalanine	0.1	Taurine	0.1
L-proline	0.1	Thiamine hydrochloride (aneurine)	0.01
L-serine	0.1	Trans-4-hydroxy-L-proline	0.1
L-threonine	0.3	Veal peptone	3
L-tryptophan	0.1	Vitamin B12	0.01
L-tyrosine	0.1	Yeast extract	0.1
L-valine	0.1	Zinc sulphate	0
Magnesium sulfate heptahydrate	0.1	$\alpha$ aminobutyric acid	0.1
Myo-inositol	0.01	Uracil	0.01

**formula**

### **A(5): List of figures**

Figure 1: The sites of action for antimicrobial drugs. Adapted from a figure in ref. 34

Figure 2: The structure of the cell walls for both Gram positive and Gram negative bacteria. ... Adapted from ref. 36.

Figure 3: The elongation stage of fatty acid synthesis. The antibiotics are shown in red, displaying where they are effective. Modified from ref. 45.

Figure 4: Examples of antimicrobials that affect the protein/ RNA synthesis. Streptomycin 7 is an example of an aminoglycoside. Tetracycline 8, erythromycin 9 is a macrolide and dafopristin 10 is an example of a streptogramin. The MIC data displayed shows their activities against *S. pneumoniae*. Refs. 50,51.

Figure 5: Systemic antibacterial new molecular entities approved by the US Food and Drug Administration from ref. 56.

Figure 6: A timeline of when antibiotics were introduced and when resistance was identified. . Adapted from ref. 60.

Figure 7: A simplified diagram of the prodrug concept. Modified from ref. 92.

Figure 8: Data analysis of the composition of carbohydrate drugs records from the aforementioned pharmacopoeias. Adapted from ref. 97.

Figure 9: The structures of TTS-12 (22) and TTS-15 (23).

Figure 10: Four of the key enzymatic glycosylations in nature. Glycosyltransferase (A), reverse glycosidase (B), glycan donor transferase (C) transglycosylation (D). Adapted from 33.

Figure 11: The structure of ciprofloxacin 24 with its glucose 26 and galactose 25 conjugates. The data shown is the diameter of the zone of inhibition in a disc diffuse assay. Data adapted from ref. 113.

Figure 12: The structure of nadifloxacin 27 with its glucose 28 and galactose 29 conjugates. The data shown is the MIC determined by the bioscreen method. Work adapted from ref. 114.

Figure 13: The previously synthesised compounds, 30-33,<sup>113</sup> and the target structures, 24-25, for the bisphenol containing carbohydrate compounds.

Figure 14: The structure of triclosan 26. The MIC data is also shown; data collected using a micro-dilution assay.<sup>115</sup> A table showing triclosan's 26 mechanism of resistance and antibiotic cross-resistance in different bacteria.

Figure 15: The structures of bromochlorophen (BCP) 28, dichlorophen (DP) 29 and hexachlorophene (hex) 27. Data was collected using a bioscreen method.<sup>113</sup>

Figure 16 : The structures of the previously synthesised glycosides from Dr. Brieley's work.

Figure 17: The target compounds 24-25. The retrosynthetic route is also shown beneath the .... target compounds.

Figure 18: The possible hydrogen bond present in the acetylated intermediates in for the synthesis of 24b and 25b.

Figure 19: A table showing the different glycosylation methods used. NR = no reaction.

Figure 20: <sup>1</sup>H-NMR spectrum for 25a, the highlighted peak is the hydrogen present at the anomeric centre. The *J* value highlights that's it's the β-anomer has been synthesised. The table below shows the *J* values (Hz) for the four compounds, 24-25, as determined from their respective <sup>1</sup>H-NMRs spectra.

Figure 21: The dipole interactions shown on the α- and β- anomers.

Figure 22: The hyperconjugation model. This shows the lone pair orbital on the oxygen and the σ\* orbital in C-1 position.

Figure 23: A graph showing the growth of a bacterium, in relation to time.

Figure 24: A diagram showing the SAR collected form the different bisphenol moieties attached as glucosides and galactosides.

Figure 25: The target structure 24-25, with their respective yields and purities shown.

Figure 26: The basic structures for this series of compounds. In 35-42, the R groups are shown below the target compounds.

Figure 27: The structure of Azidothymidine 43 and thymidine 44. The hydroxyl on the 3' position of the thymidine is replaced with an azido group in AZT 43. The ID<sub>50</sub> is displayed for 43-50.

Figure 28: The mechanism of action for azidothymidine. The use of enzymes allows for the active metabolite (AZT-Thymidine 53) to be synthesised and used as a DNA chain terminator. Adapted from ref. <sup>201</sup>.

Figure 29: Examples of ester prodrugs of AZT. 54-57 are reported in ref. <sup>205</sup>, 58-61 in ref. <sup>206</sup>. . The MIC data is presented below each compound. 54-57 MIC was assayed using Mueller-Hinton broth against *Klebsiella pneumoniae* ATCC 10031. 58-61 were assayed using Mueller-Hinton broth against *Klebsiella pneumoniae*. \* compared to the parent compound, AZT 43, which had an MIC = 2 µg/mL. \*\* compared to commercial antibiotics: Norfloxacin MIC = 0.0381 µg/mL and Ciprofloxacin MIC = 0.0381 µg/mL.

Figure 30: The structures 62-69 which were tested against various bacteria. These are from ref. 212. The MIC data is also displayed for compounds 62-69.

Figure 31: Compounds 70-75, which all contain a 1,2,3- triazole in the 3' position. The data is showing the phosphorylation by *Up*TK and hTK1, with 100 M ATP and the nucleosides, respectively. The data is presented as relative activity (%) when compared to dThd. Data from ref. <sup>74</sup>.

Figure 32: Cefatrizine 76 is a commercial drug that contains a 1,2,3,-triazole. The MIC data (µg/mL) is displayed, with good activity against the bacteria shown. Data from ref. 213.

Figure 33: Annotated structures, 35-42, showing the justification for their drug design.

Figure 34: Three different 'click' reactions. (A) is the Huisgen 1, 3-Dipolar Cycloaddition, stereocontrol is achieved. (B) uses CuAAC and (C) uses RuAAC.

Figure 35: The general reaction schemes for the synthesis of the 1,4 and 1,5 isomers of the 1,2,3- triazoles. The target compounds 35-42 are shown below the general reaction scheme.

Figure 36: The copper catalytic cycle for the formation of a 1,4-isomer. Adapted from ref. <sup>219</sup>. R<sup>1</sup> = AZT, This shows the formation of 35.

Figure 37: The ruthenium catalytic cycle for the formation of the 1,5-isomer. Adapted from ref. <sup>220</sup>. R = AZT. This figure displays the formation of 39.

Figure 38: The key resonance forms on the 1,2,3-triazole ring. The 1,4 and 1,5 isomers are shown. The hydrogen coloured is the hydrogen resonance peak on the <sup>1</sup>H NMR spectra that is being shown.

Figure 39: A diagram showing the SAR collected from the different triazole containing compounds.

Figure 40: A computer model of AZT triphosphate chelating to the magnesium ion. AZT 43 is incorporated into the DNA and causes the chain to end.

Figure 41: The fitting of the compounds 35-42 with the active site of HIV reverse transcriptase. A = 35, B = 36, C = 37, D = 38, E = 39, F = 40, G = 41, and H = 42.

Figure 42: The overlapped view of 36 and 40 (36 = blue and 40 = green) in the active site of HIV-1 reverse transcriptase.

Figure 43: The target structure 35-42, with their respective yields and purities shown.

Figure 44: The target structures for the flavonoid series, 82-87.

Figure 45: The general structures of the different flavonoids. The general flavonoid structure is numbered and displayed in the middle.

Figure 46: Quercetagenin-7-arabinosyl-galactoside 88 equivalent concentrations against select bacteria.

Figure 47: The structures of the flavonoids and their glycosidic counter parts found in *Scutellaria baicalensis*. The MIC and MBC were determined using methods described by Hansen et al.<sup>297</sup> *S. aureus* (ATCC 19115), and *L. monocytogenes* (ATCC 27217). Data adapted from ref. <sup>248</sup>.

Figure 48: Chrysin 93 MIC values against selective gram-positive and gram-negative bacteria. Four gram-negative (*Agrobacterium tumefaciens* (ATCC 11158), *Escherichia coli* (ATCC 29425), *Pseudomonas lachrymans* (ATCC 11921) and *Xanthomonas vesicatoria* (ATCC 11633)) and three gram-positive (*Bacillus subtilis* (ATCC 11562), *Staphylococcus aureus* (ATCC 6538) and *Staphylococcus haemolyticus* (ATCC 29970)). The method used was a modified broth dilution- colorimetric assay. Adapted from ref. 261.

Figure 49: Part of the elongation stage in the fatty acid synthesis in bacteria which involved FabH.

Figure 50: The structures of C (7) derivatives. The MIC were determined using broth dilution methods. *B. subtilis* (MTCC 441), *B. sphaericus* (MTCC 11), *S. aureus* (MTCC 96), *K.aerogenes* (MTCC 39), *C. violaceum* (MTCC 2656), and *P. aeruginosa* (MTCC 741). The n refers to a=1, b= 2 and c=4. Data adapted from ref.257.

Figure 51: The structures of C (7) derivatives. The MIC values were determined using the MTT method in MHB. Data adapted from ref.256.

Figure 52: The mechanism by which chrysin 93 undergoes glucuronidation. Modified from ref. 261.

Figure 53: The glucosides 84 and 86 and galactosides 85 and 87 of their respective parent flavonoids.

Figure 54: The glucosides 82 and galactosides 83 of 7-hydroxyflavone 100.

Figure 55: The target compounds 82-87. The retrosynthetic route is also shown beneath the target compounds.

Figure 56: The catalytic cycle for the formation of the glycosidic flavonoids. The transition state is formed due to the reaction going through an S<sub>N</sub>2 reaction style.

Figure 57: The acetylated intermediates, 102-107, that are the products of the PTC reactions.

Figure 58: The possible hydrogen bond present in the acetylated intermediates in the synthesis for 84 and 85.

Figure 59: A table that summeries the different conditions used for glycosylation of 104. The scheme for the reaction is shown above the table.

Figure 60: The structures of glufosfamide 105 and ifosfamide 106 with their LD50 data for rats and mice. Adapted from ref. 279.

Figure 61: The target compounds, 24-25, for the bisphenol containing compounds.

Figure 62: The MIC<sub>100</sub> values for compounds 98-102. The work was performed by ref. 282

Figure 63: The target compounds, 35-42, for the 1,2,3-triazole containing compounds.

Figure 64: Potential carbohydrate prodrugs, 115 (Glu) and 116 (Gal), of AZT.

Figure 65: The target compounds, 82-87, for the flavonoid containing glycosides.

Figure 66: The MIC<sub>100</sub> data for four compounds in the pleutmultin class: Pleuromutilin 117, retapamulin 118, valnemulin 119 and tiamulin 120. Data was collected using a liquid both method.

Figure 67: The MIC<sub>100</sub> values for 121 and 122, displaying how masking the hydroxyl moiety lowers the biological activity. The reaction scheme and yield for the reaction is also shown.

Figure 68: The MIC<sub>100</sub> data for 123 and 124. The data was collected using a liquid broth method. This work was performed by 292.

Figure 69: The structures of azidamfenicol 125 and chloramphenicol 126.

## A(6): List of Tables

Table 1: A table showing examples of different classes of antibiotics. Table adapted from ref. 10 and 5.

Table 2: A table showing the priority list provided by the WHO for which bacteria need new

Table 3: Relating antibiotic class to its target and mechanism of action.<sup>62</sup>

Table 4: A table showing examples of biocides, their targets and mechanism of action. Adapted from tables from ref. <sup>65,66</sup>.

Table 5: A table showing the four different categories of culture media. Adapted from ref. 68.

Table 6: The different glycosidase profiles for three different bacteria: *Es. coli*, *B. cereus* and *P. aeruginosa*. Adapted from ref. 68. Key: glu=glucose, gal = galactose, man = mannose, Xyl = xylose, L-Fuc = L-fructose.

Table 7: A table showing examples of why selective media is used for certain bacteria

Table 8: A table showing examples of media used to selectively recover or grow certain bacteria. The names in red denote an antibiotic. \* Not technically an antibiotic but was added to provide selectivity.

Table 9: A table showing the results of screening several bis-phenol compounds attached to various sugars against a range of bacterial strains, as performed by L. Brierley.<sup>116</sup> It is highlighted in yellow where the value  $\leq 32 \mu\text{g/ml}$ . The microbials labelled in red are gram-positive bacteria. The broth is CM5.

Table 10: A table showing the yields and purity of the target compounds 24-25.

Table 11: The MIC<sub>100</sub> data for the underivised compounds, BP 33 and HPM 34. The NB and MHB refer to the media used in the bioscreen. NG – No growth. The ClogP data was calculated using Chem BioDraw Ultra software version 13.0. It is highlighted in yellow where the value  $\leq 64 \mu\text{g/ml}$ .

Table 12: The MIC<sub>100</sub> data for the glycosidic compounds, BP and HMP. The broth is NB. NG – No growth. The ClogP data was calculated using Chem BioDraw Ultra software version 13.0. It is highlighted in yellow where the value  $\leq 64 \mu\text{g/ml}$

Table 13: The MIC<sub>100</sub> data for the glycosidic compounds, 33 and 34. The broth is MHB and CM5. NG – No growth. It is highlighted in yellow where the value  $\leq 64 \mu\text{g/ml}$

Table 14: Antimicrobial compounds containing 1,2,3-triazole moieties. MIC ( $\mu\text{g/mL}$ ) for compounds 77 and 78 were determined by two-fold serial dilution method for microdilution plates. Compounds 81 the lowest concentration of the compound which inhibits the growth of mycobacterium >90%.

Table 15: The different experimental condition used to synthesis 32. The reaction can be seen above the table. NR = No reaction

Table 16: A table showing the yields and purity of the target compounds 35-41.

Table 17: MIC<sub>100</sub> data for AZT 43 in two different media; MHB and NB. The values highlighted yellow show MIC<sub>100</sub> ≥64 µg/mL. NG – No growth. The bacteria in red refer to gram-positive strains.

Table 18: Cell extracts of the bacteria were examined for TK activity at a protein concentration of 50 pg ml<sup>-1</sup> in the reaction mixture. Where the bacteria originated from *a*, Y. Kanemasa, Okayama University, Okayama, Japan; *b*, A. Takagi, Tottori University, Tottori, Japan; *c*, A. Matsumae, Kitasato Institute, Tokyo, Japan; *d*, M. Kuwabara, Hiroshima Prefectural Hospital, Hiroshima, Japan. Adapted from data in ref. 200

Table 19: The MIC<sub>100</sub> data for the underivised compound AZT and the 1,4-isomers 35-38. The broth is NB. NG – No growth. The values highlighted yellow show MIC<sub>100</sub> ≥64 µg/mL. The ClogP data was calculated using Chem BioDraw Ultra software version 13.0.

Table 20: The structure 35-38 and 43 shown with their ClogP and select gram-negative bacteria's MIC<sub>100</sub> values.

Table 21: The MIC<sub>100</sub> data for the underivised compound AZT and the 1,5-isomers 35-38. The broth is NB. NG – No growth. The values highlighted yellow show MIC<sub>100</sub> ≥64 µg/mL. The ClogP data was calculated using Chem BioDraw Ultra software version 13.0.

Table 22: The MIC<sub>100</sub> data for the underivised compound AZT and both the 1,4- the 1,5-isomers 35-42. The broth is MHB. NG – No growth. The values highlighted yellow show MIC<sub>100</sub> ≥64 µg/mL

Table 23: A table showing the yields and purity of the target compounds 82-87 and the acetylated intermediates, 104-107.

Table 24: A table summarising the solubility of chrysin. A concentration of 1 mg/mL was used.

Table 25: The starting material for these reactions was acetobromo- $\alpha$ -D-glucose. All produced the  $\beta$ -anomer. The R group = sugar attached to the various products. R<sup>1</sup> = sugar attached.

Table 26: The *J* values (Hz) for the six compounds 82-87, as determined from their respective <sup>1</sup>H-NMR spectra. CD = cannot be distinguished

Table 27: A table showing the differences between the resonance peaks using <sup>1</sup>H-NMR spectra. \* = The resonance peaks falls under other peaks

Table 28: The MIC<sub>100</sub> data for the underivised parent compounds 93, 100-101. The agar is MH. NG – No growth. The values highlighted yellow show MIC<sub>100</sub> ≥32 µg/mL. The ClogP data was calculated using Chem BioDraw Ultra software version 13.0.

Table 29: A table showing the different conditions used to try and solubilise the parent flavonoid compounds for the bioscreen method.

Table 30: A summary of the different conditions in which the agar was prepared

Table 31: The MIC<sub>100</sub> data for the underivised parent compounds 100 and its respective glycosides 82 and 83. The agar is MH, with the broth shown NB (82-83). NG – No growth. The values highlighted yellow show MIC<sub>100</sub> ≥32 µg/mL. The ClogP data was calculated using Chem BioDraw Ultra software version 13.0.

Table 32: The MIC<sub>100</sub> data for the underivised parent compounds 93 and its respective glycosides 84 and 85. The agar is MH, with the broth shown NB (84-85). NG – No growth. The values highlighted yellow show MIC<sub>100</sub> ≥32 µg/mL. The ClogP data was calculated using Chem BioDraw Ultra software version 13.0.

Table 33: The MIC<sub>100</sub> data for the underivised parent compounds 101 and its respective glycosides 86 and 87. The agar is MH, with the broth shown NB (86-87). NG – No growth. The

values highlighted yellow show  $\text{MIC}_{100} \geq 32 \mu\text{g/mL}$ . The ClogP data was calculated using Chem BioDraw Ultra software version 13.0.

Table 34: The  $\text{MIC}_{100}$  data for the glycosidic flavonoid compound 82-87. The broth is MHB. NG – No growth.

Table 35: The MIC values ( $\mu\text{g/mL}$ ) for *St. agalactiae* and *Es. coli* the underivised compounds. Compounds 2-4 data was adapted from ref. 104.

Table 36: A comparison of clinically available antimicrobials MIC values with the bisphenol parent compounds 33 and 34 and their respective glycosides 24-25 MIC values. The values are reported by EUCAST for the clinically used compounds.

Table 37: A comparison of clinically available antimicrobials MIC values with the AZT 43 and its triazole containing compounds 35-42 MIC values. The values are reported by EUCAST for the clinically used compounds.

### **A(7): List of equations**

Equation 1: The general process used in PTS.

Equation 2: An equation to express the exponential stage of growth in bacteria.

Equation 3: The Lineweaver-burke rearrangement and how it relationship to  $Y=Mx+C$

### **A (8): List of Schemes**

Scheme 1: The pathway used for folate synthesis is displayed. Where the antibiotics are effective is summarised. Modified from ref. 52.

Scheme 2: The cleavage of the glycosidic bond, by  $\beta$ -galactosidase, to produce *ortho*-nitrophenol 18 and galactose.

Scheme 3: The cleavage of the glycosidic bond in X-GAL 19 to produce 4-chloro-3-bromo-indol-3-ol 20. This compound then dimerises to produce the insoluble indigo 21.

Scheme 4: The different methods for drug design.

Scheme 5: An example of a tripartite prodrug. The example is ampicillin 19.

Scheme 6: The reaction scheme for the synthesis of 24 and 25. The compound in the square bracket represents an intermediate that was partially purified.

Scheme 7: The mechanism for the formation of the  $\beta$ -anomer.